# CHARACTERIZATION AND FUNCTION OF TWO G-PROTEIN REGULATORS, VERTEBRATE LGN AND *DROSOPHILA* RAPGAP

**RACHNA KAUSHIK**

**A THESIS SUBMITTED**

**FOR THE DEGREE OF DOCTOR OF PHILOSOPHY**

**INSTITUTE OF MOLECULAR AND CELL BIOLOGY**

**NATIONAL UNIVERSITY OF SINGAPORE**

**2004**

# Acknowledgements

I thank Drs. Sami Bahri, Xiaohang Yang and Bill Chia for accepting me as a graduate student in their lab and for their continual support throughout. I am especially grateful to Sami for mentoring me and for giving me the freedom to shape my projects. His suggestions, critical comments and patience have been instrumental in shaping this thesis into its present form. I thank Xiaohang for all his invaluable guidance and support, and Bill who made the time for many insightful discussions about my work.

I am grateful for the support of the many scientists in IMCB who have made this thesis possible. Dr. Inna Sleptsova-Friedrich initiated me into the zebrafish field and patiently helped me perfect embryo injections over the period of many months. Dr. Fengwei Yu has been a valuable collaborator and has provided me the anti-mLGN serum and some DRapGAP reagents. Dr. Bor Luen Tang helped with golgi analysis in mammalian cell cultures. HWJ, CXM and GG labs generously shared their reagents with me. I also thank Dr. Chee Wai Fong and Dr. Canhe Chen for help with reagents for GDI assays. Hing Fooksion and Mak Kah Jun provided not only excellent technical assistance, but also equally important humorous diversions, keeping the lab's spirits high.

I am grateful to the members of my supervisory committee Drs. Ed Manser and Thomas Dick for their suggestions during the yearly committee meetings. I also thank the IMCB graduate student committee Drs. Graeme Guy and Mingjie Cai for their help with student matters. I also thank Drs. Sudipto Roy and Dr. Peter Currie for their comments and suggestions on my work.

I thank all the past and present members of the Fly lab at IMCB for providing a great atmosphere in the lab. Thanks to Cai Yu, Devi, Fengwei, Fitz, Hue-Kian, Kate, Kavita, Linda, Marita, Martin, Mike Z, Murni, Priya, Tong-wey, and Xavier for all their suggestions for my work and for allowing me to pick their brains, and thankfully still remaining sane at the end of the day.

I am especially grateful to Kavita for being a great friend throughout the course of my PhD and Kate for providing both professional and moral support during the tiring days of thesis-writing. Special thanks to my husband JC for all his patience and support without which none of this would have been possible. Lastly, I thank my mom and brother for all their encouragement and support.

# Table of Contents

# List of Figures and Tables

## Figures

## Tables

# Abbreviations

| | |
|---|---|
| A/P | Anterior/Posterior |
| aa | amino acid |
| Ab | Antibody |
| AGS3 | Activator of G-Protein Signalling 3 |
| Amp | Ampicillin |
| aPKC | atypical Protein Kinase C |
| APS | Ammonium Persulphate |
| ATP | Adenosine 5' Triphosphate |
| *baz* | *Bazooka* |
| bp | basepairs |
| BSA | Bovine Serum Albumin |
| *C. elegans* | *Caenorhabditis elegans* |
| $CaCl_2$ | Calcium Chloride |
| cAMP | cyclic Adenosine Monophosphate |
| Cdc42 | Cell division cycle 42 |
| cDNA | complementary DNA |
| CIP | Calf Intestinal Phosphatase |
| CNS | Central Nervous System |
| CS | Canton-S (wild type fly strain) |
| C-terminal | Carboxy (COOH) terminal |
| Cy3 | Cyanine 3 conjugated |
| dbd | dorsal bidendritic |
| DBDN | Dorsal bidendritic neuron |

| | |
|---|---|
| DEPC | Diethyl Pyrocarbonate |
| DIG | Digoxygenin |
| DNA | Deoxyribonucleic acid |
| dNTP | deoxynucleotide triphosphate |
| DRapGAP2 | *Drosophila* RapGAP isoform 2 |
| *Drosophila* | *Drosophila melanogaster* |
| DTT | 1, 4-Dithiothreitol |
| *E. coli* | *Escherichia coli* |
| ECL | Enhanced Chemilluminescence |
| EDTA | Ethylenediaminetetraacetic acid |
| EGTA | Ethylene glycol-bis(2-aminoethylether)-N,N,N',N'-tetraacetic acid |
| F-actin | Filamentous actin |
| FITC | Fluorescein isothiocyanate |
| FRT | FLP recombinase recombination target |
| g | Grams |
| G-actin | Globular actin |
| GDI | Guanine Dissociation Inhibitor |
| GEF | Guanine Exchange Factor |
| GIPs | Inhibitory G-proteins |
| GM130 | golgi matrix protein 130KD |
| GoLoco | $G\alpha_{i/o}$ – Loco interaction motif |
| GPCR | G-Protein Coupled Receptor |
| GPR | G protein regulatory |
| GS28 | 28-kilodalton golgi SNARE protein |

| | |
|---|---|
| GST | Glutathione-S-Transferase |
| GTPase | Guanine 5'-Triphosphatase |
| $H_2O$ | Water |
| HCl | Hydrochloric acid |
| HEPES | N-2-hydroxyethyl piperazine-N'-2-ethanesulphonic acid |
| Hh | Hedgehog |
| hr | Hour |
| HRP | Horse Radish Peroxidase |
| IgG | Immunoglobulin |
| Insc | Inscuteable |
| IP | Immunoprecipitation |
| IPTG | Isopropyl-β-thiogalactopyranoside |
| kb | Kilobase |
| KCl | Potasium Chloride |
| KD | Kilodalton |
| *LacZ* | Lactose converting reporter gene from *E. coli* |
| Lat B | Latrunculin B |
| LB | Luria Broth |
| LGN | leucine-glycine-asparagine tripeptide containing protein |
| LiCl | Lithium Chloride |
| M | Molar |
| m21 | DRapGAP mutant |
| mAb | monoclonal Antibody |
| MDCK | Madin-Darby Canine Kidney cell line |
| $MgCl_2$ | Magnesium Chloride |

| | |
|---|---|
| mins | Minutes |
| Mir | Miranda |
| ml | Milliliter |
| mM | Millimolar |
| mm | Millimeters |
| MNs | Motor Neurons |
| mRNA | messenger RNA |
| MTOC | Microtubule Organising Centre |
| NaCl | Sodium Chloride |
| NB | Neuroblast |
| nm | Nanometers |
| NRK | fibroblast-like cell line from normal rat kidney |
| N-terminal | Amino ($NH_2$) terminal |
| NuMA | Nuclear mitotic apparatus protein |
| ORF | Open Reading Frame |
| Par | Partitioning defective |
| pBS | plasmid BlueScript |
| PBS | Phosphate Buffered Saline |
| PC12 | pheochromocytoma cells from rat |
| PCR | Polymerase Chain Reaction |
| PDZ domain | PSD-95, Dlg and ZO-1/2 domain |
| PFF | Paraformaldehyde fixative |
| PFS | Paraformaldehyde solution |
| pGMR | plasmid Glass Multimer Reporter |
| *Pins* | *Partner of Inscuteable* |

| | |
|---|---|
| PKA | Protein kinase A |
| PKI | Protein kinase A inhibitor |
| PMNs | primary motor neurons |
| *Pon* | *Partner of numb* |
| Ptx | Pertussis toxin |
| *Rac* | Ras homology gene family |
| *Rap* | GTP-binding protein - a close homolog of Ras |
| *Ras* | small GTPase |
| *REPO* | Reversed Polarity |
| RGS | Regulator of G-protein Signalling |
| *Rho* | Ras homology gene family |
| RNA | Ribonucleic acid |
| rpm | Revolutions per minute |
| RT | Room Temperature |
| *Sb* | *Stubble* |
| SDS-PAGE | Sodium Dodecyl Sulphate-Polyacrylamide Gel Electrophoresis |
| Shh | sonic hedgehog |
| SMNs | Secondary motor neurons |
| TE | Tris EDTA |
| TEMED | N, N, N', N' tetramethylethylene diamine |
| Thr | Threonine |
| TPR | Tetrotricopeptide repeat |
| Tris | Tris (hydroxymethyl) aminomethane |
| Tyr | Tyrosine |

| | |
|---|---|
| *UAS* | *Upstream Activator Sequence* |
| V | Volts |
| Vti1α | Vesicle transport v-SNARE protein |
| WISH | human cell line from amnion epithelium |
| Wnt | Mammalian Wingless |
| WT | Wild Type |
| ZPA | Zone of polarizing activity |
| β-Gal | β-Galactosidase |
| μg | Microgram |
| μl | Microliter |
| μM | Micromolar |

# Summary

Heterotrimeric guanine nucleotide binding regulatory proteins (G-proteins) are critical players in cellular signaling and their regulation is important for growth and development. This thesis focuses on characterizing two GoLoco motif-containing regulators of G-protein signaling, vertebrate LGN and *Drosophila* RapGAP using mammalian cell culture systems, zebrafish neurogenesis and *Drosophila* neurogenesis as model systems.

Mammalian LGN/Activator of G-protein signalling 3 (AGS3) proteins and their *Drosophila* Pins ortholog are cytoplasmic regulators of G-protein signalling. The results in chapter 3 show that like *Drosophila* Pins, LGN exhibits enriched localization at the cell cortex in a cell cycle-dependent manner in mammalian cultured cell lines. This LGN cortical localization is dependent on actin and influenced by Gα subunits of heterotrimeric G-proteins and interfering with LGN function in cultured cell lines causes early disruption to cell cycle progression. In chapter 4, a role for *LGN* in zebrafish primary motor neuron formation is described. For this work two homologs of LGN from zebrafish were identified and named *LGN and AGS3.* The results show that *LGN* and *AGS3* are expressed in distinct subdomains during development and that *LGN* has important roles in formation of primary motor neurons in zebrafish embryos. The data indicate that LGN interferes with Hh signaling during this process by somehow lowering the expression of patched mRNA. In chapter 5, another G-protein regulator RapGAP is described. RapGAPs are GAPs for Rap1 GTPase and generally contain a GoLoco motif that allows them to interact with Gα. In this work, a GoLoco motif-containing protein isoform, DRapGAP2 from *Drosophila* is characterized. DRapGAP2 shares high homology with human Rap1GAP. The results show that *DRapGAP2* is heavily expressed in the embryonic peripheral nervous system (PNS)

and is asymmetrically localized at metaphase in precursor cells of dorsal bidendritic (dbd) neuronal lineage. Mutants specifically removing *DRapGAP2* were isolated and they show loss of dbd neurons and gain of glial cells. This phenotype is also seen in *Gαi* mutants. Gαi is asymmetrically localized in the dbd precursor cell similar to DRapGAPs, suggesting that these two proteins may influence the same step in regulating asymmetric division of the PNS precursor cell.

Taken together the data on *LGN* presented in this thesis show that in mammalian and vertebrate systems, LGN is required in the execution of proper cell division as well as cell differentiation. The work presented here also indicates an important function for DRapGAP2 in asymmetric division of the PNS dbd precursor cell and dbd neuron formation during PNS development in *Drosophila*.

# CHAPTER 1 : Introduction

Normal cell function and its contribution to overall physiology largely depend on the proper response of cells to extracellular signals and stimuli. The first critical component of signal transduction is communication of signal from its origin outside the cell across the cell membrane to evoke a response inside the cell. Signaling via heterotrimeric and Ras-related family of Guanine nucleotide binding proteins (G-proteins) play pivotal roles in signal transduction events within the cell (Gilman 1987; Preininger *et al*., 2004). Regulators that influence the activation and inactivation state of these G-proteins in time and space are therefore equally important (Chidiac *et al*., 2003). Of particular interest to this thesis work were two such regulators: LGN and RapGAP. Both of these proteins contain GoLoco/G-protein regulatory (GPR) motifs that mediate their interaction with Gαi/o subunits of heterotrimeric G-proteins. LGN and RapGAP also contain additional conserved protein domains that allow for interaction with other proteins, adding to their functional complexity within the cell. LGN contains tetratricopeptide domains (TPR domains) in its N terminus whereas RapGAP contains a GAP domain for Ras-related GTPase, Rap1 (Mochizuki *et al.,* 1996; Chen *et al.,* 1997). TPRs mediate protein-protein interaction and have been shown to be important in LGN function in the cell (Blatch and Lassle, 1999). Through these GoLoco motifs, LGN and RapGAP have the potential of modulating heterotrimeric G-protein activities in the cell. This introductory chapter deals with heterotrimeric G-protein signaling (section 1.1) and then regulatory GoLoco motif-containing proteins (section 1.2) with special emphasis on the LGN/Pins family (section 1.3) and RapGAPs (section 1.6).

For the functional studies of LGN and RapGAP in model organisms, the zebrafish embryonic nervous system and the *Drosophila* embryonic peripheral nervous system

were used. These two systems are also considered in details in this chapter sections 1.4 and 1.7.

## 1.1 Heterotrimeric G-protein signaling

Heterotrimeric G-proteins are critical players in cellular signaling and they generally act via linking activated seven transmembrane receptors, also known as G-protein coupled receptors (GPCRs), to effector molecules. G-proteins play important part in this transmembrane signaling process as they participate in processing and sorting of incoming signals as well as in adjusting the sensitivity of the system. When a hormone interacts with receptor on the surface, this interaction either stabilizes or induces a conformational change in the receptor that activates heterotrimeric-G proteins on the inner membrane of the cell (For review see : Cabrera-Vera *et al*., 2003).

Heterotrimeric G-proteins are composed of three subunits: α, β and γ. The alpha subunits are GTPases which range in size from 39 to 52 kDa (Gilman *et al*., 1987). These enzymes bind and hydrolyse GTP. Some α subunits show specificity for effectors; for example, $\alpha_s$ activates adenylyl cyclases, $\alpha_i$ inhibits adenylyl cyclases, and $\alpha_q$ activates phospholipase C isozymes. Specificity of α subunit types for certain receptors has also been demonstrated in a few cases (Gudermann *et al*., 1997, Conklin *et al*., 1993). The β subunit is tightly bound to the γ subunit and is known to function only as part of such a complex. This βγ complex modulates the activity of several effectors. The β subunit binds a variety of effectors and is therefore directly involved in the modulation of effector activity (Buck E., 1999, Clapham *et al.,* 1997). The γ subunits have been grouped into four subfamilies (Gautam *et al.,* 1998); γ subunits that share identical C-terminal sequences interact with the same receptor while γ subunits

with different C-terminal sequences interact with distinct receptors, thereby adding additional level of selectivity to the heterotrimeric G-protein signaling.

In the inactive receptor state, GDP is bound to the Gα subunit and in this form the Gα subunit is also bound to Gβγ and the intracellular domain of the GPCRs. Upon receptor activation, GDP is released, GTP binds to the Gα subunit and subsequently Gα-GTP dissociates from Gβγ and from receptor. Both Gα and Gβγ subunits are then free to activate their effectors. Examples of the effector molecules include second messengers like cyclic adenosine monophosphate (cAMP) and inositol triphosphate (IP3). The duration of signal is determined by intrinsic GTP hydrolysis rate of Gα and the subsequent reassociation of Gα-GDP with Gβγ (Hamm HE, 1998, Sprang SR, 1997; Sato *et al*., 2004). Changes in the activity of the effector molecules eventually lead to the regulation of multiple cellular functions ranging from short term regulatory processes like the control of secretion rates, muscle tonus or metabolic processes to long term effects like regulation of growth and differentiation.

### 1.1.1 Structural and molecular basis for regulation of heterotrimeric G-protein signaling

The molecular structure of Gα in its GDP-bound and GTP-bound heterotrimeric complexes has been determined. These have provided a framework for understanding the basis for G-proteins acting as biomolecular switches (Rens-Domiano *et al*., 1995). Each Gα subunit contains two domains; one GTPase domain that is involved in binding and hydrolysis of GTP and a helical domain that buries the GTP within the core of the protein (Lambright *et al*., 1994). By comparing the crystal structure of Gα-GDP with Gα-GTPγS, it has been shown that there are three flexible regions in Gαi subunit designated switches I, II and III which become more rigid and well ordered in

GTP bound form (Lambright *et al*., 1994; Noel *et al*., 1993). Within heterotrimeric complexes, the N-terminal helix of Gα is ordered via its interaction with the β propeller domain of Gβ (Lambright *et. al.*, 1996). The βγ dimer binds to a hydrophobic pocket present in Gα-GDP and GTP binding to Gα removes the hydrophobic pocket and reduces the affinity of Gα for Gβγ (Lambright *et al*., 1994).

Based on structural and biochemical studies, it is proposed that the rate limiting step in G-protein activation is the release of GDP from the nucleotide binding pocket. GDP is spontaneously released at a rate that varies depending on the Gα subunit (Denker *et al*., 1995). However the inactive state of the Gα subunit is primarily controlled by Gβγ binding and GDP release is greatly facilitated by receptor activation of the G-protein (Stryer *et al.*, 1986). The intrinsic GTPase activity and the amplitude of signal generated are also under a feedback control (Casey *et al*., 1997; Berstein *et al*., 1992). The duration of G-protein mediated effector activation is dependent on the intrinsic GTPase activity of the Gα subunit (Fields *et al.*, 1997). The amount of available active GTPase can be changed in several ways: 1) acceleration of GDP dissociation by guanine exchange factors (GEFs) speeds up the building of active GTPase, 2) acceleration of GTP hydrolysis by GTPase-activating proteins (GAPs) reduces the amount of active GTPase, 3) inhibition of GDP dissociation by guanine nucleotide dissociation inhibitors (GDIs) slows down the building of active GTPase and 4) GTP analogues like γ-S-GTP, β,γ-methylene-GTP, and β,γ-imino-GTP that cannot be hydrolyzed fix the GTPase in its active state.

### 1.1.2 Model for GPCR mediated activation of heterotrimeric G-protein signaling

The standard model of GPCR-mediated activation of G protein signaling is schematically presented in Fig. 1.1. The Gβγ heterodimer couples Gα-GDP to the receptor and inhibits the release of GDP, thus implying a type of GDI activity for Gβγ dimer. Ligand-occupied GPCRs stimulate signal onset by acting as guanine-nucleotide exchange factors (GEFs) for Gα subunits, thereby facilitating GDP release, subsequent binding of GTP, and release of the Gβγ dimer (Bourne *et al*., 1997). Effector interactions with the GTP-bound Gα and free Gβγ subunits propagate the signal forward.

### 1.1.3 Regulation of GTPase signaling of Gα

#### 1.1.3.1 The role of guanine exchange factors or GEFs

Traditionally, activation of heterotrimeric G-proteins has been thought to be accomplished exclusively by the action of GPCRs, the seven transmembrane-spanning proteins that reside in the plasma membrane (Fig. 1.1A). The activated receptors act as guanine nucleotide exchange factors (GEFs) and stimulate the release of GDP from Gα. To ensure directionality of exchange, activated GPCRs/GEFs stabilize a nucleotide-free transition state of Gα that is disrupted by binding of GTP (Coleman *et al*., 1994). This facilitates dissociation of Gα–GTP from the Gβγ dimer and release of these proteins from the receptor. In addition to GPCRs, intracellular proteins such as Ric-8A and Ric-8B have been isolated as Gα binding proteins with potent GEF activity towards $G\alpha_q$, $G\alpha_{i1}$, and $G\alpha_o$ but not $G\alpha_s$ (Tonissoo *et al*., 2003; Tall *et al*., 2003).

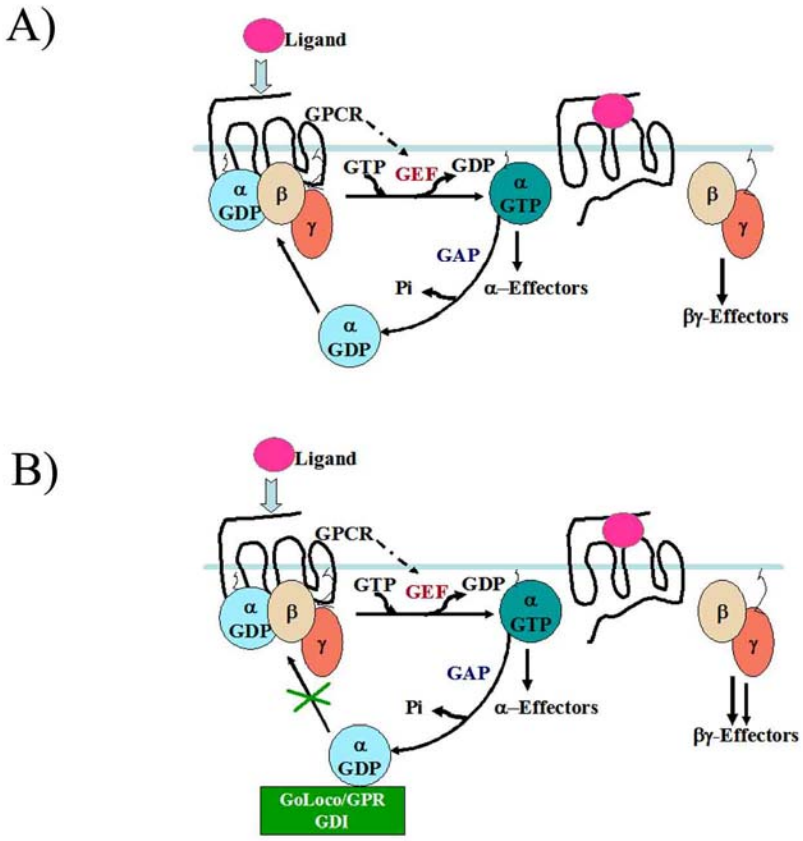


**Figure 1.1: Model of the GDP-GTP cycle governing activation of heterotrimeric G-protein-coupled receptor (GPCR) signaling pathways.**

Panel A shows a model of the GDP-GTP cycle governing activation of heterotrimeric G-protein-coupled receptor (GPCR) signaling pathways. In the standard model of heterotrimeric G protein signaling, GPCRs are associated with the membrane bound heterotrimeric G-proteins comprising of Gα, Gβ and Gγ subunit. In the absence of ligand-mediated activation, the Gβγ dimer is tightly bound to Gα-GDP and intracellular domain of GPCR. The binding of an extracellular ligand to GPCR causes conformational changes in the intracellular loops of the receptor that in turn promote replacement of bound GDP by GTP on the Gα subunit (i.e. activated GPCR exhibits GEF activity). GTP binding changes the conformation of the three flexible "switch" regions within Gα allowing its dissociation from Gβγ. Gβγand GTP bound Gα subunits, once freed of one another, can initiate signals by interacting with downstream effector proteins, including different isoforms of adenylyl cyclase, phospholipase-C as well as various ion channels. Termination of signals generated by Gα-GTP and free Gβγ subunits relies on the intrinsic guanine triphosphatase (GTPase) activity of Gα; this activity is greatly augmented by proteins which act as GTPase activating proteins or GAPs. These GAPs help Gα to convert to the GDP-bound state which then reassociates with Gβγ and terminates all effector interactions. Panel B depicts a revised model of heterotrimeric G protein signaling due to the presence of guanine dissociation inhibitors GDIs such as the Goloco/GPR motif-containing proteins Pins/LGN/AGS3. These GDIs bind to Gα-GDP and this results in the inhibition of Gα-GDP/Gβγ complex formation and thus allowing free Gβγ to activate downstream effector pathways for a longer period of time in a manner independent of receptor mediated "GEF-like" activity.

Ric-8A interacts with GDP-bound Gα subunits in the absence of Gβγ, causing release of GDP and formation of a stable, nucleotide-free Gα–Ric-8A complex. GTP then binds to Gα and disrupts the complex, releasing Ric-8A and an activated Gα–GTP protein.

#### 1.1.3.2 The role of GTPase activating proteins or GAPs

GTPase-activating proteins act to inactivate G-protein signaling pathways by enhancing the intrinsic GTPase activity of Gα subunits thereby converting them from GTP-bound form to a GDP-bound form. Examples of GAP proteins include the RGS proteins (Regulators of G-protein signaling) which all share approximately 125-amino acid domain termed the RGS box (Koelle *et al*., 1996). The RGS box is conserved in various proteins from various systems (Hollinger *et al*., 2002). The RGS proteins are multifunctional and act by accelerating the GTPase activity of Gα subunits to promote signal termination and formation of Gαβγ heterotrimer.

#### 1.1.3.3 The role of guanine dissociation inhibitor proteins or GDI

The discovery of this additional class of regulatory proteins for Gα has challenged the standard model of heterotrimeric G-protein activation (see section 1.1.2 for details). These proteins contain a characteristic GoLoco/G-protein regulatory motif with which they selectively bind Gα-GDP (Fig. 1.1B). This GDI– Gα–GDP interaction inhibits the release of GDP from Gα and excludes Gβγ binding. Thus, GDI proteins are capable of permitting continued Gβγ–mediated effector signaling in the absence of receptor-catalyzed Gα-GTP formation. Examples for this class of proteins include Partner of Inscuteable (Pins) in *Drosophila*, LGN and AGS3 in vertebrates and GPR1 and GPR2 in *C elegans*. This important class of GoLoco-motif containing G-

protein regulators and their function during animal development are described in detail in following sections 1.2 and 1.3.

## 1.2 GoLoco/GPR motifs and GoLoco motif-containing proteins

### 1.2.1 GoLoco/GPR motifs

The GoLoco/GPR motif is a 19-amino-acid sequence with guanine nucleotide dissociation inhibitor activity against Gα subunits of the adenylyl-cyclase inhibitory subclass. The GoLoco/GPR motif has now been identified in several distinct classes of proteins encoded in metazoan genomes (Fig. 1.2). They include modulators of Ras family G-protein signaling (RGS12, RGS14, Rap1GAP), several variations on the tetratricopeptide repeat (TPR), multi-GoLoco architecture of heterotrimeric G-protein regulators (AGS3, LGN, Pins, GPR-1/-2), and two short polypeptides with multiple GoLoco motifs (G18, Pcp-2) (For review see Willard *et al*., 2004; Takesono *et al*., 1999; Yu *et al*., 2000; Kimple *et al*., 2001). The GoLoco motifs were first discovered in studies done on plasma membrane-delimited GPCR signaling and they have been used as a tool to examine GPCR-effector coupling due to their ability to bind Gα–GDP and to exclude Gβγ binding (Siderovski *et al*., 1999). These GoLoco-containing proteins can also regulate heterotrimeric G-protein signaling independent of receptor activation (Cismowski *et al*., 1999; Takesono *et al*., 1999). Recently, there have been some reports indicating that GoLoco/GPR proteins might function in regulation of heterotrimeric G-proteins activity that does not reside near the plasma membrane and that cannot be activated directly by GPCRs: Examples of this include heterotrimeric G-proteins that reside in the Golgi and regulate vesicular trafficking (Jamora *et al*., 1997) and heterotrimeric G-proteins that are involved in the control of mitotic spindle force generation and the act of cell division (Review by Kimple *et al*.,

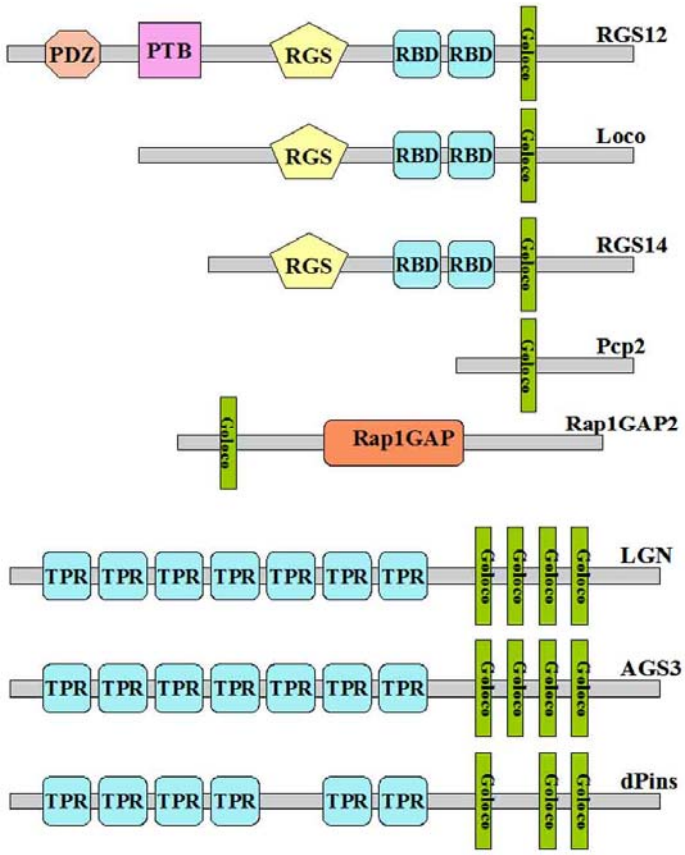


**Figure 1.2: GoLoco/GPR motifs are present in a diverse set of signaling regulatory proteins.**

Domain organization of the single RGS 12 (accession number : O08774), Loco (accession number : Q9UB06), RGS14 (accession number : Q8K2R4), Pcp2 (accession number : Q8IVA1), and Rap1GAP2 (accession number : Q9UQ51) and the multi LGN (accession number : P81274), AGS3 (accession number : Q86YR5 and *Drosophila* Pins (accession number : Q9NH88) GoLoco/GPR motif containing proteins as obtained from SMART (Simple Modular Architecture Research Tool: http://smart.embl-heidelberg.de). PDZ domain : domain present in PSD-95, Dlg, and ZO-1/2 and known for protein-protein interaction; PTB domain : Phosphotyrosine-binding domain; RGS domain : Regulator of G-protein signalling domain; RBD : Raf-like Ras-binding domain; TPR : Tetratricopeptide repeats mostly implicated in protein- protein interaction forming multiple aggregate complexes. The GoLoco motifs mediate interaction with Gα subunits.

2002). GoLoco motif-containing proteins specifically bind to Gα–GDP subunits and this GoLoco– Gα–GDP interaction excludes Gβγ binding, thus capable of permitting continued Gβγ effector signaling in the absence of receptor-catalyzed free Gβγ formation. The formation of GβγGα–GDP and GoLoco-Gα–GDP complexes are mutually exclusive events (Schaefer *et al*., 2001; Knust *et al*., 2001). In this respect GoLoco motif-containing proteins act as activators of G-protein signaling via Gβγ. Concurrently, the inhibition of GDP dissociation by GoLoco motif-containing GDIs in turn contributes to slowing down the building of GTP-bound forms of GTPases in the cell.

### 1.2.2 Structural basis and role of phosphorylation in GoLoco motif function

By structural analysis, the N-terminus of the GoLoco motif is predicted to fold as an amphipathic α-helix (Kimple *et al*., 2002). Binding of the GoLoco motif-containing peptide to the Gα–GDP results in a significant displacement of switch II away from the α3-helix (Kimple *et al*., 2002), thus deforming positions within Gα–GDP that normally serve as critical contact sites for the Gβγ heterodimer (Lambright *et al*., 1996). This further supports the observation that the formation of Gα–GDP-Gβγ and Gα-GDP-GoLoco motif-containing protein complexes are mutually exclusive events (Natochin *et al*., 2000; Takesono *et al*., 1999; Bernard *et al*., 2001).

GoLoco/GPR motif-containing proteins are subject to posttranslational modifications that affect their GDI activity. Recently, two reports have proposed that phosphorylation of GoLoco-motif containing proteins might be the mechanism by which their GDI activity can be modulated. A GoLoco-motif containing protein from mammals RGS14 has been shown to be phosphorylated in rat B35 neuroblastoma cells

by cAMP-dependent protein kinase (PKA) (Hollinger *et al*., 2003). *In vitro* phosphorylation of the recombinant RGS14 protein by PKA occurs at two sites, Ser-258 and Thr-494; the latter site is just N-terminal to the start of the GoLoco motif. At this point, it remains unclear whether phosphorylation at this site contributes directly to the interaction with Gα or results in structural changes within RGS14 that increase GoLoco motif accessibility. Increased cellular PKA activity is the principal outcome of Gαs-coupled receptor stimulation (via adenylyl cyclase activation and the accumulation of cyclic AMP) and it has been speculated that enhancement of Gαi-directed GDI activity mediated by PKA phosphorylation could play a role in cellular cross-modulation of adenylyl cyclase-stimulatory (Gαs) and adenylyl cyclase-inhibitory (Gαi) GPCR signaling pathways, either by decoupling Gαi-linked receptors and/or augmenting effector modulation by Gβγ subunits freed from Gαi heterotrimers (Hepler *et al*., 1999; Hollinger *et al*., 2003).

In a separate study aimed at looking for AGS3 interactors, Blumer and colleagues (2003) identified LKB1/STK11, the mammalian homolog of serine/threonine kinases of *C. elegans* PAR-4 and *Drosophila* LKB1 which are required for establishing early embryonic anterior-posterior axis formation (Watts *et al*., 2000; Martin *et al*., 2003), as a protein which potentially phosphorylates AGS3. These investigations showed that immunoprecipitated LKB1 is able to phosphorylate a recombinant protein consisting of the four Goloco motif C-terminal region of AGS3 and containing 24 serine and threonine residues, only 9 of which are present within the conserved GoLoco motifs. It is currently unknown which specific serine/threonine residue(s) within AGS3 are phosphorylated by LKB1 *in vivo*. However, AGS3 was further shown to be phosphorylated at Ser-16 and it was concluded that phosphorylation at this site diminishes GDI activity *in vitro*. The physiological relevance of this finding is

unknown in the absence of evidence that this serine is actually targeted for phosphorylation *in vivo*. Nonetheless, these studies have highlighted that posttranslational modificiations such as phosphorylation would add additional level of control in the signaling pathways in which the GoLoco/GPR motif- containing proteins function.

### 1.2.3 GoLoco/GPR motif-containing proteins

The Goloco motifs are either present singly or repeated in tandem array within several proteins. Although initially identified and named as heterotrimeric G-protein regulatory proteins, most GoLoco motif- containing proteins possess additional protein interaction domains ranging from a PDZ domain in RGS12, GAP domain for Rap1 in RapGAP and TPR domains in *Drosophila* Pins and its LGN/AGS3 mammalian homologs (Fig. 1.2)(Kimple *et al*., 2001; Mochizuki *et al*., 1999; Yu *et al*., 2000; Schaefer *et al*., 2000; Takesono *et al*., 1999; Mochizuki *et al*., 1996). The presence of these conserved multidomain structures indicates that GoLoco motif-containing proteins might play important roles in integrating various cellular processes with heterotrimeric G-protein signaling. Hence, understanding the function of these GPR-containing molecules would allow for a more integrative understanding of cellular and physiological processes involving their function during development. The work described in this thesis has focused on studying the function of two such GoLoco/GPR motif-containing proteins, vertebrate LGN (chapters 3 and 4) and *Drosophila* RapGAP (chapter 5).

#### 1.2.3.1 GoLoco/GPR motif-containing proteins in development and differentiation

GoLoco/GPR motif-containing proteins are conserved from flies to humans and work done in various systems has indicated critical roles for these proteins during

growth, differentiation and development. In flies and worms for examples, GoLoco motif-containing RGS proteins regulate several aspects of embryonic development including glial differentiation, embryonic axis formation, and skeletal and muscle development (Granderath *et al*., 2000; Fukui *et al*., 2000; Wu *et al*., 2000). The *Drosophila* gene product Loco is another example of a GoLoco/GPR protein where a mutation in the gene results in defects in glial cell-cell interactions such that axons remain partially unsheathed and embryos lack a blood-brain barrier suggestive of an important role for Loco in glial cell adhesion and motility (Granderath *et al*., 2000). Similarly, mouse knock-outs of the closely related mammalian GoLoco/GPR gene, *RGS14,* are lethal at early embryonic stages due to improper attachment to the uterus (Zhong *et al*., 2001), indicating that this gene may also be involved in cell adhesion during development in mammals and that its functions in cell adhesion and motility might be conserved. Overexpression of these proteins can also cause developmental defects; for example, exogenous GoLoco/GPR proteins, RGS2 or RGS4, in *Xenopus* embryos results in severe skeletal and muscular abnormalities (Wu *et al*., 2000), exogenous axin (axin is a scaffold protein which binds beta-catenin and GSK3beta among other proteins and is a negative regulator of Wnt signalling pathway) inhibits axis formation in embryos by scaffolding binding partners together to alter gene transcription, and exogenous mammalian RGS3 can directly affect renal tubule cell migration which underlies the formation of the kidney (Gruning *et al*., 1999; Bowman *et al*., 1998). Interestingly, it has been shown that some of the RGS proteins that affect cell migration block $G\alpha_{12/13}$ signals in addition to being GAPs for Gαi/o and Gαq (Moratz *et al*., 2000; Reif and Cyster, 2000). $G\alpha_{12/13}$ promote both cell migration and oncogenesis more effectively than other Gα subunits (Radhika and Dhanasekaran, 2001) and therefore the $G\alpha_{12/13}$ antagonist function of these RGS proteins may explain

their effects on cell motility. In addition to their role in differentiation and migration, some GoLoco/GPR-containing proteins have also been implicated in having a role in cell proliferation and apoptosis. For example, inhibition of astrocyte proliferation by astrial natriuretic peptide occurs through translocation of RGS3 and RGS4 to the membrane (Pedram *et al*., 2000).

#### 1.2.3.2 GoLoco/GPR motif containing proteins in cell division

Cells can divide symmetrically or asymmetrically to generate two daughter cells during development. Symmetric cell division produces two daughter cells with identical developmental potential or cell fate and it is usually used during cell proliferation to increase cell numbers, whereas asymmetric cell division generates two daughter cells with different fates or developmental potential. The *Drosophila* gene product, partner of inscuteable (Pins), was the first GoLoco/GPR motif-containing protein to be described as having important functions in asymmetric cell divisions. It was shown that Pins in a partnership with Gα forms a crucial part of a complex dictating asymmetric cell division in *Drosophila* neuroblasts (Yu *et al*., 2000; Schaefer *et al*., 2000).

The modular structure of Pins with its N- terminal TPR domains for protein- protein interaction and C-terminal GoLoco motifs is conserved from *C.elegans* to humans (Gotta *et al*., 2003; Yu *et al*., 2000, Schaefer *et al*., 2000 and Du *et al*., 2001). Pins homologs in *C. elegans*, *GPR-1* and *GPR-2* also play important functions in asymmetric cell division and spindle dynamics (Gotta *et al*., 2003). In mammals, LGN is the homolog of Pins and its function in cell division has been described (Du *et al*., 2001). LGN binds NuMA and controls spindle dynamics during cell division. Section 1.3 describes *Drosophila* Pins and mammalian LGN/AGS3 proteins and their functions in some detail.

## 1.3 LGN/Pins family of GoLoco/GPR motif-containing proteins

The LGN family of heterotrimeric G-protein regulators includes Pins in *Drosophila*, GPR1/GPR2 in *C. elegans* and LGN/AGS3 in vertebrates (Gotta *et al*., 2003; Yu *et al*., 2000, Schaefer *et al*., 2000 and Du *et al*., 2001). These proteins have a highly conserved modular structure containing N-terminal TPR domains for protein-protein interaction and C-terminal GoLoco motifs. They form a complex with a Gα subunit and are increasingly becoming crucial components in various cellular processes including asymmetric cell division, spindle dynamics and animal development.

### *1.3.1* Pins in *Drosophila melanogaster*

*Drosophila* Pins was independently identified by two groups to be binding partner of Inscuteable (Insc) and Gαi (Yu *et al*., 2000; Schaefer *et al*., 2000). It encodes a novel protein with multiple repeats of the Tetratricopeptide (TPR) motif that complexes/interacts *in vivo* and *in vitro* with the Insc asymmetric localization domain. *Pins* RNA is maternally deposited and is ubiquitously expressed until stage 12 of embryonic development. Its expression becomes progressively restricted to the CNS starting with stage 13 (Schaefer *et al*., 2000). The Pins protein is present in both dividing neuroblasts and epithelial cells. In epithelial cells, Pins is concentrated at the cell cortex whereas in neuroblasts it is apically localized in a cell cycle dependent manner. In the CNS, Pins is first detected in the apical stalk of delaminating neuroblasts and colocalizes with Inscuteable at the apical cell cortex in fully delaminated neuroblasts and this apical colocalization of Inscuteable and Pins is maintained through metaphase. In anaphase, Insc disappears and in telophase, Pins shows a weak cortical distribution and disappears only after telophase. Apical cortical

crescents of Pins can also be found in the dividing cells of the procephalic mitotic domain 9 (Schaefer *et al*., 2000; Yu *et al*., 2000).

#### 1.3.1.1 Pins function in asymmetric Neuroblasts division in *Drosophila*

The segmented *Drosophila* embryonic central nervous system (CNS) derives from neuronal precursor cells (Neuroblasts or NBs) and each hemisegment contains about 30 NBs. Each NB has a unique developmental potential and gives rise to a distinct lineage of neurons and/or glia during development (Bossing *et al*., 1996; Doe *et al*., 1992; Schmidt *et. al*., 1999). Through lateral inhibition mediated by Notch signaling, one NB is singled out from a small group of cells expressing proneural genes expressing cells (also called an equivalence group). This NB undergoes DNA replication and delamination from single cell-layered neuroectoderm during the G2 cell cycle phase (Doe and Skeath, 1996). During and after delamination, NBs still maintain contacts with the neuroectoderm cells lying just underneath, retain the apical-basal polarity and undergo repeated asymmetric cell divisions which are characterized by apical/basal localization of protein complexes, spindle re-orientation and unequal daughter cell sizes (Fig. 1.3A). Each NB division yields another neuroblast and a smaller secondary precursor cell: the ganglion mother cell (GMC). In the *Drosophila* embryonic central CNS, GMCs only divide once to produce two postmitotic sibling neurons/glia with different fate. The process of binary fate decision of two pairs of sibling neurons that occurs during GMCs division is accomplished through the intrinsic cell fate determinant, Numb. GMCs themselves have apical-basal polarity and Numb basal localization and the orientation of division are coordinated to segregate Numb to only one sibling daughter cell. The correct basal positioning of Numb and the proper orientation of division require the activity of an apical complex of proteins.

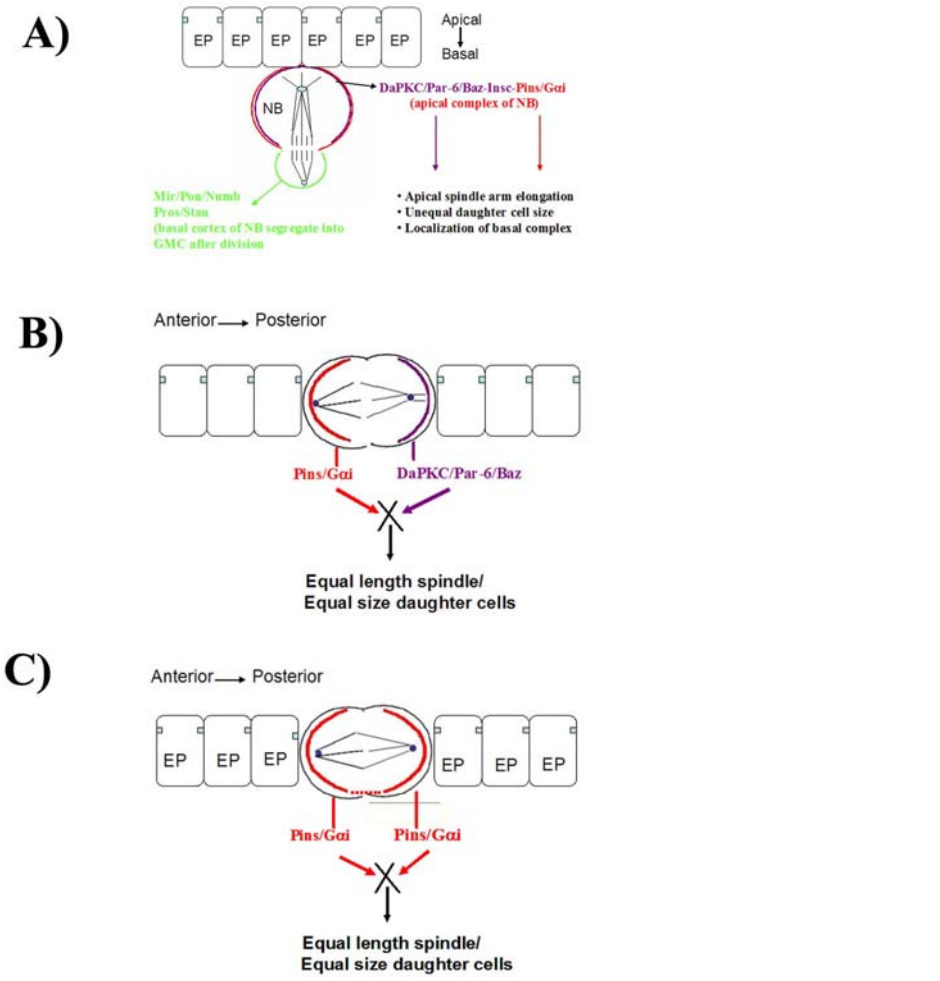


**Figure 1.3 : The subcellular localization of Drosphila Goloco motif-containing protein, Pins.**
A) Pins in dividing Drosophila Neuroblasts; during NB division the two-apical pathways depicted by Baz/DaPKC/Par6/Insc (purple) and Pins/G I (red) are brought together at the apical half of the cortex and results in elongation of apical spindle and ultimately results in bigger apical neuroblasts and smaller ganglion mother cell. B) Pins in the adult sensory organ precursor cell, pI.; the pI cell does not express Insc and the two pathways controlling spindle elongation, Baz/aPKC (purple) and Pins/G I (red) localized to the opposite anterior/posterior halves of the cortex in the dividing pI cells; this results in equal magnitude of force on the two halves of the spindle and in two equal sized daughter cells.
C) Pins in embryonic epithelial cells, the Pins/G i(red) complex is localized to the basolateral cortex during division and during division the magnitude of force on each spindle is equal and two daughters are of equal sizes.
(Adapted from Cai et al., 2003).

The NB apical complex includes Insc (Kraut *et al*., 1996), Pins (Yu *et al*., 2000, Schaefer *et al.*, 2000), Gαi (Schaefer *et al*., 2001), atypical PKC (Wodarz *et al*., 2000) and mutiple PDZ domain protein: Bazooka (Baz)( Schober *et al*., 1999). This apical complex helps localize various cell fate determinants and adapter proteins to the basal side. The basal complex includes Numb (Spana and Doe, 1996), Partner of Numb (Pon) (Lu *et al*., 1998), Miranda (Schuldt *et al*., 1998; Shen *et al*., 1998), Staufen (Li P *et al*., 1997) and Prospero (Doe *et al*., 1991). Pon and Miranda are adapter proteins and they act as a link between the apically localized Insc and the basally localized cell fate determinants (reviewed by Chia and Yang, 2002). Baz, the fly homologue of *C.elegans* Par-3, is the only gene known to be required for asymmetric Insc localization in NBs. Baz is localized apically in the neuroepithelium as well as in dividing NBs and may act to link NB polarity to the apical/basal polarity of the epithelium by recruiting Insc to the apical cortex. While the apical complex in a NB mediates basal localization of cell fate determinants and apico-basal orientation of the mitotic spindle, it is believed that mitotic spindle geometry and unequal daughter cell size are controlled by two parallel pathways within the apical complex: one comprising of Baz and DaPKC and the other comprising of Pins and Gαi. The localized activity of either pathway alone is sufficient to mediate the generation of an asymmetric mitotic spindle and unequal size daughters, but the loss of both pathways results in symmetric divisions (Yu *et al*., 2003; Cai *et al*., 2003; Chia and Yang, 2002).

Analyses of both loss and gain of function approaches suggest that Pins is required for maintenance of apical Insc later in interphase and in mitosis and for spindle dynamics (Yu *et al*., 2000; Schaefer *et al*., 2000). The fact that Pins contains three GoLoco domains, that bind Gα and modulate its signaling, has implicated Pins in the activation of a receptor-independent heterotrimeric G-protein signaling cascade

leading to the establishment of cell polarity. Recent work done on Gαi loss-of-function mutants has shown that Gαi and Gβ13F (Gβ subunit in flies) play distinct roles during *Drosophila* NB asymmetric cell division. Gαi is required for Pins to localize to the cortex, and the effects of loss of Gαi or Pins are highly similar, supporting the idea that Pins/Gαi act together to mediate various aspects of neuroblast asymmetric division. In contrast, Gβ13F appears to regulate the asymmetric localization/stability of all apical components, and Gβ13F loss-of-function exhibits phenotypes resembling those seen when both apical pathways Baz/DaPKC and Pins/Gαi are compromised, suggesting that it acts upstream of the apical pathways (Yu *et al*., 2003a; Izumi *et al*., 2004).

At present, no direct evidence exists that would suggest the involvement of extracellular signals (through G-protein coupled receptors) in orienting *Drosophila* NB divisions. Furthermore, asymmetric localization of Insc and other asymmetrically localized proteins during metaphase and asymmetric cell division can occur in cultured NBs in the absence of any extracellular signal (Broadus and Doe, 1997). Therefore, knowing exactly how heterotrimeric G-proteins are involved in asymmetric cell division awaits identification of some additional pathway elements. In any case, Pins acts as a receptor- independent modulator of heterotrimeric G-protein signaling in this system and has provided some insights into the functions of GoLoco/GPR motif-containing proteins in the context of asymmetric cell division.

#### 1.3.1.2 Pins function in *Drosophila* PNS precursor cells

During the development of the *Drosophila* peripheral nervous system (PNS), a sensory organ precursor (SOP or pI) cell undergoes rounds of asymmetric divisions to generate four distinct cells of a sensory organ. The SOP divides to give rise to two secondary precursors, IIa and IIb. For a simple external sensory (es) organ, IIa divides

once to give rise to hair and socket, and IIb divides twice to produce neuron, glia, and sheath. The Notch antagonists cell fate determinant protein, Numb, is asymmetrically distributed to the anterior IIb daughter and is necessary to specify IIb cell fate (Knoblich *et al*., 1995; Spana *et al*, 1995; Rhyu *et al*., 1994). The pI cell does not express Inscuteable and it is polarized along the anteroposterior (AP) axis by Frizzled (Fz) receptor signaling (For review see Adler and Lee 2001). Fz itself is localized at the posterior cortex of the pI cell prior to mitosis, whereas transmembrane protein Strabismus (Stbm) and LIM domain protein Prickle (Pk), which are both required for AP polarization of the pI cell, co-localize at the anterior cortex. The asymmetric localization of Fz, Stbm and Pk define two opposite cortical domains prior to mitosis of the pI cell. During mitosis, Stbm forms an anterior crescent together with Pins, Gαi and Discs-large (Dlg) and this anterior Dlg-Pins-Gαi complex regulate the localization of cell-fate determinants such as Numb to the same side to give rise to two daughter cells with unequal fates. At this stage, Baz-DaPKC localize posteriorly to the opposite cortical side and function in opposition to Dlg-Pins-Gαi complex to generate a symmetric spindle and equal size of the two daughter cells. At prophase, Stbm promotes the anterior localization of Pins. In this way, Stbm-dependent recruitment of Pins at the anterior cortex of the pI cell provides a read-out of planar cell polarity and translates it into symmetric spindle and sibling cell size during division (Fig. 1.3B) (Cai *et al*., 2003; Bellaïche *et al*., 2004 ; For review see Bardin *et al*., 2004). Overexpression of Insc in pI shifts Pins localization to the posterior cortex and generates asymmetric division and unequal cell size daughters (Cai *et al*., 2003).

#### 1.3.1.3 Pins in symmetrically dividing epithelial cells in the *Drosophila* embryo

In the early *Drosophila* embryo, epithelial cells normally express but do not apically localize Pins or Gαi and do not express Insc (Kraut and Campos-Ortega

1996). These cells divide in the anterior posterior axis with their spindle parallel to the A-P axis (Fig. 1.3C). Insc is necessary for the apical localization of Pins in NBs and ectopic expression of Insc in epithelial cells is sufficient to recruit Pins to the apical cortex of epithelial cells and redirect spindle orientation from parallel to perpendicular (similar to what is seen in NB division) to the A-P axis (Kraut *et al*., 1996). Conversely, apical localization of ectopically expressed Insc in epithelial cells is dependent on Pins. In pins mutants, the exogenous Insc does not localise as an apical crescent; rather it adopts a cytoplasmic distribution (primarily towards the apical side of the cell) during interphase and is undetectable during mitosis, presumably due to rapid degradation. These findings indicate that the ectopic expression of Insc is sufficient for Pins to be recruited to the apical cortex of epithelial cells; moreover, similar to NBs, the mutual dependence between Pins and ectopically expressed Insc is indicated by the apical localization of both proteins in these cells (Yu *et al*., 2000).

It is becoming clear that the role of Pins in *Drosophila* is very much dependent on other Pins-interacting proteins present in a particular cellular context (Inscuteable and Strabismus). These Pins partners can influence its subcellular localization and ultimately the site at which it modulates Gα activity in a receptor-independent manner. It should be noted that most of the asymmetrically localized proteins have conserved counterparts in vertebrates except Insc and Mir for which no mammalian counterparts have been reported so far (For review see Wodarz and Huttner, 2003).

### 1.3.2 LGN & AGS3 proteins in vertebrates

In vertebrates, the family of cytoplasmic nonreceptor-linked heterotrimeric G-protein signaling regulators signified by Pins in *Drosophila* includes two proteins, LGN and AGS3 (Mochizuki *et al*., 1996; Takesono *et al*., 1999). Like Pins, LGN and AGS3 contain N-terminal TPR repeats and C-terminal GoLoco motifs and this

conserved modular structure is indicative towards a conserved role for this family of proteins during evolution. Although the functional interplay between components of plasma membrane-delimited GPCR signaling and GoLoco/GPR motif containing proteins is well defined in mammalian systems (Gilman *et al*., 1987; Hamm *et al*., 1998), investigations into the role of heterotrimeric G-protein signaling in mammalian cell division have lagged behind studies in lower metazoans. A relatively limited number of reports which predict a role for heterotrimeric G-protein signaling in mammalian mitosis exists (for example Willard *et al*., 2000; Crouch *et al*., 1997) and while there is evidence that asymmetric cell division is important during mammalian neurogenesis (Reviewed by Cayouette & Raff 2002), no role for heterotrimeric G-protein signaling in such a process has been reported so far. Gαs, Gαi, and Gαq subunits have been shown to bind tubulin with high affinity and this interaction between tubulin and Gα subunits also activates the GTPase activity of tubulin, inhibits microtubule assembly and accelerates microtubule dynamics (Roychowdhury *et al*., 1999). Thus, the possibility exists where GoLoco/Gα complexes signal directly to tubulin to modulate spindle dynamics. Indeed it has been demonstrated that microtubules at the posterior cortex are less stable during spindle displacement in the *C. elegans* embryo (Labbe *et al*., 2003). In contrast, microtubules are equally stable at the anterior and posterior cortex in *goa-1/gpa-16* (RNAi) embryos (Labbe *et al*., 2003), thus reinforcing a role for heterotrimeric G-proteins and GoLoco/GPR motif containing proteins in the control of cortical microtubule dynamics.

#### 1.3.2.1 Identification of LGN & AGS3

The mammalian Pins homologue LGN (named after the leucine-glycine-asparagine tripeptide present in its TPR regions) was initially isolated in a two hybrid screen for interactors/activators of G-protein signaling (Mochizuki *et al*., 1996;

Takesono *et al*., 1999). LGN is a 677 amino acid mosaic protein with seven repeated sequences of about 40 aa in length at its N-terminal end (TPRs), and four repeated sequences of about 34 aa at its C-terminal end (GoLoco/GPR motifs). Each of the two repeat regions shows substantial similarity to proteins found in other organisms. RT-PCR analysis has shown that the mRNA of *LGN* is ubiquitously expressed in human tissues (Mochizuki *et al*., 1996).

The activator of G-protein signaling, *AGS3,* was identified in a screen for other modes of stimulus input to heterotrimeric G-proteins (other than the GPCR mediated ones) using a functional screen based on the pheromone response pathway in *Saccharomyces cerevisiae* (Takesono *et al*., 1999). In that screen, AGS3 activated the pheromone response pathway at the level of heterotrimeric G-proteins in the absence of a typical receptor. In protein interaction studies, AGS3 was shown to bind Gαi/o and to exhibit a preference for Gαi/o–GDP versus Gαi/o-GTP, thereby indicating that the mechanisms of heterotrimeric G-protein activation by AGS3 are distinct from that of a typical G-protein-coupled receptor.

#### 1.3.2.2 LGN/AGS3 subcellular localization, distribution and function in mammalian cells

Given the knowledge from studies in model organisms where *Drosophila* Pins and *C. elegans* GPR-1 and GPR-2 proteins can assume different cortical localization depending on their interacting proteins and their role in asymmetric cell division, serious efforts have been made to study the tissue and subcellular localization of their mammalian counterparts in different mammalian cell types. It is reported that while *LGN* transcript is expressed in all rat tissues and cell lines tested, *AGS3* transcript is primarily enriched in the brain, testes, and heart (Pizzinat *et al*., 2001).

The subcellular localization of LGN is reported by two separate studies using reagents based on the human LGN sequence. In one study, Blumer and colleagues (2002) used PC12 cells to show that LGN exhibits dramatic differences in its localization at specific stages of the cell cycle. The authors have shown that LGN moves from the nucleus to the midbody structure separating daughter cells during the later stages of mitosis, suggesting a role in cytokinesis. In another study, Du and coworkers (2001) have shown that LGN, unlike *Drosophila* Pins, accumulates at the spindle poles of dividing polarized MDCK cells. The authors have also shown that LGN plays essential roles in the assembly and organization of the mitotic spindle via binding to the nuclear mitotic apparatus protein NuMA, which tethers spindles at the poles (Du *et al*., 2001; Du *et al*., 2002).

Ectopic expression of LGN causes severe mitotic abnormalities in several mammalian cell lines and RNAi-mediated knockdown of endogenous LGN levels disrupts microtubule organization and chromosome segregation during mitosis (Du *et al*., 2001). The first two TPRs domains of LGN specify its binding to NuMA *in vitro* and *in vivo*. This interaction provides a direct link between GoLoco-Gα signaling and the regulation of spindle dynamics because NuMA has been shown to regulate spindle formation and organization at the level of the centrosome (Du *et al*., 2001). Assays of aster formation in *Xenopus* mitotic extracts using recombinant NuMA fragments and anti-LGN antibodies indicate that LGN acts negatively on the intrinsic ability of NuMA to stabilize microtubules and form asters (Du *et al*., 2001). Mechanistically, it appears that the LGN- and tubulin-binding sites on NuMA partially overlap, suggesting that LGN sterically inhibits NuMA-mediated microtubule stabilization (Du *et al*., 2002).

In addition to the reported subcellular localization of LGN, the work described in chapter 3 shows a cell cycle-dependent cortical localization for LGN in dividing cells (Kaushik *et al*., 2003). Furthermore, the data shows that the C-terminal GoLoco-containing domain of LGN alone is sufficient for cortical localization. Factors affecting the cortical localization of LGN in mammalian cells include microfilaments and the Gα subunits of heterotrimeric G-proteins (Kaushik *et al*., 2003). The data presented in chapter 3 also show that overexpression of the mouse LGN protein or prevention of LGN translation in cell lines by a antisense morpholino results in cell cycle arrest (Kaushik *et al*., 2003).

In addition to the previous studies and my work, recently it has been shown that endogenous LGN in human neural precursor cells (hNPCs- recovered from postmortem human brains) can localize asymmetrically in a cell cycle-dependent manner, although this apical localization is not strictly cortical as is seen for Pins in *Drosophila* NB division (Fuja *et al*., 2004). When hNPCs are grown in conditions favouring cell division, the LGN protein localizes to one side of the dividing cell and gets segregated to one of the daughter cells and colocalizes with progenitor cell marker, Nestin. When hNPCs are grown under conditions favoring differentiation, LGN accumulates in double foci similar to those containing the mitotic apparatus protein NuMA, and in a pattern shown previously for LGN and NuMA in differentiated cells (Fuja *et al*., 2004).

As for subcellular localization of AGS3, the protein has been reported to be primarily cytoplasmic throughout the cell cycle (Blumer *et al*., 2002) and a truncated version of AGS3 (AGS3-Short) lacking the N-terminal TPR repeats has also been identified (Pizzinat *et al*., 2001). It is enriched in the heart and shows a punctuate subcellular cytoplasmic distribution that is different from AGS3. The localization data

suggested that the TPR domains might account for the differences between a homogeneous cytoplasmic staining for AGS3-Short and a punctate cytoplasmic distribution for AGS3. During cell division, AGS3 seems to be cytoplasmic throughout (Blumer *et al*., 2002). A role for AGS3 in mammalian cell division has not been reported so far. However, an interaction between the mammalian PAR-4 homolog LKB-1 and AGS3 has recently been demonstrated *in vitro* and in cotransfection studies in culture (Blumer *et al*., 2003). Although PAR-4/LKB-1 are known to function in cell polarity and division, the functional consequences of AGS3 interaction with these proteins have yet to be determined. Still, given recent findings regarding LGN function in mammalian cell division, it appears likely that AGS3 may have a function in this process.

AGS3 function in mammalian cells has been reported in two studies. In one study, ectopic AGS3 was shown to attenuate amino acid deprivation-induced autophagy in HT-29 cells (Pattingre *et al.*, 2003). In another study, AGS3 has been shown to increase the stability of Gαi-GDP in the membrane, which influences the adaptation of the cell to prolonged activation of heterotrimeric G-protein coupled receptors (Sato *et al*., 2004).

#### 1.3.2.3 LGN/AGS3 function in animal development

A role for LGN or AGS3 in animal development has not been studied. However, our laboratory has studied the behaviour of mouse LGN (mLGN) in *Drosophila* and its potential to replace Pins function in this system (Yu *et al*., 2003b). Our findings showed that LGN localizes asymmetrically to the apical cortex of mitotic neuroblasts when ectopically expressed in *Drosophila* embryos. Like Pins, the N-terminal tetratricopeptide (TPR) repeats of mLGN can directly interact with the asymmetric localization domain of Insc and its C-terminal GoLoco-containing region can direct

localization to the neuroblast cortex. It was further shown that mLGN can fulfill all aspects of pins function in *Drosophila* neuroblast asymmetric cell divisions by being able to rescue all Pins functions when expressed in *pins* mutant backgrounds (Yu *et al*., 2003b).

As a means to characterize the function of LGN/AGS3 during animal development, the tissue expression patterns of these genes have been analyzed during embryonic development. *LGN* RNA is found ubiquitously expressed in many tissues with enrichment in the ventricular zone of the developing central nervous systems (Yu *et al*., 2003b), while *AGS3* RNA is mainly enriched in the brain it is uniformly distributed in the neural tube (Blumer *et al*., 2002; Yu *et al*., 2003b). Unfortunately, these studies have not addressed function of LGN or AGS3 in animal development. In my work, I have attempted to characterize the role of LGN in animal development using zebrafish, *Danio rerio* and I named the zebrafish LGN paralogs, *lgn* and *ags3* (See chapter 4). In my study, I have analyzed the expression pattern of *zebrafish lgn* and *zebrafish ags3* and described a role for LGN protein during primary motor neuron formation in the developing zebrafish embryo. My findings show that LGN may interfere with hedgehog signaling pathway to allow formation of correct number of primary motor neurons in the zebrafish embryo (See Chapter 4). In the following sections (1.4 and 1.5), zebrafish neurogenesis and the Hh signaling pathway, which are relevant to this part of my work are described.

## 1.4 Zebrafish as a model system to study vertebrate development

As a model species, zebrafish has several advantages: 1) it has small size and high fecundity, 2) the embryo develops externally, 3) the embryo is transparent during embryogenesis making it an excellent system to study vertebrate embryonic

development, 4) transparency of embryos also allows high resolution analysis of gene expression often at a single cell level and 5) the zebrafish genome is almost completely sequenced and availability of genomic and EST sequences and the development of knock-down techniques using morpholinos are increasingly making zebrafish a popular model system for studying various conserved proteins functions.

### 1.4.1 Neurogenesis in the developing zebrafish embryo

Although there are many similarities in which neurulation takes place in vertebrates, there are features in which zebrafish neurulation is different form the other vertebrates such as chick and mouse (Kimmel *et al*., 1994; Papan and Campos-Ortega 1997). The central nervous system of zebrafish comprises of the brain and the spinal cord and it develops from a specialized region of the ectoderm, the neuroectoderm or neural plate, which is specified during gastrulation (Kimmel *et al*., 1995). The onset of gastrulation occurs at 50% epiboly (5 1/4 hpf) at this time, a thickened marginal region termed the germ ring appears around the blastoderm rim. Within the germ ring, there are the upper and lower germ layers with the upper layer (the epiblast) continuing to feed cells into the lower layer (the hypoblast) throughout gastrulation. The cells remaining in the epiblast when gastrulation ends correspond to the ectoderm and will give rise to such tissues as epidermis, the central nervous system, neural crest, and sensory placodes. The hypoblast gives rise to both the mesoderm and endoderm, although it is unclear how this layer subdivides into endoderm and mesoderm. A marked streaming of cells toward the presumptive dorsal side of the germ ring in both the epiblast and the hypoblast produces the embryonic shield (6 hpf).

Narrowing and elongation of the primary embryonic axis occur as the shield extends toward the animal pole. The dorsal epiblast begins to thicken rather abruptly anteriorly and at the midline near the end of gastrulation, producing the first indication

of development of the rudiment of the central nervous system: the neural plate. Below this is the axial hypoblast, flanked by the paraxial hypoblast. In the trunk region, these will form the notocord and somites, respectively. After epiboly, the somites and neural tube develop, the rudiments of the primary organs become visible, the tail bud becomes more prominent and the embryo elongates. The first somites form anteriorly, and the posterior ones form last. The neural plate is then converted into a solid structure called the neural keel which later develops in a neurocoel. The brain and spinal cord in vertebrates are hollow and are filled with cerebrospinal fluid. The hollow is the neurocoel and it is lined by the epithelium. The neural keel forms in an anterior to posterior progression (Kimmel *et al*., 1995).

The first neurons are formed shortly after gastrulation and before the transformation into neural keel has started (Mendelson *el al*., 1986; Kimmel *et al*., 1995). Motor neurons develop on both sides of the floor plate in the ventral neural tube and zebrafish have two distinct populations of motor neurons: 1) primary motor neurons (PMNs) which are born earlier and are larger than 2) secondary motor neurons (SMNs), which are born later and are smaller. It is not yet known whether PMNs are specific to anamniote vertebrates such as fish and amphibians (Kimmel *et al*., 1994). As a consequence of this early development of functional neurons, embryos are motile after the first day of development, show spontaneous twitching of the body axis and respond to touch after the second day of development. This response is coordinated by relatively few differentiated neurons and a simple scaffold of pioneering axons which relay the touch inputs to muscle cells surrounding the neural tube. The neural tube of zebrafish embryos is like that of other vertebrates, highly polarized along its dorsoventral axis. In the spinal cord, sensory neurons form at dorsal position whereas motor neurons (MNs) and floor plate develop at ventrolateral and ventral positions respectively and interneurons occupy intermediate regions (Fig. 1.4).

Patterning of the neural tube along its dorsoventral axis is initiated during the neural plate stages. Initially, the mediolateral coordinates and then later dorsoventral coordinates of the neural tube are established by secretion of signaling molecules from non-neural tissue surrounding the neural plate (Tanabe and Jesell, 1996). The notochord instructs neural tube precursor cells to differentiate into floor plate during the early stages of somitogenesis (i.e., the time of formation of somites whose blocks of similar cells that differentiate into muscles, bone, and other tissues). In zebrafish, as in other vertebrates, Hedgehog signals function as a messenger protein from the embryonic midline to induce PMNs in the ventral neural tube on both sides of the floor plate (Eisen *et al*., 1999; Lewis and Eisen, 2001). In all vertebrates examined so far, additional signals from the paraxial mesoderm then specify distinct subpopulations of PMNs that occupy specific motor columns at particular anterior-posterior (AP) axial levels. For example, lateral motor column PMNs are generated only at limb levels and visceral PMNs are generated at thoracic levels (Eisen, 1999; Ensini *et al*., 1998; Liu *et al*., 2001). These motor neurons will ultimately relay information between the spinal cord and muscles.

### 1.4.2 Molecular mechanisms governing neural precursor cell formation and division in vertebrates

Molecular mechanisms leading to the establishment of neuronal fate are less well understood in vertebrates than in invertebrates. The presence of genes homologous to *Drosophila Notch* and *Delta* and proneural genes *achaete-scute* as well as *atonal* suggests that similar molecular mechanisms of neurogenesis may exist in vertebrates and flies (Salzberg and Bellen, 1996; Lewis *et al*., 1996; Lee *et al*., 1997).

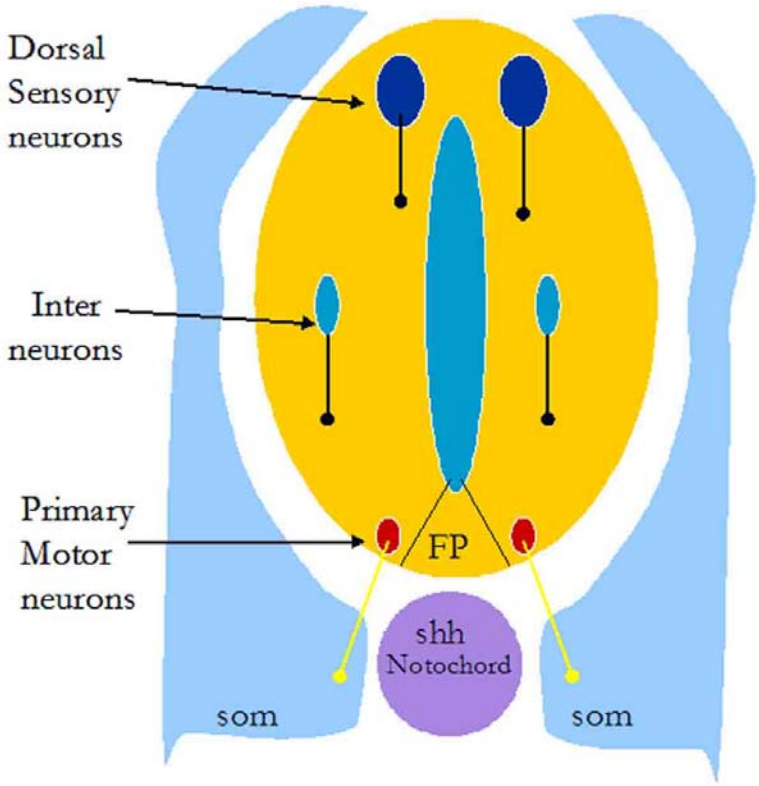


**Figure 1.4 : Distribution of primary neurons in zebrafish.**

Schematic representation of a cross section of 22 somites stage zebrafish embryo at the level of trunk is shown. In the neural tube (nt), primary motor neurons form ventrally and are specified by the activity of Hh that is secreted from ventral structures such as floor plate (FP) and notochord. Interneurons and sensory neurons are formed as a distance further away from the source of signal. The neural tube is in contact with the somites (som) which provide signals that activate neuronal differentiation. Dorsal is up.

In all animal models tested so far, mutations in the Notch receptor invariably result in developmental abnormalities and a conserved picture is emerging with respect to neural fate commitment and the role of Notch signaling (For review see Artavanis-Tsakonas *et al*., 1999). In vertebrate and invertebrate embryos, neuronal precursor cells are born within small proneural clusters as a result of Notch- and Delta-dependent lateral inhibitory interactions.

Simplistically, Notch mediated signaling starts when the extracellular domains of the Notch-ligands (Delta and Serrate in *Drosophila*, Delta and Jagged in vertebrates, LAG-2 and APX-1 in *C. elegans*) are expressed on the surface of one cell and interact with the extracellular domain of the Notch receptor on an adjacent cell. In *Drosophila* and as a result of this Notch-receptor activation, the transcription factor Suppressor of Hairless, Su(H)(CBF1/RBPj-k in mammals, LAG-1 in *C. elegans*) binds to regulatory sequences of the genes of the Enhancer of split (E(spl)) locus and up-regulates expression of their encoded bHLH proteins (For review see Schweisguth F., 2004; Lai EC., 2004). The bHLH factors, in turn, affect the regulation of downstream target genes. One well-defined target is the Achaete-Scute complex, which contains proneural genes that encode proteins involved in the segregation of neuronal and epidermal lineages, a process affected by mutations in Notch. The differential regulation of cell fates is in part achieved by asymmetrically segregating cell fate determinants (such as Numb) that function through inhibition of Notch signaling in the cells they are present. Notch and its inhibitor Numb are also important for later events of sibling cell fate choice in postmitotic cells in *Drosophila* (Buescher *et al*., 1998; Schuldt and Brand, 1999).

In support of conserved function for these molecules in vertebrates, overexpression of *neuroD* or *neurogenin*, the vertebrate homolougue of *Drosophila* proneural gene *atonal* has been shown to form ectopic neurons in zebrafish (Blader *et al*., 1997; Ma *et*

*al.*, 1996) and the expression pattern of vertebrate *Delta* homologs within the neural plate suggests a process similar to lateral inhibition acts within the neuroectoderm of the vertebrate embryo to single out precursor cells that divide and give rise to develop to become neurons (Haddon et *a.l,* 1998; Appel and Eisen*,* 1998). In addition, Numb, and a related protein, Numblike (Nbl), have been identified in vertebrates and like the *Drosophila* Numb proteins, vertebrate Numb is asymmetrically localized in cortical and retinal progenitors (Zhong *et al*., 1996; Cayouette *et al*., 2001). Through the use of different experimental paradigms, multiple roles for Numb and Numblike during neurogenesis have been proposed in maintaining progenitor populations and promoting neuronal differentiation (Zhong *et al*., 2000; Zilian *et al*., 2001; Petersen *et al*., 2002). However, the complexity of neuronal types in the neural tube makes drawing parallels between *Drosophila* and zebrafish mutant phenotypes difficult. In vertebrates, the location, origin and identity of endogenous neural stem cells are just being elucidated but much is known about factors that modulate precursor cell differentiation and maintenance in invertebrates. These factors have been well characterized in *Drosophila* NB and they include many asymmetrically localized proteins such as Pins/Insc/dAPKC/Gαi/Baz/ Staufen/Pros/Mir/Numb proteins. Like in other vertebrates, in zebrafish the types of precursor neuronal cell divisions have not been well elucidated and most work done in these organisms have focused on the identity of the neuron formed in different mutant background (Chen *et al*., 2001; Beattie *et al*., 2000; Eisen *et al*., 1991; Grunwald *et al*., 1988).

### 1.4.3 Primary motor neuron formation in zebrafish

In addition to distinct motor columns at particular AP axial levels (Eisen *et al*., 1991), zebrafish embryos have a more fine-grained, segmentally reiterated pattern of different PMN subtypes along the spinal cord AP axis. The individually identifiable

PMNs are also useful in facilitating analysis of mechanisms that pattern neurons at the level of single cells. Zebrafish have three different PMN subtypes: rostral primary (RoP), middle primary (MiP) and caudal primary (CaP). One PMN of each subtype forms per spinal hemisegment, with the exception that about half the hemisegments initially have two CaP-like PMNs, one of which is called variably present (VaP) and usually dies (Lewis and Eisen, 2004). Hence, at mid-somitogenesis each PMN subtype is uniquely identifiable by soma position relative to overlying somites and by axon trajectory. For example, MiP and RoP are present adjacent to overlying somite boundaries and CaP somatic position is adjacent to overlying somite middles (Fig. 1.5). CaP axons project into ventral myotome, MiP axons project into dorsal myotome and RoP axons project into medial myotome (Fig.1.5).

PMNs can first be identified molecularly by expression of LIM domain/homeodomain-type transcription regulator *islet1*. Prospective PMNs express islet1 soon after birth; at mid-somitogenesis stages CaPs initiate expression of *islet2* and then within 1 hour downregulate expression of *islet1*. By contrast, MiPs and RoPs never express *islet2* (Appel *et al*., 1995; Inoue *et al*., 1994; Tokumoto *et a*l., 1995), but can be distinguished by their temporal expression of *islet1* RoPs express *islet1* later than MiPs or CaPs (Appel *et al*., 1995). Therefore, at mid-somitogenesis stages CaPs can be identified by *islet2* expression and MiPs by *islet1* expression, RoPs do not yet express *islet1*.

#### 1.4.3.1 Mesodermal signals and PMN formation in zebrafish embryos.

The tight spatial correlation between the reiterated pattern of PMNs and the overlying somites suggests that signals from paraxial mesoderm might specify different PMN subtypes. Consistant with this idea, transplantation experiments have

shown that environmental signals can specify zebrafish PMN subtypes (Appel *et al*., 1995; Eisen, 1991).

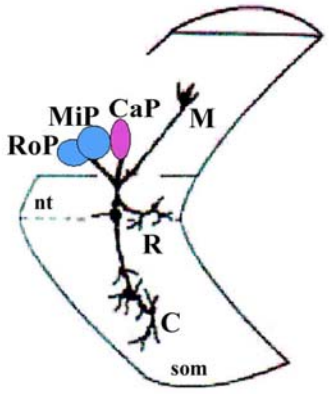


**Figure 1.5 Primary motor neurons in zebrafish embryo.**

Schematic representation of a 22 hour zebrafish embryo showing primary motoneuron positions within the spinal cord and their axonal projections into the adjacent somite (som). Blue represents *islet1*, and red represents *islet2*. MiP : middle primary; RoP : rostral primary; CaP : caudal primary and M indicates the MiP axon, R the RoP axon and C the CaP axon. Anterior is to the left. (Modified from Appel *et al.,* 1994)

For example, when MiP is transplanted 2-3 hours before axogenesis to the position where CaP normally develops, the transplanted cell forms a CaP-like axon and initiates expression of *islet2*. However, when MiP is transplanted in the same way just 1 hour before axogenesis, it remains committed to its original fate, extends a MiP-like axon and does not express *islet2* (Appel *et al*., 1995; Eisen, 1991). The role of signals from paraxial mesoderm in controlling primary motoneuron specification has also been studied in several zebrafish mutants that have distinct effects on paraxial mesoderm development (Lewis and Eisen, 2004). For example, PMN specification and development is disturbed in *spadetail (spt)* mutants, which cause a dramatic reduction of trunk paraxial mesoderm, and the position and axonal morphology of PMNs are also disturbed when somite segmentation is affected by heat shock (Kimmel *et al*., 1988; Roy *et al*., 1999; Bisgrove *et al*., 1997; Eisen and Pike, 1991; Inoue *et al.,* 1994; Tokumoto *et al.,* 1995). These studies have also suggested that signals from the paraxial mesoderm are required to specify MiPs and CaPs, and additional signals from the somites are then required to fine-tune or maintain correct spatial organization of PMN subtypes (Lewis and Eisen, 2004). Together these observations suggest that in addition of Hh signaling (discussed in section 1.4.3.2), signals from the paraxial mesoderm have a role in specifying PMN subtypes.

#### 1.4.3.2 Hedgehog signaling and PMNs formation in zebrafish embryos

One of the most important signaling pathways in patterning the neural tube during neurogenesis in vertebrates is Hedgehog (Hh). The Hh pathway has been extensively studied in model organisms and is highly conserved from flies to humans. Vertebrate hedgehog genes were first reported in 1993, following a cross-species (fish, chick, and mouse) collaborative effort involving three groups (Echelard *et al.,* 1993; Krauss *et al*., 1993; Riddle *et al*., 1993); additional reports of Hh homologs appeared in the

following year (Chang *et al*., 1994; Roelink *et al*., 1994). Unlike the fly which has a single Hh gene, there are several Hh-related genes in vertebrate species. Three Hh genes were identified in the mouse: Desert hedgehog (Dhh), Indian hedgehog (Ihh) and Sonic hedgehog (Shh) (Echelard *et al*. 1993). Dhh is most closely related to *Drosophila* hedgehog; Ihh and Shh are more related to one another, representing a more recent gene duplication event. Further duplication events appear to have occurred in teleosts fishes within the Shh and Ihh classes (Krauss *et al*., 1993; Ekker *et al.,* 1995; Currie and Ingham, 1996). In zebrafish, the Hh family is represented by sonic hedgehog (Shh), tiggy-winkle hedgehog (twhh) and echidna hedgehog (ehh) of which Shh is the best studied. Shh in zebrafish and other vertebrates is expressed in three key signaling centers in the vertebrate embryo: the notocord, the floor plate, and the zone of polarizing activity (ZPA), a population of apical/posterior mesenchyme cells in the limb bud, but not within the mid/hindbrain region where Wnt-1/Engrailed interactions have been observed. Signaling by Shh controls important developmental processes, including dorsoventral neural tube patterning, neural stem cell proliferation, and neuronal and glial cell survival. The graded activity of Shh in patterning the neural tube has been demonstrated using various concentrations of purified Shh to elicit dose-dependent gene activity in neural tube explants (Briscoe *et al*., 2001). Shh organizes the developing neural tube by establishing distinct regions of homeodomain transcription factors production along the dorsoventral axis including Nkx, Pax, and Dbx family members, which specify neuronal identity (reviewed in Briscoe *et al*., 2001). By ectopically activating Shh signaling in medial and dorsal cells of the neural tube, it has been shown that Shh signaling acts directly on target cells, and not through other secreted mediating factors to specify neural cell fates (Briscoe *et al*., 2001 and Hynes *et al*., 2000). Conversely, elimination of Shh signaling from the notocord prevents the differentiation of primary motor neurons (Lewis and Eisen 2001).

Different concentrations of Shh thus cause cells to choose appropriately among many potential cell fates. Shh also plays important patterning roles elsewhere in the nervous system, in the ventral forebrain, Shh is necessary for the generation of cells of the medial and lateral ganglionic eminences in the midbrain and hindbrain and is one of the signals necessary to generate dopaminergic and serotonergic neurons (Reviewed in Briscoe *et al*., 2001). In zebrafish, *Cyc* mutant embryos which lack *twhh* and *shh* expressing forebrain cells lose proximal fates and dorsal expression of Shh in the neural tube results in the induction of ventral marker gene expression (Echelard *et al*., 1993; Krauss *et al*., 1993; Roelink *et al*., 1994). Anterior expression of Shh in the limb mesenchyme produced a mirror image duplication of limb pattern resembling those produced by anterior grafts of ZPA cells (Riddle *et al*., 1993; Chang *et al*., 1994).

The Hh signal is perceived at the cell surface by transmembrane receptors, Patched (Ptc: a multipass transmembrane protein that binds Hh with nanomolar affinity and required for repression of target genes in the absence of Hh) and Smoothened (Smo: a segment polarity gene which encodes a transmembrane protein with high resemblance to G-protein coupled receptors and acts downstream of Hh and Ptc (Alcedo *et al*., 1996). In the absence of Hh signal, Ptc destabilizes Smo at the cell surface (Denef *et al*., 2000) and as a result a cytoplasmic multi-protein complex comprising kinesin-like protein Cos2 and Suppressor of Fused (Su(fu)) binds to the zinc finger transcription factor Cubitis interruptus (Ci) and prevents Ci activation by retaining it in the cytoplasm. These events are coupled with the cleavage of Ci in the cytoplasm from its full length 155-kDa form to a smaller N-terminal fragment called Ci75, or CiRep which lacks the transcriptional activation domains that are found C-terminal to the cleavage region (Chen *et al*., 1999). The cleaved Ci75 form is imported to the nucleus where it represses transcription of Hh target genes, including Ptc (Fig. 1.6).

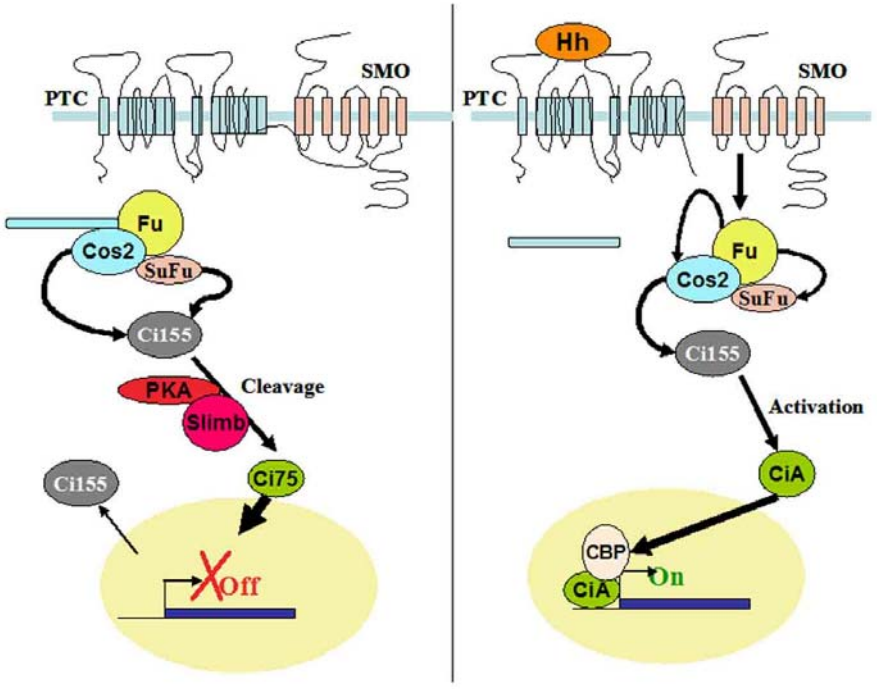


**Figure 1.6 Model of Hedgehog signaling.**

In the absence of Hh signal (left), Costal2 (Cos2) and Supressor of fused Su(fu) binding to Cubitus interruptus (Ci) keeps it bound to microtubules and prevents Ci155 activation and retains it in the cytoplasm. Most of Ci155 is available for cleavage in a process that is dependent upon its phosphorylation by PKA and which involves Slimb. The cleaved Ci75 form then moves to the nucleus and the uncleaved full-length Ci155 is actively exported from the nucleus so that there is no activation of gene transcription by Ci. Upon Hh reception (right), Fused (Fu) is activated and phosphorylates Cos2 and Su(fu). As a result, Ci cleavage is reduced, Ci155 nuclear import overcomes its export driving gene transcription. Activated nuclear Ci155 (CiA) interacts with transcriptional coactivator CBP (CREB binding protein) to fully activate the transcription of Hh target genes.

Most of Ci155 is available for cleavage in a process which is dependent upon its phosphorylation by the serine/threonine kinase PKA and involves Cos2, Su(Fu) and an F-box family of proteasomal targeting proteins, Slimb (Jiang *et al*., 1998). The remaining uncleaved full length Ci155 is actively exported from the nucleus in the absence of Hh signal.

Upon Hh reception, Hh binds Ptc and inactivates it and thus alleviates Ptc-inhibition effect on Smo. Downstream of a free and activated Smo, the kinase protein Fused is activated and it acts on Cos2 and Su(fu) to alleviate the negative effect on Ci. As a result, Ci155 cleavage is reduced and its nuclear import overcomes its export and Ci is activated. Ci activation requires Fu to antagonize Su(fu) and the Cos2-mediated negative effect. Activated nuclear Ci155 interacts with the transcription coactivator CREB binding protein, CBP to fully activate the transcription of Hh target genes. Thus, the Hh signal induces expression of target genes (including Ptc transcription) by binding and inactivating Ptc and allowing Smo to become active leading to transcription of downstream targets (Fig. 1.6). When Ptc is inactivated by mutation, inappropriate transcription of Hh target genes results. Ptc also regulates the movement of Hh through tissues and binding of Hh to Ptc limits the spread of Hh from its source. Ptc-mediated control of Smo signaling might involve vesicular transport as extensive structural similarity is shared between Ptc proteins (Ptc1 and Ptc2 in vertebrates) and the Niemann-Pick C1 (NPC1) protein. NPC1 functions in the sorting and recycling of cholesterol and glycosphingolipids in the late endosomal/lysosomal system (Incardona *et al*., 2002). Moreover, Ptc might regulate Smo activity by promoting activity of a phosphatase that dephosphorylates Smo in the absence of Hh (Denef *et al*., 2000). PKA has been shown to have negative regulation on the Shh pathway similar to Ptc, but PKA does not act downstream of Ptc rather it is epistatic to Smo. Activation of Smo might modulate PKA activity (Alcedo *et al*., 1996) and as Smo has similarities

with GPCRs it is speculated to regulate PKA activity via heterotrimeric G-proteins and adenylyl cyclase.

The other zebrafish Hh family members Twhh and Shh are involved in patterning the ventral CNS and proximal eye (Ekker *et al*., 1995) and a negative regulatory role for PKA in these processes have been reported. Zebrafish embryos injected with RNAs encoding Shh, Ihh, or a dominant-negative regulatory subunit of PKA, PKI, have equivalent phenotypes (Hammerschmidt *et al*., 1996). Moreover, ectopic expression of PKI partially rescues somite and optic stalk defects in mutants that lack midline structures that normally synthesize Shh (Hammerschmidt *et al*., 1996). While a role for Shh signaling is implicated in primary motor neuron formation (Lewis and Eisen 2001) it has never been shown whether PKA mediated negative regulation of Shh signaling affects PMNs formation.

## 1.5 LGN and PMN formation in zebrafish embryo

Many receptors for neurotransmitters, hormones and chemokines utilize heterotrimeric G-proteins as second messengers in signaling cascades leading towards growth and development of most organisms. Smo, which is a receptor for Shh, has similarities with the GPCRs. Hence it was speculated that heterotrimeric G-proteins might have a role in Hh signaling. Some support for this speculation was provided from human Smo when expressed in *Xenopus* melanophores was shown to be sufficient to stimulate persistent pigment aggregation in these cells, and it was shown that this effect can be blocked by pertussis toxin (DeCamp *et al*. 2000). On the other hand, in another experiment involving primary fish myoblast assay system, the effects of Shh were found to be insensitive to pertussis toxin (Norris *et al*. 2000). In another report, Hammerschmidt and McMahon (1998) described developmental defects upon

injection of RNA encoding pertussis toxin (Ptx) into zebrafish embryos. Ptx promotes ADP-ribosylation of inhibitory G-proteins (GIPs) and therefore inhibits the release of Giα from Gβγ dimers on ligand binding (Gilman, 1987). The authors have reported that Ptx-injected embryos developed phenotypes opposite to embryos injected with dominant negative PKA and that heterotrimeric G-proteins might be involved in modulating Hh signaling downstream of Hh in some but not all target cells (Hammerschmidt and McMahon, 1998).

The information on the *in vivo* function of heterotrimeric G-proteins during embryonic nervous system development in zebrafish is rather limited and mostly based on toxin studies. The identification and analysis of the different subunits of heterotrimeric G-proteins in zebrafish would grant a better understanding of the role of this signaling process during developement. In this regard, the gamma3 subunit has recently been identified and it is expressed during late somitogenesis preferentially in the forebrain and in ventrolateral regions of the mid- and hindbrain including the spinal cord (Kelly *et al*., 2001). Overexpression of the human β2/zebrafish γ3 complex in zebrafish embryos leads to the loss of dorsoanterior structures and heart defects, possibly owing to an up-regulation of mitogen-activated protein kinase (MAPK) activity and/or decline in PKA signaling (Kelly *et al*., 2001).

Still to date, a function for heterotrimeric G-proteins in PMNs formation in zebrafish embryos has not been reported. In this thesis, the work described in chapter 4 deals with the identification of LGN/AGS3 homologs from zebrafish and the characterization of LGN function in neuronal formation using zebrafish as a model system. The data show that zebrafish LGN (LGN) plays a negative role in the formation of PMNs and that it may influence Hh signaling in this process at the level of *ptc* transcription (See chapter 4 for details).

## 1.6 RapGAPs

In addition to the LGN family and RGS proteins, some RapGAP protein isoforms also contain GoLoco motifs. The GoLoco motif in RapGAP is located at its N-terminus and is able to bind Gα. RapGAP is defined as a negative regulator of the Ras-related small GTPase, Rap1 as it stimulates intrinsic GTPase activity of Rap1, (Rubinfeld *et al.*, 1999). Rap1 is the Ras family small GTPase closest to Ras (Bos, *et al.,* 1998; For review Bos *et al*., 2001) and its activation can be regulated by specific GEFs which catalyze the conversion of Rap1 from GDP- to GTP-bound forms and by GAPs which accelerate the hydrolysis of bound GTP to GDP (Bos *et al*., 1997). Many proteins with apparent Rap1 GEF activity have been isolated including Crk SH3-domain-binding guanine-nucleotide releasing factor (C3G), exchange protein directly activated by cAMP (Epac1), CD-GEFs, Nsp2 and PDZ-GEFs (Gotoh *et al*., 1995; Kawasaki *et al.,* 1998; de Rooij *et al.,* 1998). On the other hand, at least two distinct proteins have been shown to exhibit Rap1-specific GAP activity *in vitro*, namely Rap1GAP (Rubinfeld *et al.,* 1991) and SPA-1 (Kurachi *et al.,* 1997). In mammals, Rap1GAP and Spa-1 exhibit quite distinct expression profiles with the former being selectively expressed in brain, pancreas, and kidney and the latter predominantly in lymphohematopoietic tissues (Kurachi *et al*., 1997).

### 1.6.1 RapGAP in mammalian cells

While some work has been done to understand RapGAP functions in mammalian cells, not much is known about its *in vivo* roles during development. Rap1GAP has two alternatively spliced isoforms in humans which differ in their N- terminal sequences. Studies done on both RapGAP isoforms form the clearest demonstration of

a GoLoco/Gα interaction being involved in GPCR-mediated modulation of a Rap1-mediated cellular signaling pathway (Meng *et al*., 1999, Rubinfeld *et al*., 1999).

In one study Meng and coworkers (1999) have found that Rap1GAP isoform 1 binds Gαz in its activated, GTP-loaded form (a departure from the normal GoLoco motif requirement for a GDP-bound Gα subunit). Gαz activation in PC12 cells, via agonist stimulation of α2A-adrenergic receptors, is able to recruit Rap1GAP1 to the plasma membrane (Meng *et al*., 2002) and this Gαz-mediated recruitment of Rap1GAP attenuates Rap1-mediated ERK activation and neurite development, suggesting that Gα-linked GPCR signaling can antagonize the Rap1/B-Raf/ERK signal transduction cascade in PC12 cells via RapGAP translocation to the plasma membrane. In another study, Mochizuki and coworkers (1999) have found that an N-terminally extended variant of Rap1GAP isoform 2 binds to activated Gαi1 and Gαi2 subunits (again a departure from the normal GoLoco motif requirement for a GDP-bound Gα subunit). Moreover activation of the Gαi-linked M2 muscarinic acetylcholine receptor was shown to recruit Rap1GAP2 to the plasma membrane and to lower cellular levels of GTP-loaded Rap1in human embryonic kidney 293T fibroblasts cells (Mochizuki *et al*., 1999). However, this reduction in activated Rap1 correlated with an increase in ERK activation. Differences between the findings of the two groups could be the result of differing Rap1GAP isoforms examined and/or differing operative Rap1-effector pathways in the cell lines used.

### 1.6.2 RapGAP in *Drosophila*

Biochemical and cell culture methods have provided a significant state of understanding of the cross talk between regulatory pathways (as described above), but these studies have not addressed the function of these molecules within the context of

the many tissues and developmental stages of the multicellular organism. Functional studies in model organisms such as *Drosophila* help better understand how the proteins work *in vivo* during animal development. A *Drosophila* RapGAP1 (isoform1 which does not have a GoLoco motif) encoding a 850-amino acid protein with a central region that displays substantial sequence similarity to human RapGAP has been reported (Chen *et al*., 1997). This protein can potently stimulate Rap1 GTPase activity *in vitro*. Unlike Rap1, which is ubiquitously expressed, RapGAP1 expression is highly restricted. RapGAP1 mRNA is localized in the pole plasm in an oskar-dependent manner in the early embryo and in late embryogenesis its expression is restricted to the PNS. RapGAP1 is also expressed at high levels in the developing photoreceptor cells and in the optic lobe (Chen *et al*., 1997). In the eye, *RapGAP* is expressed in specific groups of cells including those of the photoreceptor clusters posterior to the morphogenetic furrow, but not in the proliferating cells anterior to the morphogenetic furrow. Thus, different subpopulations of cells in the same tissue differ in terms of RapGAP expression. Chen and coworkers (1997) have also reported that *rapgap* mutants are viable and fertile and over-expression of RapGAP induces a rough eye phenotype that is exacerbated by reducing Rap1 gene dosage. In the eye, Rap1 is a regulator of morphogenesis that is distinct from functions attributed to Ras1-mediated signaling and is important for morphological aspects of differentiation in post-mitotic cells (Asha *et al.,* 1999).

In this thesis, chapter 5 deals with the identification of a novel GoLoco motif-containing isoform of RapGAP in *Drosophila* (RapGAP2). The Goloco motif in DRapGAP2 isoform is present N-terminus to the GAP domain. Findings from my work show that DRapGAP2 is heavily expressed in the *Drosophila* embryonic PNS and that RapGAP2 protein can assume asymmetric localization in dividing PNS precursor cells (See chapter 5). The results also show that RapGAP has important

functions in asymmetric cell division of neuronal precursor cells in the PNS and affects the md-bd lineage of neurons (See Chapter 5). In the following section (1.7) the development of the *Drosophila* embryonic PNS is described in detail.

## 1.7 *Drosophila* embryonic peripheral nervous system (PNS)

The embryonic PNS of *Drosophila* is a well-characterized model system for studying genes involved in basic processes of neurogenesis. Because of its simplicity and stereotyped pattern, each cell of the PNS can be individually identified and the phenotypic consequences of mutations can be studied in detail.

In *Drosophila*, sensory neurons in the embryonic PNS are two types: Type I (monodendritic) and Type II (multidentritic). Both these type of neurons innervate the the sensory organs to which they are related by lineage (Bodmer *et al*., 1989; Hartenstein *et al*., 1989). Type I sensory organs contain type I monodendritic sensory neurons and their supporting glial cells and are classified into two major classes: 1) mechano or chemosensory organs (es organs) that have external sensory structures in the cuticle such as bristles, campaniform and basiconical sensilla and 2) chordotonal organs (ch organs) that are internally located stretch receptors (Fig. 1.7). In contrast to type I sensory organs, type II organs contain multidendritic sensory neurons (md neurons, Ghysen *et al*., 1989; Bodmer and Jan, 1987) and no supporting glial cells (with one exception of dorsal bidendritic- dbd neuron).

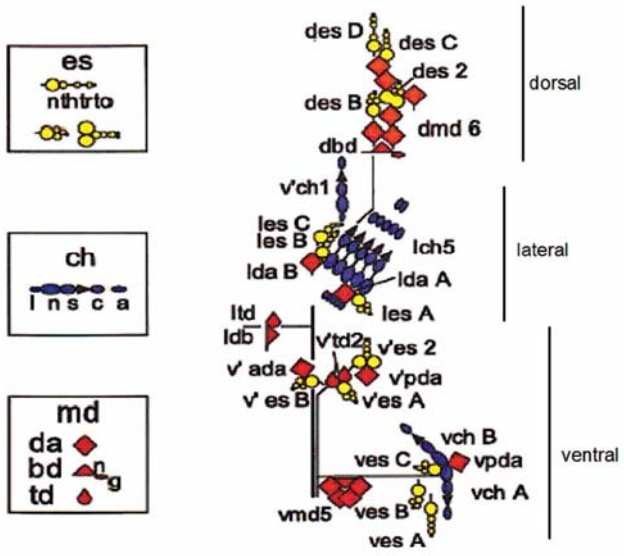


**Figure 1.7 Schematic representation of embryonic Drosophila PNS in each abdominal hemisegment are shown.**
In blue: chordotonal (ch) organs; in yellow: external sensory (es) organs; in red: multiple dendritic neurons (md). Nomenclature is according to Ghysen and Dambly-Chaudiere (1986), Bodmer and Jan (1987) and Bodmer *et al*. (1989); da, neuron with large dendritic arbors (diamond shape); td, tracheae; innervating neuron (drop shape); bd, bipolar dendrite neuron (triangle shape); n, neuron; g, glial cell; th, thecogen cell; tr, trichogen cell; to, tormogen cell; l, ligament cell; s, scolopale cell, c, cap cell; a, attachment cell; v,v' refer to two ventral clusters and l and d refer to lateral and dorsal clusters respectively. Anterior is always to the left and dorsal is up.
(Adapted with changes from Brewster et al., 2001)

md sensory neurons are thought to function as stretch or touch receptors and they have been subdivided into three different subclasses based on their morphology (Bodmer *et al*., 1987): 1) md-da neurons which are the most abundant subclass and have extensive subepidermal dendritic arborisations, 2) md-bd neurons which have bipolar dendrites and some of these contain associated glial cells and 3) md-td neurons which extend their dendrites along tracheal branches.

Despite having distinct neuronal activities and sensory structures, the mechanisms of early cell fate specification for these three types of sensory organs (es, ch and md) are quite similar. Each sensory organ seems to be generated by a stereotyped pattern of cell division of individual ectodermal precursor cells (SOPs). The program to develop SOPs is initiated by the activities of proneural genes which are limited to small patches of ectodermal cells, termed proneural clusters. The expression of proneural genes confers on each cell within the proneural cluster the potential to become a SOP cell. However, only one, or at most, a few cells within a cluster are selected to become SOP cells by a process of lateral inhibition involving the Notch/Delta pathway (reviewed in Artavanis-Tsakonas *et al*., 1995; Bray, 1998). This SOP cell(s) maintains the proneural gene expression by autoactivation. Proneural genes *achaete (ac)* and *scute (sc)* of the Achaete-Scute complex (AS-C) are required for the formation of es organs, whereas *atonal (ato)* directs the formation of ch organs. Proneural gene products form heterodimers with the bHLH protein Daughterless (Da) (Caudy *et al*., 1988), and this complex binds to E-box sequence found in promoter regions of many downstream target genes (Jarman *et al*., 1993).

### 1.7.1 PNS lineages

Cell lineage analyses have provided a detailed picture of almost all the lineages in the PNS. In type I monodendritic, es organ formation, the SOP (p1) divides

asymmetrically and gives rise to two secondary SOPs (pIIa and pIIb); pIIa then divides and gives rise to tormogen (socket cell) and trichogen (shaft cell) while pIIb further divides to give rise to the sensory neuron and thecogen (sheath cell). For the ch organ formation, the SOP (p1) division produces two second order precursors (pIIa and pIIb), pIIa divides further and gives rise to the ligament, neuron and scolopale cell lineage, and pIIb divdes to generate the cap and another (ectodermal) cell (For details see Brewster and Bodmer, 1995).

In type II multidendritic md organ formation, most SOPs are related in lineage to SOPs of type I organs and hence are derived from secondary precursors of either es or ch organ lineages and these lineages are referred to as md-es or md-ch lineages respectively. The cell fate choice between the sibling md and es neurons of the md-es lineages is controlled by asymmetric cell division of the secondary precursor which results in differential distribution of the product of *numb*, a cell fate determinant that prevents *Notch* activation and allows for md differentiation (Uemura *et al*., 1989; Rhyu *et al*., 1994; Guo *et al*., 1996). The polarity in this md-es secondary precursor that gives rise to the md and the es neuron depends on apical localization of the product of the *inscuteable* gene (Orgogozo *et al*., 2001).

The remaining type II SOPs which are not related to type I SOPs can either divide once or a few times to give rise to md neurons called solo-md neurons. A particular solo-md neuron, the dorsal bipolar (dbp/dbd or md-bd) neuron, is generated from an asymmetric division (in terms of size of daughter cells) of a dorsal SOP cell, which also generates an associated glial cell (Huang *et al*., 2000; Brewster and Bodmer, 1995). In mutants lacking both *AS-C* and *atonal* (genes coding for bHLH proteins known to establish SOP cell fate), two to three neurons of the solo-md type remain in the dorsal region of each abdominal hemisegment. The identity of these remaining neurons is controlled by another proneural gene called *absent solo-md neurons and*

*olfactory sensilla or amos* (Huang *et al*., 2000). However, the solo-md neurons that exist in *AS-C; ato* double mutants are eliminated in *daughterless (da)* mutants. Since Da protein physically interacts with AS-C and Atonal, this observation implies that the bHLH protein amos may also directly interact with Da to specify the solo-md neuronal cell identity (Huang *et al*., 2000).

### 1.7.2 The dbd lineage in the embryonic PNS

The SOP cell of the dbd lineage is identified at the beginning of stage 12 as a large cell, weakly expressing POU domain genes *Pdm-1/2* in the anterior-dorsal region of abdominal segments. This cell divides asymmetrically (in terms of size of daughters) producing two unequal sized Pdm-1 positive cells, a larger one located basal to the smaller one. The larger cell expresses neuronal marker protein ELAV and differentiates as dbd neuron (DBDN), while the smaller one expresses glial cell marker REPO and becomes a dbd-associated glial cell (DBDG) (Brewster and Bodmer, 1995). No further cell division has been reported for the progenies.

Shortly after mitosis of the SOP cell in the dbd lineage, *Pdm-1/2* genes are temporally downregulated in the presumptive glial cell and this coincides with *glial cell missing (gcm)* transcription being initiated. Upon establishment of high levels of *gcm* during embryonic stage 12, the *Pdm-1/2* expression is reinitiated in this glial cell. *gcm* then disappears rapidly and subsequently *Pdm-1/2* expression is also downregulated in DBDG (Fig. 1.8), resulting in expression of *Pdm-1/2* specifically to the DBDN at stage 16 (Dick *et. al*., 1991; Lloyd *et al*., 1991).

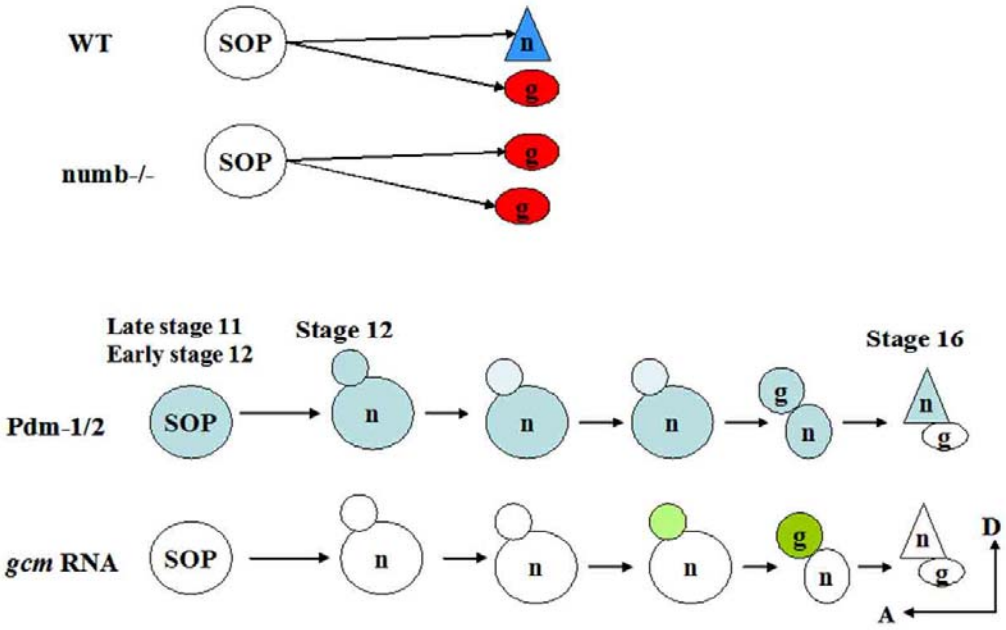


**Figure 1.8: Diagramatic representation of the dbd lineage in Drosophila embryonic peripheral nervous system.**

A) The precursor SOP cell divides and produces one dbd neuron and another glial cell in the wt embryo. In *numb* mutants there is no dbd neuron formed and instead two glial cells are formed indicating cell fate change of dbd neuron to glia. In wt, Numb segregates with the dbd neuron where it can block Notch signaling and allow neuronal fate specification. B) Summary of the expression dynamics of gcm mRNA (green) and Pdm-1/2 protein (blue) in the dbd lineage (based on Brewster et al., 2001 and Umesano et al., 2002). g, glial cell; n, neuron. Pdm-1/2 is initially detected in the SOP cell at stage 11. After SOP division, the smaller daughter cell located apicodorsally to the larger daughter cell differentiates as glia. Pdm-1/2 are down-regulated in the presumptive glial cell prior to the onset of gcm expression. The expression of gcm is initiated in the smaller daughter cell where Pdm-1/2 expression is low. After gcm becomes highly activated, Pdm-1/2 is re-expressed in the glial daughter cell. At stage 16, Pdm-1/2 expression is again restricted to the dbd neuron whereas gcm expression is no longer expressed in the glia cell at this stage. Dorsal is up.

Numb and Notch are also important for cell fate specification in the dbd lineage. Notch signaling positively regulates glial cell differentiation in this lineage (Umesono *et al*., 2002) while Numb is required in the dbd neurons to block Notch signaling and to promote neuronal fate (Uemura *et al.*, 1989; Rhyu *et al*., 1994). In *numb* mutants, a normal number of es or ch SOPs are formed, but the second order precursor cells give rise mainly to support cells instead of neurons and their glial-like sibling cells. Many md neurons are also missing in *numb* mutants (Uemura *et al*., 1989; Rhyu *et al.*, 1994).

# CHAPTER 2 : Materials and Methods

All chemicals and reagents were obtained from BDH Laboratory supplies (UK) and Sigma Chemical Company (USA) unless otherwise stated. Restriction enzymes and DNA modifying enzymes were purchased from New England Biolabs, USA

## 2.1 Molecular Biology

### 2.1.1 Recombinant DNA methods

General recombinant DNA methods were performed essentially as previously described (Sambrook *et al*). Polymerase Chain Reaction (PCR) was done with Taq DNA polymerase. Restriction enzyme digestions were performed using appropriate buffers supplied by the manufacturers. Blunt ending of DNA fragments was carried out using Klenow DNA polymerase (large fragment). Dephosphorylation of DNA fragment was done using calf intestinal phosphatase (CIP). T4 DNA ligase was used for ligation of DNA fragments. Double-stranded DNA sequencing was performed with automatic PCR-based Big-Dye sequencing method.

### 2.1.2 Strains and growth conditions

The *E. coli* strain DH5α (GIBCO BRL, USA) was used throughout this study for all cloning procedures. *E. coli* cells were either cultured in LB broth (1% bacto-tryptone, 0.5% bacto-yeast extract. 1% NaCl pH 7.0) or maintained or LB agar plates (LB containing 1.5% bacto-agar) at 37$^{o}$C. When recombinant plasmid-containing cells were cultured, the media was supplemented with 100µl/ml of Ampicillin.

### 2.1.3 Cloning strategies and constructs used in this study

In most cases, when the cDNA molecules were obtained by PCR amplification, they were first cloned into cloning vector pBlueScript (pBKS from Stratagene, USA), before being cloned into other vector such as expression vectors and transgenic vectors. A brief summary of PCR cloning is as follows:

The PCR product was first separated on an appropriate agarose gel. The product was then recovered from the agarose gel using Qiaquick gel extraction kit according to the manufacturer's instructions (Qiagen, Germany). The DNA was then dissolved in 26µl elution buffer. The PCR product was then digested with required enzymes (most of the contructs made in this study had EcoRI and Xho I sited engineered in the PCR products). At the same time the vector (initially pBS and later the required vector) was cut with the same enzymes and treated with Calf intestinal phosphatase. The vector was recovered after CIP treatment using Qiaquick gel extraction kit. Ligation of the insert with vector was set along with ligase buffer and ligase enzyme. This reaction was done overnight at 16$^{o}$C. Transformation of the ligation mixture was then done using heat shock transformation or electroporation transformation method.

#### 2.1.3.1 m-LGN constructs

The generation of full length *Pins*-related *LGN* sequence from mouse, *m-LGN* (or *m-Pins*) cDNA (accession number AY081187), was initially based on a partial EST sequence (AA543923; IMAGE: 949074) and is described elsewhere (Yu *et al*., 2003). Another EST (BC021308; IMAGE: 5007832) encoding the full length mouse LGN protein homolog is also found in the database. FLAG-tagged versions of full length, N-terminal (aa1-384) and C-terminal (aa385-650) mouse LGN were generated by cloning into the *Bam*HI / *Xho*I sites of pXJ40 (Manser *et al*., 1997) vector and expressing them under CMV promoter. The His-G$\alpha_{i3}$ and His-G$\alpha$o fusion constructs (in pQE60) were a

kind gift from Chen Canhe (Chen *et al*., 1997, 2001). The mouse $G\alpha_o$ transfection construct was kindly provided by Graeme Milligan (Hoffmann *et al*., 2001).

**List of constructs for mLGN work**

| Construct name | Use | Reference |
|---|---|---|
| pXJ40-FLAGmLGN-FL (*EcoR1-Not1*) | Transient transfection in mammalian cells | This study |
| pXJ40-FLAGmLGN-N term (aa 1-384) (*BamH1- Xho1*) | Transient transfection in mammalian cells | This study |
| pXJ40-FLAGmLGN-C term (aa 385 – 650) (*BamH1 – Xho1*) | Transient transfection in mammalian cells | This study |
| pXJ40-FLAGmLGN-N term 1-3 TPR (*BamH1-Xho1*) | Transient transfection in mammalian cells | This study |
| pQE60-His-Gαi | His-tagged fusion protein used in GDI assay | Chen *et al*., 1997, 2001 |
| pQE-60-His-Gαo | His-tagged fusion protein used in GDI assay | Chen *et al*., 1997, 2001 |
| pCMV-Gαo | Transient transfection in mammalian cells | Hoffamnn *et al*., 2001 |
| pCMV-Gαi2 | Transient transfection in mammalian cells | Chen *et al*., 1997 |
| pCMV-Gαi3 | Transient transfectrion in mammalian cells | Chen *et al*., 1997 |
| pGEX-Cterm mLGN (aa478-672) | GST-tagged fusion protein for raising antibody and for GDI assay | Yu *et al*., 2003 |

### 2.1.3.2 LGN and AGS3 constructs

Initial database searches using full length protein sequences of mouse LGN and fly Pins identified a partially sequenced EST clone, fj65e03.x1, as a LGN-related clone. This clone was then purchased from RZPD (RZPD Deutsches Ressourcenzentrum fur Genomforschung, Gmbh) and fully sequenced (genbank accession number: AY619722). The full length *LGN* cDNA contains 2574 nucleotides. The longest ORF encoding LGN protein is from nt 274 – nt 2217. The *Eco*RI – *Xho*I cDNA fragment containing this ORF was cloned in pBluescript II KS (Stratgene, USA). DNA sequencing was performed by using an automated sequencer with the ABI prism BigDye Termination, Cycle sequencing Ready Reaction Kit (Perkin Elmer, USA).

The RZPD clone ID: MPMGp609B0724Q8 was ordered based on high homology to rat AGS3 and sequenced completely and found to encode partial sequence for AGS3

of 1628bp. This partial sequence was digested from the RZPD clone and recloned in pBKS vector in *BamHI* and *SmaI* site. Based on this sequence 3' RACE was performed on total RNA from 6 somites stages fish embryos and the resulting fragment of 300bp was sequenced and found to contain *AGS3* sequence. This fragment was ligated in the the 1628bp partial clone and resulting 1928bp fragment was cloned in *EcoR1* and *Spe1* site of pBKS resulting in FL AGS3 of 2.1 kbp. This clone encoded full length *AGS3* sequence and the sequence was deposited to genebank database (accession number: AY619723). The 3' RACE was performed as per manufacturer's instructions using First Choice RLM-RACE kit (catalogue number #1700, Ambion Inc., USA).

For the RT-PCR amplification to study RNA expression pattern of Lgn, RKZF17and RKZF5 primers were used. For the RT-PCR amplification to study RNA expression pattern of Ags3, RKZF18 and RKZF21 primers were used.

**List of constructs for zebrafish work**

| Construct name | Use | Reference |
|---|---|---|
| pBKS-*LGN*-FL (*EcoR1-Xho1*) | For making antisense probe, linearise construct with EcoR1 and use T3 polymerase | Unpublished, This study |
| pXJ40-*LGN*-FL (*BamH1- Xho1*) | For making in vitro translated protein and transient transfection in mammalian cultured cells under CMV promoter | Unpublished, This study |
| pBSK-*AGS3*-FL (*EcoR1-Spe1*) | For making antisense probe, linearise construct with EcoR1 and use T7 polymerase | Unpublished, This study |
| pXJ40-AGS3-FL (*BamH1-Kpn1*) | For making in vitro translated protein and transient transfection in mammalian cultured cells under CMV promoter | Unpublished, This study |
| *Islet-2* | For making antisense probe | Appel *et al*., 1995 |
| *twist* | For making antisense probe | Yan *et al*., 1995 |
| *patched-1* | For making antisense probe | S. Roy |
| Construct name | Use | Reference |
| *Shh* | For making antisense probe, linearise with EcoR1 and use T7 polymerase | I. Sleptsova-Freidrich |
| *PKA* | For making RNA, linearise with *Xba1* and use SP6 polymerase | Hammerschmidt *et al*., 1996 |
| *PKI* | For making RNA, linearise with *BamH1* and use SP6 polymerase | Hammerschmidt *et al*., 1996 |
| *Shh* | For making RNA, linearise with *BamH1* | Hammerschmidt *et al*., 1998 |

| | | |
|---|---|---|
| | and use SP6 polymerase | |
| Pertussis toxin (pSP64T-*PT*) | For making RNA, linearise with EcoR1 and use SP6 polymerase | Hammerschmidt *et al*., 1998 |
| pGEX4T-1-*LGN(BamH1-Not1)*(aa 468- 647) | For making GST-tagged fusion protein used in GDI assay | Unpublished, This study |
| pGEX4T-1-*AGS3(BamH1-Not1)*(aa 450– 634) | For making GST-tagged fusion protein used in GDI assay | Unpublished, This study |
| pGEX*Gαi* | For making GST-tagged fusion protein used in GDI assay and binding studies | Chen *et al.,* 2001 |
| pGEX*Gα0* | For making GST-tagged fusion protein used in GDI assay and binding studies | Chen *et al*., 2001 |

#### 2.1.3.3 Rap1GAP constructs

The EST encoding the DRapGAP2 isoform was ordered from Research genetics (Clone ID: RE68074) which encodes full length DRapGAP2. This clone is 2.998kb and encodes the DRapGAP2 of 877 amino acids. This clone was fully sequenced and used for subcloning.

**List of constructs for RapGAP work**

| Construct name | Use | Reference |
|---|---|---|
| pBKS-*amos* | For making *amos* anti-sense probe | Huang *et al*., 2000 |
| pBKS-*DRapGAP1* | For making pUAST-RapGAP | Hariharan IK |
| His-*Rap1GAPII* (aa640-aa870) | For making antibody | R.Kaushik and F. Yu ; This study |
| MBPGαi (FL-*DGαi* in pMal-c2x) | For GDI assay | F. Yu; This work |
| pGEX4T-*DRapGAP2*(aa21-aa116) | For GDI assay | F. Yu ; This work |
| pGEX4T-*Pins(*C-term) | For GDI assay | Yu *et al*., 2002 |
| pGEX4T-*Loco* (C-term) | For GDI assay | F. Yu ; This work |

### 2.1.4 Transformation of *E. coli* cells

#### 2.1.4.1 Preparation of competent cell for heat shock transformation

400ml of LB was inoculated with 10ml DH5α culture (that was grown overnight). The cells were shaken vigorously at 37°C until the $OD_{600}$ was about 0.5 (approximately 2 hours). The cells were then harvested by centrifugation in 50ml falcon tubes at 4$^{o}$C and spinning at 3,500 rpm for 5 minutes. The cell pellet was then

resuspended in 20ml of ice-cold Buffer A (10 mM MOPS, 10 mM RbCl, pH7.0) and centrifuged as before. The cell pellet was then gently resuspended in 20ml of Buffer B (100 mM MOPS, 50 mM $CaCl_2$, 10 mM RbCl, pH 6.5) by inverting each tube. The cells were chilled on ice for 15 minutes and the pellet was resuspended in 5ml of ice-cold Buffer B containing 10% volume of glycerol. These cells were then snap-frozen in aliquots of 200µl and stored at –80°C.

#### 2.1.4.2 Heat shock transformation of E. coli

The competent cells were thawed on ice, and 10 µl of the ligation reaction mix was added and the cells kept on ice for 30-45 minutes. The cells were then heat shocked at 42 $^{o}$C for 60 seconds in a water bath. And then chilled on ice for 1 minute. The cells were then recovered in 1ml of LB lacking antibiotic at 37$^{o}$C for 1 hour. They were then briefly spun and resuspended in 100µl of LB. The cells were then spread on LB agar plate containing the appropriate antibiotic.

#### 2.1.4.3 Preparation of competent cells for electroporation

A liter of LB was inoculated with 10 ml DH5α culture that was grown overnight. The cells were shaken vigorously at 37°C until the $OD_{600}$ reached about 0.9-1 (about 4 hours). The cells were chilled on ice for 30 minutes, and centrifuged in a cold SS34 rotor for 15 minutes at 3000 rpm at 4°C. The supernatant was then removed and the pellet resuspended in 1:l cold deionised water. This was followed by another round of centrifugation as was done previously and the pellet was resuspended in 500ml of cold water and centrifuged again. The supernatant was then removed and the pellet resuspended in 20-30 ml of cold 10% glycerol. Another round of centrifugation followed this step. The supernatant was then removed and the pellet was resuspended in 2-3 ml of cold 10% glycerol. Aliquots of 50µl were made and snap-freezed and stored at –80°C.

#### 2.1.4.4 Electroporation transformation of *E. coli*

The electrocompetent cells were allowed to thaw on ice. 1-2µl of ligation reaction was added to the cells and mixed gently. The mixture was then kept on ice for 1 minute and then transfered to a cold, 0.2 cm electroporation cuvette. The Gene Pulser Apparatus (Biorad) was set to 25µF and 2.5 kV., and the Pulse Controller set to 200 Ω. The cell suspension was knocked to the bottom of a cuvette and a pulse applied with a time constant of 4 to 5 msec and field strength of 12.5 kV/cm. 1 ml of LB was added to the cells immediately after electroporation and this was followed by transfer of the suspension to a 1.5 ml eppendorf tube. The cells were then incubated at 37°C for 1 hr, with occasional shaking and plated on selective medium.

### 2.1.5 Plasmid DNA preparation

#### 2.1.5.1 Plasmid Miniprep

3ml LB culture was set up and the cells were shaken vigorously for 8-12 hours at 37°C. The cells were then collected in 1.5 ml eppendorf tubes and spun at maximum speed (14,000 rpm) in microfuge for 30 sec. The cells were resuspended in 350 µl of STET buffer (8% Sucrose. 50mM Tris pH 8.0, 50mM EDTA, 0.5% triton X-100) and boiled for 2-4 minutes on a heat block. This is followed by centrifugation of the cell lysate at 14,000 rpm for 10 minutes. The pellet was then removed with a sterile toothpick and the supernatant was retained. An equal volume of isopropanol (350 µl) was added to each tube prior to mixing by vortexing. Each tube was then centrifuged at 14,000 rpm for 5 minutes at room temperature. The supernatant was then discarded and the pellet air-dried. The DNA pellet was then dissolved in 50µl of TE-RNAse and used for restriction enzyme digestion or double-stranded DNA sequencing.

Alternatively, plasmid minipreps of bacterial cultures (1-3ml) were also carried out using the QIAprep Miniprep kit from QIAGEN according to manufacturer's instructions. This system is based on alkaline lysis. DNA purity with this method is higher than that in STET boiling method, however, STET boiling method is more rapidly manipulated.

#### 2.1.5.2 Plasmid Midi/Maxiprep

Plasmid midi/maxipreps of bacterial cultures (500 ml) were performed with the Qiagen Plasmid Midi/ Maxi Kit using Qiagen-tip 100/500 resin columns. These plasmid purifications that are based on alkaline lysis procedure were carried out according to the manufacturer's protocol.

### 2.1.6 PCR reactions and Primers used in this study

PCR was performed using a reaction mixture containing 1µl of template DNA (50ng), 1µl of thr N-terminal primer (100ng/µl), 1µl of the C-terminal primer (100ng/µl), 10ml of dNTPs (2.5mM each), 10 µl of PCR buffer, 76 µl of double distilled water and 1 µl of Taq polymerase enzyme mix. The reaction cycles carried out using a thermocycler (Perkin Elmer) were 25 cycles of 94$^{o}$C for 30s, 60$^{o}$C for 30s and 72$^{o}$C for 1 min/1kb of DNA. The DNA bands required were isolated on standard DNA gels.

**List of primers used in this study:**

| Construct name | Primer name | Sequences (read in 5'-3' direction) |
|---|---|---|
| mLGN-FL (for PCR) | MPF1 | CGCGGATCCATGAGGGAAGACCATTCCTTTCAT |
| | MPB1 | CCGGAGCTCACCAAGAACCATCTGCAGGTCTTGA |
| mLGN-Nterm (for PCR) | MPF1 | Same as above |
| | TPR7 | CCGCTCGAGCATCTGCAGGTCTGAGAGGTT |
| mLGN-Cterm (for PCR) | MPF2 | CGCGGATCCATGGTTCTTGGTCTGAGCTACAGC |
| | MPB2 | CCGCTCGAGTATTTTCCCGAATGCTTAAATTC |
| MDCK 5'RACE | MpsRACE1 | AAGCTGTCTGACATTGACCTCCTTTCATTA |

| | | |
|---|---|---|
| fragment I (for PCR) | MpsRACE2 | GGCGTAGTCATGCAAGTAGAAGTAAGCATT |
| MDCK 5' RACE fragment II (for PCR) | MpsRACE3 | ATTGCCGGCTGGCTTTAGCTTCCCCAAGTTG |
| | MpsRACE4 | AAGCTGTCTGACATTGACCTCCTTTCATTA |
| LGN FL (for PCR) | RKZF31 | CCACACACACAGGTTTTCCTGCAGGAATCCCCT |
| | RKZF30 | TCGGATCCGGCCAGCAAGCGCCTACACTCCAGG |
| AGS3 FL (for 5'RACE) | 5'RACE | CTCCAGAAGGCGGTCCCCGG |
| AGS3 FL (For PCR) | RKZF20 | CTCCAGAAGGCGGTCCCCGGGGCCCCGACGGTTC |
| | RKZF21 | ACCGTCGGGGCCCCGGGGACCGCCTTCT |
| LGN-GST fusion (for PCR) | RKZF34 | CGCGGATCCATCCTGCAGGATACCAGCAACA |
| | RKZF35 | ATAAGAATGCGGCCGCCAGGAGGGAAGCGTGACTCTCT |
| AGS3-GST fusion (forPCR) | RKZF32 | CGCGGATCCCCGTCAGATGAAGACTGCTTCT |
| | RKZF33 | ATAAGAATGCGGCCGCGACTCCTGCTGGTCCTCCGGGA |
| DRapGAP2 mutant checking (for PCR of SFP3) | RK29 | CATGTAGCGTTTGCGTGCCACCAATGTGTAGGATTCCTT |
| | RK30 | CAAATATTGATAATGCCAATGGCTTGATAAGGTCGGCTCC |
| Construct name | Primer name | Sequences (read in 5'-3' direction) |
| DRapGAP2mutant checking (for PCR of SFP4) | RK31 | CACAGAGAGCAAGTCATGTGTGAACAGACGCTGAG |
| | RK32 | CGCGCACCGTGTGGGTGTCAAAGTGCAGCTGAAATGCG |
| DRapGAP2 mutant checking (for PCR of SFP2) | RK33 | TTCGATGCATGAAGAGATTGCGTGCTCGC |
| | RK34 | GGGCCGATGACCAACGTTGGACAATTGCCA |
| DRapGAP2 mutant checking (for PCR SFP1) | RK17 | ATGAAATATACGAATACACACAAGGAA |
| | RK18 | GTGCTGCAGCCCACCGTTGTGCGGATGGCC |
| AGS3 sequencing | RKZF13 | CCGGAATTCCTGGAGGCAGAGCGTCTGTGTAAG |
| | RKZF14 | GAGGGCGAGAGGCTGTGTAAAGCGG |
| | RKZF18 | GGGTGGGCGAGGGCCGGGCCTG |
| | RKZF1 | GGATCCATGGAGGCGTCGTGTCTGGA |
| | RKZF2 | GTAGCTTGGATCCTCTAGAGCGGCCG |
| | RKZF3 | CTCAAGAGCAGGGAGACAAGGT |
| LGN sequencing | RKZF4 | GCTGGGTACCGGGCCCCCCCTCGAG |
| | RKZF5 | GATCATCTGTCTGTTGTTGGTGCTGC |
| | RKZF6 | GATTGTCTGCTGCCAGAGACAT |
| | RKZF7 | GCCAGGGAACTGGGTGACAAGG |
| | RKZF8 | TCATCCATCCGGTTGCTCTGAAA |
| | RKZF12 | GGAGGCGTCCTGTTTGGATCTGGCT |
| | RKZF15 | GGCCTGCTACAGTCTGGGTAACACA |
| | RKZF16 | CGCCAATGGTCAGAAGTGGACCAG |
| | RKZF17 | GCTGGCGAATGCTCAGGGCAGGAG |

## 2.2 Cell culture and animal biology

### 2.2.1 Mammalian cell culture and transfection

The human amniotic-derived cell line WISH (ATCC CCL 25), monkey kidney COS-1 and normal rat kidney NRK cells were grown in DMEM medium supplemented with 2mM Glutamine, 5% FCS, 100 U/ml penicillin and 10 μg/ml streptomycin. The Mouse neuronal-derived PC12 cell line was grown as described by Greene and Tischler (1976). For subculturing the cells, the monolayer was rinsed with PBS. This rinsing step removes any residual serum from the monolayer that could inactivate the trypsin. About 3ml was used 25- cm2 flasks and 5ml for 75-cm2 flasks. Remove and discard the solution. Repeat the washing step, this time using the dissociation solution (trypsin). For more fastidious cell lines, the flask was placed in a 37°C incubator to facilitate the enzymatic reaction. The cells were also observed microscopically to monitor progress and prevent over-exposure of the cells to the enzyme activity. Once the cells were detached, the desired amount of growth medium was added to the flask, creating a cell suspension. It is not unusual for a small amount of cells to remain attached to the flask or substrate. However, more vigorous pipetting may be necessary to break up cell clumps. Using the cell suspension, determine the appropriate inoculum and seeding density for subculturing the particular cell line was determined by counting the cells using the hemacytometer device using trypan blue (MT 25-900-CI). Simply remove a small amount of the cell suspension, such as 500ul and mixed with an equal amount of trypanblue. The concentration of tryptan blue used was 0.025% w/v. The number of cells/ml in the suspension and calculate the volume of suspension required to seed the desired density for each subculture. Aliquots were dispensed into clean, sterile, labeled culture vessels with the desired amount of culture

medium and culture vessles were returned to a 37°C incubator with a carbon dioxide level of 5%.

For immunofluorescence microscopy, coverslips were coated with 20μg/ml laminin (Upstate Biotechnology) for 1 hour at 37°C prior to seeding the cells. MDCK cells (strain II), a polarized epithelial cell line derived from dog kidney, were cultured on polycarbonate filters (Transwell Clear, Costar, Cambridge, MA) in DMEM medium supplemented with 10% fetal bovine serum and 1% penicillin (100 U/ml) and 10 μg/ml streptomycin. The cells were plated at 2.5 X $10^6$ cells/ filter for 2 days before fixing and processing for immunofluorescence.

For transient transfection, Lipofectamine from Gibco-BRL (Life Technologies) was used according to manufacturer's instructions. Cells were seeded at ~ 1-3 X $10^5$ per 35mm tissue culture plates in 2ml of appropriate medium and kept at 37$^o$C in a $CO_2$ incubator until a confluency of 50-80% was reached, typically about 18-24 hours. For each transfection, 1-2μg of DNA was diluted in 100μl OptiMEM and mixed with solution B containing 30μl of Lipofectamine in 100μl OptiMEM. The mixture was incubated at room temperature for 45 minutes to form a DNA-liposome complex. 0.8ml of OptiMEM was then added to the complex and the diluted complex was overlayed on the rinsed cells. The cells were incubated with the complex for 6 hours at 37$^o$C in a $CO_2$ incubator following which fresh serum-containing medium was added to the cells. The cells were typically recovered for fixing and further analysis after about 20 hours. Typically depending on the cell line used, about 20-40 percent of the cells showed expression of the transfected plasmid.

### 2.2.2 Fish Biology

Wild type (*Danio rerio*) and mutant zebrafish embryos were obtained from the fish facility of the Institute of Molecular and Cell Biology and were staged according to

Kimmel *et al*. (1995) in hours post fertilization (hpf). For analysis at 36 and 48 hpf, embryos were treated with phenyl-2- thiourea (Westerfield, 1995) at 18hpf to prevent formation of melanin. Treated embryos were then incubated at 28.5 degrees Celsius, raised to the desired stage, fixed and processed for whole mount in-situ hybridization or immunohistochemistry.

## 2.2.3 Fly genetics

### 2.2.3.1 Basic fly keeping

The Canton S and yw flies were used as controls. The life cycle of the fly is 10 days at 25 $^0$C and 21 days at18 $^0$C. Fly stocks were turned over every 14-17 days if they were being reared at room temperature, and every 30 days if they were being reared at 18 $^0$C. Females for crosses must be virgins. Females remain virgins for ~6 hrs at 25$^o$C, and for ~18 hrs at 18$^o$C.

### 2.2.3.2 Mobilisation of EP element

EP(2)BG02277 carrying a P element derivative that contains the *mini-white* gene inserted about 3Kbp upstream of the first exon of *D-RapGAP* at cytological position 28A6. For generation of lines containing mutation in DRapGAP : EP(2) BG02277 was crossed with double balancer fly stock containing [Sp/CyO; Delta2-3, sb/Tm6,Ubx] to obtain male flies with EP(2)BG02277/Cyo;delta 2-3,Sb/+ genotype. Single males with mosaic eyes(to indicate the jump) were then crossed to yw; Gla/CyO females in single vials. The flies that have lost EP and contain CyO were selected and sibling crosses were set up to select for reveratnats. The remobilised lines were then subjected to single fly PCR to select mutant lines. A total of 450 viable lines were screened for mobilised P element via single fly PCR using the primers detailed in section 2.1.4. In the WT, *Rapgap*$^{m21}$ (m21) homozygous and *BG02277* flies a 700 bp fragment (SFP1)

can be amplified using primers RK17 and RK18 and this fragment can not be amplified from genomic DNA from homozygous flies of *Rapgap*$^{vh183}$ (VH183) homozygous and *Rapgap*$^{vh329}$ (VH329) homozygous genotype. The 700 bp fragment (SFP2) can be amplified from *WT*, *BG02277* using primers RK33/34. Using another set of PCR primers (RK 31/32), a fragment of 500bp (SFP4) can be amplified from genomic DNA of *Rapgap*$^{vh18\ 3}$ and *Rapgap*$^{vh329}$ but not from genomic DNA of *Rapgap*$^{m21}$. However, genomic DNA from the *WT, BG02277*, *Rapgap*$^{m21}$; *Rapgap*$^{vh183}$ and *Rapgap*$^{vh329}$flies can be used for amplifying a 650bp fragment (SFP3) using primers RK29/RK30. The primer sequences are detailed in 2.1.6

#### 2.2.3.3 Single Fly PCR

A single fly was placed in a 0.5 ml tube and mashed for 5 - 10 seconds with a pipette tip containing 50µl of buffer (10 mM Tris-Cl pH 8.2, 1 mM EDTA, 25 mM NaCl, and 200 ug/ml Proteinase K. The remaining buffer was then expelled into the tube and incubated at 25-37$^{o}$C for 20-30 minutes. This incubation was then followed by heating the tube to 95$^{o}$C for 1-2 minutes, which inactivates the Proteinase K. 0.5µl of the DNA from a single fly was then used for one PCR reaction.

**List of Fly stocks used in this study**

| Fly stocks | Source | Reference |
|---|---|---|
| *Rapgap*$^{m21}$ homozygous viable mutation in the 2$^{nd}$ chromosome | I.S. Hariharan | Chen et. al., 1997 |
| *Rapgap*$^{vh183}$ homozygous viable mutation in the 2$^{nd}$ chromosome | R. Kaushik | Unpublished/this study |
| *Rapgap*$^{vh328}$ homozygous viable mutation in the 2$^{nd}$ chromosome | R. Kaushik | Unpublished/this study |
| *Rapgap*$^{vh29}$ homozygous viable mutation in the 2$^{nd}$ chromosome | R. Kaushik | Unpublished/this study |
| *Rapgap*$^{vh187}$ homozygous viable mutation in the 2$^{nd}$ chromosome | R. Kaushik | Unpublished/this study |
| pGMR-GAL4 on the 2nd chromosome | M. Freeman | Hay *et al*., 1997 |
| Scabarous GAL4; *Rapgap*$^{m21}$/CyO | R. Kaushik | Unpublished/This study |
| UAS-amos/Tm6 | T. Chien | Huang *et al*., 2002 |
| *Rapgap*$^{m21}$/CyO, UAS-amos/Tm6 | R. Kaushik | Unpublished/This study |

| | | |
|---|---|---|
| *Rap* mutant lethal | N. Brown | Knox and Brown 2002 |
| Rap-GFP homozygous | N. Brown | Knox and Brown 2002 |
| $G\alpha i^{LL8}$/Tm6 | F. Yu | Yu *et al*., 2003 |
| $Pins^{P89}$/Tm6 | F. Yu | Yu *et al*., 2001 |
| $Pins^{P62}$/Tm3 | F. Yu | Yu *et al*., 2001 |
| $Insc^{nem22}$/CyO | R. Kraut | Kraut et. al., 1996 |

## 2.3 Biochemistry

**Frequently used buffers and solutions**

| Buffer | Composition |
|---|---|
| 2x SDS gel-loading buffer | 100 mM Tris HCl pH 6.8, 200 mM dithiothreitol (DTT), 4% SDS, 0.2% bromophenol blue, 20% glycerol. DTT (1 M stock) added before use. |
| 10x Tris-glycine electrophoresis (PAGE) buffer, pH 8.3 | 30.2 g Tris, 188 g glycine, 50 ml 20% SDS, distilled water to 1000 ml. |
| Resolving Gels for Tris-glycine SDS-Polyacrylamide Gel Electrophoresis (PAGE) | Required amounts of 30% acrylamide mix and deionized water, ¼ vol. 1.5 M Tris (pH 8.8), 0.01 vol. 10% SDS, , 0.01 vol. 10% ammonium persulfate (APS), 0.0008 vol. TEMED. |
| Stacking gels for PAGE | 0.68 vol. $H_2O$ (deionised), 0.17 vol. 30% acrylamide, 0.125 vol. 1.0 M Tris (pH 6.8), 0.01 vol. 10% SDS, 0.01 vol. 10% APS, 0.001 vol. TEMED. |
| Western transfer buffer, pH 8.3 | 3.03 g Tris, 14.4 g glycine, 200 ml methanol, distilled water to 1000 ml (do not adjust pH). |
| Blocking solution | TBS, 3% skimmed milk powder, 0.05% Triton X-100. |
| Washing Buffer for Western Blotting (WB) | PBS, 0.1%Tween-20 |
| Blocking buffer for WB | PBS, 5% BSA, 0.5% Tween-20 |

### 2.3.1 Cell extract preparation

#### 2.3.1.1 Mammalian cell culture extract

Cells were washed twice with PBS and overlaid with 0.5ml of lysis buffer (20mM Tris-HCl, 150mM NaCl, 1mM EDTA,1mM EGTA,1% Tx-100, 2.5mM Sodium Pyrophosphate (optional), 1mM Sodiumorthovanadate (optional), Protease Inhibitors

(added just before use), 1mM PMSF). The cell scraper was then used to scrape cells from the plate and the cell lysate was sonicated for 15 seconds prior to centrifugation at top speed (14K) at 4 degrees for 30 minutes. The supernatant recovered at this stage was either used for Immunoprecipitation or quantified using a Bradford assay and stored at -20°C.

#### 2.3.1.2 Protein extract from zebrafish embryos

Embryos were obtained from cages and dechorionated manually under a microscope with a 21gauge needle. Dechorionated embryos were then transferred to glass petri-dishes containing ice-cold Opti-MEM and de-yolked. The embryonic tissue was then transferred to the 1.5ml Eppendorf tube washed with lysis buffer (20mM Tris-HCl, 150mM NaCl, 1mM EDTA,1mM EGTA,1% TritonX-100, 2.5mM Sodium Pyrophosphate (optional), 1mMSodiumorthovanadate (optional), Protease Inhibitors (added just before use), 1mM PMSF) and embryos were ground for about 3 minutes using a blue grinder. The extract was centrifuged at 14 K, 4 degrees for 30 minutes. The supernatant was recovered and protein quantified using a Bradford assay and stored at -20°C.

#### 2.3.1.3 Protein extract from *Drosophila* embryos

Embryos were obtained from cages and dechorionated for 5 minutes with 50% bleach and then rinsed 3X with PBT and then 2X with water. After the last wash, much of the water was removed leaving embryos at the bottom. Approximately, 5 times the bed volume of lysis buffer (20mM Tris-HCl, 150mM NaCl, 1mM EDTA,1mM EGTA,1% Tx-100, 2.5mM Sod Pyrophosphate (optional), 1mMSodiumorthovanadate (optional), Protease Inhibitors (added just before use), 1mM PMSF) The embryos were then ground using blue grinder for about 1 minute or so. Following which the extract is passed thru 21G needle with a 1ml syringe 10X and

the extract was centrifuged at top speed (14K) at 4 degrees for 30 minutes. The supernatant recovered at this stage was either used for Immunoprecipitation or quantified using a Bradford assay and stored at -20°C.

### 2.3.2 PAGE and western blotting of protein samples

100-200µg of protein extracts were mixed with equal volume of 2X SDS loading buffer and boiled for 6 minutes, after which the sample was loaded on the gel. Electrophoresis was carried out in a minigel apparatus (Biorad) at 50 V for 20 minutes and subsequently at 100 V for 1.5-2 hours. Transfer onto a Hybond C-extra nitrocellulose (Amersham) membrane was carried out in a Trans-Blot Electrophoretic transfer cell from Biorad. The transfer was performed at 100 V for 1.5 hr in a cold room. A magnetic stirrer was used to recirculate the transfer buffer.

### 2.3.3 Immunological detection of proteins

The membrane was blocked overnight at 4°C in blocking solution (5% non-fat milk powder in PBT). It was then incubated in primary antibody diluted in blocking solution for 3 hours at RT. This incubation was followed by 7 washes in PBT (PBS, 0.1% Triton) for 5-7 minutes per wash. The membrane was then incubated in secondary anti-mouse and anti-rabbit IgG antibodies coupled with HRP (Immuno Jackson), at a dilution of 1:2000 in blocking solution, for 1 hour. The membrane was then washed as before and the antibodies bound to the membrane were detected by chemiluminescence using the ECL system from Amersham.

### 2.3.4 Immunoprecipitation experiments

The total protein extract prepared as described above was used for co-IP. The extract was first pre-cleared with protein A/G beads for one hour followed by

incubation of pre- cleared extract with antibody for either 4 hours or overnight at 4$^{o}$C. The immune complex was then recovered by adding sepahrose conjugated protein A/G beads for 1 hour at 4$^{o}$C. The complex was then washed three times with ice-cold lysis buffer and subjected to western blotting using standard protocols described above. The blot was then probed with antibodies to see if two or more proteins were present in the same complex *in vivo.*

### 2.3.5 GST-fusion protein expression

A single clone was picked and inoculated in 2ml of culture media (LB + Amp) and allowed to grow overnight. 50ul of this culture was then inoculated into 1ml LB+ Ampicillin. The culture was grown till it reached an $OD_{600}$ of 0.6-0.8 (2-3 hours). IPTG was added to induce protein expression and the culture was grown for a further 3-4 hours at 37degree celcius. The entire culture was then spun down and resuspended in 250µl of 2XSDS buffer and boiled for 10 minutes.

### 2.3.6 Affinity purification of antibodies

Polyclonal anti-LGN antibodies were produced in rabbits by injecting a GST-fusion product containing 194 amino acids from the C-terminal domain of mouse LGN (aa478-672). The anti-LGN antibodies were affinity purified and used at a dilution rate of 1:100 for immunflourescence. Polyclonal anti-RapGAP antibodies were produced in rats by injecting a HIS-Tagged fusion protein containing C terminal of fly RapGAP (aa640-aa870). The polyclonal rat serum was used at a dilution of 1: 100 for immunofluorescence.

### 2.3.7 Protein binding and GDI assay

Direct binding between mouse LGN and LGN/AGS3 and various Gα subunits was assayed using His columns. Various $^{35}$S-labelled LGN protein products were generated using the TnT coupled transcription/translation kit from Promega and incubated with 1 μg His-$G\alpha_{i2/3/o}$ protein and His beads in 250 μl binding buffer (20 mM Tris 7.5, 70 mM NaCl, 1 mM DTT, 0.6 mM EDTA, 0.01% Triton X, 20 μM GDP) for 40 minutes at 25°C. The reaction mixtures were washed at room temperature and protein complexes were analyzed on acrylamide gels. Protein gels were dried under vacuum and autoradiographed.

In order to assay the GDI activity of mouse LGN, [$^{35}$S]GTPγ binding experiments were performed with some modification to the protocol described by De Vries *et al*., (2000). Reaction mixtures containing 50 nM His-$G\alpha_{i3/o}$-GDP, and 1 μM GST-LGN (aa385-672) or control GST were incubated in buffer A (50 mM Tris pH 8.0, 1 mM DTT, 1 mM EDTA, 10 mM $MgSO_4$). Experiments were started by adding 2 μM [$^{35}$S]GTPγ in a 50 μl reaction volume and incubated at 30°C for different time periods. The reactions were terminated by washes with ice-cold buffer before measuring by scintillation.

In order to assay the GDI activity of LGN and AGS3, [$^{35}$S]GTPγ binding experiments were performed with some modification to the protocol described by De Vries *et al*., (2000). Reaction mixtures containing 50 nM GST-$G\alpha_{i3/o}$-GDP, and 1 μM LGN (aa468-aa647), AGS3 (aa450-aa647) or control GST were incubated in buffer A (50 mM Tris pH 8.0, 1 mM DTT, 1 mM EDTA, 10 mM $MgSO_4$). Experiments were started by adding 2 μM [$^{35}$S]GTPγ in 50 μl reaction volume and incubated at 30°C for different time periods. The reactions were terminated by washes with ice-cold buffer

and filtering the reaction mixture through nitrocellulose membrane before measuring by scintillation.

In order to assay the GDI activity of *Drosophila* proteins, [$^{35}$S] GTPγ binding experiments were performed with some modification to the protocol described by De Vries *et al*., (2000). Reaction mixtures containing 50 nM MBP-Gαi -GDP, and 1 μM GST-DRapGAP (aa21-aa116), GST-Pins, GST-Loco or control GST were incubated in buffer A (50 mM Tris pH 8.0, 1 mM DTT, 1 mM EDTA, 10 mM $MgSO_4$). Experiments were started by adding 2 μM [$^{35}$S] GTPγ in 50 μl reaction volume and incubated at 30°C for different time periods. The reactions were terminated by washes with ice-cold buffer and filtering the reaction mixture through nitrocellulose membrane before measuring by scintillation.

### 2.3.8 *In-vitro* translational assay for morpholino specificity

For determining the specificity of morpholino probes on LGN translation *in vitro*, the full length *LGN* cDNA was cloned in pXJ40 vector (Manser *et al*., 1997) under the CMV promoter and $^{35}$S-labeled LGN protein products were generated using the TnT-coupled transcription/translation kit from Promega (Madison, WI; Cat.no. L1170) either in the presence of LGN-MO or in the presence of controls LGN-mismatch MO and FGF-MOs. The TNT products were then analyzed on 12% acrylamide gels, dried under vacuum and autoradiographed.

### 2.3.9 BrdU labeling and morpholino treatments

For BrdU labelling, Cells were transfected with various mouse LGN constructs (FL-FLAG, N-FLAG or C-FLAG). 36 hours after transfection, the cells were incubated for 60 minutes in 1 mM BrdU, fixed, and then stained with anti-FLAG (Affinity Bioreagents) and anti-BrdU (Boehringer Manheim) antibodies according to

manufacturer's instructions. Transfected cells positive for FLAG were scored for BrdU staining under confocal microscopy. Typically, about 100 cells were counted for each experiment. The experiments were repeated three times to obtain the percentage of FLAG-positive cells that are labelled with BrdU.

Morpholino treatment of cells was performed as described by Gene-Tools. Typically, morpholino phosphorodiamidate oligonucleotides (MOs) contain about 25 bps overlapping with the first AUG translational start site. They have high affinity for RNA, although they do not recruit RNAseH but exhibit high efficacy through non-classical antisense approach (Larson and Ekker, 2001; Summerton, 1999). Morpholino oligos can block translation of mRNA by steric blocking, preventing assembly of a functional ribosome complex. The delivery of morpholino to cells was performed as per manufacturer's protocol. Briefly, the special delivery solution was mixed with morpholino for 15 minutes at room temperature and then added to the cells for about 3 hours, following which the cells were allowed to recover for about 20 hours before being harvested for further analyses. Harvested cells were fixed and analyzed by FACSCAN using WinMDI3.5 software. A Becton and Dickinson FACSCAN machine was used to acquire and analyze 21,000 events (using Cellquest and Modfit). DNA analysis was by propidium iodide staining (50 μg/ml at 37°C for 30 minutes) or ethanol (80%, 12 hours at -20°C). The morpholino experiment was repeated three times and each time it was done in triplicates. Morpholino-treated cells were also used for immunoblotting and probed with affinity purified anti-LGN antibodies to determine the effect of morpholino on LGN protein levels. The band intensity was quantified using the Bio-Rad multianalyst version 1 software and Bio-Rad (model GS-700) imaging densitometer.

For morpholino studies in zebrafish, the morpholinos were solubilized at 1 mM stock concentration in Danieau's solution and they were constituted to 0.5 mM for

injection; 20 pl of the 0.5mM morpholino probe was injected into each embryo and approximately two hundred embryos at the one-cell stage were injected in each round.

**Morpholinos used in this study**

| Morpholino | Target/source | Sequence |
|---|---|---|
| *LGN-MO1* | -25 bps in the UTR of LGN/Unpublished, this study | 5'-TGACTTCAGTAACGTACAAACCTCC-3' |
| *LGN-MO2* | -99 bps in the UTR of LGN/Unpublished, this study | 5'GGGTCCAAACAAAAATCAATTACAT-3' |
| *LGN-MO* | targeting the translational start site (underlined) of *LGN/* Unpublished, this study | 5'-CCAGATCCAAACAGGACGCCTCCAT-3' |
| *LGN-mismatchMO* | control mismatch-morpholino based on LGN-MO, in which four mismatch bases (in italics)/ Unpublished, this study | 5'- CCAGATCCAAACAGGAC*T*C*A*T*T*C*G*T -3' |
| *fgf8*-MO | Furthauer, 2002 | 5'-GAGTCTCATGTTTATAGCCTCAGTA -3' |
| *fgf3-MO* | Furthauer, 2002 | 5'-CATTGTGGCATGGCGGGATGTCGGC-3' |
| mLGN-MO | targeting the translational start site (underlined) of *mLGN/* Kaushik et. al., 2003 | 5' GAATGGTCTTCCCTCATGCTTATCA-3' |
| mLGNmismatch-MO | control mismatch-morpholino designed based on mLGN-MO, in which four mismatch bases (in italics)Kaushik et. al., 2003 | 5' GAATGGTCTTCCCTCATG*A*TC*A*T*A*A-3' |

## 2.4 Immunohistoshemistry and microscopy

**Frequently used reagents and buffers for immunohistochemistry**

| Buffer | Composition |
|---|---|
| PBS (Phosphate Buffer Saline) | 130mM NaCl, 7mM $Na_2HPO_4$, 3mM $NaH_2PO_4$, pH 7.5 |
| PBT | PBS, 0.1% Triton X-100 unless otherwise specified |
| 20 % paraformaldehyde solution (PFS) | Add 20 g paraformaldehyde into 100 ml PBS, neutralise with 200 µl 10 M NaOH and dissolve at 65°C (keep for about 2 weeks at 4°C). |
| 4% paraformaldehyde fixative (PFF) | Mix 0.8 ml 20% PFS with 3.2 ml 0.1 M HEPES pH 7.4 or PBS. Prepare fresh fixative each time. |
| HRP staining solution | 1 ml 0.1 M Na acetate pH 6.0 (optional 2.5% $NiNH_4SO_4$), 50 µl DAB (5 mg/ml), 10 µl glucose (0.2 g/ml), 2 µl $NH_4Cl$ (0.2 g/ml), 1-2 µl glucose oxidase (2 mg/ml) |
| TO-Pro3 DNA dye | 1:5000-7000 (Molecular probes) |

## 2.4.1 Fixing and immunoflurescence

### 2.4.1.1 Fixing of embryos (*Drosophila*)

Embryos were first rinsed in PBT and dechorinated with 50% bleach/50% PBT for 2-3 minutes, and then washed in PBT. The embryos were then transferred to scintillation vials containing 5ml 4% PFF and 5ml heptane, and were fixed by shaking vigorously for 15 minutes. The lower fixative phase was then removed and 5ml methanol added. The vials were shaken vigorously for 30-60 seconds to devitellinise the embryos. The devitellinised embryos sank to the bottom. Embryos were then collected and washed in 3 changes of ethanol. Embryos in ethanol were stored at –20°C. Prior to immunostaining, the embryos were rehydrated 3 washes of PBT for 10 min/wash.

### 2.4.1.2 Fixing of embryos (zebrafish)

Embryos were washed in PBST (PBS + 0.1% Tween 20) and fixed overnight in 4% paraformaldehyde solution in cold room with gentle rocking. The embryos were then washed for 1-2 hours at room temperature in PBST and dechorionated manually. Embryos were then washed in PBST and then pre-hybridised overnight at 65°C and stored at -20°C. Prior to whole mount *in-situ* hybridisation the embryos were subjected to a further 2 to 3 hours of pre-hybridization.

### 2.4.1.3 Fixing of cultured cells

Cells were washed in PBS and fixed in either 3.7% paraformaldehyde for 20 minutes at room temperature or kept in chilled methanol for 10 minutes at 4 degrees. They were then permeablised with PBS containing 0.1% TritonX-100 for 5 minutes and blocked in 10% FBS for 1 hour at room temp. Fixed cells were incubated with primary antibody at $4^{o}$C overnight, washed with PBS and then treated with fluorescent

secondary antibody for 2 hours at room temperature. DNA was stained with TOPRO-3 dye from Molecular Probes. Coverslips were mounted with Vectashield (Vector Laboratories) and examined by confocal microscopy (BioRad, MRC1024).

#### 2.4.1.4 Immunoflurescence staining for cells and embryos

The fixed embryos or cells were rehydrated and blocked in PBT, 3% BSA or goat serum for at least 30 minutes. They were then incubated with primary antibody in PBT, 3% BSA or goat serum for 2 hr at RT or overnight at 4°C. In case of phalloidin staining, TRITC labeled phalloidin (Sigma) was added to the blocking solution or after blocking at 1:200 dilution in PBT for 2 hours at RT or Alexa-488 or 568 phalloidin (Molecular Probes) was used at 1:250 dilution in PBT at RT. Phalloidin was also added again with the secondary antibody. The tissue was washed thrice in PBT for 10 minutes/wash and incubated in secondary antibody (HRP (1:150), FITC labeled secondary antibody (1:150) or Cy3 labelled secondary (1:750) (Jackson Laboratory) or Alexa fluor secondary antibodies at light wavelengths 488, 543 and 633 ( Molecular Probes) in PBT, 3% BSA or goat serum for 2 hr at RT. The washing procedure was repeated after the secondary antibody incubation. In some cases the DNA staining dye TOPRO-3 was added at 1:5000 to 1:7000 dilution to the last wash. Fluorescently labelled samples were mounted in Vectashield (Vector Laboratories).

#### 2.4.1.5 Whole mount *in-situ* hybridisation

For whole mount in-situ hybridization on zebrafish embryos, the embryos were prehybrisidised for 2-3 hours and linearized sense or antisense digoxiginin labeled probes prepared as per manufacturer's directions (Roche, USA) were added at 65 degrees overnight. Following which the embryos were processed and stained as described in Oxtoby and Jowett (1993).

**List of antibodies used in this study :**

| Antibody | Dilution | Source/Reference | |
|---|---|---|---|
| mAb 22c10 | 1:3 | Developmental hybridoma | Zipursky, S.L., 1984 |
| mAb E7(anti B-tubulin) | 1:5 | Developmental Hybridoma | Chu, D.T.W., 1989 |
| Rabbit polyclonal anti-FLAG (PA1-984A) | 1: 100 | Affinity Bioreagents, USA | |
| mouse monoclonal anti-FLAG (M2) | 1:1000 | Sigma – Aldrich., USA | |
| Vti1α | 1: 100 | BD Transduction Laboratories | Advani RJ., 1998 |
| ZO-1 | 1: 100 | Zymed | |
| Gαi3/2/0 | 1: 100 | Upstate Biotechnology, USA | |
| TRITC-Phalloidin | 1: 1000 | Sigma | |
| Polyclonal anti-mLGN | 1: 50 | Yu F. and Kaushik R. | Kaushik R., et. al., 2003 |
| anti-Bazooka | 1: 500 | Fumio M. | |
| anti-Gai | 1: 100 | Yu. F | Yu et. al., 2003 |
| anti-Miranda (Monoclonal) | 1: 5 | Fumio M. | |
| anti-Insc | 1:25 | | Kraut et. al., 1996 |
| Polyclonal anti-RapGAP | 1:50 | Yu F and Kaushik R | Unpublished |
| Monoclonal anti-RapGAP | 1: 5 | Hariharan I. | Chen F., 1997 |
| anti – Revesed Polarity | 1: 100 | Technau G | Halter DA., 1995 |
| anti-Pdm-1/anti – dPOU19 | 1: 500 | Dick T | Yeo SL., *et al*., 1995 |
| anti – ZNP-1 | 1: 5 | Hybridoma bank | |
| anti- acetylated tubulin | 1: 1000 | Sigma Aldrich., USA | |
| anti - engrailed | 1: 5 | Hybridoma Bank | Patel NH et. al., 1989 |
| anti - eve | 1: 10000 | Hybridoma Bank | |
| anti - numb | 1: 1000 | Jan YN | Uemura T et. al., 1989 |
| anti – B-gal | 1: 3000 | Cappel | |
| anti - PON | 1:1000 | Jan YN | Lu B. et. al., 1998 |
| anti - Asense | 1: 1000 | Jan YN | Brand M. et. al., 1993 |

### 2.4.2 Confocal analysis and image processing

Stained and mounted tissue samples were analyzed with a Zeiss Axiophot microscope. Photographs were taken with an attached 35 mm camera or using a Kontron Prog Res 3012 digital camera (Kontron Elektronik) connected to a Personal Computer. The fluorescently labelled tissue samples were visualised using confocal microscopy using the MRC1024 laser scanning microscopes from Biorad or the Zeiss LSM510 confocal. All digital images were processed using Adobe Photoshop (Adobe, USA).

For the zebrafish work, photomicrographs were taken using a Zeiss microscope equipped wit Normarski differential interference contrast optics and images were compiled using Adobe Photoshop (Adobe, USA)

## 2.5 Drug Treatments

For drug treatments, WISH or MDCK cells were plated on on 35mm dishes and allowed to grow until 80 % confluent. For microfilaments depolymerization, cells were washed with PBS and inculabted with serum free medium (SFM) with or without 1μM latrunculin A (Molecular Probes) for 60 min in a $CO_2$ incubator (Rosin-Arbesfeld, 2001). For microtubule depolymerization, cells were washed with PBS and then overlaid with or without 0.5μg/ml colchicine (Sigma) in complete culture medium. The cells were cultured for 24 hours in the $CO_2$ incubator. The treated cells were rinsed twice with PBS and then fixed for 20 minutes in 4% paraformaldehyde or for 10 minutes with chilled methanol at –20$^{o}$C before proceeding with the immunofluorescence analysis.

# CHAPTER 3 : Subcellular localization of LGN during mitosis: evidence for its cortical localization in mitotic cell cultures and its requirement for normal cell cycle progression.

## 3.1 Background

In mammals, two proteins that are related to *Drosophila* Partner of Inscuteable (Pins) have been identified (Mochizuki *et al*., 1996; Takesono *et al*., 1999). They define a class of cytoplasmic non-receptor linked regulators of G-protein signaling. Members of this class of proteins generally contain two types of repeats: seven tetratricopeptide repeats (TPR) at the amino-terminus and three $G\alpha_{i/o}$-Loco (GoLoco) repeats at the carboxy-terminus. TPR motifs usually mediate protein-protein interactions (Blatch and Lassle, 1999) whereas GoLoco motifs are responsible for association with Gα subunits of heterotrimeric G-proteins (Siderovski *et al*., 1999; Natochin *et al*., 2000; Bernard *et al*., 2001). These cytoplasmic signaling regulators behave as guanine dissociation inhibitors (GDI), preventing the exchange of GDP-bound for GTP-bound Gα (De Vries *et al*., 2000; Natochin *et al*., 2000).

In *Drosophila*, Pins was originally discovered as a protein that interacts with Inscuteable (Insc) in dividing neuroblasts (NBs) (Yu *et al*., 2000; Schaefer *et al*., 2000) and that both Pins and Insc (Kraut *et al*., 1996) are asymmetrically localized to the apical cortex of NBs during mitosis and play important roles in the localization of basal cell fate determinants and mediate correct spindle orientation in dividing NBs (Yu *et al*., 2000; Schaefer *et al*., 2000; Kraut *et al*., 1996). The apical cortical

localization of Pins in dividing *Drosophila* NBs depends not only on the N-terminal sequences that interact with Insc but also on the C-terminal region that binds to Gα subunit of heterotrimeric G-proteins. However, in epithelial cells, which lack Insc expression, Pins associates with the lateral cortex instead (Yu *et al*., 2000; Schaefer *et al*., 2000).

The subcellular localization of the mammalian proteins related to *Drosophila* Pins, AGS3 and LGN, has also been reported. As for AGS3, the protein is reported to be primarily cytoplasmic throughout the cell cycle (Blumer *et al*., 2002). A truncated version of AGS3 (AGS3-Short) lacking the N-terminal TPR domains has also been identified (Pizzinat *et al*., 2001). It is enriched in the heart and shows a subcellular cytoplasmic distribution that is different from AGS3. The localization data suggested that the TPR domains might account for the differences between a homogeneous cytoplasmic staining for AGS3-Short and a punctate cytoplasmic distribution for AGS3. As for LGN, its subcellular localization has been reported by two separate studies using reagents based on the human LGN sequence. In one study, Blumer and colleagues (2002) used PC12 cell to show that LGN exhibits dramatic differences in its localization at specific stages of the cell cycle. The authors have shown that LGN moves from the nucleus to the midbody structure separating daughter cells during the later stages of mitosis, suggesting a role in cytokinesis. In another study, Du and co workers (2001) have shown that LGN, unlike *Drosophila* Pins, accumulates at the spindle poles of dividing polarized MDCK cells. The authors have also shown that LGN plays essential roles in the assembly and organization of the mitotic spindle via binding to the nuclear mitotic apparatus protein NuMA, which tethers spindles at the poles (Du *et al*., 2001; Du *et al*., 2002).

The mammalian LGN has so far been shown to assume various subcellular localizations that are different than that reported for fly Pins. Our group had previously isolated a mouse homolog of LGN, mLGN, and shown that it can functionally replace all aspects of defects seen in *Drosophila pins* mutants. Using reagents generated based on mLGN, further characterization of LGN localization profile in various mammalian cell lines was analyzed. My data shows that similar to fly Pins, transfected tagged versions of mouse LGN as well as endogenous LGN are found enriched at the cortex of some but not all cell lines tested in a cell cycle-dependent manner (Kaushik *et al*., 2003). Furthermore, my results show that the C-terminal GoLoco-containing domain of LGN is sufficient for cortical localization. I also report that factors affecting the cortical localization of LGN include microfilaments and the Gα subunits of heterotrimeric G-proteins. The data presented in this chapter also shows that overexpression of the mouse LGN or prevention of LGN translation via the use of a morpholino in cell lines results in cell cycle arrest.

## 3.2 Results

### 3.2.1 Subcellular localization of LGN in mammalian cells

#### 3.2.1.1 LGN-FLAG is enriched at the cell cortex in mitotic cells

Fly Pins displays cortical localization in dividing cells (Yu *et al*., 2000; Schaefer *et al.*, 2000) whereas the mammalian LGN homolog localizes to spindle poles (Du *et al*., 2001) or midbody structures (Blumer *et al.,* 2002) depending on the cell lines used. In order to characterize the subcellular localization profile of LGN in a variety of dividing mammalian cells, I carried out a transient transfection study of an LGN-FLAG construct in various cell line systems and followed the localization of this exogenous LGN during mitosis using anti-FLAG antibody. Depending on the cell line

used, the transient transfection experiments revealed a cortical localization profile for LGN during mitosis that has not been reported before (Fig. 3.1; Fig. 3.2).

In human amniotic WISH cells, the full length LGN-FLAG (FL-FLAG) localized to the perinuclear region/cytoplasm during interphase and was mainly redirected to the cortex during mitosis (Fig. 3.1A-B; Fig. 3.2A-B). Similarly in normal rat kidney NRK fibroblast cells, LGN-FLAG was largely perinuclear during interphase (Fig. 3.1C) and enriched at the cell cortex during mitosis (Fig. 3.1D). This cell cycle dependent localization profile for LGN-FLAG was also observed in PC12 cells (Fig. 3.1E-3.1F). In contrast monkey kidney derived COS cells, on the other hand, did not show cortical localization for LGN-FLAG as they enter mitosis. In these cells, LGN-FLAG was perinuclear during interphase (Fig. 3.1G) and remained in the cytoplasm throughout mitosis (Fig. 3.1H). These experiments showed that LGN-FLAG can localize to the cortex during mitosis of some cell lines tested, and this property could be similar to that of fly Pins.

#### 3.2.1.2 The C-terminus of LGN is sufficient for its cortical localization

Pins and Pins-related proteins have a conserved modular structure containing N-terminal TPR domains and C-terminal GoLoco repeats. The N-terminal TPR domains have been shown to be involved in the interaction with other proteins such as Insc and NuMA (Yu *et al*., 2000; Schaefer *et al*., 2000; Du *et al*., 2001) whereas the C-terminal GoLoco repeats mediate binding to Gα subunits of heterotrimeric G-proteins (De Vries *et al*., 2000). In flies, the C-terminus of Pins has been shown to be required for cortical localization of the Pins protein in neuroblasts and epithelial cells (Yu *et al.,* 2002).

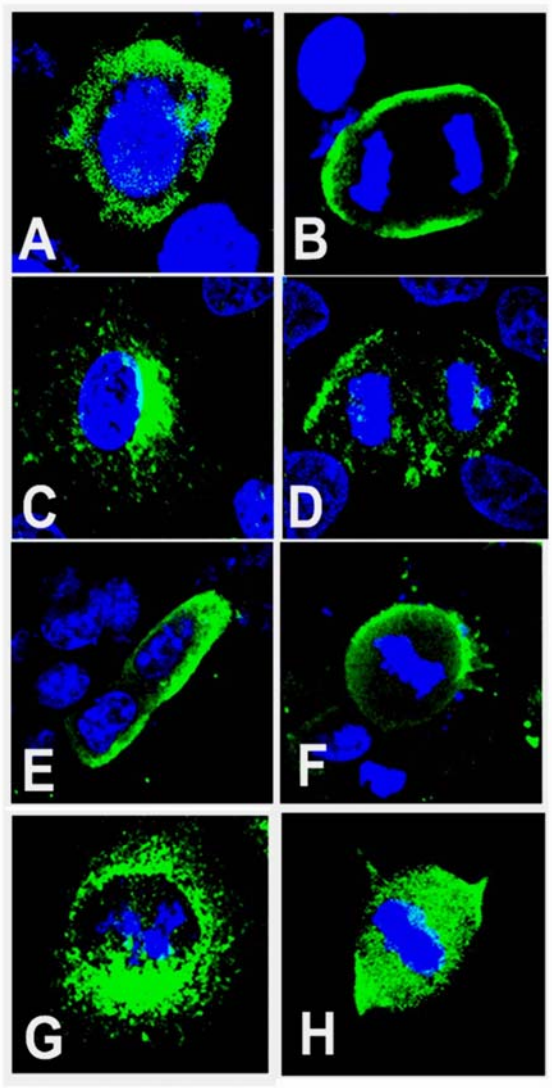


**Figure 3.1 Overexpression and localization of exogenous LGN-FLAG in cell lines.** LGN-FLAG was overexpressed in WISH (A, B), NRK (C, D), PC12 (E, F) and COS (G, H) cells. LGN localization was detected with anti-FLAG (green) and DNA was stained with TOPRO3 (blue). LGN-FLAG is localised to the perinuclear/cytoplasm in interphase WISH (A), NRK(C), PC12(E) and COS (G) cells. During mitosis, LGN is localized to the cortex in WISH (B), NRK(D) and PC12(F) but not in COS (H) cells where it remains cytoplasmic.

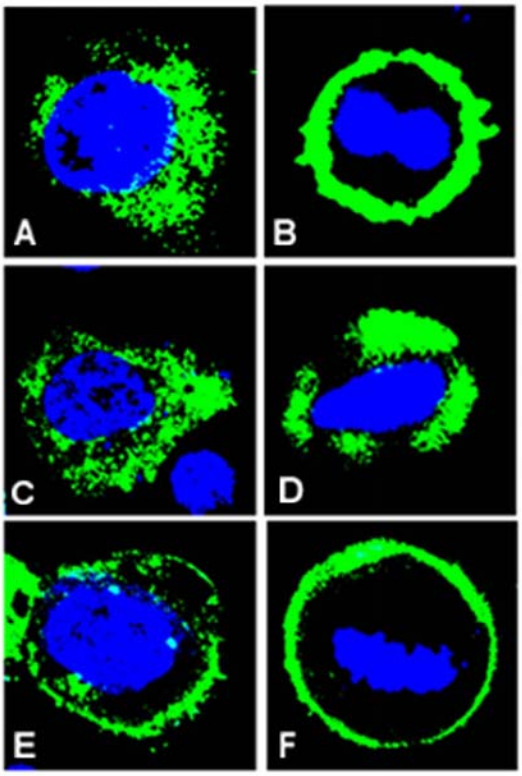


**Figure 3.2 Domain dissection of LGN.**
FLAG-tagged LGN constructs were transfected into WISH cells and their subcellular localization was detected using anti-FLAG antibody (green). Panel A shows perinulear/cytoplasmic staining for FL-LGN at interphase whereas panel B shows a cortical localization for FL-LGN at metaphase. N-FLAG (amino acids 1-384) remains mainly in the cytoplasm during interphase (C) and metaphase (D). C-FLAG (amino acids 385-672) is enriched at the cell cortex during both interphase (E) and metaphase (F). Residual cytoplasmic/perinuclear staining for C-FLAG can also be seen at interphase (E). The cell cycle stage was determined by DNA staining (blue).

To dissect the domains responsible for directing LGN to different localization sites within the cell, I generated and expressed constructs containing various FLAG-tagged fragments of the mouse LGN protein in WISH cells and assayed their localization during the cell cycle using an anti-FLAG antibody (Fig. 3.2). Transfected cells expressing the N-terminus (N-FLAG; amino acids 1 –384) or the C-terminus (C-FLAG; amino acids 385–672) of LGN showed different subcellular localization profiles. N-FLAG was predominantly cytoplasmic during interphase (Fig. 3.2C) and failed to localize to the cortex during mitosis (Fig. 3.2D). In contrast, C-FLAG was predominantly associated with the cell cortex throughout the cell cycle from interphase to telophase (Fig. 3.2E-F). These experiments indicate that the C-terminus of LGN contains a cortical localization signal; similar to that reported for fly Pins and perhaps directing LGN to the cortex during mitosis.

## 3.2.2 Endogenous LGN also localizes to the cortex of mitotic cells

The overexpression studies showed preferential cortical localization for LGN-FLAG during mitosis in WISH, PC12 and NRK but not COS cell lines (Fig. 3.1). In order to examine the localization profile of endogenous LGN in these cell lines, anti-LGN antibodies were raised against mLGN in rabbits and used for immunostaining on various cell lines.

### 3.2.2.1 LGN antibody is specific

As a first approach to determine the specificity of the antibody, affinity purified anti-LGN antisera were used on immunoblots to probe total protein extracts from PC12, WISH and COS cells. In this experiment, a single band of the expected LGN size was detected in the PC12 cell extract (Fig. 3.3A).

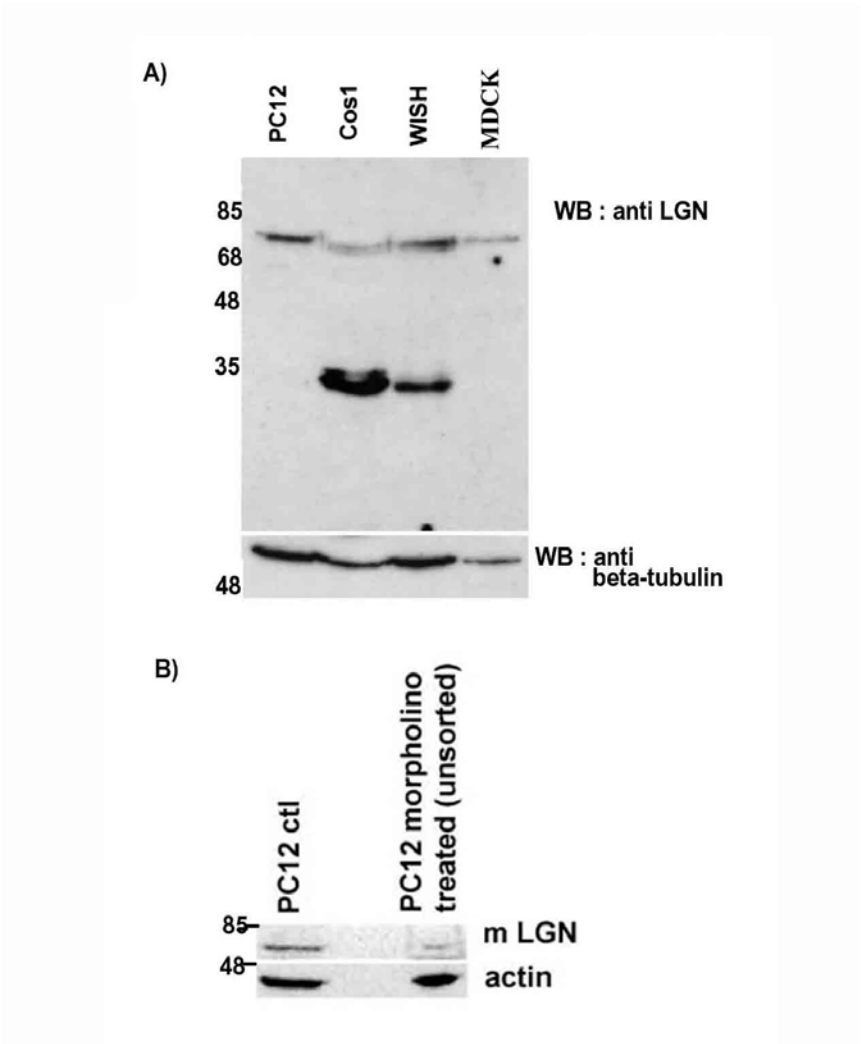


**Figure 3.3 Immunoblot analysis.**

100μg of total protein extracts were loaded in each lane and immunoblotted.Panel A shows protein extracts from PC12, COS, WISH and MDCK cell lines probed with anti-LGN antibody at a concentration of 1μg/ml. Anti-LGNdetects a prominent band of the expected LGN molecular weight in the PC12 and MDCK cell extracts. COS and WISH cell extracts show the LGN band and other additional lower size bands. β-tubulin is used as a protein-loading marker. Panel B shows an immunoblot of PC12 cell extracts before and after morpholino treatment. The intensity of the LGN band is reduced 5 fold upon morpholino treatment as compared to that of the control untreated PC12 cells. In this immunoblot, actin was used as a protein-loading marker.

The intensity of the single LGN band obtained in the PC12 cell extract was reduced 5 fold upon treatment of PC12 cells with an *LGN*-specific morpholino prior to blotting, suggesting that the anti-LGN antibody is specific (Fig. 3.3B). WISH and COS cell extracts, on the other hand, showed in addition to the LGN band other lower size bands (Fig. 3.3A). No protein bands were detected in PC12, WISH, MDCK or COS cells extracts on the immunoblot when a preimmune serum was used or when the cell extracts were subjected to antigen absorption treatment prior to immunoblotting again indicating that the anti-LGN antibody is specific. Additional lower molecular weight bands for LGN were also reported by other researchers (Blumer *et al.,* 2002) and they are either LGN degradation products or possibly LGN isoforms produced by alternative splicing events. Nevertheless, the single LGN band obtained in PC12 cells and the dramatic reduction of its intensity upon pre-treatment of PC12 cells extracts with an *LGN*-specific morpholino, shows that the anti-LGN antibody is specific (Fig. 3.3B). This anti-LGN antibody was then used to determine LGN localization in various cell lines and this is described in the following section 3.2.2.2.

#### 3.2.2.2 LGN localizes to golgi during interphase

In interphase COS cells, LGN was found in the perinuclear region that is usually occupied by golgi and other membrane compartments (Fig. 3.4A) and colocalized with Vti1α (Fig. 3.4A-C). Vti1α is a SNARE protein that colocalizes with golgi markers in various cell lines (Antonin *et al*., 2000; Xu *et al*., 1998). In addition, during interphase, mLGN colocalizes to the golgi as seen with double labelling of mLGN with the 28-kilodalton protein (GS28) of the cis-golgi (Fig. 3.4D-F) and golgi matrix protein GM130 (Fig. 3.4G-I) (Lowe *et al*., 1998).

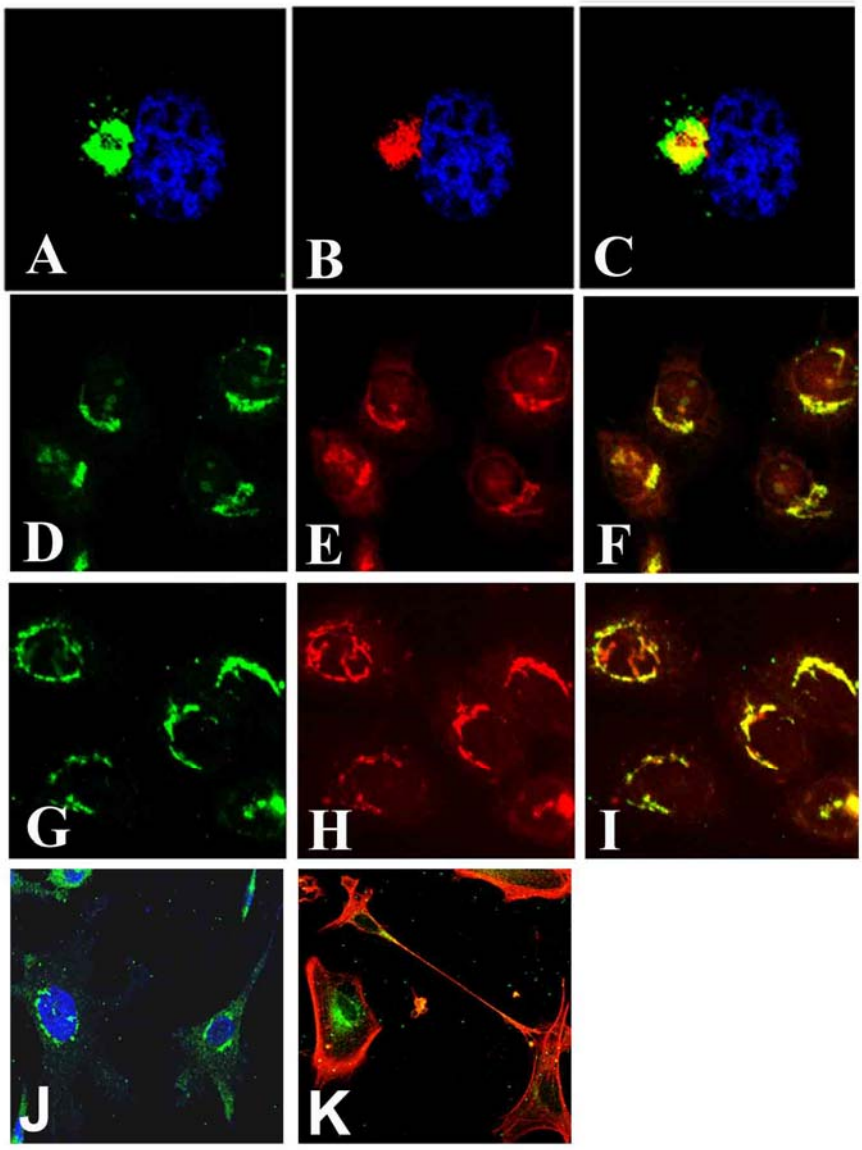


**Figure 3.4 Colocalization of LGN with golgi markers during interphase.**

COS cells (A-C) and A431 (D-I) were stained with LGN (green) and various golgi markers (red). Panels A-C show colocalisation with Vti1α in interphase cells; panels D-F show colocalisation with GS28 in A431 interphase cells; Panels G-I show colocalisation with GM130 in A431 interphase cells. Areas of overlap between LGN and various golgi markers are in yellow in the merged images (C, F and I). Panels J-K show primary cultured cells from postnatal mouse brain with LGN (green) and phalloidin (red) and DNA (blue). LGN is perinuclear in these interphase/postmitotic cells.

GS28 is a core component of the golgi SNAP receptor (SNARE) complex and participates in the docking and fusion stage of endoplasmic reticulum(ER)-golgi transport and GM130 is a core component of golgi matrix (Subramaniam *et al*., 1996). In addition, analysis of primary neuronal cultured cells from postnatal mouse revealed that mLGN localized to perinuclear subcellular loclalization in interphase cells (Fig 3.4J-K).

#### 3.2.2.3 Endogenous LGN localizes to the cell cortex during mitosis

Staining of WISH and PC12 cell lines with anti-LGN antibody revealed a cortical localization profile for the endogenous LGN protein (Fig. 3.5) similar to that observed when a FLAG-tagged version of mouse LGN was transfected into these cells and detected with an anti-FLAG antibody (see Figs. 3.1 and 3.2). In PC12 cells, endogenous LGN was predominantly perinuclear during interphase and partially accumulated at the cell cortex during mitosis (Fig. 3.5A-C). Some LGN staining associated with the cytoplasm and spindle apparatus was also be seen in metaphase cells (Fig. 3.4B). A similar localization profile was also demonstrated for endogenous LGN in MDCK cells (Fig. 3.5D-F) and WISH cells (Fig. 3.5G-I). In these cells, LGN cortical staining appeared to be strongest at the two opposite poles at metaphase and was more intense as compared to LGN staining in other cell lines. Similar to the LGN-FLAG localization data obtained in the overexpression studies, a cortical localization for endogenous LGN was not detected in mitotic COS cells and the LGN protein remained cytoplasmic (Fig. 3.5J-L).

The localization of LGN to the cell cortex was also observed using antibodies generated in other laboratories. This was demonstrated in dividing WISH cells (Fig. 3.5M-N) using affinity-purified anti-LGN antibodies made against human LGN (Blumer *et al*., 2002).

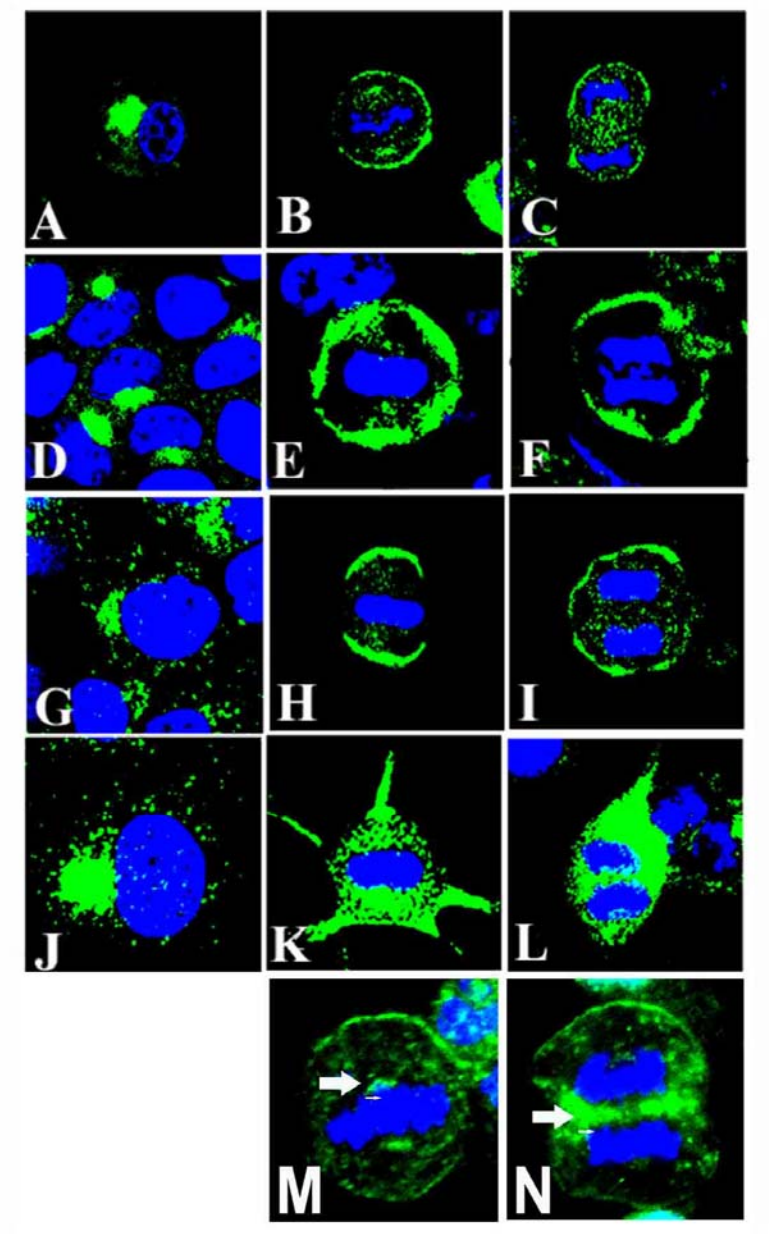


**Figure 3.5 Subcellular localization of endogenous LGN in cell lines.**

Confocal images of PC12 (A-C), MDCK(D-F), WISH(G-I) and COS cells (J-L) stained for LGN (green) and DNA (blue) are shown. In all cell lines, LGN localizes to a perinuclear space during interphase (A, D, G, J). Note the cortical localization of LGN during mitosis is only observed in PC12 (B, C), WISH (E,F) and WISH (H,I) but not COS (K, L) cells. In metaphase (K) and anaphase (L) COS cells, LGN remains in the cytoplasm. Some cytoplasmic staining of LGN can also be seen in mitotic PC12 (B-C), MDCK (E-F) and WISH (H-I) cells. Panels M and N are metaphase (M) and anaphase (N) WISH cells stained with an anti-LGN antibody generated by Blumer et al., (2002). Similar cortical localization for LGN is detected with this antibody in addition to the previously reported spindle pole (M: arrow) and mid-cell body (N: arrow).

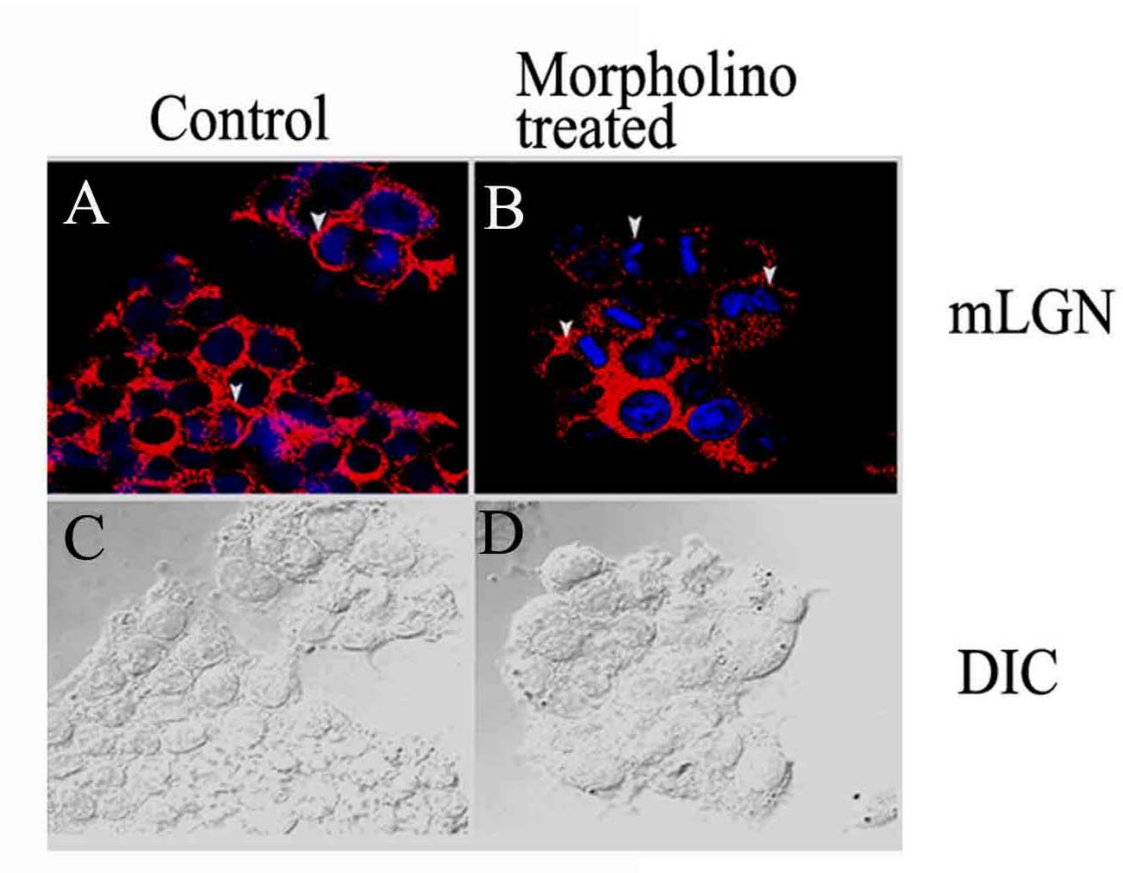


**Figure 3.6 Effect of anti-LGN morpholino on LGN translation in PC12 cells.**

PC12 cells were treated with *LGN- morpholino* (B-D) and stained for LGN (A-B : red) and DNA (blue). During metaphase LGN localises to cell cortex in (A: arrowhead) control but not in LGN morpholino treated cells (B: arrowhead). In the LGN morpholino treated cells there is a knockdown of LGNprotein levels (B : arrowheads). The DIC image of control as well as morpholino treated cells is shown in C-D.

Interestingly, these antibodies also stained midbody and spindle poles in WISH cells (Fig. 3.5J-L). The cortical localization of LGN during mitosis has not been reported in previous studies. Treatment of the PC12 cells with an antisense *LGN* morpholino that blocks LGN translation resulted in loss of cortical staining during mitosis (Fig. 3.6B) suggesting that it is the endogenous LGN that localizes to the cortex. In *LGN* morpholino treated cells there is no translated LGN protein and no cortical staining is seen providing further evidence that the cortical localization detected using the antibody is indeed *LGN* specific.

#### 3.2.2.4 LGN is localized to a basolateral sub-domain of cortex in polarized cells

As in WISH, NRK and PC12 cells, LGN localizes to the cell cortex during mitosis in dog kidney derived polarized epithelial MDCK cells (Fig. 3.5D-F). The plasma membrane of polarized epithelial cells is divided into two functionally and biochemically distinct domains, the apical and basolateral plasma membranes (Simons and Fuller, 1985) and it forms junctional complexes such as tight junctions and adherens junctions that play crucial roles in the structure and function of epithelial cells. The tight junction forms a continuous belt at the boundary between the apical and lateral plasma membrane domains and selectively regulates the passage of molecules across the plasma membrane pathway (gate function) and passively separates molecules into the apical and basolateral plasma membrane domains (fence function) (Farquhar and Palade, 1963). The adherens junction is localized below the tight junction and consists of cell adhesion and signaling molecules that may regulate the formation of other junctional complexes (Yap *et al*., 1997). In order to determine which membrane sub-domain LGN is associated with during mitosis, polarized epithelial MDCK cells were stained with an anti-LGN antibody and analyzed using confocal microscopy. Analysis of the images showed that LGN is not distributed

randomly over the cortex (Fig. 3.7D); staining was generally absent from the basal and apical membrane and was largely confined to the lateral cell membrane during mitosis.

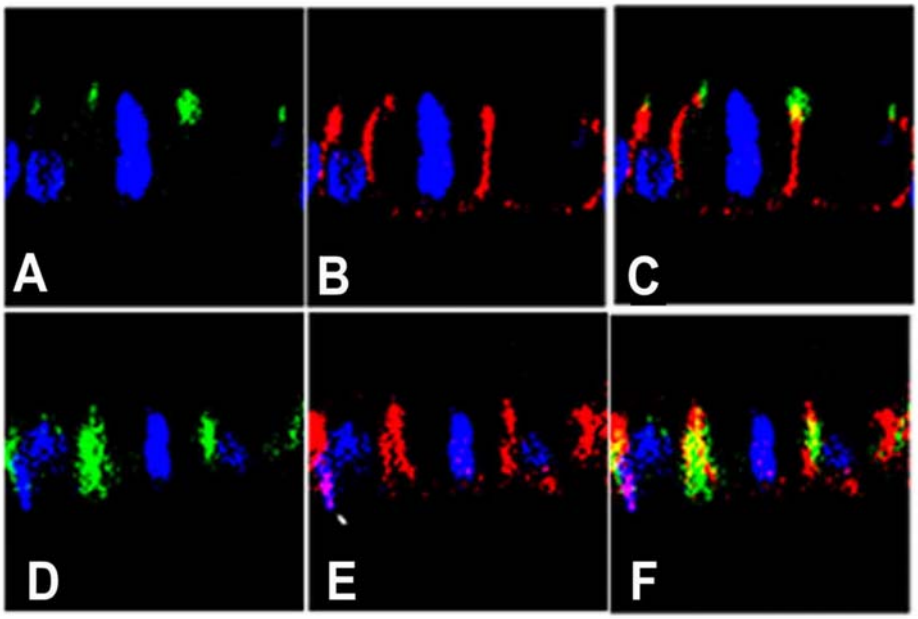


**Figure 3.7 Cortical subdomain localisation of LGN in polarised MDCK cells.**

Confocal vertical (xz) sections of polarized MDCK cells at metaphase are shown. Panels A-C show a metaphase MDCK cell double stained for apical membrane marker ZO-1 (A; green) and β-Catenin basolateral membrane marker (B; red). There is little overlap between the two membrane markers (C; yellow). Panels D-F show a metaphase MDCK cell double stained for LGN (D; green) and β-catenin (E; red). LGN and β-catenin show colocalization at the lateral membrane subdomain (F; yellow). Weak cytoplasmic staining of LGN can also be seen at this stage. The cell cycle stage was determined by DNA staining (blue).

The localization of LGN was compared to that of two other membrane proteins, ZO-1 (Fig. 3.7A; Fig. 3.7C) and β-catenin (Fig. 3.7B-C; Fig. 3.7E-F). In polarized cells, ZO-1 protein is localized in apical tight junctions (Stevenson *et al*., 1986, 1989; Anderson *et al*., 1988) whereas β-catenin a known member of cadherin-catenin complexes at adherens junctions is localized to basolateral membrane subdomain in polarized epithelial cells (Miranda *et al*., 2003; For a review see Yap *et al*., 1997). In vertical optical sections, LGN staining was absent from the apical and basal membrane but was present on the lateral membrane where its localization overlaps with β-catenin (Fig. 3.7F).

## 3.2.3 Factors important for localizing LGN to cell cortex.

### 3.2.3.1 LGN cortical localization is dependent on microfilaments but not microtubules

In order to assess the role of microfilaments and microtubules on LGN cortical localization, WISH and MDCK cells were subjected to treatments with latrunculin B and colchicine (Figs. 3.8 and 3.9). Cells treated with the microfilament destabilizing drug, Latrunculin B, were double stained with anti-LGN antibody and phalloidin. In interphase cells, Latrunculin treatment did not affect the perinuclear localization of LGN in WISH cells (Fig. 3.8E; 3.8F). On the other hand, the cortical LGN localization that is normally seen in control WISH cells during mitosis (Fig. 3.8H; Fig. 3.8I) was abolished upon latrunculin treatment (Fig. 3.8K-3.8L). As expected, the cortical microfilament staining was also abolished in treated cells (Fig. 3.8D; Fig. 3.8J). MDCK cells treated with Latrunculin B also showed similar results (Fig. 3.8M-R).

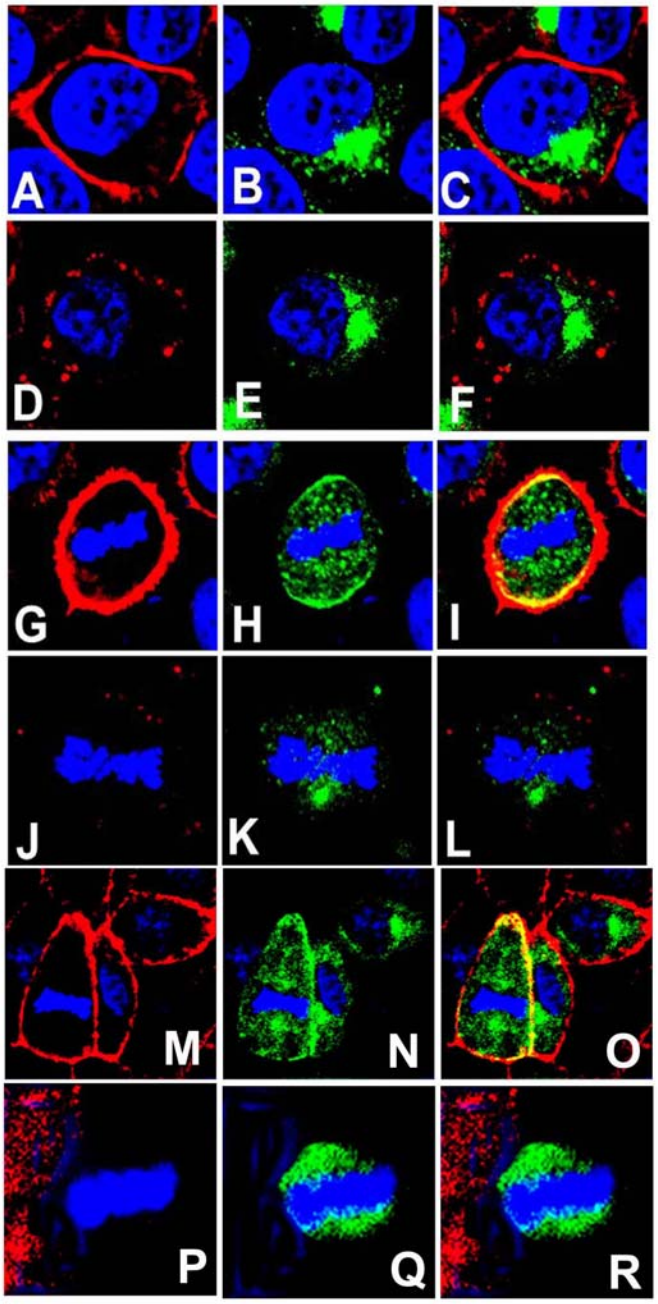


ctd on next page

**Figure 3.8 Effects of cytoskeleton on LGN cortical localization**.

Panels A-L are confocal (xy) images of cycling WISH cells stained with phalloidin (red), LGN (green) and DNA ( blue); Panels A-C show a control interphase cell with LGN localizing at the perinuclear region and actin microfilaments at the cell cortex ; Panel C is a merged image of A and B; Panels D-F show the loss of cortical actin microfilaments upon latrunculin treatment but the perinuclear LGN staining remains unaffected in the interphase drug-treated cell. Panel F is a merged image of D and E; Panels G-I is a cortical metaphase WISH cell showing LGN colocalising with actin at the cell cortex (yellow in I). Note that some LGN staining in the cytoplasm is also visible at this stage. Panels J-L show a metaphase cell treated with latrunculin B; note the cytoplasmic staining of LGN (K) and the absence of phalloidin staining in the treated cell (J); L is a merged image of J and K. Panels M-R are confocal (xy) images of cycling MDCK cells stained with phalloidin (red), LGN (green) and DNA ( blue); Panels M-O shows control cells in metaphase and colocalisation of LGN and F-actin at the cell cortex with phalloidin (O: yellow). Panels P-R show a metaphase cell treated with latrunculin B; note the cytoplasmic staining of LGN (Q) and the absence of phalloidin staining in the treated cell (P); R is a merged image of P and Q.

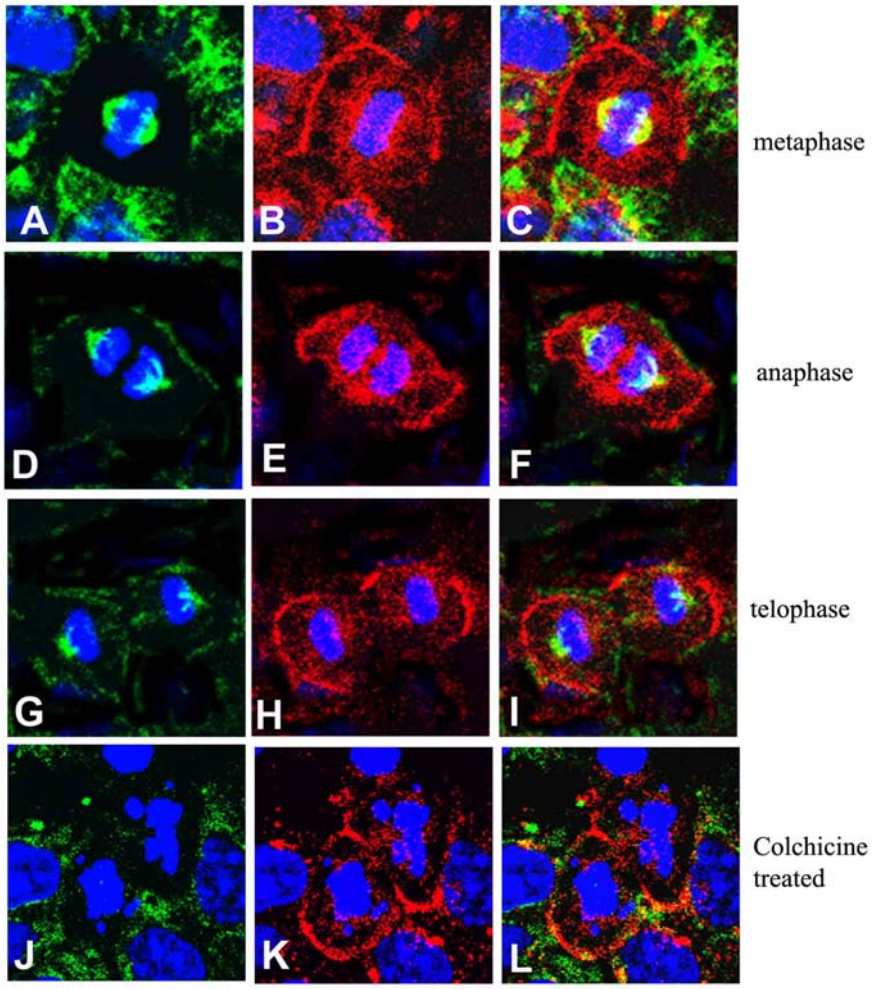


**Figure 3.9 The effect of colchicine treatment on cortical localisation of LGN during mitosis.**

Panels A-L are confocal images of cycling WISH cells without (A-I) or with (J-L) colchicine treatment and stained for LGN (red) and β-tubulin (green) and DNA (blue). Without colchicine treatment, β-tubulin stains the spindle and LGN stains the membrane cortex during metaphase (A-C), anaphase (D-F) and telophase (G-I) in WISH cells. After colchicine treatment, no spindle staining can be seen in the metaphase WISH cell (J) but LGN cortical localisation is not affected (K), L is the merged image of J and K.

In contrast, treatment of cells with colchicine, the microtubule-destabilizing drug, disrupted the mitotic spindle (Fig. 3.9J) but did not affect LGN cortical localization at metaphase (Fig. 3.9K-L). The data indicates that LGN cortical localization during mitosis is dependent on microfilaments but not microtubules. There is some cytoplasmic staining for *LGN* seen in these cells (Fig. 3.9 A-L: red) in addition to the cortical localization of the *LGN* during mitosis. This localization has previously been reported for human *LGN* (Blumer et al., 2001).

#### 3.2.3.2 Gα subunits of heterotrimeric G-proteins can cortically localize LGN

The C-terminus of LGN contains four GoLoco motifs and the identification of a cortical localization signal in that region implicated a role for Gα subunits of heterotrimeric G–proteins in the localization of LGN. To investigate the role of heterotrimeric G–proteins in LGN cortical localization, COS cells were transfected with various $G\alpha_{i/o}$ constructs. I used COS cells because our data showed that they do not localize LGN to the cortex during mitosis (Fig. 3.10A; Fig. 3.10C). Incidentally, COS cells also lack the expression of some heterotrimeric G-protein subunits including $G\alpha_o$ (Luo and Denker, 1999; Fig. 3.10B), but still express $G\alpha_{i3}$ and $G\alpha_{i2}$. Ectopic expression of $G\alpha_o$ in COS cells redirected most of LGN to the cell cortex (Fig. 3.10D; Fig. 3.10F), indicating that the $G\alpha_o$ can localize LGN to the cortex in these cells. The cortical localization of LGN was observed in all $G\alpha_o$-transfected COS cells. The transfected COS cells also directed the ectopically expressed $G\alpha_o$ protein to the cell cortex (Fig. 3.10E-3.10F). In this system, the overexpression of $G\alpha_o$ was associated with abnormal rounded-cell morphology. In contrast to $G\alpha_o$ overexpression, transfection with $G\alpha_{i3}$ and $G\alpha_{i2}$ failed to localize LGN to the cortex (Fig 3.10G-I; Fig3.10J-L), indicating that LGN cortical localization might require specific

interaction with $G\alpha_o$. LGN has been shown to directly interact with $G\alpha_{i3}$ and act as a GDI for $G\alpha_{i3}$ but this interaction is not sufficient for its cortical localization as seen in these experiment, indicating that although various G protein isoforms can interact with LGN within the cell, only $G\alpha_o$ is able to localize LGN to the cell cortex in dividing COS cells and this further adds to the complexity of LGN mediated G protein signaling in the cell.

#### 3.2.3.3 LGN interacts directly with Gα subunits of heterotrimeric G-proteins and acts as GDI

Pins and its related proteins are characterized by the presence of C-terminal GoLoco repeats, that bind Gα proteins (Siderovski *et al*., 1999; Natochin *et al*., 2000; De Vries *et al*., 2000; Bernard *et al*., 2001). Like its mammalian homologs, mouse LGN binds $G\alpha_{i3}$-GDP *in- vitro* via its C-terminus (Fig. 3.11A). No binding to $G\alpha_{i3}$ was observed with mouse LGN constructs lacking the C-terminal GoLoco repeats (Fig. 3.11A). As expected, binding of mouse LGN to $G\alpha_{i3}$ inhibited its rate of exchange of GDP for GTP (Fig. 3.11B) thereby acting as a guanine dissociation inhibitor (GDI – For details on GDI assay, See materials and methods section 2.3.7). Mouse LGN was also able to bind Gαo (Fig. 3.11A) but no GDI activity was observed with Gαo (Fig. 3.11B).

### 3.2.4 Effect of LGN protein levels on cell cycle

#### 3.2.4.1 Loss / ectopic expression of LGN causes cell cycle defects

To study the function of LGN in cell cycle progression, we carried out 5-Bromodeoxyuridine (BrdU) labeling experiments in PC12 and MDCK cells ectopically expressing three LGN constructs, FL-FLAG, N-FLAG, and C-FLAG (Fig. 3.12). BrdU, is a halogenated thymidine analog that is permanently integrated into the

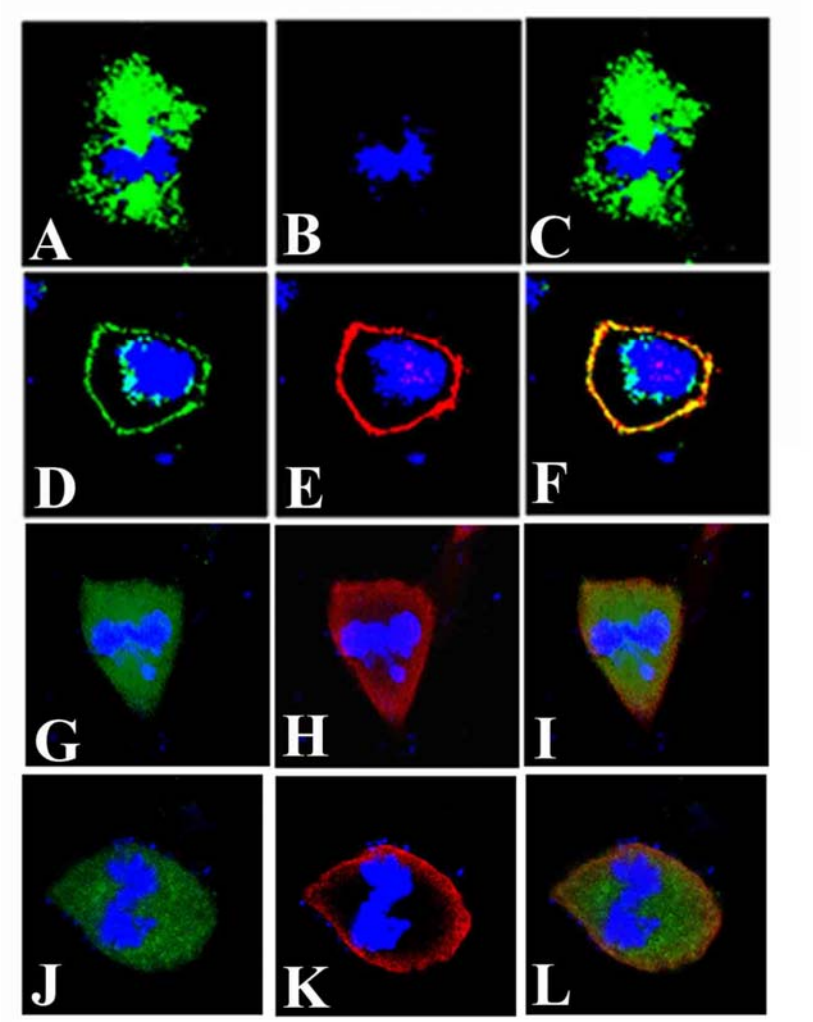


**Figure 3.10 Effects of G-proteins on LGN cortical localization.**

In all images LGN is green and $G\alpha_{i/o}$ is in red. Panels A-F show confocal images of COS cells stained for LGN and $G\alpha_{i/o}$. Panels A-C show a control vector transfected metaphase COS cell with cytoplasmic LGN (A) and no $G\alpha_o$ expression (B); C is a merged image of A and B. Panels D-F show a COS cell transfected with $G\alpha_o$; LGN (D) and exogenous $G\alpha_o$ (E) are directed to the cell cortex; Note that a residual perinuclear staining for LGN can still be seen in this experiment; F is a merged image of D and E showing areas of overlap (yellow) between $G\alpha_o$ and LGN. Panels G-I show a metaphase COS cell transfected with $G\alpha_{i3}$ and Panels (J-L) show a metaphase COS cell transfected with $G\alpha_{i2}$ ; LGN remains cytoplasmic in these $G\alpha_{i3}$ and $G\alpha_{i2}$ transfected cells. In all images, DNA staining is TOPRO3 and is shown in blue.

DNA of dividing cells during DNA synthesis in S-phase and is used as a marker for detection of cells that were dividing during the period of BrdU exposure. In these experiments, ectopic expression of FL-FLAG or N-FLAG prevented incorporation of BrdU in transfected cells, indicating cell cycle arrest at the G1/S transition stage.

In contrast, ectopic expression of the C-FLAG construct or the FLAG vector alone (control) did not affect cell cycle progression as indicated by BrdU incorporation in transfected cells. For each of these construct, 100 transfected cells were counted and the whole set was repeated three times to get average percentage which is plotted in Fig. 3.12.

The effect of LGN removal on cell cycle progression was assayed by treating cycling PC12 cells with the *LGN*-specific morpholino and carrying out FACSCAN analysis. In these experiments, a higher percentage of cells accumulated at G1 as compared to control untreated cells, indicating a delay / disruption of the cell cycle progression at the G1/S boundary in PC12 cells (Fig. 3.13). For each of these FAC-SCAN mediated cell cycle analysis, 21000 cells were scanned at one time and the experiment was repeated three times and showed reproducible results.

## 3.3 Discussion

In this chapter, I have characterized a novel dynamic cortical localization pattern of mammalian LGN that partly resembles that of fly Pins. I have mapped the cortical localization signal of LGN to its C-terminal domain which contains GoLoco motifs for G-protein interaction (as shown in Fig 3.2 and Fig 3.11A) and shown that LGN function is required for cell cycle progression. The cell cycle dependent cortical localization of LGN requires microfilaments and is influenced by the Gα subunits of heterotrimeric G-proteins.

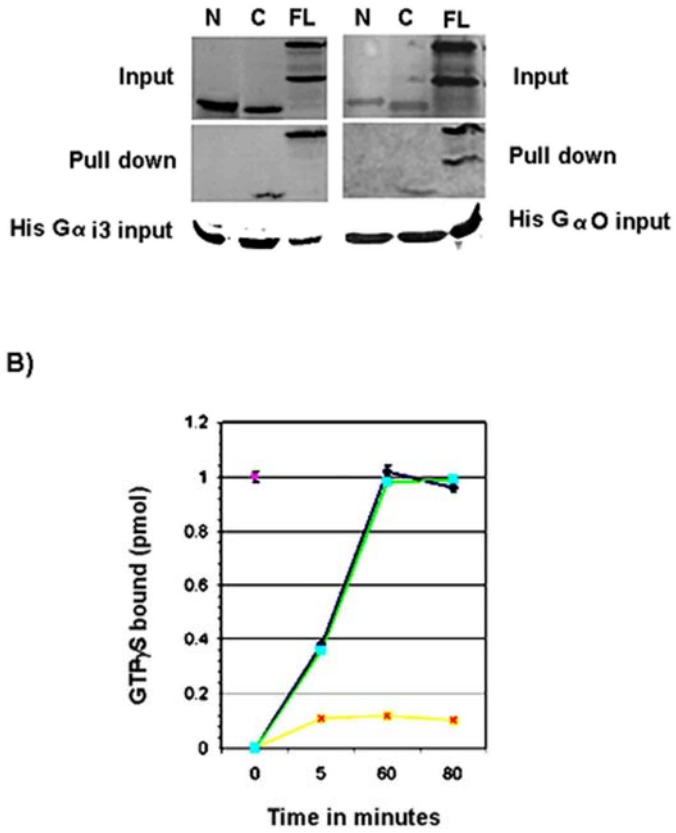


**Figure 3.11 GDI activity of mLGN.**
Panel A shows binding of mouse LGN to Gα subunits of heterotrimeric G-proteins. *In vitro*-translated LGN constructs containing amino acids 1-384 from the N-terminus (N), amino acids 385-670 from the C-terminus (C) or full length (FL) were incubated with His-G$\alpha_{i3}$ or His-G $\alpha_o$ bound to His columns. Only FL and C products copurify with His-Gai3/o. No binding is detected between construct N and G $\alpha_{i3}$ or G $\alpha_o$. In the FL lane, two bands are detected, an upper band corresponding to LGN and a lower band being a by-product of the translation reaction. Panel B shows GDI activity of mouse LGN on G $\alpha_{i3}$. Time course experiments showing the rate of [$^{35}$S] GTPγ binding by G $\alpha_{i3}$ were carried out in the presence of 1mM GST- LGN (yellow). Control experiments using GST alone are shown in blue. GST-LGN inhibits about 90% of [$^{35}$S] GTPγ binding to G $\alpha_{i3}$ but the GST control has no effect. The effect of LGN on G $\alpha_{i3}$ activity is observed as early as 5 minutes and lasts over 80 minutes time period. GST-LGN effect on G $\alpha_o$ (green) is similar to the GST control (blue), indicating mouse LGN has no GDI activity on G $\alpha_o$.

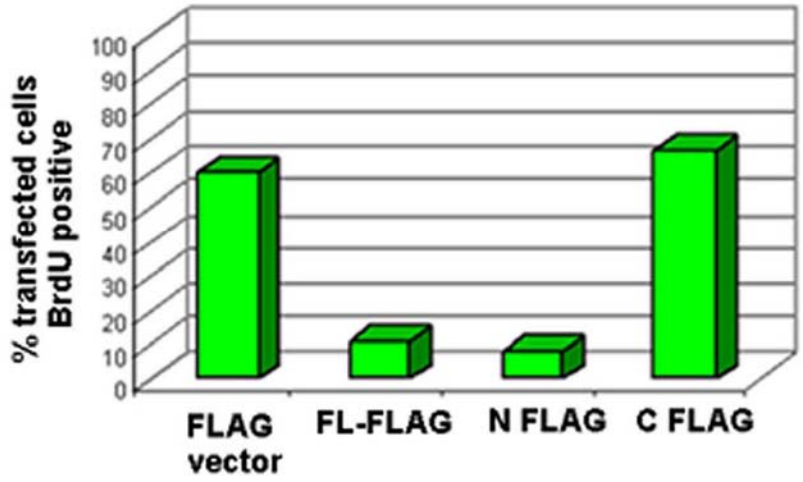


**Figure 3.12 Effects of LGN on cell cycle progression.**

Graph showing the effect of ectopic expression of various mouse LGN constructs, FL-FLAG, N-FLAG and C-FLAG on cell cycle in PC12 cells. Anti-BrdU and anti-FLAG antibodies were used for detection purposes. The bars represent percentage of BrdU positive cells. The majority of FL-FLAG or N-FLAG transfected cells were BrdU-negative whereas C-FLAG or FLAG-vector transfected cells are BrdU-positive would indicate that overexpression of either FL or N-FLAG; but not C-FLAG results in cell cycle arrest.

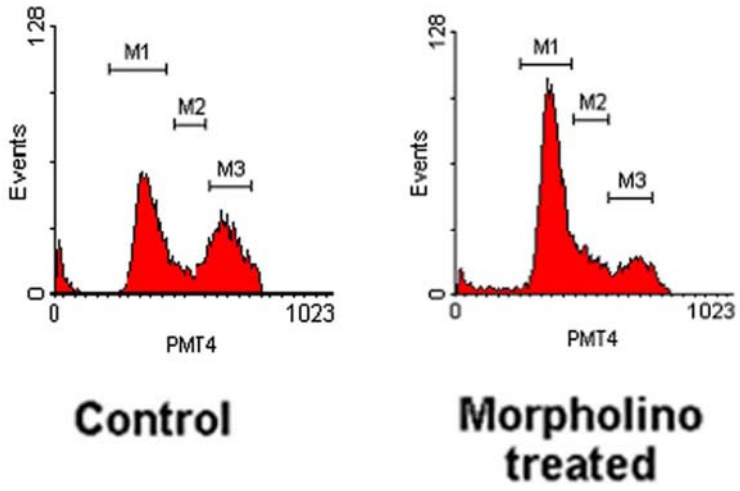


**Figure 3.13 Effect of LGN removal on cell cycle progression**

Panel A and B shows the effect of LGN removal by morpholino treatment on cell cycle in PC12 cells. For control cells, (A) the percentage of cells in G1 phase (M1) was ~52%, S phase (M2) ~11 % and G2 phase (M3) ~37%. For morpholino-treated cells, (B) the scores were ~70% for M1, ~10% for M2 and ~21% for M3, indicating that the loss of LGN causes partial delay/disruption of the cell cycle progression at the G1/S phase boundary.

Evidence for a cortical localization of LGN during mitosis is supported by several observations. Firstly, ectopically expressed full length tagged-LGN protein can localize at the cell cortex in various mitotic cell lines. Secondly, the over-expression studies show that the LGN C-terminus alone is able to accumulate at the cell cortex during mitosis. Thirdly, COS cells which normally do not localize LGN redirect this protein to their cortex upon overexpression of heterotrimeric G-proteins alpha subunits. The mitotic cortical localization of LGN described in this paper has not been previously reported. Du and coworkers (2001) have shown that LGN associates with the spindle poles during mitosis and its function is required to regulate mitotic spindle organization. They have also shown that the N-terminus of human LGN binds the nuclear mitotic apparatus protein NuMA, which tethers spindles at the poles, and that this interaction is required for the LGN phenotype. In a separate study, LGN was reported to be nuclear and to move to midbody domain in late mitotic phases (Blumer

*et al*., 2002). The different LGN localization data shown in these studies is surprising since they all describe the same LGN protein but using different reagents.

The various localization data suggest an ability of LGN to localize to different subcellular compartments depending on the cell cycle stage and the cellular context. Interestingly, a partial cortical staining for LGN in WISH cells is also observed with LGN antibodies obtained from other laboratories (Blumer *et al*., 2002). Mouse LGN and human LGN share a high degree of identity at the amino acid level. Mouse LGN shares 92% identity with human LGN, 60% with AGS3, and 49% with fly Pins (Yu *et al*., 2003). The difference in LGN localization data between these studies may reflect variations in the multiple LGN isoforms produced in the cell.

It has been previously reported the *LGN* locus produces several LGN peptides (Blumer et. al., 2002), suggesting the existence of splice variants or alternative promoters as reported for AGS3 (Pizzinat *et al*., 2001). The human LGN gene contains 14 exons and exon 1 encodes an amino-terminal 12aa that is not found in all ESTs for LGN (Blumer *et al*., 2002). Therefore, it is possible that the different antibodies generated for the human and mouse LGN proteins may recognize distinct protein epitopes that are present on the various LGN isoforms produced in the cell. In this scenario, it could be envisaged that, since different LGN isoforms might be localized differently to various subcellular sites, our reagents perhaps preferentially recognize the LGN isoforms that localize to the cortex during mitosis. Cell lines may also localize proteins differently. Indeed, no cortical localization for LGN could be detected in COS cells but WISH cells accumulate higher levels of LGN at their cell cortex compared to other cell lines (this study) and this may facilitate the detection of the protein in these cells.

In addition, it has been shown recently that endogenous LGN in human neural precursor cells (hNPCs- recovered from postmortem human brains) can localize

asymmetrically in a cell cycle-dependent manner. Although this apical localization is not strictly cortical as is seen for Pins in *Drosophila* NB division. When hNPCs are grown in conditions favouring cell division, the LGN protein localizes to one side of the dividing cell and gets segregated to one of the daughter cells and colocalises with progenitor cell marker, Nestin. When hNPCs are grown under conditions favoring differentiation, LGN accumulates in double foci similar to those containing the mitotic apparatus protein NuMA, and in a pattern shown previously for LGN and NuMA in differentiated cells (Fuja *et al*., 2004).

Domain dissection analysis suggests that the region containing the C-terminal GoLoco motif of LGN is sufficient for membrane targeting and that the cortical localization of this domain is cell cycle-independent. This implies roles for heterotrimeric G-proteins in LGN cortical localization, which would be consistent with the observations that LGN can directly bind $G\alpha_{i2/3/o}$ subunits. A function for heterotrimeric G-proteins in LGN cortical localization is also supported by evidence from ectopic expression studies in COS cells, which cannot normally localize endogenous LGN to the cortex during mitosis. The ectopic expression studies in COS cells indicate a requirement for $G\alpha_o$ in directing the cortical localization of LGN during mitosis in these cells. Since LGN does not act as a GDI for $G\alpha_o$, its $G\alpha_o$-driven cortical localization in COS cells may be independent of its GDI activity. LGN can bind directly to $G\alpha_o$ *in-vitro* and this lends support to the notion that LGN cortical localization by $G\alpha_o$ may be a direct event. This notion can also be supported by the cortical localization data of $G\alpha_o$ in transfected COS cells.

Work on the Pins-related protein from rat, AGS3, has also shown that in crude fractionation assays overexpression of G-proteins can direct AGS3-Short to the membrane (Pizzinat *et al*., 2001). Interestingly, fly Pins also contains a cortical

localization domain in its C-terminus (Yu *et al*., 2002) and the C-terminus of mouse LGN exhibits similar cortical localization when expressed in fly neuroblasts (Yu *et al*., 2003a). Gα subunits have been found segregated onto the plasma membrane and membranes of several organelles such as the endoplasmic reticulum, golgi complex, and the nucleus (de Almeida *et al*., 1994; Ercolani *et al*., 1990; Stow *et al*., 1991). Based on the localization data and interaction of LGN with heterotrimeric G-proteins, it is plausible to suggest that during mitosis, LGN is released from the perinuclear domain and becomes accessible to binding by plasma membrane-associated heterotrimeric G-proteins.

The functional significance of the cell cycle-dependent cortical localization of LGN is not yet clear. It is interesting to note here that LGN localization to the cell cortex during mitosis is somewhat similar to what is described for fly Pins. In *Drosophila*, Pins is normally found in the lateral cortex of epithelial cells and only become asymmetrically localized upon the expression of *inscuteable* in neuroblasts, for which a mammalian homolog has not been found so far (Yu *et al*., 2000 and Schaefer *et al*., 2000). Pins is also dependent on heterotrimeric G-protein activity for its localization (Schaefer *et al*., 2001). Furthermore, Pins plays important roles in neuroblast asymmetric cell divisions and the available data suggests that its interaction with Gα facilitates receptor-independent G-protein signaling (Scheafer *et al*., 2000, 2001). Interestingly, the mouse *LGN* gene reported in this study can also bind fly Inscuteable and rescue defects associated with *pins* mutations in the fly (Yu *et al*., 2003a), showing functional conservation. In conclusion, LGN and Pins share the domains required for cortical localization and both proteins can assume this dynamic localization depending on the presence of a suitable partner.

LGN, like other Pins-related proteins, complexes with Gα subunits of heterotrimeric G-proteins and inhibits dissociation of GDP from $G\alpha_i$ (Mochizuki *et al*., 1996; Natochin *et al.*, 2000; Bernard *et al*., 2001; DeVries *et al*., 2000; Peterson *et al.,* 2000; Scheafer *et al.*, 2000). Whether LGN interferes with G-protein activity at the plasma membrane remains to be determined. Interestingly, interfering with LGN expression causes cell cycle arrest. However, the cell cycle arrest at the G1/S stage is incomplete as we were still able to find some treated cells in the mitotic phase. The role of LGN in cell cycle progression may be due to interference with G-proteins activity or the function of some other protein(s) at different cellular sites. Interestingly, a nuclear localization for LGN has also been reported (Blumer *et al.*, 2002).

## 3.4 Future Directions

The role of C terminal mediated cortical localization in a cell cycle dependent manner is still not clear and the question whether or not LGN is required at the nucleus or other subcellular sites for the cell cycle progression is still not clear and further investigations are required to address these issues. Also work from other systems indicates that heterotrimeric G-protein and Pins interaction is important for spindle orientation and spindle asymmetry generated during asymmetric cell division (Cai *et. al*., 2003). In this respect, it would be interesting to specifically express the C-terminal of LGN in dividing polarized MDCK cells to analyze its effect on spindle orientation.

# CHAPTER 4 : Characterization of the LGN/AGS3 homologs from zebrafish: *LGN* is required for proper formation of primary motorneurons in the zebrafish embryo

## 4.1 Background

Studies in *Drosophila* have shown that LGN-related Pins binds Inscuteable via its N-terminal TPR domains and plays important roles in invertebrate development by controlling asymmetric cell division during neurogenesis. In mammals, the N-terminal TPR domains of LGN mediate binding to NuMA and this subsequently blocks the ability of this protein to stabilize microtubules (Du *et al*., 2001; Du *et al*., 2002). Mammalian LGN also binds to LKB1 serine/threonine kinase via its N-terminal TPR domains, which can then phosphorylate the C-terminal GoLoco motifs in AGS3 and reduce its ability to bind heterotrimeric G-proteins (Blumer *et al*., 2003). This interaction is evolutionarily conserved in *Drosophila*. Other studies have also described various cell cycle-dependent subcellular localizations for LGN in mammalian cell culture systems and its function in cell cycle progression (Blumer *et al*., 2002; Blumer and Lanier, 2003; Kaushik *et al*., 2003; Fuja *et al*., 2004). Recently, it has been shown that mammalian LGN is able to substitute for all Pins functions in *Drosophila* asymmetric neuroblast division (Yu *et al*., 2003).

So far the function of LGN/AGS3 proteins during vertebrate development has not been reported. In vertebrate animal systems, LGN and AGS3 are detected in various tissues including brain and they are differentially regulated during development, which may be indicative of distinct functionality. In order to study the function of these

proteins in vertebrate nervous system development, I have identified the zebrafish, homologs of LGN/AGS3 and analyzed the consequences of LGN removal and overexpression on neuronal formation.

As a model species, *D. rerio* offers many advantages. It is small in size and has high fecundity and embryos develop externally and are transparent during embryogenesis which also allows high resolution analysis of gene expression often at a single cell level. The genome is almost completely sequenced and full length expressed sequence tags (ESTs) are largely available. For simplicity, I focused my study on primary motorneurons (PMNs) which are the first motorneurons to form within the spinal cord in zebrafish. PMNs can be divided into three subtypes: rostral primary (RoP), middle primary (MiP) and caudal primary (CaP). At mid-somitogenesis stages only CaPs can be identified by *islet2* expression, with one *islet2*-positive PMN per spinal hemisegment (Appel *et al*., 1995; Lewis *et al*., 2001; Lewis *et al*., 2004). Any alterations to this simple pattern in a mutant background can be easily identified. This system also allows for the study of interaction between mutant backgrounds and important signaling pathways such as the Hedgehog (Hh) pathway. The data described in this chapter shows that *LGN* but not *AGS3* is enriched in the embryonic central nervous system at mid-somitogeneis stages in zebrafish and that LGN plays important negative roles in the formation of proper number of primary motor neurons in the developing embryonic spinal cord. The data also suggests that LGN may negatively interfere with Hh signaling pathway in Hh target cells to allow the formation of only one *islet2*-positive PMN per spinal hemisegment in zebrafish.

## 4.2 Results

### 4.2.1 Identification of LGN/AGS3 homologs in zebrafish

Members of the LGN/AGS3 family of heterotrimeric G-protein regulators have been characterized in several vertebrate and invertebrate species including human, mouse, rat, *Drosophila* and *C. elegans* (Takesono *et al*., 1999). In order to study the function of LGN in vertebrate nervous system development, zebrafish *LGN (LGN)* and zebrafish *AGS3 (AGS3)* were identified by homology searches. In zebrafish, *LGN* and *AGS3* appear to be paralogues, formed by duplication after divergence of vertebrates and flies.

#### 4.2.1.1 Identification of LGN

To isolate the zebrafish homologs of *LGN*, we searched zebrafish EST databases with the deduced amino acid sequences from mouse *LGN* and its *Drosophila* homolog, *Pins*. One partially sequenced EST clone, RZPD clone ID: CHBOp575c0517Q3, showed significant homology to both LGN and Pins. This zebrafish EST clone was obtained from RZPD and its full sequence was determined and deposited in Genbank under accession number AY619722. This full length cDNA comprises of 2430 nucleotides and encodes for an open reading frame of 647 amino acids with a predicted protein size of 72Kda. The deduced amino acid sequence of this putative protein contains seven N-terminal TPRs and four C-terminal GoLoco motifs (Fig. 4.1A) and is 66.0% identical to mouse LGN, 54.8% identical to rat AGS3 and 45% identical to fly Pins (Fig. 4.1B). As this putative zebrafish protein shares a higher identity percentage with mouse LGN than with rat AGS3, I named it LGN.

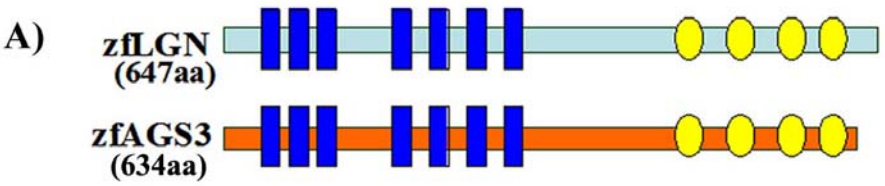


B)

| | zfLGN | zfAGS3 |
|---|---|---|
| mLGN | 66.0% | 57.5% |
| ratAGS3 | 54.8% | 65.3% |

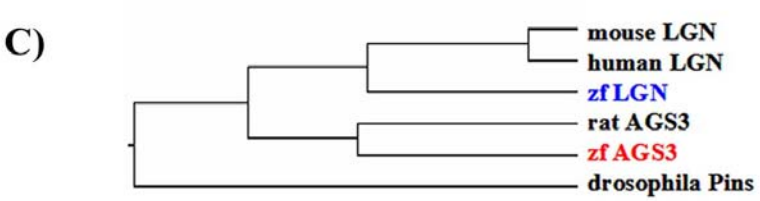


**Figure 4.1 Structural domains and sequence similarities of the zebrafish LGN/AGS3 proteins.**

A shows a schematic representation of the conserved domains structure of LGN and AGS3; both proteins contain seven N-terminal TPR domains (in blue) and four C-terminal GoLoco motifs (in yellow). B is a table showing the degree of amino acid identity between LGN, AGS3 from zebrafish and their counterparts from mouse (mLGN) and rat (AGS3); LGN shares highest identity (66.0%) with mLGN whereas AGS3 shares highest identity (65.3%) with rat AGS3. C is a phylogenetic tree for the LGN/AGS3 proteins from different vertebrate and invertebrate species.

#### 4.2.1.2 Identification of AGS3

The homology search also identified another partially sequenced EST clone in the zebrafish database, RZPD clone ID: MPMGp609B0724Q8. This EST clone was fully sequenced and found to contain an incomplete ORF truncated at the 3'-end. The complete cDNA sequence of this gene was obtained following RACE-amplification of the remaining 3' sequences that were missing in the EST clone and it was deposited in Genbank under accession number: AY619723. The complete ORF of this gene codes for 634 amino acids and shares 57.5% identity with mouse LGN and 65.3% identity with rat AGS3 (Fig. 4.1B). As this putative zebrafish protein shares a higher identity percentage with rat AGS3 than with mouse LGN, we named it AGS3.

### 4.2.2 Expression pattern of *LGN* and *AGS3*

As a first step in this study, expression patterns of *LGN* and *AGS3* during development of zebrafish embryos were examined by performing whole mount in-situ hybridizations with DIG-labeled antisense probes. The antisense probes detected *LGN* and *AGS3* signals throughout embryonic development and starting at very early stages, suggesting that the *LGN* RNA and the *AGS3* RNA are both maternally deposited.

#### 4.2.2.1 Expression pattern of *LGN*

The *LGN* transcript is ubiquitously expressed at the 8-cell stage (Fig.4.2A) and sphere stage (Fig. 4.2B). Enrichment of *LGN* transcript at the dorsal side of the embryo becomes discernible at the 60% epiboly stage (Fig. 4.2C ) and in 72hpf embryos, the *LGN* transcript becomes localized to the central nervous system in the developing head region and to segmentally repeated neuromast cells (Fig. 4.2H-I).

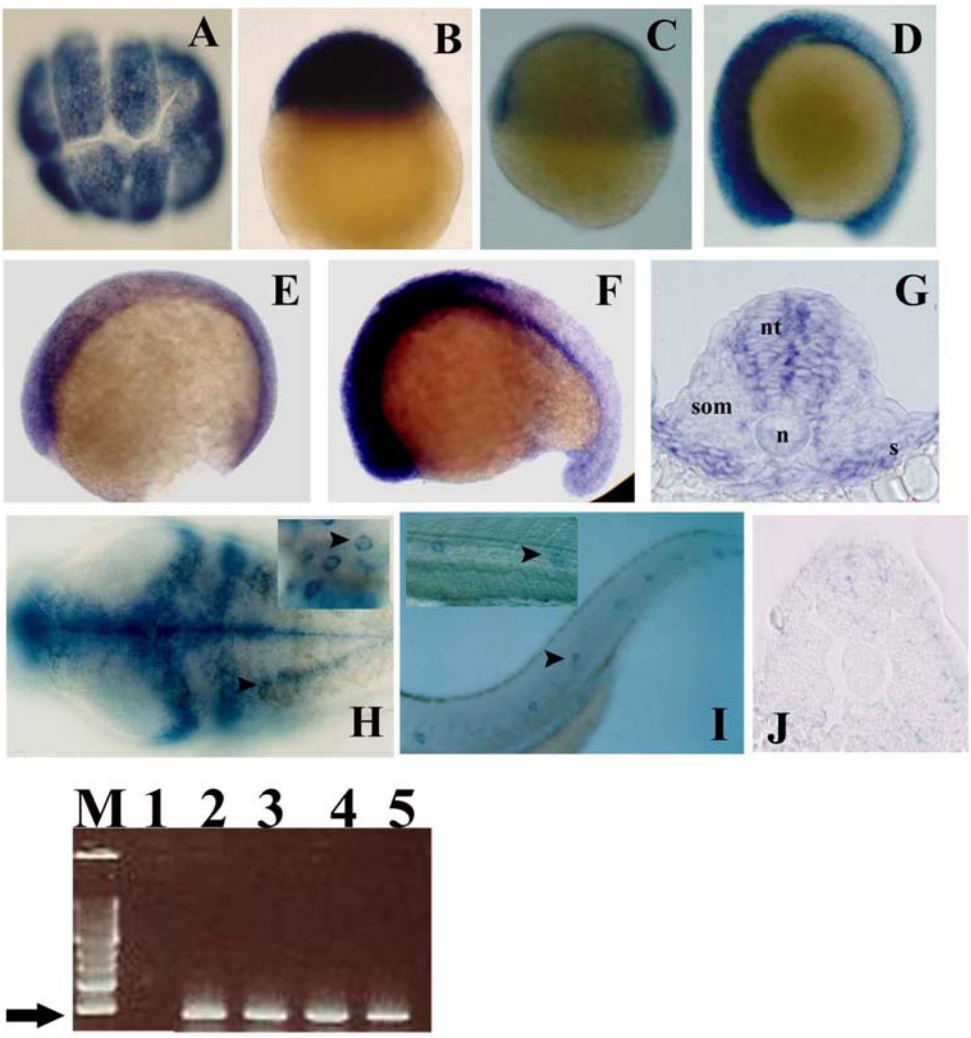


**Figure 4.2 RNA expression patterns of *LGN* in the developing zebrafish embryo.**

The RNA expression patterns of *LGN* A-I. Panel A is a top view of 8-cell stage; panel B shows lateral view of sphere stage embryo; panel C is the lateral view of 60% epiboly stage embryo showing enrichment of *LGN* at the dorsal side; panels D and E are lateral views of shield and 6 somites stage embryos showing that *LGN* is highly expressed in the developing head and brain region respectively. Panel F is a 18 somite stage embryo showing that the *LGN* transcript levels remain high in the anterior part of the embryo but are lower in the trunk; panel G is a cross section at the trunk level of 22 somites stage embryos showing *LGN* expression in the neural tube (nt) and sclerotome (s) ; at this stage, *LGN* (E) is not detected in notochord (n) . Panel H and I show expression of *LGN* in 72hpf embryo. *LGN* staining is intense in the head region (H) and further localized to groups of neurons in the head (inset arrowheads in H). *LGN* transcript is also present in segmentally repeated neuromast cells in the posterior part of the embryo(I). Panel J is a cross section at the trunk level of a 22 somite stage embryo hybridized with a DIG-labelled sense proble against *LGN*. The autoradiogram shows the results of RT-PCR performed on total RNA using primers based on *LGN* sequence. Lane 1 is negative control where total RNA from mouse tissue was used. Lane 2 contains total RNA from 64-128 cell stage embryo while Lanes 3, 4 and 5 contain total RNA from 60% epiboly, 18 somite stage and 26somite stage zebrafish embryo respectively. The arrow shows the location of 500 bp position on the DNA marker (marked as lane M).

Cross sections of embryos at 22 somite revealed high enrichment of *LGN* transcript in the central nervous system and the sclerotome (Fig. 4.2G) The *LGN* transcripts is not detected in the notochord, which is the source for important signals such as Hedgehog (Fig. 4.2G). RNA *in-situ* hybridizations of embryos with negative control DIG-labeled sense probes did not yield any signals.

#### 4.2.2.2 Expression Pattern of *AGS3*

*AGS3* transcript is ubiquitously expressed at 4 and 8-cell stages (Fig.4.3A-B) and differential expression patterns for *AGS3* transcript becomes visible in the somites of the developing embryo during epiboly stages and during somitogenesis (Fig.4.3C-F). Cross sections through the trunk of 22 somites embryos revealed enrichment of the *AGS3* transcript mainly in the somitic myotome (Fig4.3G). Like *LGN* the *AGS3* transcript is not detected in the notochord, which is the source for important signals such as Hedgehog (Fig. 4.3G). RNA *in-situ* hybridizations of embryos with negative control DIG-labeled sense probes did not yield any signals.

#### 4.2.2.3 LGN and AGS3 directly interact with Gα subunits of G-proteins.

LGN-like proteins are characterized by the presence of C-terminal GoLoco motifs, which bind Gα subunits of heterotrimeric G-proteins (Siderovski *et al*., 1999; Natochin *et al*., 2000; De Vries *et al*., 2000; Bernard *et al*., 2001). Like their vertebrate and invertebrate homologs, LGN contains C terminal GoLoco motifs and are expected to bind Gα. In order to test this, LGN and AGS3 were *in-vitro* translated in the presence of $^{35}$S-Methionine and radiolabeled products were mixed with GST-Gαio and Gαi3 or GST alone in the *in-vitro* binding assay (see materials and methods section 2.3.7 for details). The bound products were analyzed by SDS-PAGE.

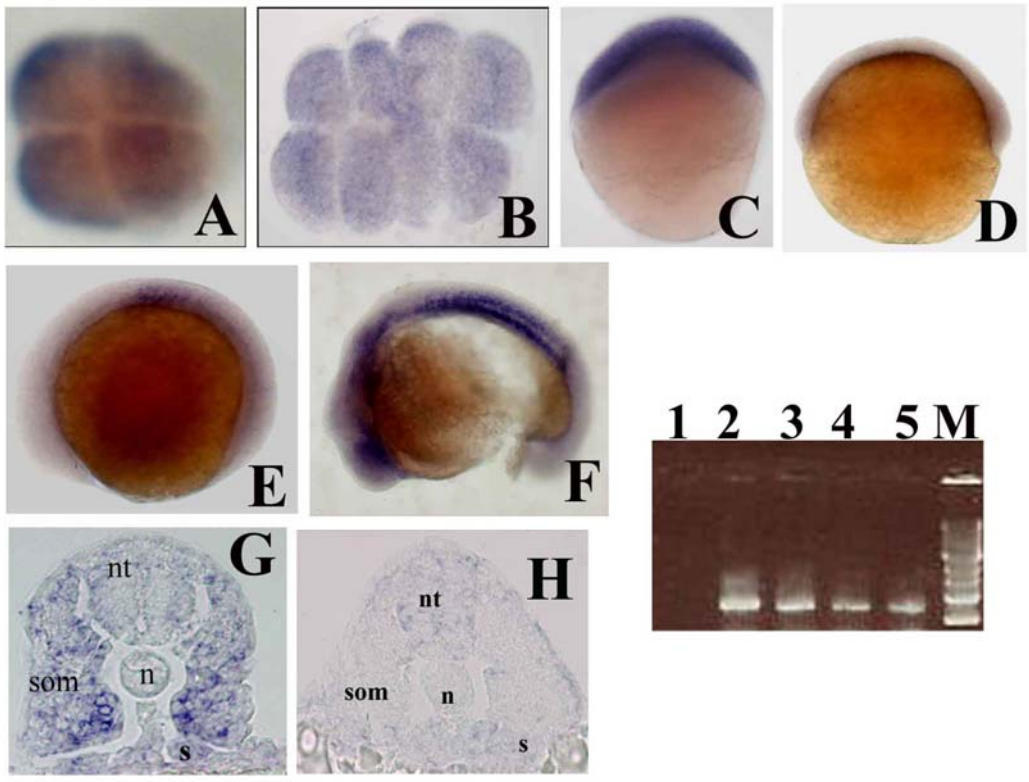


**Figure 4.3 RNA expression patterns of *AGS3* in the developing zebrafish embryo.**

Panels A and B are top views of 4-cell and 8-cell stage embryos showing ubiquitous expression of the *AGS3* transcripts; panels C is lateral view of sphere stage embryo and D is lateral view of 60% epiboly stage embryos showing enrichment of *AGS3* at the dorsal side; panels E is lateral view of 6 somites stage embryo showing that *AGS3* is hardly expressed in the head and brain region but mainly detectable in the CNS.Panel F is a 22 somites stage embryo showing that the *AGS3* transcript expression in both anterior and trunk regions. Panel G is a cross section at the trunk level of 22 somites stage embryos showing *AGS3* expression in the myotome (m) and *AGS3* is not detected in the neural tube (nt), notochord (n) and scelerotome (s). The autoradiogram shows the results of RT-PCR performed on total RNA. Lane 1 is negative control where total RNA from mouse tissue was used. Lane 2 contains total RNA from 64-128 cell stage embryo while Lanes 3, 4 and 5 contain total RNA from 60% epiboly, 18 somite stage and 26somite stage zebrafish embryo respectively. The arrow shows the location of 500 bp position on the DNA marker (marked as lane M).

In this assay, AGS3 was able to bind to both GST-Gαi3 and Gαo (Fig4.4B) and this binding is dependent on the presence of GDP in the assay. However, LGN showed stronger binding to Gαi3, while its binding to Gαo was weak (Fig4.4A). LGN binding to Gαi3 was also dependent on the presence of GDP in the assay.

#### 4.2.2.4 LGN is a guanine dissociation inhibitor(GDI) for Gαi3 and Gαo

LGN/AGS3 proteins are known to bind GDP-Gαi/o subunits and they are able to inhibit the rate of exchange of GDP for GTP on these subunits *in-vitro*, thereby acting as guanine dissociation inhibitors or GDI (Kaushik *et al*., 2003; Natochin *et al*., 2001). As shown in the previous section 4.2.2.3, LGN and AGS3 can bind Gαi/o subunits *in-vitro*. Since these proteins are highly homologous, they are expected to exert a GDI function on Gα subunits. To check this, an *in-vitro* GDI assay was carried out using Gαi3 and Gαo subunits. The results show that as expected both LGN and AGS3 acts as GDI for Gαi3 and Gαo but with varying degree of intensity (Fig. 4.5A-B). LGN inhibited the rate of exchange for Gαi3 by ~70% but its GDI activity towards Gαo was less at ~40%. In contrast, AGS3 had higher inhibition on Gαo (~80%) than on Gαi3 (~40). These results indicate that even though LGN and AGS3 are both capable of providing the GDI function, they exhibit different degree of GDI activity on different Gα subunits, which may be crucial for their in vivo function.

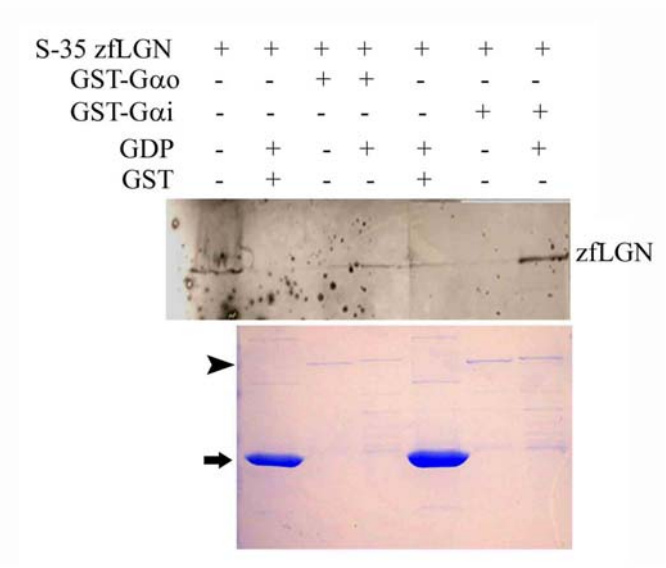


**Figure 4.4A Binding of zebrafish LFN to $G\alpha_{i/o}$.**
In the *in-vitro* binding assay, $^{35}S$ - Methionine labeled LGN was mixed with GST or GST-$G\alpha_i$ or GST-$G\alpha_o$ as indicated by the + and the - signs above. Bound products were separated by SDS-PAGE, dried and autoradiographed. The top panel shows the autoradiogram and the bottom panel shows the Coomassie blue staining of GST(arrow) and GST- $G\alpha_i$ (arrowhead) GST-$G\alpha_o$ (arrowhead) proteins used in this assay. LGN shows binding to GST-$G\alpha_i$ or GST-$G\alpha_o$ in presence of GDP but not to GST alone. The first lane in the top panel is the amount of $^{35}S$ - Methionine labeled LGN used in each experiment.

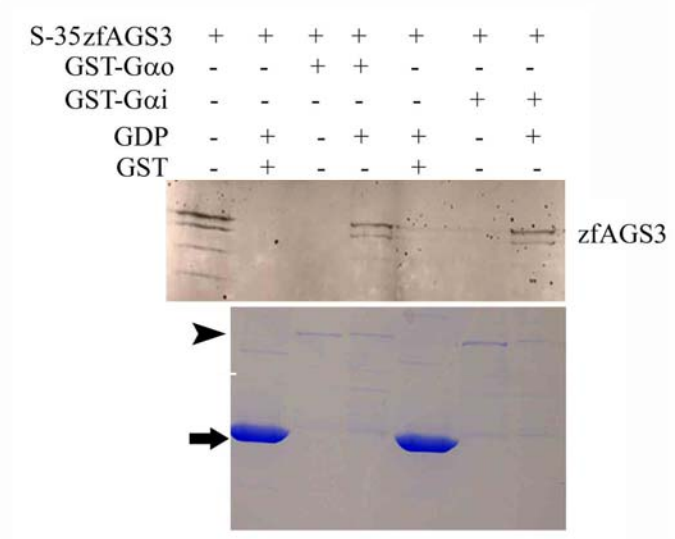


**Figure 4.4B Binding of zebrafish AGS3 to $G\alpha_{i/o}$.**
In the *in-vitro* binding assay, $^{35}S$ - Methionine labeled AGS3 was mixed with GST or GST-$G\alpha_i$ or GST-$G\alpha_o$ as indicated by the + and the - signs above. Bound products were separated by SDS-PAGE, dried and autoradiographed. The top panel shows the autoradiogram and the bottom panel shows the Coomassie blue staining of GST(arrow) and GST- $G\alpha_i$ (arrowhead) GST-$G\alpha_o$ (arrowhead) proteins used in this assay. AGS3 shows binding to GST-$G\alpha_i$ and GST-$G\alpha_o$ in presence of GDP but not to GST alone. The first lane in the top panel is the amount of $^{35}S$ -Methionine labeled AGS3 used in each experiment.

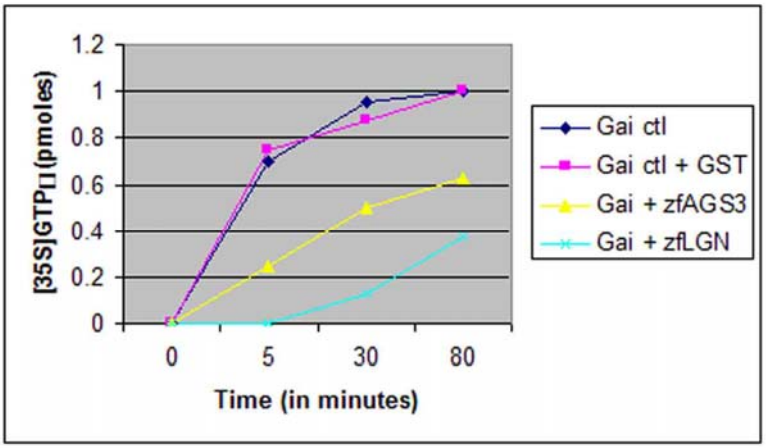


Figure 4.5A Zebrafish LGN and AGS3 can act as a GDI for $G\alpha_{i3}$
Time course experiments showing the rate of [$^{35}$S]GTPγ binding by $G\alpha_{i3}$ were carried out in the presence of 1mM GST- LGN (cyan), GST-AGS3 (yellow). Control experiments using GST alone are shown in pink and control experiment without GST is shown in black. GST-LGN inhibits 70% of [$^{35}$S]GTPγ binding to $G\alpha_{i3}$ and GST-AGS3 inhibits about 40% of [$^{35}$S]GTPγ binding to $G\alpha_{i3}$. The GST control has no effect on [35S]GTPg binding to $G\alpha_{i3}$. The effect of LGN, AGS3 on $G\alpha_{i3}$ activity is observed as early as 5 minutes and lasts over the 80 minute time period. All the experiments were repeated three times and their average is shown above.

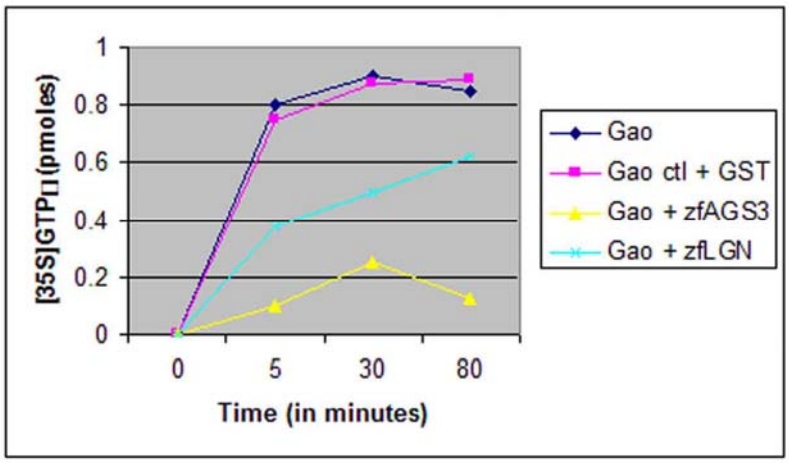


Figure 4.5B Zebrafish LGN and AGS3 can act as a GDI for $G\alpha_o$.
Time course experiments showing the rate of [$^{35}$S] GTPγ binding by $G\alpha_o$ were carried out in the presence of 1mM GST- LGN (cyan), GST-AGS3 (yellow). Control experiments using GST alone are shown in pink and control experiment without GST is shown in black. GST-LGN inhibits 40% of [$^{35}$S] GTPγ binding to $G\alpha_o$ and GST-AGS3 inhibits about 80% of [$^{35}$S] GTPγ binding to $G\alpha_o$. The GST control has no effect on [$^{35}$S] GTPγ binding to $G\alpha_o$. The effect of LGN, AGS3 on $G\alpha_o$ activity is observed as early as 5 minutes and lasts over the 80 minute time period. All the experiments were repeated three times and their average is shown above.

### 4.2.3 Effect of Removal and overexpression of LGN in zebrafish embryos

#### 4.2.3.1 Role of LGN in primary motor neuron formation

Since the *LGN* transcript is strongly expressed in the developing central nervous system of zebrafish embryos, we checked whether or not *LGN* is required for neuronal formation by injecting embryos with a *LGN*-specific antisense morpholino and determining neuronal phenotypes using *islet2* as a neuronal marker. On western blots, the LGN protein levels were downregulated by *LGN-MO* but they were not affected by the negative control *LGN-mismatchMO* or unrelated *fgf3-MO* (Fig. 4.6), suggesting that LGN was specifically knocked down by *LGN-MO*. In addition, the presence of *LGN-MO* but not the negative control *LGN-mismatchMO* inhibited LGN translation in *in-vitro* translation assays (Fig. 4.6B). In this assay, *LGN-MO* had no effect on the translation of a luciferase cDNA control unrelated to LGN (Fig. 4.6B, lane 6), indicating that *LGN-MO* is specifically inhibiting LGN translation.

Using *islet2* as a neuronal marker, an increase in the number of primary motoneurons was observed in *LGN-MO*-injected embryos (Fig. 4.7B). In 22 hpf wt embryos, *islet2* normally labels two rows of cells, the ventral primary motoneurons (PMNs) and the dorsal Rohan Beard (RB) sensory neurons (Tokumoto *et al*., 1995; Fig. 4.7A). In *LGN-MO*-treated embryos, multiple *islet2*-positive PMNs were observed as compared to one per somite in the wt embryo (Fig. 4.7B). Conversely, over expression of LGN by injecting *LGN* mRNA into the embryo resulted in reduction in the number of *islet2*-positive PMNs (Fig. 4.7C). However, a DAPI counterstain would

be useful in order to determine that only islet-2 positive PMNs are affected in these embryos and not dorsal sensory RB neurons which is not clear from these results.

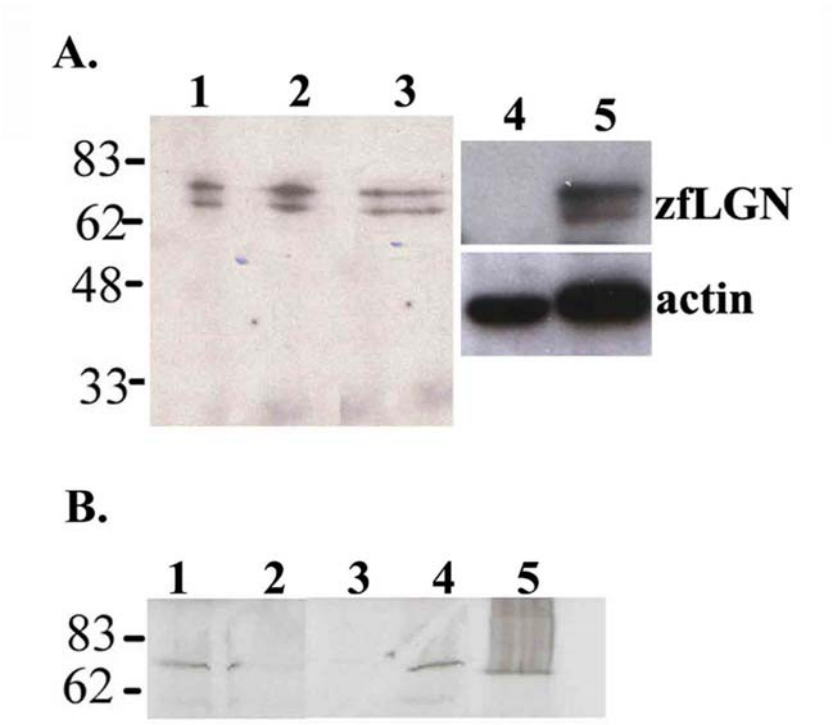


**Figure 4.6 Downregulation of zebrafish LGN protein levels by morpholino.**

A shows two immunoblots (Lanes1-3; Lanes 4-5) of total cell lysates from 22 hpf stage embryos hybridized with anti-LGN antibody. In wt untreated embryos (Lanes 1, 5), two closely segregating protein bands of ~72-74 Kda in size are present. The LGN protein bands are in the range of the expected size of LGN as deduced from its amino acid sequence (647aa). The LGN protein bands are unaffected in negative controls *LGN-mismatchMO*-treated (Lane 2) and LGN-unrelated *fgf3-MO*-treated (Lane 3) embryos but they are absent in embryos treated with *LGN-MO* (Lane 4). This shows that LGN is specifically knocked down by *LGN-MO*. For lanes 4-5, actin was used as loading control. B shows the effect of morpholino on LGN translation in *in-vitro* translation assays; the radiolabeled LGN protein product is present in the control (Lane 1) and its translation is not inhibited by the presence of 0.5mM negative control *LGN-mismatchMO* (Lane 4). The presence of *LGN-MO* at 0.5mM (Lane 2) and 0.25 mM (Lane3) specifically inhibits the translation of LGN in the in vitro assay but not the translation of LGN-unrelated luciferase control (Lane 5). In the luciferase reaction, *LGN-MO* was used at 0.5mM.

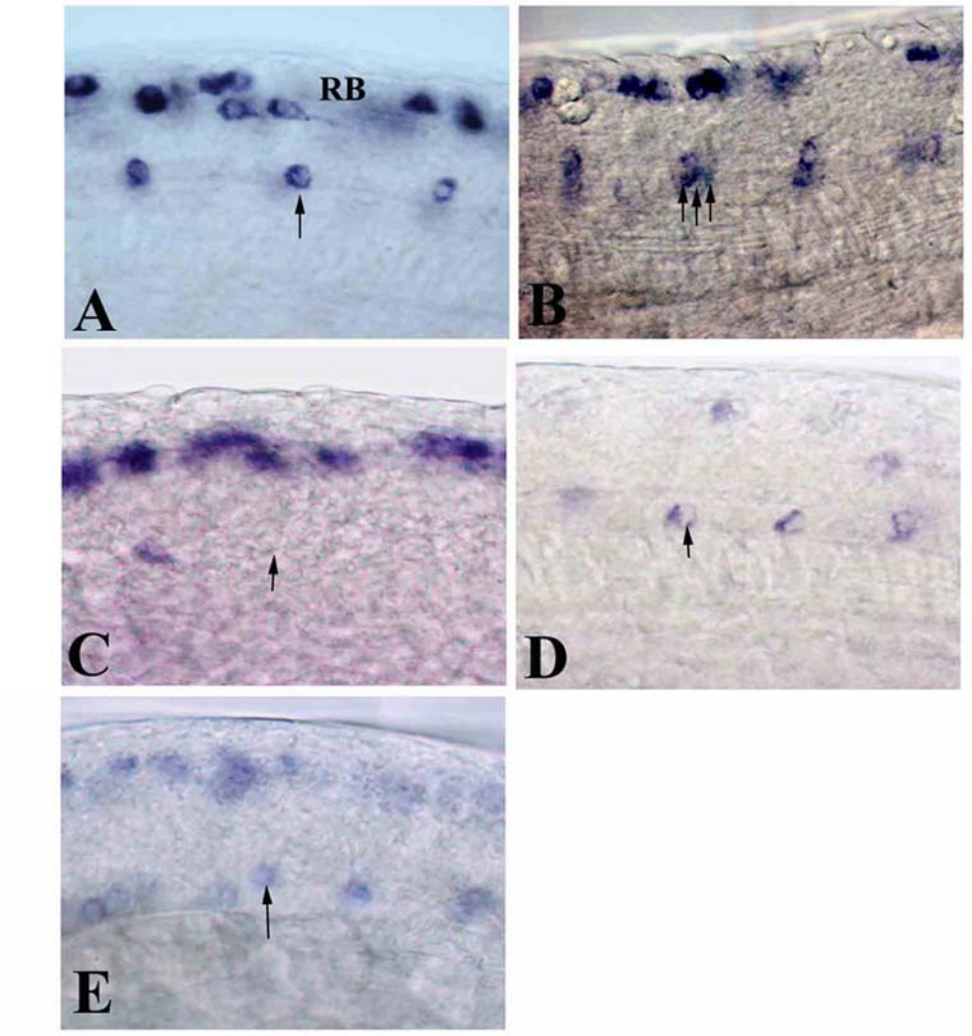


**Figure 4.7 Effects of LGN on primary motoneurons formation.**

Lateral views of trunk regions from 22 hpf zebrafish embryos that were hybridized with *islet-2* as a probe are shown in A-E; panel A is a representative image from a control embryo showing two rows of *islet2*-positive cells, the ventral PMNs (one per somite, arrow) and the dorsal RB sensory neurons; panel B shows multiple *islet2*-positive PMN formation in an embryo injected with *LGN-MO*; panel C shows loss of *islet2*-positive PMNs (arrow) in an embryo overexpressing LGN; panel D is an embryo overexpressing *AGS3* with no effect on the number of *islet2*-positive PMNs (arrow) but the number of RBs is reduced; panel E is an embryo injected with pertussis toxin RNA showing no change in the number of *islet2*-positive PMNs (arrow).

The data suggests that LGN normally inhibits the formation of these PMNs in zebrafish embryos. The number of *islet2*-positive PMNs in anterior somites, 1-5, was not affected in this experiment. In contrast to the LGN phenotypes, injection of embryos with *AGS3* RNA or pertussis toxin RNA did not affect the number of *islet2*-positive PMNs (Fig. 4.7D,E)**.** These data suggest that LGN plays a negative role in the formation of ventral *islet2*-positive primary motor neurons in developing zebrafish embryos and its function in this process may be independent of its activity on heterotrimeric G-proteins signaling.

#### 4.2.3.2 Role of *LGN* in other tissues

The function of LGN is not restricted to the central nervous system as *LGN-MO*-injected zebrafish embryos displayed patterning defects (Fig. 4.8A-D) including blocky somites and disorganized tail, absence of a well-defined midbrain – hindbrain region, abnormal size and shape of the retina and changes in the number and size of otoliths in the otic capsule (Table 4.1). In addition, *LGN-MO*-injected embryos showed dramatic reduction in *twist* expression in both the scleortome and other twist positive cells (Fig. 4.9), suggesting that LGN plays a positive role in the differentiation of these tissues.

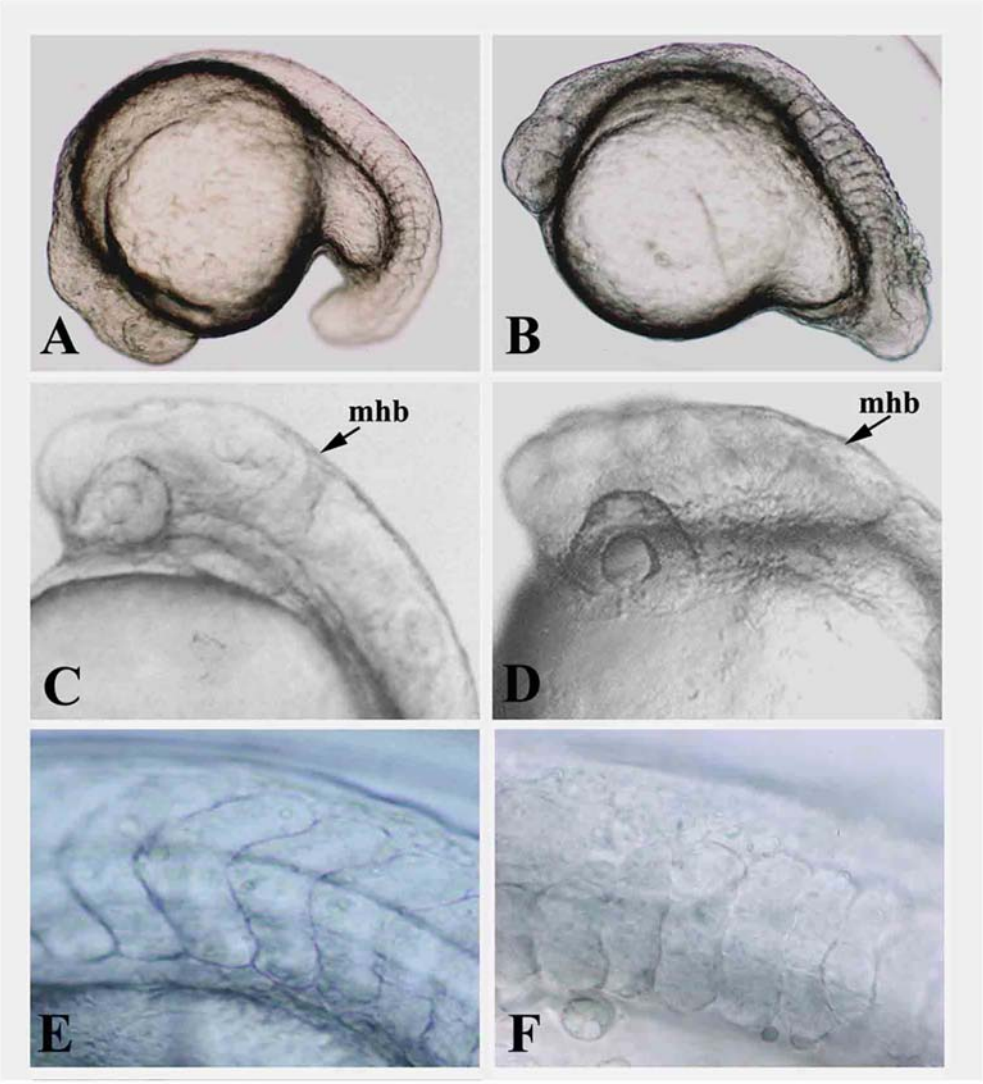


**Figure 4.8 Patterning defects of LGN-morphant embryos.**

DIC images of 18 somites stage embryos from control (A, C, E) and *LGN-MO* injected (B, D, F) experiments; C and E are high magnification views of A whereas D and F are high magnification views of B; the morphant embryo exhibits trunk and tail defects (B) and lacks a well-defined midbrain-hindbrain boundary (D, arrow); Panel F shows loss of chevron-shaped somites in the morphant embryo as compared to control (E).

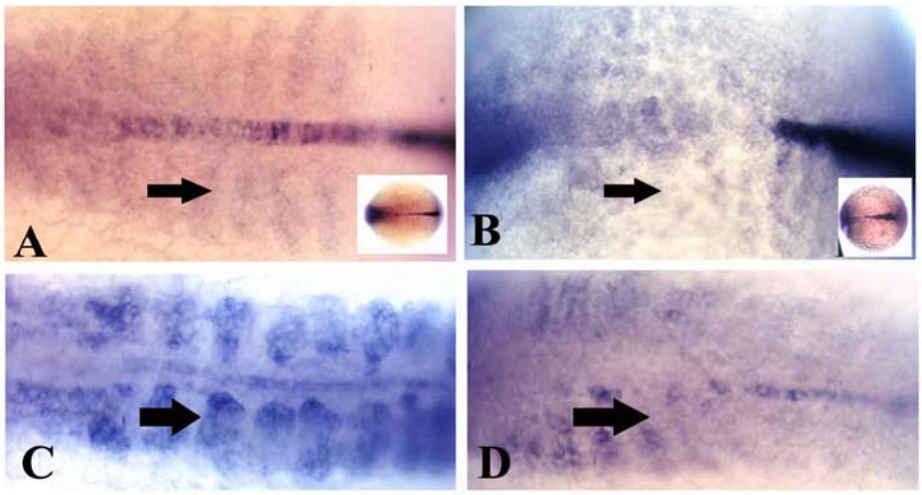


**Figure 4.9 zebrafish LGN loss results in loss of twist positive sclerotome cells.**

Panel A and B show *twist* RNA expression in 6 somite stage wt and *LGN*-morphant embryo and panels C and D show *twist* RNA expression in 18 somites stage wt and *LGN*-morphant embryos respectively; the expression domain of *twist* RNA in the presumptive sclerotome (arrows) and other twist expressing cells is dramatically reduced in the *LGN*-morphant embryo (B, D) as compared to wt (A, C). The inset in A and B shows the low magnification image of the *twist* RNA expression in 6 somite stage wt and *LGN*-morphant embryo. In all images, anterior is to the left.

**Table 4.1: Phenotypes seen in *zfLGN*-morphants**

| Phenotypes | | ***zfLGN- MO*** (0.5mM) | ***zfLGN-MO1*** (1mM) | ***zfLGN* mismatch MO** (1mM) |
|---|---|---|---|---|
| **Early** (18-22 somites) | blocky somites | ~78% | ~53% | 5% |
| | mhb misorganisation | ~64% | ~49% | 6% |
| **Late** (3 days) | defects in ears | ~13% | ~8% | 2% |
| | eye phenotypes | ~12% | ~5% | nil |

For each phenotype counted per treatment was repeated three times with about 150 embryos scored each time and the average percentage is shown above. For the late phenotypes, a defect in ears refers to changes in number and size of otoliths and eye phenotypes refers to changes in the shape and size of the eye.

## 4.2.4 Interaction of *LGN*-mediated signaling with other signaling pathways

### 4.2.4.1 *LGN* interferes with Hh signaling during specification of PMN fate

The proper induction and specification of PMNs fate is known to require the integration of many signaling pathways including the Hedgehog pathway. Based on the similarities between the *islet2* phenotypes associated with *LGN-MO* and *Shh* overexpression or those associated with *LGN*-overexpression and Hedgehog signaling downregulation, we simultaneously manipulated the levels of LGN and Hh and used *islet2* as neuronal marker for phenotypic analysis. Overexpression of LGN in embryos overexpressing Shh or PKI led to a partial rescue of the *islet2* expansion phenotype caused by Shh or PKI overexpression alone (Fig. 4.10 A, B-C), suggesting that LGN may have a negative influence on Hedgehog signaling pathway during PMNs formation.

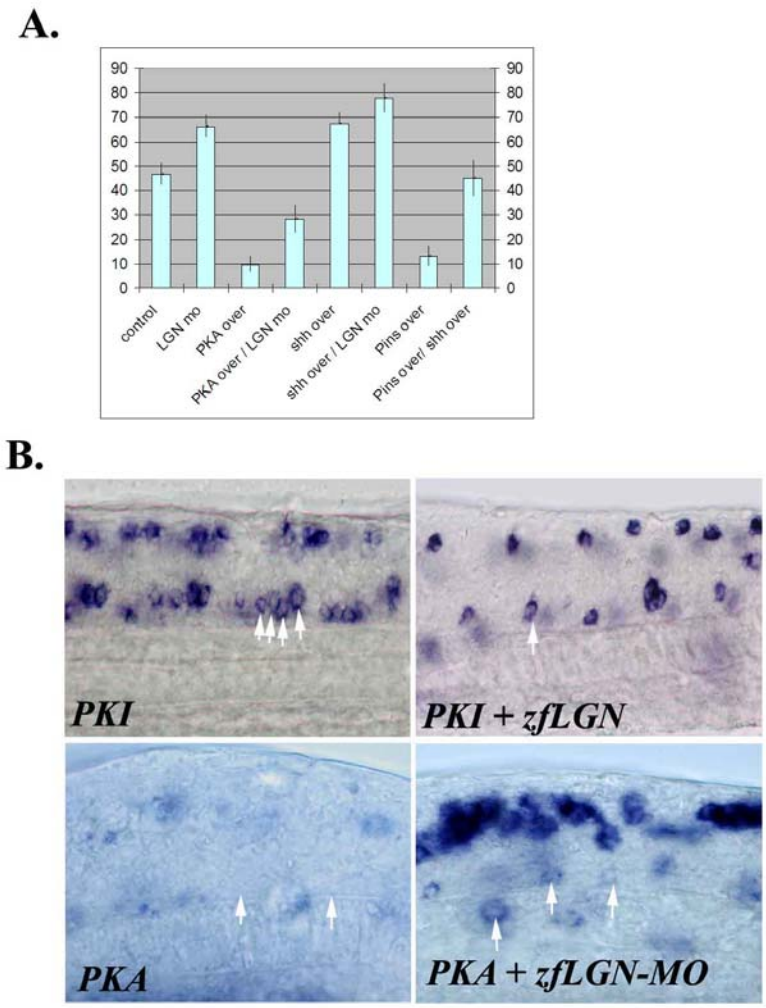


**Figure 4.10 Interference of LGN with hedgehog signaling during primary motorneurons formation in zebrafish embryos.**

A representative graph showing the average numbers of *islet2*-positive PMNs in 22 hpf zebrafish embryos of different genetic backgrounds is shown in A; the average number was derived from counting total numbers of *islet2*-positive PMNs in all somites from 15 embryos. Increase in the PMNs average number is observed in embryos injected with *LGN-MO* (average number ~68) or embryos overexpressing Shh (average number ~68) as compared to wt (average number ~48); combining *LGN-MO* injection with *Shh* overexpression leads to a further increase in the average number of PMNs (average number ~75) as compared to each one alone (average number ~ 68); combining *Shh* overexpression with *LGN* overexpression rescues (average number ~45) the *Shh* overexpression phenotype, indicating that *LGN* may have an antagonistic effect on Hh signaling pathway. *LGN* overexpression or *PKA* overexpression alone decreases the average number of PMNs to ~12 and ~8 (as compared to ~48 in wt) respectively; the phenotype of *PKA* overexpression can be partially rescued by simultaneous injection of *LGN-MO* (average number ~28). Overexpression of *PKA* inhibitor, *PKI*, leads to an increase in the average number of *islet2*-positive PMNs (~ 87) and this increase is partially reduced when *PKI* is coexpressed with *LGN* (~ 43). Lateral views of representative islet2-stained images are shown in B; the number of islet2-positive PMNs is increased upon *PKI* overexpression (*PKI*, arrows) and this phentotype is partially rescued by co-expressing *LGN* with *PKI*; simultaneous injection of *LGN-MO* in an embryo overexpressing *PKA* partially rescues the reduced PMNs phenotype observed in *PKA* overexpression alone.

Conversely, the *islet2* expansion phenotype caused by shh overexpression was enhanced by simultaneous injection of *LGN-MO* (Fig. 4.10 A). Furthermore, injection of *LGN-MO* into embryos overexpressing PKA partially rescued the PMNs-loss phenotype associated with PKA overexpression (Fig. 4.10 A, D-E), again suggesting that LGN might be exerting a negative regulatory role on Hedgehog signaling pathway. This LGN mediated rescue of excessive PMN numbers in case where LGN is overexpressed in conjunction with PKI is considered partial as although the overall number of the PMNs is close to wildtype levels, there are still clusters of multiple PMNs combined with some losses of PMNs (due to LGN overexpression) that leads to an overall numbers. Since the effect of LGN overexpression on PMNs seen is intermediate to that of PKI overexpression and LGN overexpression by themselves, I believe that the LGN does not show an obvious epistatic relationship with PKI in this respect and interferes with Hedgehog signaling in an indirect manner.

#### 4.2.4.2 Effects of LGN levels in the zebrafish embryo on expression of Hh target gene *patched*

Transduction of Hedgehog signals proceeds via interactions with multipass transmembrane proteins encoded by the patched (*ptc*) gene family. Patched acts to negatively regulate Hedgehog signaling by blocking the activity of smoothened (Wolff *et al*., 2003). The transcription of *ptc* itself is also positively regulated by Hedgehog signaling (Concordet *et al*., 1996). In wt zebrafish embryonic somites, *ptc* is expressed in Hedgehog target cells in the central nervous system and the myotome (Fig. 4.11 A,C). We reasoned that if LGN were to exert an effect on Hedgehog signaling pathway, manipulations of LGN levels should be expected to affect the expression of Hedgehog downstream target genes, such as *ptc*, in a corresponding manner. Consistent with this prediction, somitic *ptc* levels in both, the central nervous system

and the myotome, were dramatically reduced when LGN was ectopically expressed in the embryo (Fig. 4.11B lateral view), suggesting that ectopic LGN expression can contribute a negative effect on the expression of Hedgehog downstream target genes in Hedgehog target cells. In addition, injection of *LGN-MO* led to increased levels of *ptc* expression in the central nervous system, but did not affect its expression domain (Fig. 4.11D). The removal of LGN did not affect the levels of Hedgehog expression in the notochord (Fig.4.11E-F), which is the source of Hedgehog signals.

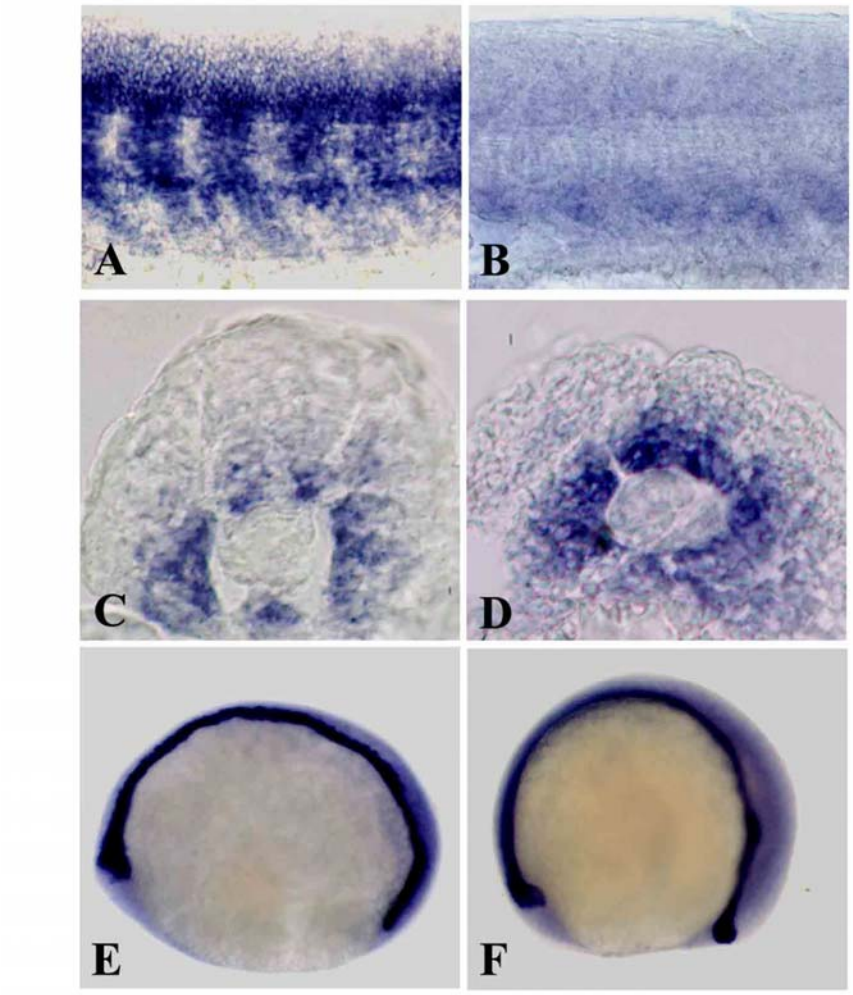


**Figure 4.11 Effects of *LGN* on *patched* RNA expression.**

18 somites stage embryos were hybridized with a *ptc* RNA probe (A-D) or shh RNA probe (E-F). Panels A (control) and B (LGN overexpression) are lateral views showing reduction in *ptc* expression levels in the *LGN*-overexpressing embryo (B) as compared to control (A); panels C (control) and D (*LGN-MO*-treated) are cross sections at the level of trunk showing no obvious effects on the expression domain of *ptc* in the neural tube but a relative increase in the intensity of *ptc* expression can be seen in the *LGN-MO*-treated embryo (D) as compared to control (C). *shh* RNA expression is not affected by *LGN-MO* (F) and it is similar to wt control (E).

## 4.3 Discussion

In this study, I have identified *LGN* and *AGS3* homologous genes from zebrafish, *LGN* and *AGS3*, and studied their expression patterns during embryonic development. I have shown that *LGN,* but not *AGS3* is expressed in the central nervous system and sclerotome and that LGN is required for the proper formation of primary motoneurons in the zebrafish embryo, possibly by antagonizing a Hedgehog signalling pathway. The deduced zebrafish LGN/AGS3 proteins are highly homologous to other members of the LGN/AGS3 family and they contain the conserved two domains structure characteristic for this family: TPR domains in the N-terminal domain and Gαi/o-binding GoLoco motifs in the C-terminal domain.

The TPR motifs serve a range of functions for LGN/AGS3 proteins in animals including binding to protein partners such as Inscuteable in *Drosophila* (Yu *et al*., 2002) and NuMA and LKB kinase in mammalian cells (Blumer *et al*., 2003; Du *et al*., 2001) and thereby affecting LGN trafficking, subcellular localization and ability to bind Gαi. The GoLoco motifs of LGN/AGS3 proteins mediate interaction with Gαi/o subunits of heterotrimeric G-proteins and inhibit dissociation of GDP from Gαi/o (De Vries *et al*., 2000; Kaushik *et al*., 2003; Natochin *et al*., 2000; Schaefer *et al*., 2000).

Based on their high sequence conservation, LGN/AGS3/Pins proteins are expected to fulfill similar functional interactions and we have recently shown that mammalian LGN can bind fly Inscuteable and replace all Pins functions in *Drosophila* (Yu *et al*., 2003), suggesting that protein domains in the LGN/AGS3 family members are conserved in structure and function across species. Like their counterparts, the

zebrafish LGN/AGS3 proteins are able to bind GDP-Gαi3/o and act as GDI for Gαi *in vitro*.

In zebrafish, *LGN* and *AGS3* show striking differences in their expression in embryonic somites, suggesting that they may have tissue-specific functions. *LGN* is enriched in the central nervous system and sclerotome but not the myotome in the zebrafish embryo. To address the function of LGN in the central nervous system, we focused our analysis on the *islet2*-positive PMNS for simplicity. Several observations support a role for LGN in the CNS for proper formation of primary motor neurons: firstly, *LGN* is expressed in the central nervous system; secondly, downregulation of LGN increases the number of *islet2*-positive PMNs; and thirdly, overexpression of LGN decreases the number of these primary motor neurons.

These observations suggest a negative role for LGN in the formation of PMNs. It is not yet clear how LGN affects PMN fate in zebrafish but it is apparent from the phenotypic interaction experiments that it exerts a negative influence on Hh signaling in this process. In zebrafish, as in other vertebrates, Hh signals from the embryonic midline induce motorneurons in the ventral neural tube (Lewis and Eisen, 2001).

However, the absence of a strict epistatic relationship between LGN and Shh/PKA suggests that the negative influence of LGN on a Hh pathway is most likely indirect. Still, the observation that the expression of the Hh downstream target gene *patched* is reduced in embryos ectopically expressing LGN, lends support to the notion that the "LGN pathway" can converge an inhibitory influence on the Hh pathway at the level of *patched* expression. One mechanism by which LGN may affect Hh signaling pathway is through its ability to affect heterotrimeric G-proteins signaling.

Interestingly, pertussis toxin, which normally blocks some types of heterotrimeric G-proteins signaling, has been shown to interfere with Hh signaling in the zebrafish

embryo with regards to controlling the binary cell fate choice of embryonic zebrafish myoblasts (Hammerschmidt and McMahon, 1998), but not in culture (Norris *et al*., 2000). Furthermore, Hh signaling has also been shown to be able to activate Gαo in culture (Decamp *et al*., 2000). Surprisingly, injection of embryos with pertussis toxin RNA has no effect on the number of *islet2*–positive PMNs. This suggests that the proper specification of these PMNs does not require toxin-sensitive heterotrimeric G-protein activity and that LGN may be acting via another mechanism in this process or in a subcellular compartment that is not accessible to the toxin.

The role of LGN during zebrafish development is obviously not restricted to the central nervous system as LGN morphant embryos also show patterning defects and a detectable decrease in the expression domain of *twist* which labels the presumptive sclerotome and other twist positive cells. LGN is expressed in the presumptive sclerotome and it may have a direct role in sclerotomal cells for their proper differentiation. The differentiation of this tissue has also been shown to be sensitive to pertussis toxin treatment (Hammerschmidt and McMahon, 1998), raising the possibility that LGN may be acting via heterotrimeric G-proteins in this process.

However, LGN removal and pertussis toxin treatment seem to produce opposite effects on *twist* expression, suggesting that LGN may have an inhibitory effect on heterotrimeric G-proteins signaling rather than the commonly expected LGN/AGS3 role of prolonging signal input to Gβγ effectors. It has been reported that cytosolic AGS3, but not membrane-associated AGS3, can interact with G(i)alpha subunits and disrupt their receptor coupling. Immunoblotting studies reveal that cytosolic AGS3 can remove G(i) alpha subunits from the membrane and sequester G(i)alpha subunits in the cytosol. These findings suggest that AGS3 may downregulate heterotrimeric G protein signaling by interfering with receptor coupling (Ma H et. al., 2003). Alternatively, it is

also possible to envisage functions for LGN in somite patterning independent of its activity on hetertotrimeric G-proteins and further experiments are needed to determine the mode of action of LGN in these important developmental processes.

Whatever the signaling complexity controlled by LGN , these observations point to an important function for this protein in the development of zebrafish. The observations described here highlight the function of LGN in the proper formation of primary motoneurons and sclerotome in the somites of developing zebrafish embryos. To my knowledge, this is the first study describing an in vivo function of LGN in a developing vertebrate embryo.

## 4.4 Future directions

The possibility of LGN negatively interfering with Hedgehog pathway opens up arena for testing other questions with regards to LGN function during growth and development. The exact mechanism of LGN-mediated control of *ptc* expression is not very clear at the moment, LGN in mammalian cells was shown to localize to the nucleus as well as cytoplasm and exactly how it regulates *ptc* transcription needs more investigation. A rescue of with *LGN* RNA lacking the sequence against which the *LGN-MO* was designed would also be very useful in order to determine the specificity of the phenotypes seen with the morpholinos. In addition, it is known that mutations in smoothened (smo), a gene that is required for Hh signalling, render cells unable to enter S phase and hence become arrested during the cell cycle. It might be interesting to overexpress *LGN* in this system and assess its role in cell cycle progression. More specifically, overexpression of N-terminal TPR containing region and C-terminal GoLoco motif containing regions can be expressed independently to analyse their effect on primary motor neuron formation. The role of AGS3 in this process also needs

to be evaluated using specific morpholinos made against *AGS3*. In addition, work on LGN in other systems indicating an important role for LGN/AGS3 family of proteins in regulating spindle dynamics and cell division, it would be very interesting to see whether or not LGN/AGS3 have any role in cell division and asymmetric protein localization, although this area of research is not fully developed in zebrafish. In addition, the discovery of novel G-protein isoforms and studying their roles in relation to *LGN* function during zebrafish development would allow for a better understanding of the signaling pathways in which *LGN* is involved.

# CHAPTER 5 : Characterization of *DRapGAP2*: its localization and requirement in the dbd neuron formation in *Drosophila* PNS

## 5.1 Background

GAPs are regulatory proteins for small GTPases such as Gα, Ras and Ras-like Rap proteins. They act as GTPase activating proteins that help increase the slow intrinsic GTPase activity in these enzymes by many orders of magnitude. The activation mechanism involves stabilization of the catalytic glutamine of the small GTPase and, in most cases, the insertion of a catalytic arginine of GAP into the active site. However for a Ras-like protein, Rap1 and its GAP (Rap1GAP), the activation mechanism seems to be different in that Rap1 does not possess the catalytic glutamine that is essential for GTP hydrolysis in all other Ras-like and Gα proteins. Also, Rap1GAPs are not related to other GAPs and although they have the conserved arginine residue, recent studies have highlighted that they do not use this catalytic arginine residue. Instead, Rap1GAP provides a catalytic asparagine to stimulate GTP hydrolysis (Scheffzek, *et al*., 1998; Daumke *et al.*, 2004).

RapGAP proteins have other conserved protein motifs in addition to the GAP domain that allows for interactions with proteins other than Rap1 and provides means for cross talking between signaling pathways (Mochizuki *et al*., 1999; Meng *et al*., 1999). RapGAPs contain GoLoco/GPR motifs that mediate binding with heterotrimeric G-proteins (Gα subunit). In humans, Rap1GAP has two alternatively spliced isoforms that differ in N terminal region. The Rap1GAP1 isoform 1 binds GTP- bound heterotrimeric G-protein alpha subunit and this interaction blocks the

ability of RGSs (regulators of G protein signaling- also known to act as GAPs for G-proteins) to stimulate GTP hydrolysis by Gα ( Meng *et al*., 1999). In humans, Rap1GAPII isoform 2 on the other hand, binds specifically to Gα upon GPCR stimulation and translocates from cytosol to the membrane where it can act as GAP for Rap1 and therefore decreases the amount of GTP-bound Rap1. This decrease in GTP-bound Rap1 activates ERK/MAPK (Mochizuki *et al*., 1999).

RapGAP proteins are highly conserved in structure and function during evolution from *Drosophila* to humans. In *Drosophila,* a *RapGAP1* isoform was initially isolated as a protein with high homology to human *Rap1GAP1* isoform I but unlike the human isoforms RapGAP1 does not contain GoLoco motifs in the N terminus of the protein (Chen *et al*., 1997). DRapGAP ESTs with GoLoco motifs encoding sequences have been isolated and this isoform is referred to as *RapGAP2*. Overexpression of RapGAP1 has been reported to cause rough eye phenotype that can be enhanced by reducing Rap1 gene dosage (Chen *et al*., 1997). Mutations that abolish *RapGAP1* function exist but no phenotypic abnormalities have been reported for these mutants. The work described in this chapter shows that RapGAP plays important role in the formation of the dorsal bipolar dendritic neuron (dbd neuron) lineage of PNS neurons. I have found that RapGAP is localized asymmetrically in SOPs and that RapGAP mutants show loss of dbd lineage of sensory neurons in the PNS.

The PNS of *Drosophila* is a very well-characterized model system for studying the genes involved in basic processes of neurogenesis. One particular type II neuron, dbd, is easily identifiable by its dorsal location and its bipolar dendritic shape. The dbd sensory neuron is the only type II neuron which has associated glia (Huang *et al*., 2000; Brewster and Bodmer, 1996). The sensory organ precursor (SOP) cell of the dbd neuron lineage is identified at the beginning of stage 12 as a large cell, weakly

expressing POU domain genes, *Pdm-1/2* in the anterior-dorsal region of abdominal segments. This cell divides asymmetrically (in terms of size of daughter cells) producing two unequal Pdm-1 positive cells, a larger one located basal to the smaller one. The larger cell expresses the neuronal marker protein, ELAV (embryonic lethal and abnormal vision) and differentiates as a dbd neuron (DBDN), while the smaller sibling cell expresses REPO (reverse polarity, glial cell marker) and becomes a dbd associated glial cell (DBDG) (Brewster and Bodmer, 1995). No further cell division has been reported for this lineage. Shortly after mitosis, *Pdm-1/2* genes are temporally downregulated in the presumptive glial cell and this coincides with *glia cell missing (gcm)* transcription being initiated. Upon establishment of high levels of gcm during stage 12 embryo, the *Pdm-1/2* expression is reinitiated in this glia cell. *gcm* expression remains at high levels during stage 12 and then disappears rapidly. Subsequently, *Pdm-1/2* expression is also downregulated in DBDG, resulting in expression of *Pdm-1* specifically to the DBDN at stage 16 (Dick *et al*., 1991; Lloyd *et al*., 1991) (Fig. 5.1). In addition to these genes, Notch and Numb play important roles in specifying cell fate in the dbd lineage (Brewster *et al*., 2001; Umesono *et al*., 2002).

## 5.2 Results

### 5.2.1 Identification of the GoLoco motif-containing isoform of *DRapGAP*, *DRapGAP2*.

Unlike the human RapGAPs, the previously reported RapGAP isoform in *Drosophila* does not contain GoLoco motifs (Chen *et al*., 1997). To identify the *Drosophila* RapGAP isoform with a Goloco motif, the *Drosophila* EST collection was searched for homology with human Rap1GAPII.

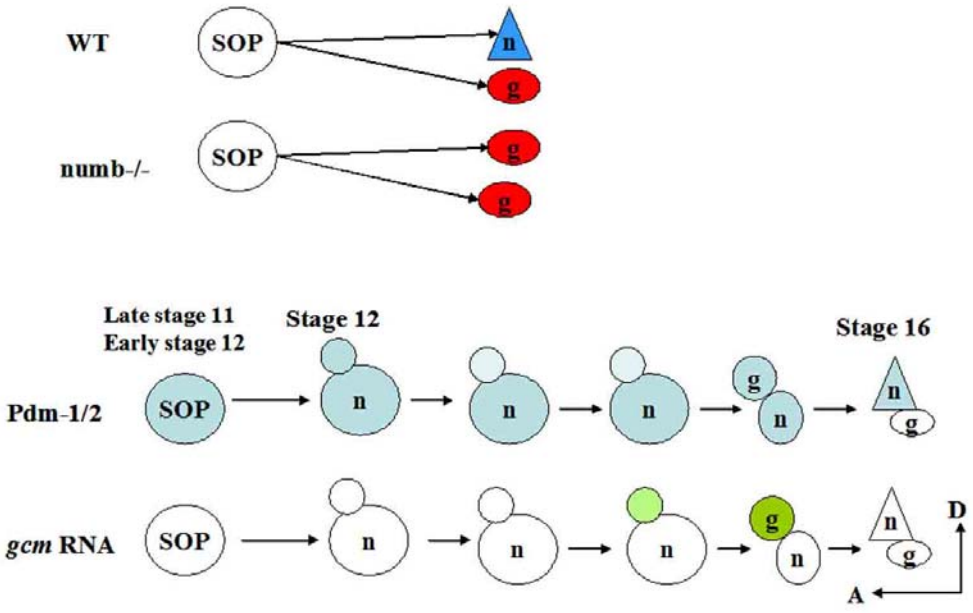


**Figure 5.1: Diagramatic representation of the dbd lineage in *Drosophila* embryonic peripheral nervous system.**
The precursor SOP cell divides and produces one dbd neuron and another glial cell in the wt embryo. In *numb* mutants there is no dbd neuron formed and instead two glial cells are formed indicating cell fate change of dbd neuron to glia. In wt, Numb segregates with the dbd neuron where it can block Notch signaling and allow neuronal fate specification. B) Summary of the expression dynamics of gcm mRNA (green) and Pdm-1/2 protein (blue) in the dbd lineage (based on Brewster et al., 2001 and Umesano et al., 2002). g, glial cell; n, neuron. Pdm-1/2 is initially detected in the SOP cell at stage 11. After SOP division, the smaller daughter cell located apicodorsally to the larger daughter cell differentiates as glia. Pdm-1/2 are down-regulated in the presumptive glial cell prior to the onset of gcm expression. The expression of gcm is initiated in the smaller daughter cell where Pdm-1/2 expression is low. After gcm becomes highly activated, Pdm-1/2 is re-expressed in the glial daughter cell. At stage 16, Pdm-1/2 expression is again restricted to the dbd neuron whereas gcm expression is no longer expressed in the glia cell at this stage. Dorsal is up.

One EST of 3.2 kb in size was pulled out and sequence analysis revealed a single long ORF that encodes a protein of 876 amino acids with a predicted molecular weight of 97 kDa (Fig. 5.2). The domain structure of an N-terminal GoLoco motif and central GAP domain in DRapGAP2 is conserved from human to *Drosophila*. The *RapGAP2* and the previously identified *Drosophila RapGAP1* isoforms result from alternatively splicing of the DRapGAP gene located on chromosome 2 cytological location 28A6. DRapGAP2 contains an additional N-terminal 26 amino acids that are not found in DRapGAP1 (Fig. 5.2).

The central region of 287 amino acids in DRapGAP1/2 comprising the GAP domain for Rap1 GTPase, displays 82% sequence similarity to human RapGAPII whereas, the N terminal region of DRapGAP2 comprising the GoLoco motif shares 94% similarity to human RapGAP1/II. In addition, in the C-terminal portion of both RapGAP1 and RapGAP2, there is a 9-amino acid stretch (DTGLESMSS) that is highly conserved and is found in both human RapGAP isoformsI and II (DTGLESVSS). This peptide is specific to RapGAPs and is not found in any other protein in the available protein databases, but the significance of this motif is unclear.

### 5.2.2 DRapGAP2 displays a GDI activity for Gαi *in-vitro*

Based on the similarity between the *Drosophila* RapGAP2 with that of human Rap1GAP2 protein in that they both contain a similar N-terminal GoLoco motif we reasoned that DRapGAP2 may also directly bind with the heterotrimeric G-protein alpha subunit, Gαi. Furthermore and as GoLoco motifs are known to have guanine dissociation inhibitors (GDI) activity for Gαi, it was expected that DRapGAP2 would possess such an activity.

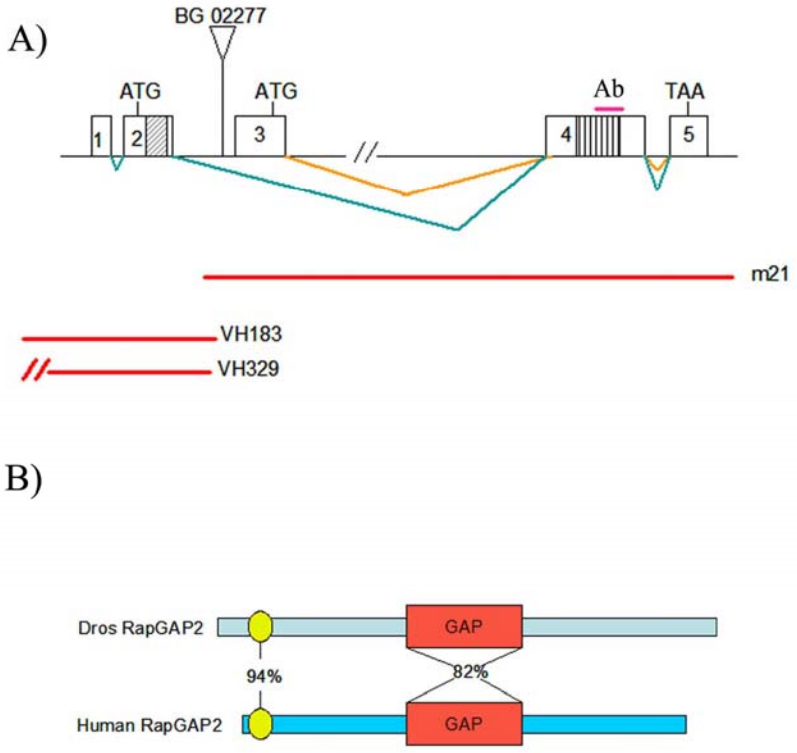


**Figure 5.2: A schematic of the representative transcripts for *DRapGAP*1 and *DRapGAP2*.**
Panel A shows that schematic of two transcripts for *DRapGAP* gene. The two transcripts differ from each other in the exon that encodes the GoLoco motif. The antibody used to study the localization of the *DRapGAP* protein was raised against conserved sequences derived from the GAP domain as indicated by Ab in red. The red lines indicate the extent of deletion in the genomic region in different *DRapGAP* alleles (m21, VH183 and 329). VH183 and VH329 are identified in my study. Panel B shows the comparison of sequences between Drosophila and Human *RapGAPII*. The GoLoco motif is indicated as yellow circle and the GAP domain is indicted by red box and the percent of similarity is shown.

To test this hypothesis, an *in-vitro* binding and GDI activity assay was carried out using purified DRapGAP2 and Gαi (see materials and methods section 2.3.7 for details). DRapGAP2 inhibited rate of exchange of GDP for GTP on Gαi (Fig. 5.3). The results showed that DRapGAP2 can act as a GDI for Gαi.

The potency of GDI activity of DRapGAP2 was also compared to two other GoLoco motif-containing proteins known in *Drosophila,* locomotion defect (Loco) and Partner of Inscuteable (Pins). Loco contains a GoLoco/GPR motif at its C-terminus and has been shown to act as a GAP specifically for Gαi/o (Granderath *et al*., 1999) whereas Pins contains multiple C-terminal GoLoco/GPR motif in tandem arrays with N terminal tetratricopeptide (TPR) domains (Yu *et al*., 2000; Schaefer *et al*., 2000). In the in-vitro assay, Loco was found to have the highest GDI activity preventing the rate of exchange of GDP for GTP on Gαi by as much as 80 % while Pins was able to inhibit this rate of exchange by 60% and RapGAP2 was only able to do so by 40% (Fig. 5.3B). These results indicated that although all these proteins may be expressed in the same cell (for example in the developing nervous system), they can potentially act as GDIs towards the Gαi subunit with a varying degree and therefore resulting in different outcomes in terms of their effects on heterotrimeric G-protein signaling and phenotypic consequences.

### 5.2.3 Isolation of mutations that remove the GoLoco motif of *DRapGAP* gene

At the start of my work, one RapGAP mutation, m21, was available (Chen *et al*., 1997). m21 deletes three common exons in both isoform of *RapGAP1/2* sequences but it does not extend to the exon encoding the GoLoco motif (Fig. 5.2A). m21 homozygous flies are healthy and viable.

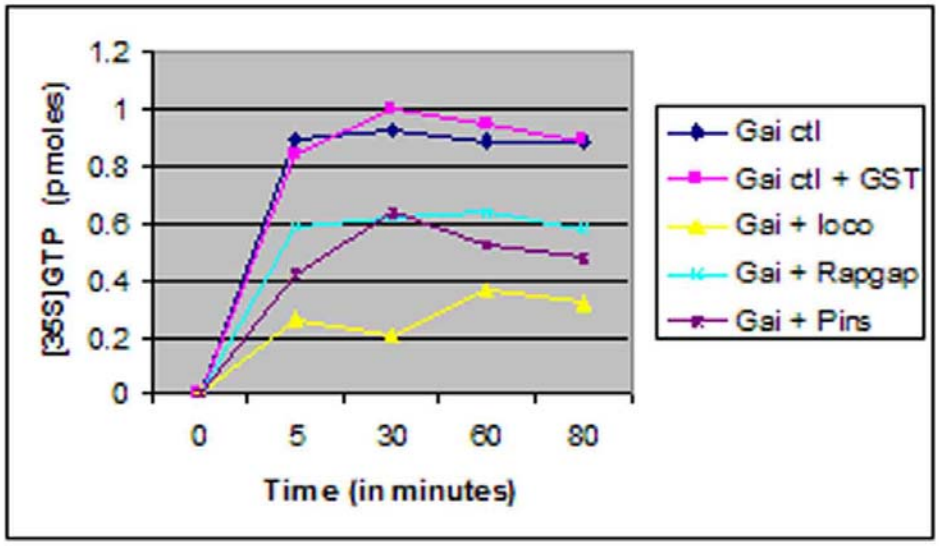


**Figure 5.3 GDI activity of DRapGAP2, Loco and Pins towards Gαi.**

Time course experiments showing the rate of [$^{35}$S]GTPγ binding by Gαi were carried out in the presence of 1μM GST GST-DRapGAP (blue), GST-Pins (purple) and GST-Loco(yellow). Control experiments without (black) and with GST (pink)alone are shown in black. GST-Loco inhibits about 80% of [$^{35}$S]GTPγ binding to Gαi, GST-Pins inhibits about 70% of [$^{35}$S]GTPγ binding to Gαi and GST-DRapGAP inhibits about 40% of [$^{35}$S]GTPγ binding to the Gαi but the GST control has no effect. The effect of DRapGAP, Loco and Pins on Gαi activity is observed as early as 5 minutes and lasts over 80 minutes time period. All the experiments were repeated three times and their average values were used in this graph.

In order to generate mutants that lack the GoLoco motif of RapGAP2, a P-element BG02277 which is inserted in the 5' flanking region of the DRapGAP gene between exon 2 and exon 3 was mobilized and excision alleles that had lost the P-element encoded eye marker were isolated. Analysis by PCR showed that two revertants, VH183 and VH329, have deletions in the region that removes the GoLoco motif of the DRapGAP gene (Fig. 5.2B). The detailed P-element excision and PCR scheme are described in chapter 2, section 2.2.3.2. Like the previously described m21 deletion allele, VH183 and VH329 mutants were completely viable. Embryo staining with anti-DRapGAP antibody showed that m21 is a completely null allele removing both isoforms of DRapGAP whereas VH183 are probably affecting only DRapGAP2 (See section 5.2.5 for details).

### 5.2.4 The dbd sensory neurons are missing in the PNS of DRapGAP mutants

Although DRapGAP is strongly expressed in the embryonic PNS (Chen *et al*., 1997; this chapter Fig. 5.7), no PNS phenotype has been reported (Chen *et al*., 1997). In my approach, I analyzed the DRapGAP mutants for PNS defects using neuronal marker 22C10 and focusing on easily identifiable dbd neuron and its lineage. In order to see if RapGAP plays a role in dbd neuron formation, I analyzed the RapGAP mutant embryos for defects in PNS using the neuronal marker 22C10. The monoclonal antibody 22C10 has been widely used to visualize neuronal morphology and axonal projections (Zipursky *et al*., 1984). Within the embryonic PNS, 22C10 labels all the sensory neurons including the dbd (DBDN). DBDN and its associated glial cell (DBDG) cell can be reliably identified by their dorsal location and characteristic cell morphologies at late stage 16 (Brewster and Bodmer, 1995) upon staining with neuronal marker 22C10 and glial cell marker REPO. There is one dbd neuron and one

associated glia in each abdominal hemisegment of the wildtype embryo. Staining with 22C10 and REPO antibodies showed that in DRapGAP mutant embryos, at least 60% of the hemisegments had loss of the dbd neuron (Fig. 5.4; Table : 5.1) and this loss of dbd neuron was associated with gain of a REPO (Fig. 5.5) positive cell. This phenotype was observed in all three alleles m21, VH183 and VH329 ( see Table 5.1). Based on the fact that VH183 and VH329 only affect DRapGAP2 but not DRapGAP1 transcript it is possible that the loss of dbd neurons is due to the loss of the GoLoco motif containing DRapGAP2 transcript. Whether or not DRapGAP1 is also essential for the dbd neurons cannot be excluded from these observations.

**Table 5.1: *DRapGAP* mutants show dbd loss phenotype.**

| | WT | VH183 | VH329 | m21 |
|---|---|---|---|---|
| No of dbd missing (%) | 0 | 55 | 58 | 65 |

Percentages of segments with dbd loss. Each embryo had atleast one dbd missing and atleast 50 embryos were counted for each genotype. VH 183 and VH 329 delete DRapGAP2 only and m21 deletes both DRapGAP1 and DRapGAP2.

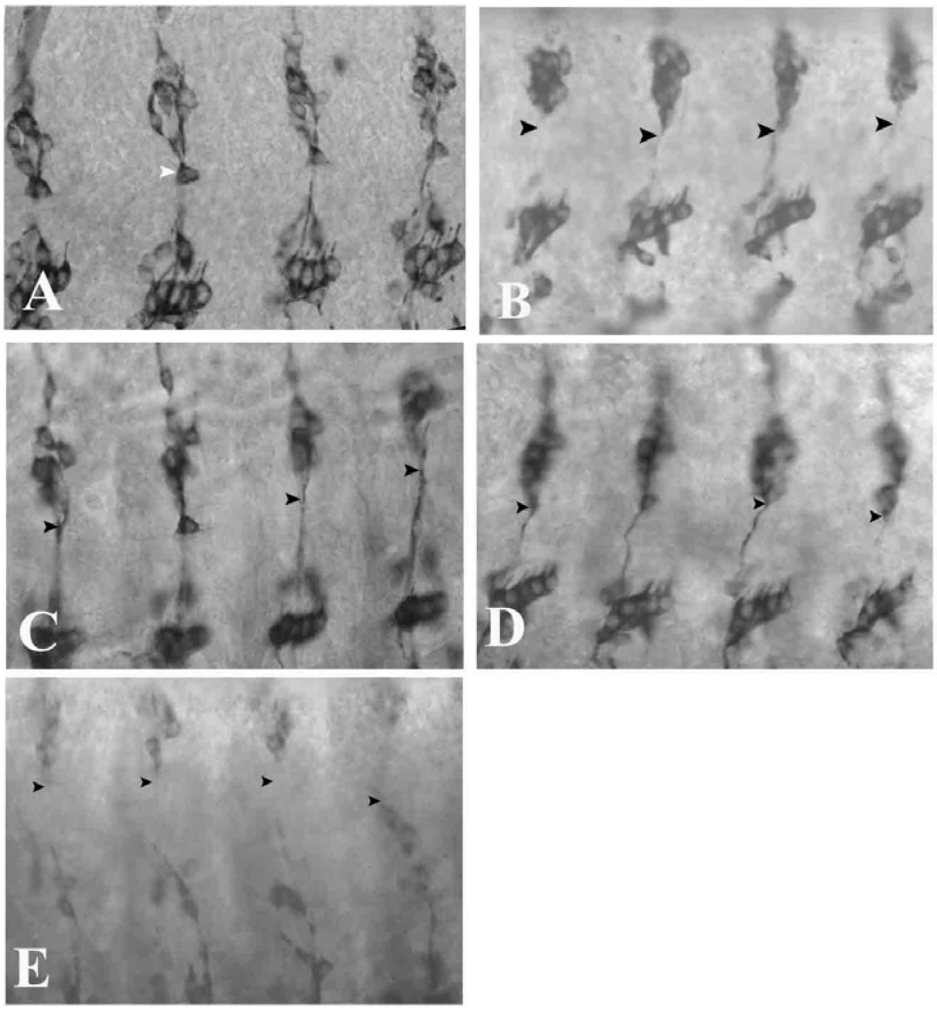


**Figure 5.4 DR*apGAP* mutants show loss of dbd neurons.**

Embryos were stained with neuronal marker 22C10. In the WT embryo, dbd is easily identifiable as a triangle- shaped cell in the dorsal segment (arrowheads in A), B is m21 showing loss of dbd neuron (arrowhead), C is VH183 showing loss of dbd neuron (arrowhead), D is VH329 showing loss of dbd (arrowhead) and E is $G\alpha_i$ mutants showing loss of dbd neuron (arrowhead).

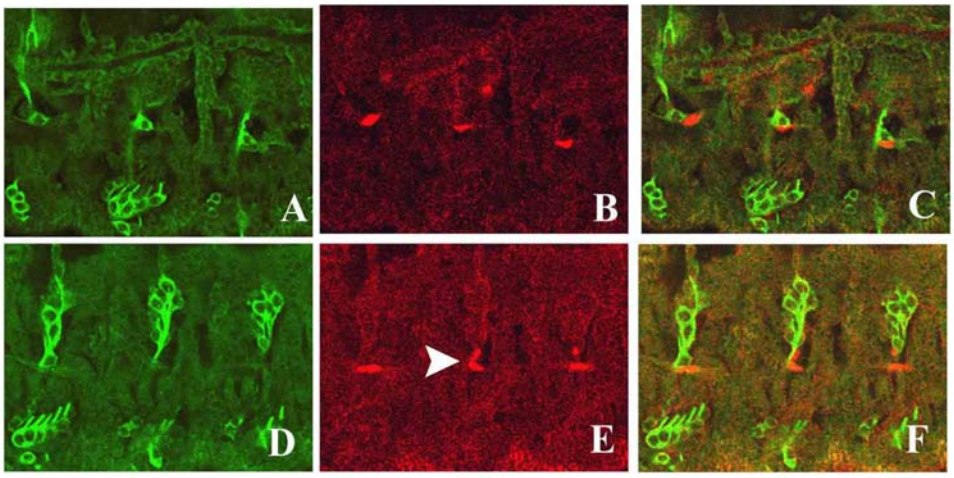


**Figure 5.5 Loss of dbd neuron is associated with gain of glia in *DRapGAP* mutants.**

Stage 16 embryos are stained with 22C10 neuronal marker (green) and REPO glial cell marker (red). Panels A and C show the 22C10 staining in the wildtype(WT) embryo and D and F show the same in *DRapGAP* mutant embryo. Panels B and C show REPO staining in WT embryo and E and F show REPO staining in *DRapGAP* mutant embryo. In the WT 22C10 labels one dbd neuron (A and C : green) and REPO labels one glia cell per hemisegment (Cand F : red). In the *DRapGAP* mutant (*m21/m21*) embryos, 22C10 is lost from the dbd location (D and F : red) and REPO labels two glia cells (E : arrowhead).

### 5.2.5 RapGAP is expressed and asymmetrically localized in the embryonic PNS in the dbd lineage precursor

To study the expression pattern and protein localization of DRapGAP1 and 2 in the embryonic PNS in *Drosophila*, sequences from the C terminus region common to both DRapGAP1 and DRapGAP2 was used to make a His-RapGAP fusion protein for antibody production in rat. Staining of the embryo with anti-DRapGAP showed specific staining in one cell per hemisegment at late stage 11. At this stage, sensory organ precursor cells (SOPs) are normally formed. The position of this DRapGAP positive cell was further defined using with anti-engrailed antibody which labels the anterior margin of each parasegment that is equivalent to the posterior portion of each segment (Ingham *et al*., 1988). The RapGAP-labeled cell is located at the anterior dorso-lateral position of each segment (Fig 5.6A) at late stage 11. This DRapGAP-labelled cell also expresses Pdm-1/2 which is an SOP marker for dbd lineage at that stage (Umesono *et al*., 2002), suggesting that this cell could be an SOP cell of the dbd lineage (Fig. 5.6B).

Using an anti-Pdm-1 antibody as a marker it has been shown that the dbd precursor SOP divides asymmetrically, producing two unequal size Pdm-1 positive daughters, a larger one located basal to the smaller apical one. The larger cell expresses the neuronal marker protein ELAV and differentiates as the dbd neuron, whereas the smaller sibling daughter cell expresses glial marker REPO, migrates dorsally and becomes DBDG (Umesono *et al*., 2002). In the DRapGAP-positive SOP cell lineage, DRapGAP localizes as a crescent at the apico/anterior cortex of the asymmetrically dividing SOP cell during metaphase and after division it segregates into the smaller daughter that is possiblly destined to become a glial cell (Fig. 5.6B-D).

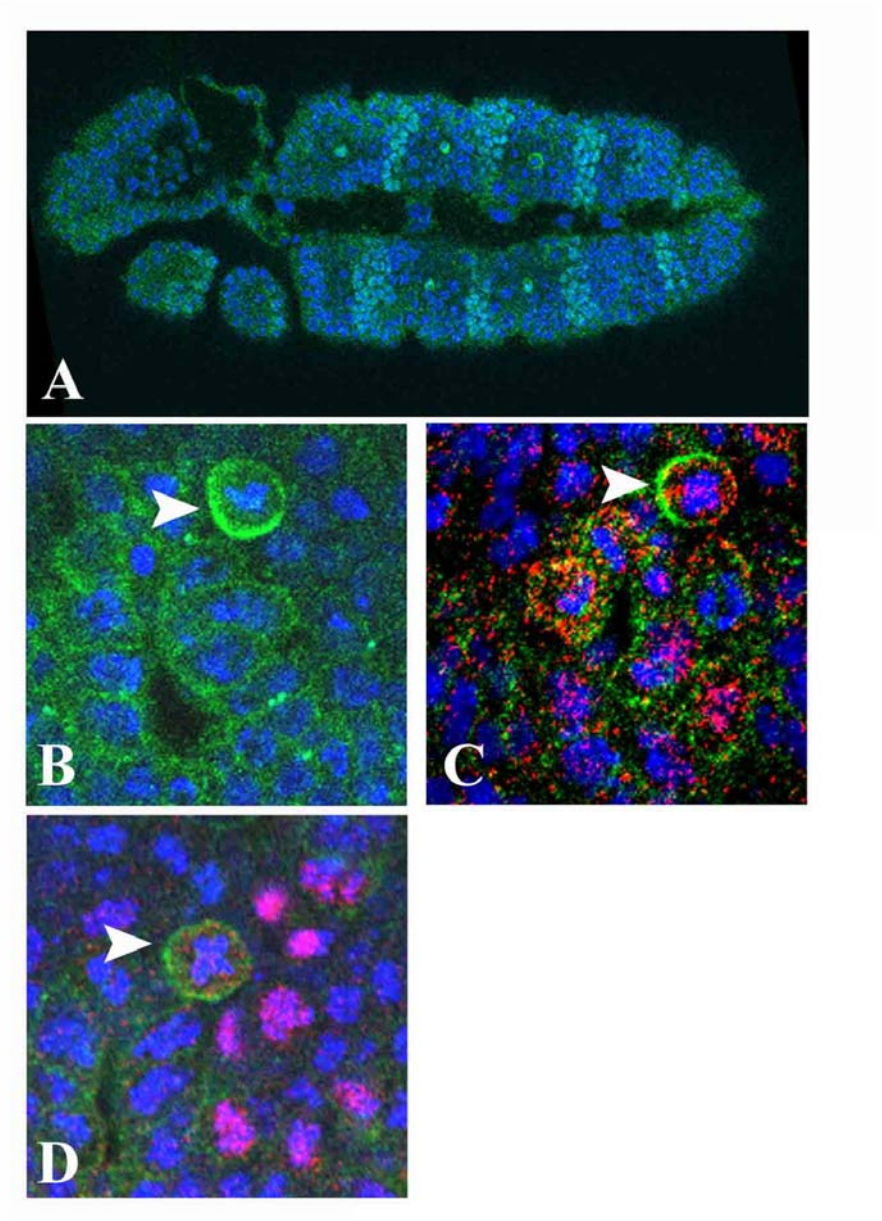


**Figure 5.6 RapGAP antibody labels one SOP cell per hemisegment.**

Panel A shows a lateral view of late stage 11 embryo stained with anti-DRapGAP and anti-engrailed antibody (both in green). DRapGAP labels a single cell per hemisegement which is located in the anterior part of the segment and engrailed is also labeled in green in the posterior part of the segment. Panel B-D shows the confocal images of one abdominal hemisegment from stage 11 embryo stained with DRapGAP (green). DRapGAP localizes to the anterior crescent at metaphase in B (arrowhead). Panel C shows double labeling of anti-DRapGAP and anti-Pdm-1 while panel D shows double labeling of DRapGAP (green) and neural precursor gene, asense (red). DNA is labeled with TOPRO3 and shown in blue in all images.

In DRapGAP m21 allele which removes both DRapGAP isoforms, the DRapGAP staining is completely abolished from both SOP cell and from glial cells in the PNS, indicating also that the antibody is DRapGAP specific (Fig. 5.7). However, in DRapGAP VH183 and VH329 alleles which delete the GoLoco motif exon but leaves exons coding for DRapGAP1 intact, only the SOP staining is abolished. Glia staining with anti-DRapGAP remained in these two alleles, suggesting that DRapGAP2 and not DRapGAP1 is the protein expressed in the SOP cell and that VH183 and VH329 only remove the DRapGAP2 and not DRapGAP1 (Fig. 5.7).

The dbd SOP is known to divide asymmetrically and produce daughter cells with unequal size and fate but the localization of the apical/basal complex proteins which have been discovered in NBs and some SOPs in *Drosophila* such as Insc, Gαi and Pon but have not been reported earlier in this dbd SOP cell. Double labeling experiments showing that DRapGAP, Insc, Pins and Gαi colocalise at the apico/anterior side of the dbd SOP cell at the metaphase (Fig. 5.8) On the opposite basal posterior cortex of the dbd SOP cell, Pon and Mir colocalize at metaphase and segregate with the larger basal cell that is destined to become a dbd neuron (Fig. 5.9-I). This SOP then undergoes a spindle rotation and ultimately divides asymmetrically to give rise to the basal, large-Pon/Mir positive cell and apical-small dRapGAP/Insc/Gαi positive cell (Fig. 5.9-II).

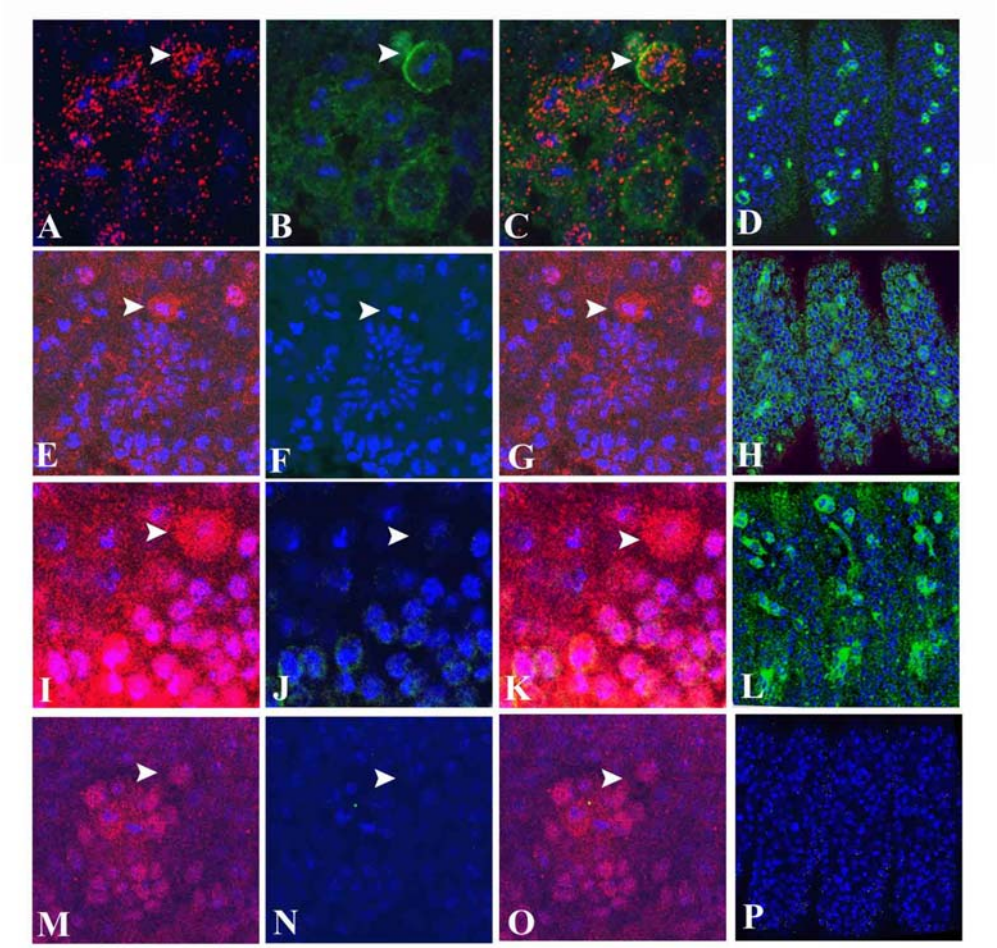


**Figure 5.7 Mutations in *DRapGAP2* gene fail to show SOP staining.**

The embryos stained with anti-DRapGAP (green) and anti-Pdm-1 (red) and the confocal images of one abdominal hemisegment from stage 11 and stage 16 embryos are shown. In WT (A-D) stage 11 embryo, DRapGAP labels one SOP (B-C : green) and this cell is also positive for Pdm-1(A, C: red) while at stage 16 DRapGAP labels a large number of cells in the PNS. In VH183 homozygous (E-H) , VH329 homozygous (I-L) and m21 homozygous (M-P) embryos at stage 11, Pdm-1 positive (E; I; M : red) SOP does not stain positive for DRapGAP (F-G : no green; J-K: no green and N-O : no green respectively). The late PNS staining for DRapGAP is still seen in VH 183 (H:green); VH329 (L:green) but not in m21 (P: lack of green). VH183 and VH329 only delete DRapGAP2 while m21 deletes both DRapGAP1 and DRapGAP2. The arrowhead in panels A-C; E-G; I-K and M-O shows the SOP location. Blue is TOPRO3 in all images.

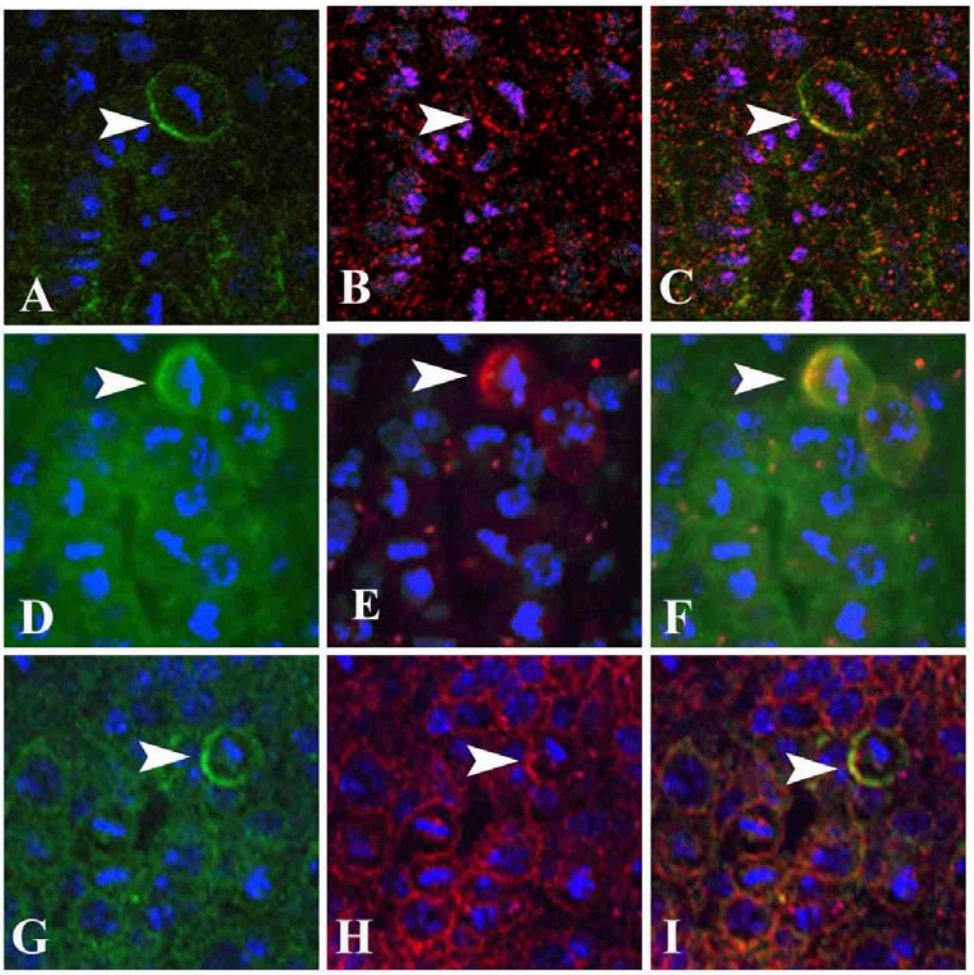


**Figure5.8 Asymmetric localization of DRapGAP in dbd-SOP cell.**

Images are taken from whole mount antibody labeling of late stage 11 WT embryos stained with anti-DRapGAP (green) and DNA (blue). At metaphase DRapGAP forms an anterior crescent in the dividing dbd SOP (A, D,G ). Double labeling with Gαi (B, C : merged image), Insc (E, F : merged image) and Pins (H, I : merged image) shows colocalisation of the DRapGAP anterior crescent during metaphase. In all the images DRapGAP is shown in green; DNA is in blue and anterior to the left.

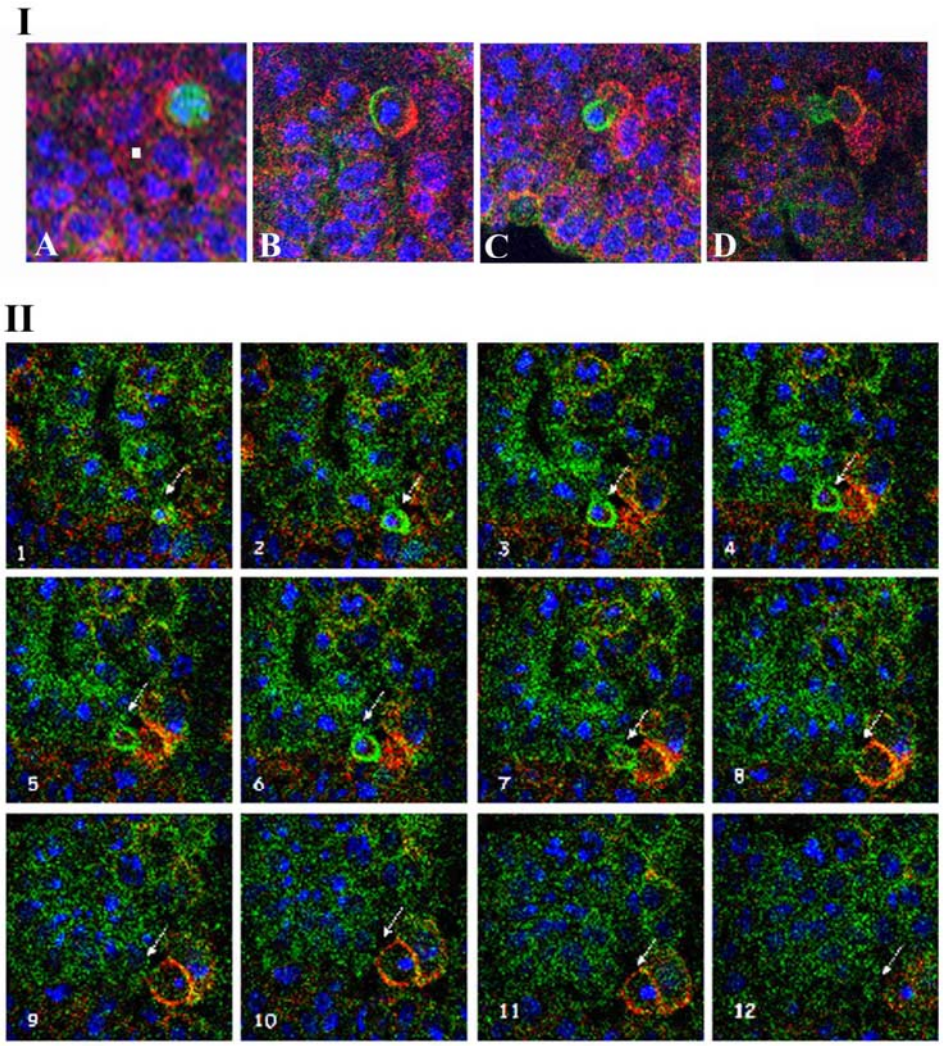


**Figure 5.9 DRapGAP segregates to the smaller apical cell during telophase.**

Panel I shows images taken from whole mount antibody labeling of late stage 11 WT embryos stained with anti-DRapGAP (green), anti-Pon (red) and DNA (blue). Double labeling with anti-Pon antibody shows that in the dbd SOP cell during interphase, DRapGAP is cytoplasmic and Pon is cortically localized (A). At metaphase DRapGAP localizes to anterior cortical crescent (B:green) which is opposite to the cortical crescent of Pon (B :red). During telophase spindle rotates and DRapGAP segregates with the smaller apical daughter cell (C, D: green) while Pon segregates to the larger basal daughter cell (C, D: red). Panel II shows confocal Z sections of one abdominal hemisegment from a late stage 11 embryo showing double labeling of RapGAP (green) and Mir (red). The DRapGAP positive SOP cell (indicated by arrow) divides asymmetrically to give rise to an apical small (positive for RapGAP-green) cell and a basal big cell (positive for Mir-red). The DRapGAP smaller cell is closer to the surface and is out of focus in the deeper sections (8-12).

### 5.2.6 DRapGAP mutants show asymmetric cell division defects in the Pdm-1 positive SOP cell

To characterize the requirement of *Drosophila* DRapGAP in asymmetric cell division of the SOP cell, mutant m21 embryos lacking both isoforms of DRapGAP (*m21*-/-) were analyzed. In the DRapGAP mutant embryos, Mir is mislocalized during mitosis and it becomes uniformly cortical/cytoplasmic and as a result segregated to both the daughter cells after division (Fig. 5.10H-I; 5.10K-L). This observation indicates that DRapGAP is important for proper asymmetric localization of cell fate determinants in the SOP cell of the dbd lineage. DRapGAP is normally localized as an anterior crescent in the SOP in mutants lacking Insc and Pins function and Insc and Pins are normally localized to the apico/anterior crescent in the DRapGAP mutants during metaphase (Fig. 5.11B, D).

### 5.2.7 Gαi mutants but not Pins or Insc mutants show loss of dbd neuron phenotype similar to that of DRapGAP mutants.

I have shown in this chapter that DRapGAP2 contains a GoLoco motif and it can act as a GDI for Gαi *in vitro*. Furthermore, I have shown that both Gαi and DRapGAP proteins localize to the apical cortical side of the SOP during metaphase. To check whether or not Gαi plays any role in the formation of the dbd lineage, Gαi mutants were stained with 22C10 and REPO. Like DRapGAP mutants, Gαi mutants showed severe loss of dbd neurons (Fig. 5.4), indicating that signaling via DRapGAP and Gαi is important for dbd formation. Surprisingly, Pins and Insc mutants did not show any dbd phenotypes (Fig. 5.11A, C).

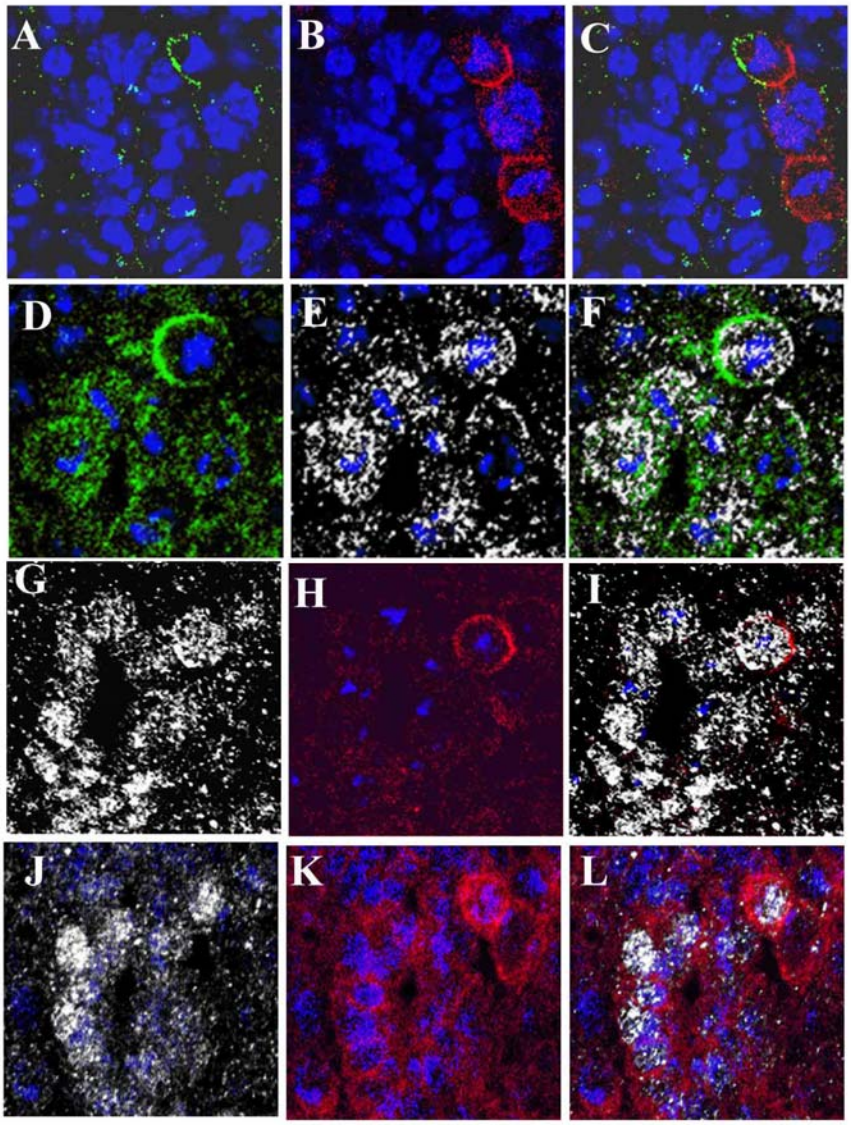


**Figure 5.10 Mir is mislocalized in *DRapGAP* mutants.**

Late stage 11 embryo is shown stained with Pdm-1(E,G,J : white), Mir (B,H,K : red) and DRapGAP(A,D,F : green) antibodies. In wt embryo, DRapGAP (A, C: green) and Mir (B, C: red) is asymmetrically localized to opposite sides of the cortex during metaphase and at this stage the DRapGAP positive cell is also positive for Pdm-1 positive (E, F : white). In DRapGAP mutants (m21), Mir is mislocalised and is now present cortically all over the cortex (H, K: red)) in the Pdm-1 positive SOP cell (G, J: white).

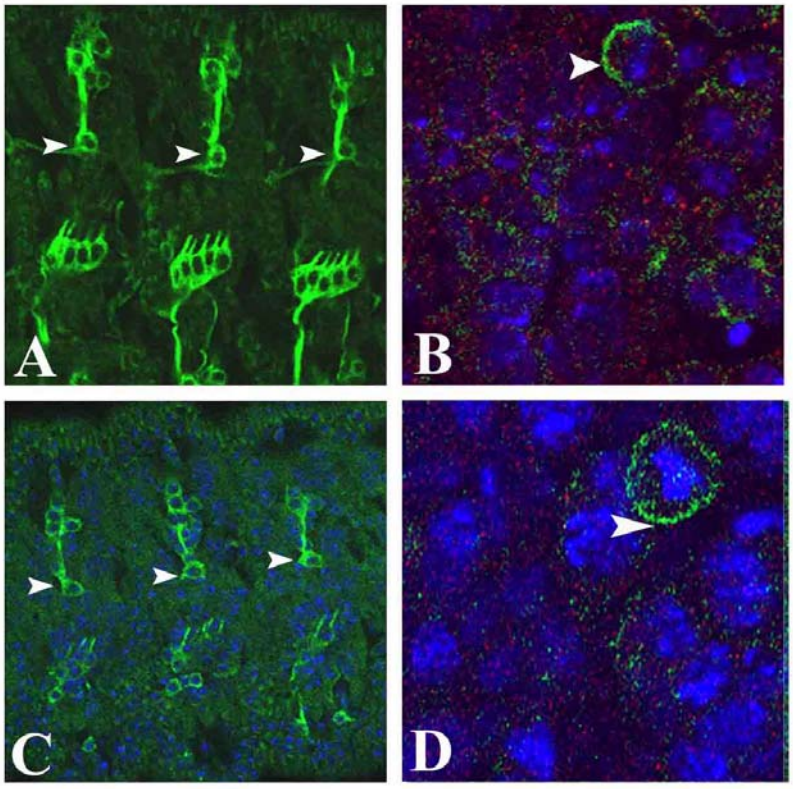


**Figure 5.11 Insc and Pins mutants do not show any dbd phenotypes.**

Stage 16 embryos were stained with 22C10 and lateral views are shown in A and C. In embryos mutant for Pins (A) and Insc (C). 22C10 antibody labels the dbd neuron (arrowheads) in WT embryos. Panel B,D shows the stage 11 embryo mutant for Pins (B) and Insc (D) and stained for DRapGAP showing that DRapGAP is localized to the anterior crescent in these embryos.

### 5.2.8 RapGAP acts downstream of *amos* in dbd lineage

*amo*s is a bHLH proneural gene that is required for the formation of the SOP cell of the dbd lineage. *amos* mutants show loss of SOPs and their dbd/glia progenies (Huang *et al*., 2001). Overexpression of *amos* in the neuroectoderm using Scabrous GAL4 causes ectopic SOPs formation and increase in number of dbd neurons per hemisegment (Fig. 5.5.12A-C). However, over-expression of *amos* in a d*RapGAP* mutant background (*m21*-/-) does not lead to ectopic dbd neurons as visualized with 22C10 staining (Fig 5.12D-F). These results suggest that dRapGAP might act downstream of *amos* and is required for the asymmetric division of SOP cells to produce dbd/glia progenies.

## 5.3 Discussion

In this chapter, I have characterized a *Drosophila* GoLoco motif-containing DRapGAP isoform which is referred to as DRapGAP2. I have shown that DRapGAP is asymmetrically localized at metaphase to an apical crescent in the SOP cell of the dbd lineage in the embryonic peripheral nervous system. I have also shown that DRapGAP mutants show loss of dbd neurons and DRapGAP plays an important role in the asymmetric division of the SOP by influencing localization of cell fate determinants to the opposite basal cortex in this sensory organ precursor cell.

The pattern of cell division in the SOP cell of the dbd lineage has remained unclear because of the lack of useful realtime markers which can be used to follow this division. Until now, the identification of this particular SOP has been based on its size, location and expression of certain molecular markers (Umesono *et al*., 2002; Brewster *et al*., 2001).

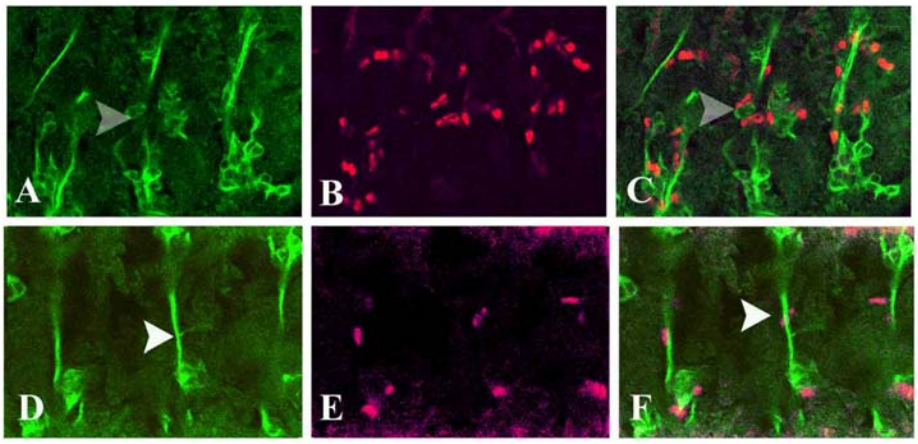


**Figure 5.12 *amos* overexpression results in ectopic dbd neurons in WT but not in *DRapGAP* mutant embryos.**

A-F shows stage 16 embryo overexpressing UAS-*amos* under Sca-GAL4 and stained with 22C10 (green) and REPO (red) in the WT genetic background (A-C) and in DRapGAP mutant background (D-F). Over expression of *amos* results in ectopic MD-bd neurons in WT (A-C: arrowheads) but not in an *amos* mutant (D-F: arrowheads) genetic background.

At the late stage 11/ beginning of stage 12 the dbd-SOP cell is identified as a large cell weakly expressing the POU domain protein, Pdm-1 in the anterior-dorsal region of embryonic abdominal segments. However, Pdm-1 expression is not exclusive to this SOP and it labels a cluster of SOP in the dbd SOP location. Three observations support the conclusion that the SOP cell expressing the DRapGAP is the dbd-SOP : 1) the DRapGAP positive cell is a large cell located in the anterior-dorsal region of the embryonic abdominal segment, 2) the DRapGAP positive cell also expresses Pdm-1 weakly and 3) DRapGAP mutants cause loss of dbd neurons. The exclusive expression of DRapGAP to this single SOP cell that is likely to be the dbd-SOP provides an additional and extremely useful marker for the cell fate specification and diversity in the dbd lineage of the embryonic PNS.

While studying the dbd lineage, it is important to consider certain salient features of the SOP dividing and generating the dbd neuron. In the dbd lineage, an SOP cell is thought to divide only once to generate a neuron and a sibling glial cell of unequal sizes through an asymmetric division. In other gliogenic PNS lineages, the first division of the SOPs generates a glial cell and a sibling cell that is not postmitotic neuron but a secondary precursor that undergoes a further division to generate neurons and associated glial (Brewster *et al*., 1995). Although the dbd SOP division has been described as asymmetric, this property is mainly based on daughter sizes. The asymmetric machinery directing this SOP division has never been studied in detail. Only numb protein has been shown to be specifically segregated to the dbd neuron and to be responsible for it cell fate (Brewster *et al*., 2001; Umesono *et al*., 2002) but Numb protein localization during SOP division has not been reported. Other asymmetric proteins widely described for asymmetrically dividing CNS neuroblast and SOP cell division have never been shown to be present in this precursor. The work described in this chapter sheds some light on the localization and function of some of

these proteins like Pins, Insc, Pon and Mir in the dividing dbd SOP cell. This work shows dbd-SOP localizes Pins, Insc and Gαi as an apico/anterior crescent at metaphase and this crescent is segregated in the smaller apical cell, on the other hand, Pon and Mir are localized as a basal posterior crescent and segregated to the large basal cell, which is slightly different from the neuroblasts in term of cell size. In addition and unlike in the neuroblasts, Pins and Insc do not seem to play any obvious role in localization of Pon and Mir in the dividing dbd-SOP and subsequently no phenotypic consequences are observed in the dbd neuronal formation in Pins and Insc mutants. Pins and Insc function is essential for localization of Mir and Pon in dividing neuroblasts in the CNS.

Of the apical complex proteins, only Gαi seems to play an important role in the dbd lineage. The observation that Gαi mutants lose of dbd neurons supports this conclusion. However, more work is needed to characterize the effect of the Gαi mutation on the other asymmetry machinery components such as Insc/Pins/Mir/Pon. In *Drosophila* neuroblast asymmetric cell division, Gαi is required for Pins to localize to the cortex, and the Pins/Gαi complex acts to mediate various aspects of neuroblast asymmetric division (Yu *et al*., 2003; Knust E, 2001).

Since Pins does not play an influential role in the asymmetric division of the dbd-SOP asymmetric division, Gαi activity might be sensitive to other factors. DRapGAP could be one factor that can affect Gαi activity in the dbd SOP. Several observations support a critical role for DRapGAP in the asymmetric division of the dbd SOP: 1) DRapGAP is expressed in the dbd-SOP, 2) DRapGAP colocalizes asymmetrically with Gαi to a cortical crescent in the dbd SOP during metaphase, 3) DRapGAP mutants show mislocalisation of basal proteins in the dbd-SOP during metaphase and 4) DRapGAP mutants show defects in cell fate specification of the progenies in this

lineage. Additionally, the presence of the GoLoco motif in DRapGAP, a Gαi binding motif, and the similarities in subcellular localization and phenotypic consequences between Gαi and DRapGAP imply that DRapGAP and Gαi may function as a complex.

In neuroblasts, Gαi function is important for Pins cortical localization and Pins then acts as a guanine nucleotide dissociation inhibitor for Gαi to regulates Gα signaling by competing with Gβγ (Schaefer *et al*., 2000; Yu *et al*., 2000; Yu *et al*., 2003). DRapGAP function in the dbd-SOP maybe similar to Pins on Gαi in NBs; Like Pins, DRapGAP can act as a GDI *in vivo*. However, DRapGAP contains an additional characteristic GAP domain for Rap1 that is not present in Pins. The function for this GAP domain *in vivo* is currently not known. Attempts to investigate DRap1 mutant phenotypes in the dbd lineage might shed some light on the function and possible interplay between DRapGAP and Gαi. Unfortunately, DRap1 mutants lacking both maternal and a zygotic DRap1 gene product do not survive till stage 12, the stage at which dbd-SOP cell divides (personal observation).

Mechanistically, it remains unclear how DRapGAP mutants promote neuron to glial cell fate change in the dbd lineage. It is possible that mislocalisation of cell fate determinants such as Pon/Mir in the DRapGAP mutant SOP subsequently segregate with both daughter cells instead of only the dbd neuron in the wildtype. As a result Numb in the cell destined to become a dbd neuron is insufficient to block Notch signaling and the cell then potentially takes on a glial fate (Fig. 5.13) (Uemura *et al*., 1989; Posakony, 1994; Guo *et al*., 1995; Jan and Jan, 1995). In the dbd lineage, *numb* mutations show a double-glial phenotype at the expense of the neuron (Brewster and Bodmer, 1995) and notch mutants show loss of dbd glia and more neurons.

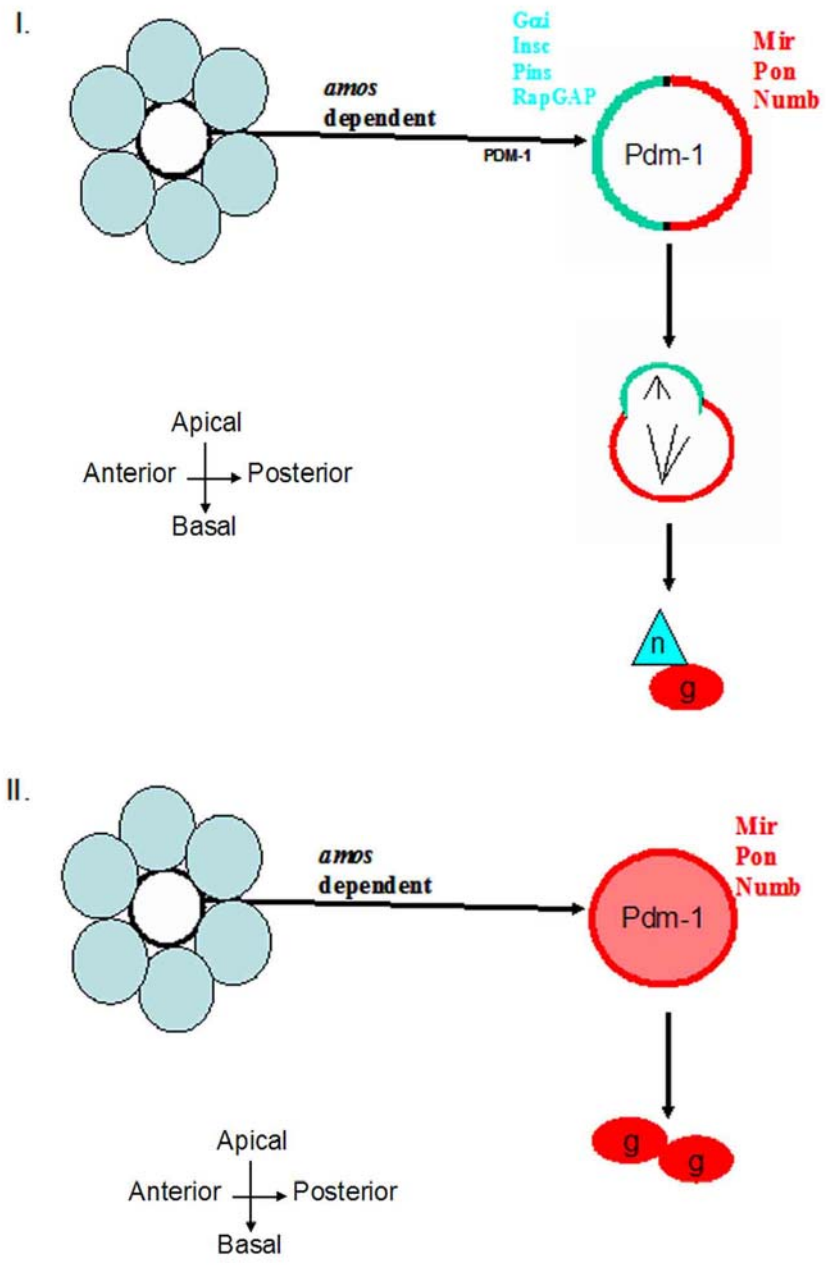


**Figure 5.13: Working model for role of RapGAP in dbd lineage formation.**

Panel I outlines the WT scenario: The amos-dependent, RapGAP-positive cell divides asymmetrically and segregates DRapGAP to the smaller apical cell and differentiates as a dbd-neuron while the larger Mir and Pon positive cell differentiates into the dbd neuron sibling glia cell. Panel II outlines DRapGAP mutant scenario: The *amos* dependent, RapGAP-positive cell is the dbd SOP shows asymmetric cell division defects and cell fate determinants such as Mir and Pon are mislocalised at metaphase and segregate to both daughter cells. The result is two glial cells and no dbd neuron.

The current understanding is that within dbd lineage *numb* mutants mislocalise *gcm* to the presumptive dbd neuron and show loss of *pdm-1* expression in the dbd neuron.

These phenotypes are similar to the artificial activation of Notch in the neurons. Hence, it is likely that Numb represses Notch activity in the neuronal daughter upon asymmetric division of the dbd SOP (Umesono *et al*., 2002)

The formation of dbd SOP (in addition to two other SOPs) is known to be dependent on the function of *amos*. *amos* is a proneural bHLH gene whose mutation results in loss of the dbd SOP and their dbd neuronal progeny (Huang *et al*., 2000; Umesono *et al*., 2002). In addition, overexpression of *amos* has been reported to cause increase in the number of dbd neurons in each hemisegment (Huang *et al*., 2000). In agreement with DRapGAP having a role the dbd-SOP division, overexpression of *amos* in a DRapGAP mutant genetic background does not show the increase in the dbd neurons. Conversely, in *amos* mutants, which remove the dbd-SOP cell, DRapGAP is not present at stage 11/12, indicating that DRapGAP is expressed in the SOP cell that is dependent on amos for its formation. Furthermore the observation that amos overexpression in DRapGAP mutant backgrounds does not result in extra dbd neurons suggests that DRapGAP controls the asymmetric division of extra dbd-SOP cells that form by amos overexpression.

## 5.4 Ongoing and Future work

In summary, I have shown that DRapGAP plays important roles in the asymmetric division of the dbd SOP and in the generation of daughter cells with correct fate. I have shown that Gαi also plays a positive important role in this lineage. More work is needed to clarify remaining pertinent questions, some of which include identification of the isoform of RapGAP that is able to rescue the dbd phenotype, to check if

DRapGAP2 is also expressed in the glia daughter cell and to check if overexpression of Numb in a DRapGAP mutant background rescues dbd loss. In addition, it would be interesting to investigate the factors that affect DRapGAP loclaization (DRapGAP in Gαi mutants and *vice versa*). Since DRapGAP has a GDI activity towards Gαi *in-vitro*, it would be interesting to ectopically express DRapGAP in neuroblasts and analyse its effects on asymmetric cell division machinery components. In addition, DRapGAP appears to act downstream of *amos* in the pathway leading to dbd formation, hence, expression of DRapGAP in *amos* mutant background should be able to rescue this phenotype.

# CHAPTER 6 : General Discussion

This thesis has dealt with characterizing two regulators of G-protein signaling, LGN and RapGAP and explored their functions using cell cultures system, zebrafish and *Drosophila* neurogenesis as model systems.

In Chapter 3 of this thesis, I have explored the subcellular localization of mouse LGN during cell division and factors that influence its localization. My results provided evidence for a novel subcellular localization of LGN during mitosis in mammalian cells. Using overexpression studies in different cell line systems, I have demonstrated that, like *Drosophila* Pins, LGN can exhibit enriched localization at the cell cortex, depending on the cell cycle and the culture system used. I have found that in WISH, PC12, and NRK but not COS cells, LGN is largely directed to the cell cortex during mitosis. Overexpression of truncated protein domains further identified the G-protein binding C-terminal portion of LGN as a sufficient domain for cortical localization in cell culture. In mitotic COS cells that normally do not exhibit cortical LGN localization, LGN is redirected to the cell cortex upon overexpression of Gα subunits of heterotrimeric G-proteins supporting that LGN cortical localization may depend on its interaction with subsets of Gα subunits.

My results have also shown that the cortical localization of LGN is dependent on microfilaments and that interfering with LGN function in cultured cell lines causes early disruption to cell cycle progression. Additionally, and similar to its fly counterpart behavior in epithelial cells, LGN in polarized mammalian cells localizes to the basolateral subdomain of the cortex and is symmetrically distributed to both daughter cells. The functional significance of this cell cycle–dependent cortical localization of LGN is not yet clear. In *Drosophila*, Pins is normally found in the

lateral cortex of epithelial cells and only becomes asymmetrically localized upon the endogenous expression of inscuteable in neuroblasts or exogenous expression of Insc in epithelial cells, for which a mammalian homolog has not been found so far (Schaefer *et al*., 2000; Yu *et al*., 2000). Pins is also dependent on heterotrimeric G-protein activity for its localization (Schaefer *et al*., 2001). Furthermore, Pins plays important roles in neuroblast asymmetric cell divisions and the available data suggest that its interaction with Gα facilitates receptor-independent G-protein signaling (Schaefer *et al*., 2000; Schaefer *et al*., 2001).

Interestingly, our group has previously reported that the mouse *LGN* gene reported in this study can also bind fly Inscuteable and rescue defects associated with *pins* mutations in the fly (Yu *et al*., 2003), supporting functional conservation. In conclusion, LGN and Pins share the domains required for cortical localization, and both proteins can assume this dynamic localization depending on the presence of a suitable partner. Biochemically and like other Pins-related proteins, mLGN complexes with Gα subunits of heterotrimeric G-proteins and inhibits dissociation of GDP from Gαi (Mochizuki *et al*., 1996; DeVries *et al*., 2000; Natochin *et al*., 2000; Peterson *et al*., 2000; Scheafer *et al*., 2000; Bernard *et al*., 2001; Kaushik *et al*., 2003), but whether or not LGN interferes with G-protein activity at the plasma membrane remains to be determined. In addition to the cortical LGN localization described in this thesis (chapter 3; Kaushik *et al*., 2003), other reports have shown that LGN can assume various subcellular localizations during mitosis (Du *et al*., 2001; Blumer *et al*., 2002), including spindle pole at metaphase and midbody during cytokinesis. Du *et al*., (2001) have also shown that LGN interferes in the spindle dynamics via binding to NuMA.

The studies of LGN function in vertebrates have depended heavily on cell culture systems (Du *et al*., 2001; Blumer *et al*., 2002; Kaushik *et al*., 2003), but expression studies in animals suggested that LGN may be involved in cell differentiation as well. In the Chapter 4 of this thesis I have identified the LGN homologs from zebrafish, *LGN* and *AGS3* and characterized their expression patterns during embryonic development. I have also studied the roles of LGN in primary motor neuron formation during zebrafish neurogenesis. My results indicate that *LGN* but not *AGS3* is expressed in the central nervous system and in the sclerotome and that LGN is required for the proper formation of primary motoneurons in the zebrafish embryo, possibly by antagonizing a Hh signaling pathway.

The deduced zebrafish LGN/AGS3 proteins are highly homologous to other members of the LGN/AGS3 family and they contain the conserved two domain structure characteristic for this family: TPRs in the N-terminal domain and Gαi/o-binding GoLoco motifs in the C-terminal domain. The TPR motifs serve a range of functions for LGN/AGS3 proteins in animals including binding to protein partners such as Inscuteable in *Drosophila* (Yu *et al*., 2002) and NuMA and LKB kinase in mammalian cells (Blumer *et al*., 2003; Du *et al*., 2001), thereby affecting LGN trafficking, subcellular localization and its ability to bind Gαi. The GoLoco motifs of LGN/AGS3 proteins mediate an interaction with Gαi/o subunits of heterotrimeric G-proteins and inhibit dissociation of GDP from Gαi/o (De Vries *et al*., 2000; Kaushik *et al*., 2003; Natochin *et al*., 2000; Schaefer *et al*., 2000). I have shown that LGN and AGS3 are similarly able to bind GDP-Gαi3/o and act as GDI for Gαi *in vitro*.

To address the function of LGN in the central nervous system, we focused our analysis on the *islet2*-positive PMNS for simplicity. Several observations support a role for LGN in the proper formation of primary motor neurons: firstly, *LGN* is

expressed in the central nervous system; secondly, downregulation of LGN increases the number of *islet2*-positive PMNs; and thirdly, overexpression of LGN decreases the number of these primary motor neurons. These observations suggest a negative role for LGN in the formation of PMNs. It is not yet clear how LGN affects PMNs fate in zebrafish but it is apparent from the phenotypic interaction experiments that it exerts a negative influence on Hh signaling in this process.

The function of LGN in zebrafish development is however, not restricted to yhe nervous system and LGN morphants also show patterning defects and a detectable decrease in the expression domain of *twist* which labels the presumptive sclerotome and other twist positive cells present in the embryo. To my knowledge this is the first report on a role for LGN- related proteins in vertebrate development. Mechanistically, it is not obvious how LGN affects *ptc* expression. LGN localization to the nucleus and cytoplasm have been reported and this suggests that LGN may theoretically directly affect nuclear processes involved in transcription or through indirect route via cytoplasmic components. At present, there is no evidence for any of these possibilities and physical interactions between Hh pathway components are not known. It is intriguing though that pertussis toxin does not have effect on PMNs formation and that may imply that LGN function in the PMNs formation may not involve heterotrimeric G-proteins. An essential question of whether or not LGN plays a role in the division of precursor cells that give rise to PMNs in the zebrafish embryo is still unanswered and this requires further investigations. Still, the data imply that LGN is important for the specification and/or formation of PMNs and that this involvement can somehow impinge on a Hh pathway in this process.

The work done in Chapter 5 of this thesis deals with the role of DRapGAP2 gene in the *Drosophila* PNS. DRapGAP2 is the GoLoco motif-containing DRapGAP isoform. I have shown that DRapGAP is asymmetrically localized at metaphase to an apical

crescent in the precursor cell of the dbd lineage in the embryonic PNS. I have also shown that *DRapGAP* mutants exhibit loss of dbd neurons and DRapGAP plays an important role in the asymmetric division of the PNS precursors by influencing localization of cell fate determinants such as Mir to the opposite basal cortex in this sensory organ precursor cell. Three observations support the conclusion that the SOP cell expressing the DRapGAP is the dbd-SOP: 1) the DRapGAP-positive cell is a large cell located in the anterior-dorsal region of the embryonic abdominal segment; 2) the DRapGAP-positive cell also expresses Pdm-1 weakly; and 3) DRapGAP mutants cause loss of dbd neurons.

The exclusive expression of DRapGAP to this single SOP cell that is likely to be the dbd-SOP provides an additional and extremly useful marker for the cell fate specification and diversity in the dbd lineage of the embryonic PNS. In the dbd lineage, an SOP cell is thought to divide only once to generate a neuron and a sibling glial cell of unequal sizes through an asymmetric division. The asymmetric machinery directing this SOP division has never been studied in detail. Only the Numb protein has been shown to specifically segregate to the dbd neuron and to be responsible for its cell fate (Brewster *et. al*., 2001; Umesono *et al.,* 2002) but Numb protein localization during SOP division has not been reported. The work described in chapter 5 sheds some light on the localization and function of some of proteins including Pins, Insc, Pon and Mir in the dividing and presumed dbd-SOP cell. This work shows dbd-SOP localizes Pins, Insc and Gαi to an anterior cortical crescent at metaphase and this crescent is segregated in the smaller apical cell whereas Pon and Mir are localized as an opposite posterior crescent and are segregated to the basal larger cell similar to the situation in NBs of the CNS.

Unlike in the NBs however, Pins and Insc do not seem to play any role in localization of Pon and Mir in the dividing dbd-SOP at metaphase and subsequently no phenotypic consequences are observed in the dbd neuronal formation in *pins* and *insc* mutants (Chapter 5). Of the apical complex, only Gαi seems to play an important role in the dbd lineage. The observation that *Gαi mutants* have loss of dbd neurons supports this conclusion. Since Pins does not play an influential role in asymmetric division of the dbd-SOP asymmetric division, Gαi activity might be sensitive to other factors such as DRapGAP.

Mechanistically, it remains unclear how DRapGAP mutants promote neuron to glial cell fate change in the dbd lineage. It is possible that mislocalization of cell fate determinants such as Pon/Mir/Numb in the DRapGAP mutant SOP subsequently segregate with both daughter cells instead of only the dbd neuron in the wildtype. As a result Numb is segregated to both sibling daughter cells at lower levels and is possibly insufficient to block Notch signaling causing the cell to assume a glial fate. In the dbd lineage, a *numb* mutation shows a ectopic glial at the expense of the neuron and notch mutants show loss of dbd glial and more neurons (Brewster and Bodmer, 1995; Umesono *et al*., 2002). The current understanding is that within the dbd lineage *numb* mutants mislocalise *gcm* to the presumptive dbd neuron and this causes loss of *pdm-1* expression from the presumptive dbd neuron. These phenotypes are similar to that of aritificial activation of Notch in neurons. Hence it is likely that Numb represses Notch activity in the neuronal daughter upon asymmetric division of the dbd SOP (Umesono *et al*., 2002). The work described in chapter 5 did not address the question of cross-talk between DRapGAP/Gα and Rap1 and more work is needed to clarify this issue.

Although, the work described in this thesis deals with three different proteins in three different paradigms, it brings out certain novel aspects of relationship of these

GoLoco motif-containing proteins with the heterotrimeric G-protein signaling in all these systems. My results highlight the importance of cross-species studies on conserved molecules to bring out the subtleties of regulation that control G-protein signaling within the cell and during development. GoLoco/GPR containing proteins are conserved from flies to humans and work done in various systems has indicated critical roles for these proteins during growth, differentiation and development. For example, in flies and worms, GoLoco motif-containing, RGS proteins, regulate several aspects of embryonic development including glial differentiation, embryonic axis formation, and skeletal and muscle development (Granderath *et al*., 1999; Fukui *et al*., 2000; Wu *et al*., 2000).

The work in this thesis has added to the existing knowledge about the complex signaling networks in which G protein regulators are involved. My results indicate that on one hand the LGN family of Goloco-motif containing protein are important players in regulating cell division and/or generation of polarity during asymmetric cell division (Cai *et al.*, 2003 and Fumio *et al*., 2004; Yu *et al*., 2001; Schaefer *et al*., 2001; Gotta *et al*., 2003; Kaushik *et al*., 2003; Du *et al*., 2001). This family also have important roles to play during neuronal differentiation of specific cell types (chapter 4). It should be noted that results in chapter 4 do not rule out the possibility that the role for LGN in primary motor neuron formation could also be at the level of precursor cell division and more work is needed to clarify this issue. The chapter describing DRapGAP function in the *Drosophila* PNS also highlights the importance of DRapGAP in a certain subset of sensory neurons found in the embryonic PNS. Although the proteins containing GoLoco motifs can act as GDI towards Gαi, the potency with which they do so varies and ultimately determines the extent they would regulate G-protein signaling in the cells. Once again, these results point toward the final outcome being a

net result of the complex signaling regulation that goes on within the cells. Finally, LGN and DRapGAP both contain additional motifs that affect their function and/or localization within the cell and ultimately the outcome of their signals. In this respect, it would be interesting to identify new partners for LGN in vertebrate systems and DRapGAP in *Drosophila* and address their functional significance on these G-protein regulators.

# References

Adler,P.N. and Lee,H. (2001). *Frizzled signaling and cell-cell interactions in planar polarity*. Curr Opin Cell Biol *13*, 635-640.

Advani,R.J., Bae,H.R., Bock,J.B., Chao,D.S., Doung,Y.C., Prekeris,R., Yoo,J.S., and Scheller,R.H. (1998). *Seven novel mammalian SNARE proteins localize to distinct membrane compartments*. J Biol Chem *273*, 10317-10324.

Alcedo,J., Ayzenzon,M., Von Ohlen,T., Noll,M., and Hooper,J.E. (1996). *The Drosophila smoothened gene encodes a seven-pass membrane protein, a putative receptor for the hedgehog signal*. Cell *86*, 221-232.

Anderson,J.M., Stevenson,B.R., Jesaitis,L.A., Goodenough,D.A., and Mooseker,M.S. (1988). *Characterization of ZO-1, a protein component of the tight junction from mouse liver and Madin-Darby canine kidney cells*. J Cell Biol *106*, 1141-1149.

Antonin,W., Riedel,D., and von Mollard,G.F. (2000). *The SNARE Vti1a-beta is localized to small synaptic vesicles and participates in a novel SNARE complex*. J Neurosci. *20*, 5724-5732.

Appel,B. and Eisen,J.S. (1998). *Regulation of neuronal specification in the zebrafish spinal cord by Delta function*. Development *125*, 371-380.

Appel,B., Fritz,A., Westerfield,M., Grunwald,D.J., Eisen,J.S., and Riley,B.B. (1999). *Delta-mediated specification of midline cell fates in zebrafish embryos*. Curr Biol *9*, 247-256.

Appel,B., Korzh,V., Glasgow,E., Thor,S., Edlund,T., Dawid,I.B., and Eisen,J.S. (1995). *Motoneuron fate specification revealed by patterned LIM homeobox gene expression in embryonic zebrafish*. Development *121*, 4117-4125.

Artavanis-Tsakonas,S., Matsuno,K., and Fortini,M.E. (1995). *Notch signaling*. Science *268*, 225-232.

Artavanis-Tsakonas,S., Rand,M.D., and Lake,R.J. (1999). *Notch signaling: cell fate control and signal integration in development*. Science *284*, 770-776.

Asha,H., de Ruiter,N.D., Wang,M.G., and Hariharan,I.K. (1999). *The Rap1 GTPase functions as a regulator of morphogenesis in vivo*. EMBO J *18*, 605-615.

Bardin,A.J., Le Borgne,R., and Schweisguth,F. (2004). *Asymmetric localization and function of cell-fate determinants: a fly's view*. Curr Opin Neurobiol. *14*, 6-14.

Beattie,C.E. (2000). *Control of motor axon guidance in the zebrafish embryo*. Brain Res Bull *53*, 489-500.

Bellaiche,Y., Beaudoin-Massiani,O., Stuttem,I., and Schweisguth,F. (2004). *The planar cell polarity protein Strabismus promotes Pins anterior localization during asymmetric division of sensory organ precursor cells in Drosophila*. Development *131*, 469-478.

Bernard,M.L., Peterson,Y.K., Chung,P., Jourdan,J., and Lanier,S.M. (2001). *Selective interaction of AGS3 with G-proteins and the influence of AGS3 on the activation state of G-proteins*. J Biol Chem *276*, 1585-1593.

Berstein,G., Blank,J.L., Jhon,D.Y., Exton,J.H., Rhee,S.G., and Ross,E.M. (1992). *Phospholipase C-beta 1 is a GTPase-activating protein for Gq/11, its physiologic regulator*. Cell *70*, 411-418.

Bisgrove,B.W., Raible,D.W., Walter,V., Eisen,J.S., and Grunwald,D.J. (1997). *Expression of c-ret in the zebrafish embryo: potential roles in motoneuronal development*. J Neurobiol. *33*, 749-768.

Blader,P., Fischer,N., Gradwohl,G., Guillemot,F., and Strahle,U. (1997). *The activity of neurogenin1 is controlled by local cues in the zebrafish embryo*. Development *124*, 4557-4569.

Blatch,G.L. and Lassle,M. (1999). *The tetratricopeptide repeat: a structural motif mediating protein-protein interactions*. Bioessays *21*, 932-939.

Blumer,J.B., Bernard,M.L., Peterson,Y.K., Nezu,J., Chung,P., Dunican,D.J., Knoblich,J.A., and Lanier,S.M. (2003). *Interaction of activator of G-protein signaling 3 (AGS3) with LKB1, a serine/threonine kinase involved in cell polarity and cell cycle progression: phosphorylation of the G-protein regulatory (GPR) motif as a regulatory mechanism for the interaction of GPR motifs with Gi alpha*. J Biol Chem *278*, 23217-23220.

Blumer,J.B., Chandler,L.J., and Lanier,S.M. (2002). *Expression analysis and subcellular distribution of the two G-protein regulators AGS3 and LGN indicate distinct functionality. Localization of LGN to the midbody during cytokinesis*. J Biol Chem *277*, 15897-15903.

Bodmer,R., Barbel,S., Sheperd,S., Jack,J.W., Jan,L.Y., and Jan,Y.N. (1987). *Transformation of sensory organs by mutations of the cut locus of D. melanogaster*. Cell *51*, 293-307.

Bodmer,R., Carretto,R., and Jan,Y.N. (1989). *Neurogenesis of the peripheral nervous system in Drosophila embryos: DNA replication patterns and cell lineages*. Neuron *3*, 21-32.

Bos,J.L. (1998). *All in the family? New insights and questions regarding interconnectivity of Ras, Rap1 and Ral*. EMBO J *17*, 6776-6782.

Bos,J.L., de Rooij,J., and Reedquist,K.A. (2001). *Rap1 signalling: adhering to new models*. Nat Rev Mol Cell Biol *2*, 369-377.

Bos,J.L., Franke,B., M'Rabet,L., Reedquist,K., and Zwartkruis,F. (1997). *In search of a function for the Ras-like GTPase Rap1*. FEBS Lett *410*, 59-62.

Bossing,T., Technau,G.M., and Doe,C.Q. (1996). *huckebein is required for glial development and axon pathfinding in the neuroblast 1-1 and neuroblast 2-2 lineages in the Drosophila central nervous system*. Mech Dev *55*, 53-64.

Bourne,H.R. (1997). *How receptors talk to trimeric G proteins*. Curr Opin Cell Biol *9*, 134-142.

Bowman,E.P., Campbell,J.J., Druey,K.M., Scheschonka,A., Kehrl,J.H., and Butcher,E.C. (1998). *Regulation of chemotactic and proadhesive responses to chemoattractant receptors by RGS (regulator of G-protein signaling) family members*. J Biol Chem *273*, 28040-28048.

Brand,M., Jarman,A.P., Jan,L.Y., and Jan,Y.N. (1993). *asense is a Drosophila neural precursor gene and is capable of initiating sense organ formation*. Development *119*, 1-17.

Bray,S. (1998). *Notch signalling in Drosophila: three ways to use a pathway*. Semin. Cell Dev Biol *9*, 591-597.

Brewster,R. and Bodmer,R. (1995). *Origin and specification of type II sensory neurons in Drosophila*. Development *121*, 2923-2936.

Brewster,R. and Bodmer,R. (1996). *Cell lineage analysis of the Drosophila peripheral nervous system*. Dev Genet *18*, 50-63.

Brewster,R., Hardiman,K., Deo,M., Khan,S., and Bodmer,R. (2001). *The selector gene cut represses a neural cell fate that is specified independently of the Achaete-Scute-Complex and atonal*. Mech Dev *105*, 57-68.

Briscoe,J., Chen,Y., Jessell,T.M., and Struhl,G. (2001). *A hedgehog-insensitive form of patched provides evidence for direct long-range morphogen activity of sonic hedgehog in the neural tube*. Mol Cell *7*, 1279-1291.

Broadus,J. and Doe,C.Q. (1997). *Extrinsic cues, intrinsic cues and microfilaments regulate asymmetric protein localization in Drosophila neuroblasts*. Curr Biol *7*, 827-835.

Buck,E., Li,J., Chen,Y., Weng,G., Scarlata,S., and Iyengar,R. (1999). *Resolution of a signal transfer region from a general binding domain in gbeta for stimulation of phospholipase C-beta2*. Science *283*, 1332-1335.

Buescher,M., Yeo,S.L., Udolph,G., Zavortink,M., Yang,X., Tear,G., and Chia,W. (1998). *Binary sibling neuronal cell fate decisions in the Drosophila embryonic central nervous system are nonstochastic and require inscuteable-mediated asymmetry of ganglion mother cells*. Genes Dev *12*, 1858-1870.

Cabrera-Vera,T.M., Vanhauwe,J., Thomas,T.O., Medkova,M., Preininger,A., Mazzoni,M.R., and Hamm,H.E. (2003). *Insights into G protein structure, function, and regulation*. Endocr. Rev *24* , 765-781.

Cai,Y., Yu,F., Lin,S., Chia,W., and Yang,X. (2003). *Apical complex genes control mitotic spindle geometry and relative size of daughter cells in Drosophila neuroblast and pI asymmetric divisions*. Cell *112*, 51-62.

Casey,M.L., Smith,J., Alsabrook,G., and MacDonald,P.C. (1997). *Activation of adenylyl cyclase in human myometrial smooth muscle cells by neuropeptides*. J Clin Endocrinol. Metab *82*, 3087-3092.

Caudy,M., Vassin,H., Brand,M., Tuma,R., Jan,L.Y., and Jan,Y.N. (1988). *daughterless, a Drosophila gene essential for both neurogenesis and sex determination, has sequence similarities to myc and the achaete-scute complex*. Cell *55*, 1061-1067.

Cayouette,M. and Raff,M. (2002). *Asymmetric segregation of Numb: a mechanism for neural specification from Drosophila to mammals*. Nat Neurosci. *5*, 1265-1269.

Cayouette,M., Whitmore,A.V., Jeffery,G., and Raff,M. (2001). *Asymmetric segregation of Numb in retinal development and the influence of the pigmented epithelium*. J Neurosci. *21*, 5643-5651.

Chang,D.T., Lopez,A., von Kessler,D.P., Chiang,C., Simandl,B.K., Zhao,R., Seldin,M.F., Fallon,J.F., and Beachy,P.A. (1994). *Products, genetic linkage and limb patterning activity of a murine hedgehog gene*. Development *120*, 3339-3353.

Chen,C., Wang,H., Fong,C.W., and Lin,S.C. (2001). *Multiple phosphorylation sites in RGS16 differentially modulate its GAP activity*. FEBS Lett *504*, 16-22.

Chen,C., Zheng,B., Han,J., and Lin,S.C. (1997). *Characterization of a novel mammalian RGS protein that binds to Galpha proteins and inhibits pheromone signaling in yeast*. J Biol Chem *272*, 8679-8685.

Chen,C.H., von Kessler,D.P., Park,W., Wang,B., Ma,Y., and Beachy,P.A. (1999). *Nuclear trafficking of Cubitus interruptus in the transcriptional regulation of Hedgehog target gene expression*. Cell *98*, 305-316.

Chen,F., Barkett,M., Ram,K.T., Quintanilla,A., and Hariharan,I.K. (1997). *Biological characterization of Drosophila Rapgap1, a GTPase activating protein for Rap1*. Proc Natl Acad Sci U S A *94*, 12485-12490.

Chen,W., Burgess,S., and Hopkins,N. (2001). *Analysis of the zebrafish smoothened mutant reveals conserved and divergent functions of hedgehog activity*. Development *128*, 2385-2396.

Chia,W. and Yang,X. (2002). *Asymmetric division of Drosophila neural progenitors*. Curr Opin Genet Dev *12*, 459-464.

Chidiac,P. and Roy,A.A. (2003). *Activity, regulation, and intracellular localization of RGS proteins*. Receptors. Channels *9*, 135-147.

Chu,D.T. and Klymkowsky,M.W. (1989). *The appearance of acetylated alpha-tubulin during early development and cellular differentiation in Xenopus*. Dev Biol *136*, 104-117.

Cismowski,M.J., Takesono,A., Ma,C., Lizano,J.S., Xie,X., Fuernkranz,H., Lanier,S.M., and Duzic,E. (1999). *Genetic screens in yeast to identify mammalian nonreceptor modulators of G-protein signaling*. Nat Biotechnol. *17*, 878-883.

Clapham,D.E. and Neer,E.J. (1997). *G protein beta gamma subunits*. Annu Rev Pharmacol Toxicol *37*, 167-203.

Coleman,D.E., Berghuis,A.M., Lee,E., Linder,M.E., Gilman,A.G., and Sprang,S.R. (1994). *Structures of active conformations of Gi alpha 1 and the mechanism of GTP hydrolysis*. Science *265*, 1405-1412.

Concordet,J.P., Lewis,K.E., Moore,J.W., Goodrich,L.V., Johnson,R.L., Scott,M.P., and Ingham,P.W. (1996). *Spatial regulation of a zebrafish patched homolog reflects the roles of sonic hedgehog and protein kinase A in neural tube and somite patterning*. Development *122*, 2835-2846.

Conklin,B.R., Farfel,Z., Lustig,K.D., Julius,D., and Bourne,H.R. (1993). *Substitution of three amino acids switches receptor specificity of Gq alpha to that of Gi alpha*. Nature *363*, 274-276.

Crouch,M.F. and Simson,L. (1997). *The G-protein G(i) regulates mitosis but not DNA synthesis in growth factor-activated fibroblasts: a role for the nuclear translocation of G(i)*. FASEB J *11*, 189-198.

Currie,P.D. and Ingham,P.W. (1996). *Induction of a specific muscle cell type by a hedgehog-like protein in zebrafish*. Nature *382*, 452-455.

Daumke,O., Weyand,M., Chakrabarti,P.P., Vetter,I.R., and Wittinghofer,A. (2004). *The GTPase-activating protein Rap1GAP uses a catalytic asparagine*. Nature *429*, 197-201.

de Almeida,J.B., Holtzman,E.J., Peters,P., Ercolani,L., Ausiello,D.A., and Stow,J.L. (1994). *Targeting of chimeric G alpha i proteins to specific membrane domains*. J Cell Sci *107 ( Pt 3)*, 507-515.

de Rooij,J., Zwartkruis,F.J., Verheijen,M.H., Cool,R.H., Nijman,S.M., Wittinghofer,A., and Bos,J.L. (1998). *Epac is a Rap1 guanine-nucleotide-exchange factor directly activated by cyclic AMP*. Nature *396*, 474-477.

De Vries,L., Fischer,T., Tronchere,H., Brothers,G.M., Strockbine,B., Siderovski,D.P., and Farquhar,M.G. (2000). *Activator of G protein signaling 3 is a guanine dissociation inhibitor for Galpha i subunits*. Proc Natl Acad Sci U S A *97*, 14364-14369.

DeCamp,D.L., Thompson,T.M., de Sauvage,F.J., and Lerner,M.R. (2000). *Smoothened activates Galphai-mediated signaling in frog melanophores*. J Biol Chem *275*, 26322-26327.

Denef,N., Neubuser,D., Perez,L., and Cohen,S.M. (2000). *Hedgehog induces opposite changes in turnover and subcellular localization of patched and smoothened*. Cell *102*, 521-531.

Denker,B.M., Boutin,P.M., and Neer,E.J. (1995). *Interactions between the amino- and carboxyl-terminal regions of G alpha subunits: analysis of mutated G alpha o/G alpha i2 chimeras*. Biochemistry *34*, 5544-5553.

Dick,T., Yang,X.H., Yeo,S.L., and Chia,W. (1991). *Two closely linked Drosophila POU domain genes are expressed in neuroblasts and sensory elements*. Proc Natl Acad Sci U S A *88*, 7645-7649.

Doe,C.Q. (1992). *Molecular markers for identified neuroblasts and ganglion mother cells in the Drosophila central nervous system*. Development *116*, 855-863.

Doe,C.Q. and Skeath,J.B. (1996). *Neurogenesis in the insect central nervous system*. Curr Opin Neurobiol. *6*, 18-24.

Doe,C.Q., Chu-LaGraff,Q., Wright,D.M., and Scott,M.P. (1991). *The prospero gene specifies cell fates in the Drosophila central nervous system*. Cell *65*, 451-464.

D'Silva,N.J., Mitra,R.S., Zhang,Z., Kurnit,D.M., Babcock,C.R., Polverini,P.J., and Carey,T.E. (2003). *Rap1, a small GTP-binding protein is upregulated during arrest of proliferation in human keratinocytes*. J Cell Physiol *196*, 532-540.

Du,Q., Stukenberg,P.T., and Macara,I.G. (2001). *A mammalian Partner of inscuteable binds NuMA and regulates mitotic spindle organization*. Nat Cell Biol *3*, 1069-1075.

Du,Q., Taylor,L., Compton,D.A., and Macara,I.G. (2002). *LGN blocks the ability of NuMA to bind and stabilize microtubules. A mechanism for mitotic spindle assembly regulation*. Curr Biol *12*, 1928-1933.

Echelard,Y., Epstein,D.J., St Jacques,B., Shen,L., Mohler,J., McMahon,J.A., and McMahon,A.P. (1993). *Sonic hedgehog, a member of a family of putative signaling molecules, is implicated in the regulation of CNS polarity*. Cell *75*, 1417-1430.

Eisen,J.S. (1991). *Determination of primary motoneuron identity in developing zebrafish embryos*. Science *252*, 569-572.

Eisen,J.S. (1999). *Patterning motoneurons in the vertebrate nervous system*. Trends Neurosci. *22*, 321-326.

Eisen,J.S. and Pike,S.H. (1991). *The spt-1 mutation alters segmental arrangement and axonal development of identified neurons in the spinal cord of the embryonic zebrafish*. Neuron *6*, 767-776.

Ekker,S.C., McGrew,L.L., Lai,C.J., Lee,J.J., von Kessler,D.P., Moon,R.T., and Beachy,P.A. (1995). *Distinct expression and shared activities of members of the hedgehog gene family of Xenopus laevis*. Development *121*, 2337-2347.

Ensini,M., Tsuchida,T.N., Belting,H.G., and Jessell,T.M. (1998). *The control of rostrocaudal pattern in the developing spinal cord: specification of motor neuron subtype identity is initiated by signals from paraxial mesoderm*. Development *125*, 969-982.

Ercolani,L., Stow,J.L., Boyle,J.F., Holtzman,E.J., Lin,H., Grove,J.R., and Ausiello,D.A. (1990). *Membrane localization of the pertussis toxin-sensitive G-protein subunits alpha i-2 and alpha i-3 and expression of a metallothionein-alpha i-2 fusion gene in LLC-PK1 cells*. Proc Natl Acad Sci U S A *87*, 4635-4639.

Farquhar,M.G. and PALADE,G.E. (1963). *Junctional complexes in various epithelia*. J Cell Biol *17*, 375-412.

Fields,T.A. and Casey,P.J. (1997). *Signalling functions and biochemical properties of pertussis toxin-resistant G-proteins*. Biochem J *321 ( Pt 3)*, 561-571.

Fuja,T.J., Schwartz,P.H., Darcy,D., and Bryant,P.J. (2004). *Asymmetric localization of LGN but not AGS3, two homologs of Drosophila pins, in dividing human neural progenitor cells*. J Neurosci. Res *75*, 782-793.

Fukui,R., Amakawa,M., Hoshiga,M., Shibata,N., Kohbayashi,E., Seto,M., Sasaki,Y., Ueno,T., Negoro,N., Nakakoji,T., Ii,M., Nishiguchi,F., Ishihara,T., and Ohsawa,N. (2000). *Increased migration in late G(1) phase in cultured smooth muscle cells*. Am J Physiol Cell Physiol *279*, C999-1007.

Gautam,N., Downes,G.B., Yan,K., and Kisselev,O. (1998). *The G-protein betagamma complex*. Cell Signal. *10*, 447-455.

Ghysen,A. and Dambly-Chaudiere,C. (1989). *Genesis of the Drosophila peripheral nervous system*. Trends Genet *5*, 251-255.

Gilman,A.G. (1987). *G proteins: transducers of receptor-generated signals*. Annu Rev Biochem *56*, 615-649.

Gotoh,T., Hattori,S., Nakamura,S., Kitayama,H., Noda,M., Takai,Y., Kaibuchi,K., Matsui,H., Hatase,O., Takahashi,H., and . (1995). *Identification of Rap1 as a target for the Crk SH3 domain-binding guanine nucleotide-releasing factor C3G*. Mol Cell Biol *15*, 6746-6753.

Gotta,M., Dong,Y., Peterson,Y.K., Lanier,S.M., and Ahringer,J. (2003). *Asymmetrically distributed C. elegans homologs of AGS3/PINS control spindle position in the early embryo*. Curr Biol *13*, 1029-1037.

Granderath,S., Bunse,I., and Klambt,C. (2000). *gcm and pointed synergistically control glial transcription of the Drosophila gene loco*. Mech Dev *91*, 197-208.

Gruning,W., Arnould,T., Jochimsen,F., Sellin,L., Ananth,S., Kim,E., and Walz,G. (1999). *Modulation of renal tubular cell function by RGS3*. Am J Physiol *276*, F535-F543.

Grunwald,D.J., Kimmel,C.B., Westerfield,M., Walker,C., and Streisinger,G. (1988). *A neural degeneration mutation that spares primary neurons in the zebrafish*. Dev Biol *126*, 115-128.

Gudermann,T., Kalkbrenner,F., Dippel,E., Laugwitz,K.L., and Schultz,G. (1997). *Specificity and complexity of receptor-G-protein interaction*. Adv. Second Messenger Phosphoprotein Res *31*, 253-262.

Guo,M., Bier,E., Jan,L.Y., and Jan,Y.N. (1995). *tramtrack acts downstream of numb to specify distinct daughter cell fates during asymmetric cell divisions in the Drosophila PNS*. Neuron *14*, 913-925.

Guo,M., Jan,L.Y., and Jan,Y.N. (1996). *Control of daughter cell fates during asymmetric division: interaction of Numb and Notch* . Neuron *17*, 27-41.

Guo,Y., Wang,Z., Carter,A., Kaiser,K., and Dow,J.A. (1996). *Characterization of vha26, the Drosophila gene for a 26 kDa E-subunit of the vacuolar ATPase*. Biochim. Biophys Acta *1283*, 4-9.

Haddon,C. and Lewis,J. (1996). *Early ear development in the embryo of the zebrafish, Danio rerio*. J Comp Neurol. *365*, 113-128.

Haddon,C., Smithers,L., Schneider-Maunoury,S., Coche,T., Henrique,D., and Lewis,J. (1998). *Multiple delta genes and lateral inhibition in zebrafish primary neurogenesis*. Development *125*, 359-370.

Halter,D.A., Urban,J., Rickert,C., Ner,S.S., Ito,K., Travers,A.A., and Technau,G.M. (1995). *The homeobox gene repo is required for the differentiation and maintenance of glia function in the embryonic nervous system of Drosophila melanogaster*. Development *121*, 317-332.

Hamm,H.E. (1998). *The many faces of G protein signaling*. J Biol Chem *273*, 669-672.

Hammerschmidt,M. and McMahon,A.P. (1998). *The effect of pertussis toxin on zebrafish development: a possible role for inhibitory G-proteins in hedgehog signaling*. Dev Biol *194*, 166-171.

Hammerschmidt,M., Bitgood,M.J., and McMahon,A.P. (1996). *Protein kinase A is a common negative regulator of Hedgehog signaling in the vertebrate embryo*. Genes Dev *10*, 647-658.

Hartenstein,V. and Posakony,J.W. (1989). *Development of adult sensilla on the wing and notum of Drosophila melanogaster*. Development *107*, 389-405.

Hay,B.A., Maile,R., and Rubin,G.M. (1997). *P element insertion-dependent gene activation in the Drosophila eye*. Proc Natl Acad Sci U S A *94*, 5195-5200.

Hepler,J.R. (1999). *Emerging roles for RGS proteins in cell signalling*. Trends Pharmacol Sci *20*, 376-382.

Hepler,J.R. (2003). *RGS protein and G protein interactions: a little help from their friends*. Mol Pharmacol *64*, 547-549.

Hoffmann,M., Ward,R.J., Cavalli,A., Carr,I.C., and Milligan,G. (2001). *Differential capacities of the RGS1, RGS16 and RGS-GAIP regulators of G protein signaling to enhance alpha2A-adrenoreceptor agonist-stimulated GTPase activity of G(o1)alpha*. J Neurochem *78*, 797-806.

Hollinger,S. and Hepler,J.R. (2002). *Cellular regulation of RGS proteins: modulators and integrators of G protein signaling*. Pharmacol Rev *54*, 527-559.

Hollinger,S., Ramineni,S., and Hepler,J.R. (2003). *Phosphorylation of RGS14 by protein kinase A potentiates its activity toward G alpha i*. Biochemistry *42*, 811-819.

Huang,M.L., Hsu,C.H., and Chien,C.T. (2000). *The proneural gene amos promotes multiple dendritic neuron formation in the Drosophila peripheral nervous system*. Neuron *25*, 57-67.

Hynes,M., Ye,W., Wang,K., Stone,D., Murone,M., Sauvage,F., and Rosenthal,A. (2000). *The seven-transmembrane receptor smoothened cell-autonomously induces multiple ventral cell types*. Nat Neurosci. *3*, 41-46.

Incardona,J.P., Gruenberg,J., and Roelink,H. (2002). *Sonic hedgehog induces the segregation of patched and smoothened in endosomes*. Curr Biol *12*, 983-995.

Ingham,P.W., Baker,N.E., and Martinez-Arias,A. (1988). *Regulation of segment polarity genes in the Drosophila blastoderm by fushi tarazu and even skipped*. Nature *331*, 73-75.

Inoue,A., Takahashi,M., Hatta,K., Hotta,Y., and Okamoto,H. (1994). *Developmental regulation of islet-1 mRNA expression during neuronal differentiation in embryonic zebrafish*. Dev Dyn. *199*, 1-11.

Izumi,Y., Ohta,N., Itoh-Furuya,A., Fuse,N., and Matsuzaki,F. (2004). *Differential functions of G protein and Baz-aPKC signaling pathways in Drosophila neuroblast asymmetric division*. J Cell Biol *164*, 729-738.

Jamora,C., Takizawa,P.A., Zaarour,R.F., Denesvre,C., Faulkner,D.J., and Malhotra,V. (1997). *Regulation of Golgi structure through heterotrimeric G proteins*. Cell *91*, 617-626.

Jan,Y.N. and Jan,L.Y. (1995). *Maggot's hair and bug's eye: role of cell interactions and intrinsic factors in cell fate specification*. Neuron *14*, 1-5.

Jarman,A.P., Brand,M., Jan,L.Y., and Jan,Y.N. (1993). *The regulation and function of the helix-loop-helix gene, asense, in Drosophila neural precursors*. Development *119*, 19-29.

Jiang,J. and Struhl,G. (1998). *Regulation of the Hedgehog and Wingless signalling pathways by the F-box/WD40-repeat protein Slimb*. Nature *391*, 493-496.

Kaushik,R., Yu,F., Chia,W., Yang,X., and Bahri,S. (2003). *Subcellular localization of LGN during mitosis: evidence for its cortical localization in mitotic cell culture*

*systems and its requirement for normal cell cycle progression*. Mol Biol Cell *14*, 3144-3155.

Kawasaki,H., Springett,G.M., Mochizuki,N., Toki,S., Nakaya,M., Matsuda,M., Housman,D.E., and Graybiel,A.M. (1998). *A family of cAMP-binding proteins that directly activate Rap1*. Science *282*, 2275-2279.

Kelly,G.M., Vanderbeld,B., Krawetz,R., and Mangos,S. (2001). *Differential distribution of the G protein gamma3 subunit in the developing zebrafish nervous system*. Int. J Dev Neurosci. *19*, 455-467.

Kimmel,C.B. and Warga,R.M. (1988). *Cell lineage and developmental potential of cells in the zebrafish embryo*. Trends Genet *4*, 68-74.

Kimmel,C.B., Ballard,W.W., Kimmel,S.R., Ullmann,B., and Schilling,T.F. (1995). *Stages of embryonic development of the zebrafish* . Dev Dyn. *203*, 253-310.

Kimmel,C.B., Warga,R.M., and Kane,D.A. (1994). *Cell cycles and clonal strings during formation of the zebrafish central nervous system*. Development *120*, 265-276.

Kimple,R.J., De Vries,L., Tronchere,H., Behe,C.I., Morris,R.A., Gist,F.M., and Siderovski,D.P. (2001). *RGS12 and RGS14 GoLoco motifs are G alpha(i) interaction sites with guanine nucleotide dissociation inhibitor Activity*. J Biol Chem *276*, 29275-29281.

Kimple,R.J., Willard,F.S., and Siderovski,D.P. (2002). *The GoLoco motif: heralding a new tango between G protein signaling and cell division*. Mol Interv. *2*, 88-100.

Knoblich,J.A. (1997). *Mechanisms of asymmetric cell division during animal development*. Curr Opin Cell Biol *9*, 833-841.

Knoblich,J.A. (2001). *Asymmetric cell division during animal development*. Nat Rev Mol Cell Biol *2*, 11-20.

Knoblich,J.A., Jan,L.Y., and Jan,Y.N. (1995). *Asymmetric segregation of Numb and Prospero during cell division*. Nature *377*, 624-627.

Knoblich,J.A., Jan,L.Y., and Jan,Y.N. (1997). *The N terminus of the Drosophila Numb protein directs membrane association and actin-dependent asymmetric localization*. Proc Natl Acad Sci U S A *94*, 13005-13010.

Knust,E. (2001). *G protein signaling and asymmetric cell division*. Cell *107*, 125-128.

Koelle,M.R. and Horvitz,H.R. (1996). *EGL-10 regulates G protein signaling in the C. elegans nervous system and shares a conserved domain with many mammalian proteins*. Cell *84*, 115-125.

Kohtz,J.D. and Fishell,G. (2004). *Developmental regulation of EVF-1, a novel non-coding RNA transcribed upstream of the mouse Dlx6 gene*. Gene Expr. Patterns. *4*, 407-412.

Krauss,S., Concordet,J.P., and Ingham,P.W. (1993). *A functionally conserved homolog of the Drosophila segment polarity gene hh is expressed in tissues with polarizing activity in zebrafish embryos*. Cell *75*, 1431-1444.

Kraut,R. and Campos-Ortega,J.A. (1996). *inscuteable, a neural precursor gene of Drosophila, encodes a candidate for a cytoskeleton adaptor protein*. Dev Biol *174*, 65-81.

Kraut,R., Chia,W., Jan,L.Y., Jan,Y.N., and Knoblich,J.A. (1996). *Role of inscuteable in orienting asymmetric cell divisions in Drosophila*. Nature *383*, 50-55.

Kurachi,H., Wada,Y., Tsukamoto,N., Maeda,M., Kubota,H., Hattori,M., Iwai,K., and Minato,N. (1997). *Human SPA-1 gene product selectively expressed in lymphoid tissues is a specific GTPase-activating protein for Rap1 and Rap2. Segregate expression profiles from a rap1GAP gene product*. J Biol Chem *272*, 28081-28088.

Labbe,J.C., Maddox,P.S., Salmon,E.D., and Goldstein,B. (2003). *PAR proteins regulate microtubule dynamics at the cell cortex in C. elegans*. Curr Biol *13*, 707-714.

Lai,E.C. and Orgogozo,V. (2004). *A hidden program in Drosophila peripheral neurogenesis revealed: fundamental principles underlying sensory organ diversity*. Dev Biol *269*, 1-17.

Lambright,D.G., Noel,J.P., Hamm,H.E., and Sigler,P.B. (1994). *Structural determinants for activation of the alpha-subunit of a heterotrimeric G protein*. Nature *369*, 621-628.

Lambright,D.G., Sondek,J., Bohm,A., Skiba,N.P., Hamm,H.E., and Sigler,P.B. (1996). *The 2.0 A crystal structure of a heterotrimeric G protein*. Nature *379*, 311-319.

Lee,J.E. (1997). *Basic helix-loop-helix genes in neural development*. Curr Opin Neurobiol. *7*, 13-20.

Lewis,J. (1996). *Neurogenic genes and vertebrate neurogenesis*. Curr Opin Neurobiol. *6*, 3-10.

Lewis,K.E. and Eisen,J.S. (2001). *Hedgehog signaling is required for primary motoneuron induction in zebrafish*. Development *128*, 3485-3495.

Lewis,K.E. and Eisen,J.S. (2004). *Paraxial mesoderm specifies zebrafish primary motoneuron subtype identity*. Development *131*, 891-902.

Li,P., Yang,X., Wasser,M., Cai,Y., and Chia,W. (1997). *Inscuteable and Staufen mediate asymmetric localization and segregation of prospero RNA during Drosophila neuroblast cell divisions*. Cell *90*, 437-447.

Liu,S., Aghakhani,N., Boisset,N., Said,G., and Tadie,M. (2001). *Innervation of the caudal denervated ventral roots and their target muscles by the rostral spinal motoneurons after implanting a nerve autograft in spinal cord-injured adult marmosets*. J Neurosurg. *94*, 82-90.

Lloyd,A. and Sakonju,S. (1991). *Characterization of two Drosophila POU domain genes, related to oct-1 and oct-2, and the regulation of their expression patterns*. Mech Dev *36*, 87-102.

Lu,B., Rothenberg,M., Jan,L.Y., and Jan,Y.N. (1998). *Partner of Numb colocalizes with Numb during mitosis and directs Numb asymmetric localization in Drosophila neural and muscle progenitors*. Cell *95*, 225-235.

Luo,Y. and Denker,B.M. (1999). *Interaction of heterotrimeric G protein Galphao with Purkinje cell protein-2. Evidence for a novel nucleotide exchange factor*. J Biol Chem *274*, 10685-10688.

Ma,H., Peterson,Y.K., Bernard,M.L., Lanier,S.M., and Graber,S.G. (2003). *Influence of cytosolic AGS3 on receptor--G protein coupling*. Biochemistry *42*, 8085-8093.

Ma,Q., Kintner,C., and Anderson,D.J. (1996). *Identification of neurogenin, a vertebrate neuronal determination gene*. Cell *87*, 43-52.

Manser,E., Huang,H.Y., Loo,T.H., Chen,X.Q., Dong,J.M., Leung,T., and Lim,L. (1997). *Expression of constitutively active alpha-PAK reveals effects of the kinase on actin and focal complexes*. Mol Cell Biol *17*, 1129-1143.

Martin,S.G. and St Johnston,D. (2003). *A role for Drosophila LKB1 in anterior-posterior axis formation and epithelial polarity*. Nature *421*, 379-384.

Mendelson,B. and Kimmel,C.B. (1986). *Identified vertebrate neurons that differ in axonal projection develop together*. Dev Biol *118*, 309-313.

Meng,J. and Casey,P.J. (2002). *Activation of Gz attenuates Rap1-mediated differentiation of PC12 cells*. J Biol Chem *277*, 43417-43424.

Meng,J., Glick,J.L., Polakis,P., and Casey,P.J. (1999). *Functional interaction between Galpha(z) and Rap1GAP suggests a novel form of cellular cross-talk*. J Biol Chem *274*, 36663-36669.

Miller,K.G., Emerson,M.D., McManus,J.R., and Rand,J.B. (2000). *RIC-8 (Synembryn): a novel conserved protein that is required for G(q)alpha signaling in the C. elegans nervous system*. Neuron *27*, 289-299.

Miranda,K.C., Joseph,S.R., Yap,A.S., Teasdale,R.D., and Stow,J.L. (2003). *Contextual binding of p120ctn to E-cadherin at the basolateral plasma membrane in polarized epithelia*. J Biol Chem *278*, 43480-43488.

Mochizuki,N., Cho,G., Wen,B., and Insel,P.A. (1996). *Identification and cDNA cloning of a novel human mosaic protein, LGN, based on interaction with G alpha i2*. Gene *181*, 39-43.

Mochizuki,N., Ohba,Y., Kiyokawa,E., Kurata,T., Murakami,T., Ozaki,T., Kitabatake,A., Nagashima,K., and Matsuda,M. (1999). *Activation of the ERK/MAPK pathway by an isoform of rap1GAP associated with G alpha(i)*. Nature *400*, 891-894.

Moratz,C., Kang,V.H., Druey,K.M., Shi,C.S., Scheschonka,A., Murphy,P.M., Kozasa,T., and Kehrl,J.H. (2000). *Regulator of G protein signaling 1 (RGS1) markedly impairs Gi alpha signaling responses of B lymphocytes*. J Immunol *164*, 1829-1838.

Natochin,M., Lester,B., Peterson,Y.K., Bernard,M.L., Lanier,S.M., and Artemyev,N.O. (2000). *AGS3 inhibits GDP dissociation from galpha subunits of the Gi family and rhodopsin-dependent activation of transducin*. J Biol Chem *275*, 40981-40985.

Noel,J.P., Hamm,H.E., and Sigler,P.B. (1993). *The 2.2 A crystal structure of transducin-alpha complexed with GTP gamma S*. Nature *366*, 654-663.

Norris,W., Neyt,C., Ingham,P.W., and Currie,P.D. (2000). *Slow muscle induction by Hedgehog signalling in vitro*. J Cell Sci *113 ( Pt 15)*, 2695-2703.

Ohshiro,T., Yagami,T., Zhang,C., and Matsuzaki,F. (2000). *Role of cortical tumour-suppressor proteins in asymmetric division of Drosophila neuroblast*. Nature *408*, 593-596.

Orgogozo,V., Schweisguth,F., and Bellaiche,Y. (2001). *Lineage, cell polarity and inscuteable function in the peripheral nervous system of the Drosophila embryo*. Development *128*, 631-643.

Orgogozo,V., Schweisguth,F., and Bellaiche,Y. (2002). *Binary cell death decision regulated by unequal partitioning of Numb at mitosis*. Development *129*, 4677-4684.

Oxtoby, E and Jowett, T., 1993. *Cloning of the zebrafish krox-20 gene(krx-20) and its expression during hindbrain development*. Nucleic Acid Res. 21, 1087-1095

Patel,N.H., Kornberg,T.B., and Goodman,C.S. (1989). *Expression of engrailed during segmentation in grasshopper and crayfish*. Development *107*, 201-212.

Papan C. and Campos-Ortega . J.A., (1997) *A clonal analysis of spinal cord development in the zebrafish.* Dev. Gen. and Evol. *207, 71 - 81*

Pattingre,S., De Vries,L., Bauvy,C., Chantret,I., Cluzeaud,F., Ogier-Denis,E., Vandewalle,A., and Codogno,P. (2003). *The G-protein regulator AGS3 controls an early event during macroautophagy in human intestinal HT-29 cells*. J Biol Chem *278*, 20995-21002.

Pedram,A., Razandi,M., Kehrl,J., and Levin,E.R. (2000). *Natriuretic peptides inhibit G protein activation. Mediation through cross-talk between cyclic GMP-dependent protein kinase and regulators of G protein-signaling proteins*. J Biol Chem *275*, 7365-7372.

Petersen,P.H., Zou,K., Hwang,J.K., Jan,Y.N., and Zhong,W. (2002). *Progenitor cell maintenance requires numb and numblike during mouse neurogenesis*. Nature *419*, 929-934.

Peterson,Y.K., Bernard,M.L., Ma,H., Hazard,S., III, Graber,S.G., and Lanier,S.M. (2000). *Stabilization of the GDP-bound conformation of Gialpha by a peptide derived from the G-protein regulatory motif of AGS3*. J Biol Chem *275*, 33193-33196.

Pizzinat,N., Takesono,A., and Lanier,S.M. (2001). *Identification of a truncated form of the G-protein regulator AGS3 in heart that lacks the tetratricopeptide repeat domains*. J Biol Chem *276*, 16601-16610.

Posakony,J.W. (1994). *Nature versus nurture: asymmetric cell divisions in Drosophila bristle development*. Cell *76*, 415-418.

Preininger,A.M. and Hamm,H.E. (2004). *G protein signaling: insights from new structures*. Sci STKE *2004*, re3.

Radhika,V. and Dhanasekaran,N. (2001). *Transforming G proteins*. Oncogene *20*, 1607-1614.

Reif,K. and Cyster,J.G. (2000). *RGS molecule expression in murine B lymphocytes and ability to down-regulate chemotaxis to lymphoid chemokines*. J Immunol *164*, 4720-4729.

Rens-Domiano,S. and Hamm,H.E. (1995). *Structural and functional relationships of heterotrimeric G-proteins*. FASEB J *9*, 1059-1066.

Rhyu,M.S. and Knoblich,J.A. (1995). *Spindle orientation and asymmetric cell fate*. Cell *82*, 523-526.

Rhyu,M.S., Jan,L.Y., and Jan,Y.N. (1994). *Asymmetric distribution of numb protein during division of the sensory organ precursor cell confers distinct fates to daughter cells*. Cell *76* , 477-491.

Riddle,R.D., Johnson,R.L., Laufer,E., and Tabin,C. (1993). *Sonic hedgehog mediates the polarizing activity of the ZPA*. Cell *75*, 1401-1416.

Roelink,H., Augsburger,A., Heemskerk,J., Korzh,V., Norlin,S., Altaba,A., Tanabe,Y., Placzek,M., Edlund,T., Jessell,T.M., and . (1994). *Floor plate and motor neuron induction by vhh-1, a vertebrate homolog of hedgehog expressed by the notochord*. Cell *76*, 761-775.

Roy,M.N., Prince,V.E., and Ho,R.K. (1999). *Heat shock produces periodic somitic disturbances in the zebrafish embryo*. Mech Dev *85*, 27-34.

Roychowdhury,S., Panda,D., Wilson,L., and Rasenick,M.M. (1999). *G protein alpha subunits activate tubulin GTPase and modulate microtubule polymerization dynamics*. J Biol Chem *274*, 13485-13490.

Rubinfeld,B., Munemitsu,S., Clark,R., Conroy,L., Watt,K., Crosier,W.J., McCormick,F., and Polakis,P. (1991). *Molecular cloning of a GTPase activating protein specific for the Krev-1 protein p21rap1*. Cell *65*, 1033-1042.

Rubinfeld,H., Hanoch,T., and Seger,R. (1999). *Identification of a cytoplasmic-retention sequence in ERK2*. J Biol Chem *274*, 30349-30352.

Salzberg,A. and Bellen,H.J. (1996). *Invertebrate versus vertebrate neurogenesis: variations on the same theme?* Dev Genet *18*, 1-10.

Sato,M., Gettys,T.W., and Lanier,S.M. (2004). *AGS3 and signal integration by Galpha(s)- and Galpha(i)-coupled receptors: AGS3 blocks the sensitization of adenylyl cyclase following prolonged stimulation of a Galpha(i)-coupled receptor by influencing processing of Galpha(i)*. J Biol Chem *279*, 13375-13382.

Schaefer,M., Petronczki,M., Dorner,D., Forte,M., and Knoblich,J.A. (2001). *Heterotrimeric G proteins direct two modes of asymmetric cell division in the Drosophila nervous system*. Cell *107*, 183-194.

Schaefer,M., Shevchenko,A., Shevchenko,A., and Knoblich,J.A. (2000). *A protein complex containing Inscuteable and the Galpha-binding protein Pins orients asymmetric cell divisions in Drosophila*. Curr Biol *10*, 353-362.

Scheffzek,K., Ahmadian,M.R., and Wittinghofer,A. (1998). *GTPase-activating proteins: helping hands to complement an active site* . Trends Biochem Sci *23*, 257-262.

Schmidt,A., Palumbo,G., Bozzetti,M.P., Tritto,P., Pimpinelli,S., and Schafer,U. (1999). *Genetic and molecular characterization of sting, a gene involved in crystal formation and meiotic drive in the male germ line of Drosophila melanogaster*. Genetics *151*, 749-760.

Schober,M., Schaefer,M., and Knoblich,J.A. (1999). *Bazooka recruits Inscuteable to orient asymmetric cell divisions in Drosophila neuroblasts*. Nature *402*, 548-551.

Schuldt,A.J. and Brand,A.H. (1999). *Mastermind acts downstream of notch to specify neuronal cell fates in the Drosophila central nervous system*. Dev Biol *205*, 287-295.

Schuldt,A.J., Adams,J.H., Davidson,C.M., Micklem,D.R., Haseloff,J., St Johnston,D., and Brand,A.H. (1998). *Miranda mediates asymmetric protein and RNA localization in the developing nervous system*. Genes Dev *12*, 1847-1857.

Schweisguth,F. (2004). *Notch signaling activity* . Curr Biol *14*, R129-R138.

Shen,C.P., Knoblich,J.A., Chan,Y.M., Jiang,M.M., Jan,L.Y., and Jan,Y.N. (1998). *Miranda as a multidomain adapter linking apically localized Inscuteable and basally localized Staufen and Prospero during asymmetric cell division in Drosophila*. Genes Dev *12*, 1837-1846.

Siderovski,D.P., Diverse-Pierluissi,M., and De Vries,L. (1999). *The GoLoco motif: a Galphai/o binding motif and potential guanine-nucleotide exchange factor*. Trends Biochem Sci *24*, 340-341.

Simons,K. and Fuller,S.D. (1985). *Cell surface polarity in epithelia*. Annu Rev Cell Biol *1*, 243-288.

Skeath,J.B. and Doe,C.Q. (1996). *The achaete-scute complex proneural genes contribute to neural precursor specification in the Drosophila CNS*. Curr Biol *6*, 1146-1152.

Spana,E.P. and Doe,C.Q. (1996). *Numb antagonizes Notch signaling to specify sibling neuron cell fates*. Neuron *17*, 21-26.

Spana,E.P., Kopczynski,C., Goodman,C.S., and Doe,C.Q. (1995). *Asymmetric localization of numb autonomously determines sibling neuron identity in the Drosophila CNS*. Development *121* , 3489-3494.

Sprang,S.R. (1997). *G protein mechanisms: insights from structural analysis*. Annu Rev Biochem *66*, 639-678.

Stevenson,B.R., Heintzelman,M.B., Anderson,J.M., Citi,S., and Mooseker,M.S. (1989). *ZO-1 and cingulin: tight junction proteins with distinct identities and localizations*. Am J Physiol *257*, C621-C628.

Stevenson,B.R., Siliciano,J.D., Mooseker,M.S., and Goodenough,D.A. (1986). *Identification of ZO-1: a high molecular weight polypeptide associated with the tight junction (zonula occludens) in a variety of epithelia*. J Cell Biol *103*, 755-766.

Stow,J.L., de Almeida,J.B., Narula,N., Holtzman,E.J., Ercolani,L., and Ausiello,D.A. (1991). *A heterotrimeric G protein, G alpha i-3, on Golgi membranes regulates the secretion of a heparan sulfate proteoglycan in LLC-PK1 epithelial cells*. J Cell Biol *114*, 1113-1124.

Stryer,L. and Bourne,H.R. (1986). *G proteins: a family of signal transducers*. Annu Rev Cell Biol *2*, 391-419.

Subramaniam,V.N., Peter,F., Philp,R., Wong,S.H., and Hong,W. (1996). *GS28, a 28-kilodalton Golgi SNARE that participates in ER-Golgi transport*. Science *272*, 1161-1163.

Takesono,A., Cismowski,M.J., Ribas,C., Bernard,M., Chung,P., Hazard,S., III, Duzic,E., and Lanier,S.M. (1999). *Receptor-independent activators of heterotrimeric G-protein signaling pathways*. J Biol Chem *274*, 33202-33205.

Tall,G.G., Krumins,A.M., and Gilman,A.G. (2003). *Mammalian Ric-8A (synembryn) is a heterotrimeric Galpha protein guanine nucleotide exchange factor*. J Biol Chem *278*, 8356-8362.

Tanabe,Y. and Jessell,T.M. (1996). *Diversity and pattern in the developing spinal cord*. Science *274*, 1115-1123.

Tokumoto,M., Gong,Z., Tsubokawa,T., Hew,C.L., Uyemura,K., Hotta,Y., and Okamoto,H. (1995). *Molecular heterogeneity among primary motoneurons and within myotomes revealed by the differential mRNA expression of novel islet-1 homologs in embryonic zebrafish*. Dev Biol *171*, 578-589.

Tonissoo,T., Meier,R., Talts,K., Plaas,M., and Karis,A. (2003). *Expression of ric-8 (synembryn) gene in the nervous system of developing and adult mouse*. Gene Expr. Patterns. *3*, 591-594.

Uemura,T., Shepherd,S., Ackerman,L., Jan,L.Y., and Jan,Y.N. (1989). *numb, a gene required in determination of cell fate during sensory organ formation in Drosophila embryos*. Cell *58*, 349-360.

Umesono,Y., Hiromi,Y., and Hotta,Y. (2002). *Context-dependent utilization of Notch activity in Drosophila glial determination*. Development *129*, 2391-2399.

Watts,J.L., Morton,D.G., Bestman,J., and Kemphues,K.J. (2000). *The C. elegans par-4 gene encodes a putative serine-threonine kinase required for establishing embryonic asymmetry*. Development *127*, 1467-1475.

Wickert,S., Finck,M., Herz,B., and Ernst,J.F. (1998). *A small protein (Ags1p) and the Pho80p-Pho85p kinase complex contribute to aminoglycoside antibiotic resistance of the yeast Saccharomyces cerevisiae*. J Bacteriol. *180*, 1887-1894.

Willard,F.S. and Crouch,M.F. (2000). *Nuclear and cytoskeletal translocation and localization of heterotrimeric G-proteins*. Immunol Cell Biol *78*, 387-394.

Willard,F.S., Kimple,R.J., and Siderovski,D.P. (2004). *RETURN OF THE GDI: The GoLoco Motif in Cell Division*. Annu Rev Biochem *73*, 925-951.

Wodarz,A. and Huttner,W.B. (2003). *Asymmetric cell division during neurogenesis in Drosophila and vertebrates*. Mech Dev *120*, 1297-1309.

Wodarz,A., Ramrath,A., Grimm,A., and Knust,E. (2000). *Drosophila atypical protein kinase C associates with Bazooka and controls polarity of epithelia and neuroblasts*. J Cell Biol *150*, 1361-1374.

Wolff,C., Roy,S., and Ingham,P.W. (2003). *Multiple muscle cell identities induced by distinct levels and timing of hedgehog activity in the zebrafish embryo*. Curr Biol *13*, 1169-1181.

Wu,C., Zeng,Q., Blumer,K.J., and Muslin,A.J. (2000). *RGS proteins inhibit Xwnt-8 signaling in Xenopus embryonic development*. Development *127*, 2773-2784.

Xu,Y., Wong,S.H., Tang,B.L., Subramaniam,V.N., Zhang,T., and Hong,W. (1998). *A 29-kilodalton Golgi soluble N-ethylmaleimide-sensitive factor attachment protein receptor (Vti1-rp2) implicated in protein trafficking in the secretory pathway*. J Biol Chem *273*, 21783-21789.

Yan,Y.L., Hatta,K., Riggleman,B., and Postlethwait,J.H. (1995). *Expression of a type II collagen gene in the zebrafish embryonic axis*. Dev Dyn. *203*, 363-376.

Yap,A.S., Brieher,W.M., Pruschy,M., and Gumbiner,B.M. (1997). *Lateral clustering of the adhesive ectodomain: a fundamental determinant of cadherin function*. Curr Biol *7*, 308-315.

Yap,A.S., Stevenson,B.R., Cooper,V., and Manley,S.W. (1997). *Protein tyrosine phosphorylation influences adhesive junction assembly and follicular organization of cultured thyroid epithelial cells*. Endocrinology *138*, 2315-2324.

Yeo,S.L., Lloyd,A., Kozak,K., Dinh,A., Dick,T., Yang,X., Sakonju,S., and Chia,W. (1995). *On the functional overlap between two Drosophila POU homeo domain genes and the cell fate specification of a CNS neural precursor*. Genes Dev *9*, 1223-1236.

Yu,F., Cai,Y., Kaushik,R., Yang,X., and Chia,W. (2003). *Distinct roles of Galphai and Gbeta13F subunits of the heterotrimeric G protein complex in the mediation of Drosophila neuroblast asymmetric divisions*. J Cell Biol *162*, 623-633.

Yu,F., Morin,X., Cai,Y., Yang,X., and Chia,W. (2000). *Analysis of partner of inscuteable, a novel player of Drosophila asymmetric divisions, reveals two distinct steps in inscuteable apical localization*. Cell *100*, 399-409.

Yu,F., Morin,X., Kaushik,R., Bahri,S., Yang,X., and Chia,W. (2003). *A mouse homolog of Drosophila pins can asymmetrically localize and substitute for pins function in Drosophila neuroblasts*. J Cell Sci *116*, 887-896.

Yu,F., Ong,C.T., Chia,W., and Yang,X. (2002). *Membrane targeting and asymmetric localization of Drosophila partner of inscuteable are discrete steps controlled by distinct regions of the protein*. Mol Cell Biol *22*, 4230-4240.

Zhong,H. and Neubig,R.R. (2001). *Regulator of G protein signaling proteins: novel multifunctional drug targets*. J Pharmacol Exp Ther. *297*, 837-845.

Zhong,W., Feder,J.N., Jiang,M.M., Jan,L.Y., and Jan,Y.N. (1996). *Asymmetric localization of a mammalian numb homolog during mouse cortical neurogenesis*. Neuron *17*, 43-53.

Zhong,W., Jiang,M.M., Schonemann,M.D., Meneses,J.J., Pedersen,R.A., Jan,L.Y., and Jan,Y.N. (2000). *Mouse numb is an essential gene involved in cortical neurogenesis*. Proc Natl Acad Sci U S A *97*, 6844-6849.

Zilian,O., Saner,C., Hagedorn,L., Lee,H.Y., Sauberli,E., Suter,U., Sommer,L., and Aguet,M. (2001). *Multiple roles of mouse Numb in tuning developmental cell fates*. Curr Biol *11*, 494-501.

Zipursky,S.L., Venkatesh,T.R., Teplow,D.B., and Benzer,S. (1984). *Neuronal development in the Drosophila retina: monoclonal antibodies as molecular probes*. Cell *36*, 15-26.

# List of Publications

**Kaushik,R**., Yu,F., Chia,W., Yang,X., and Bahri,S. (2003). *Subcellular localization of LGN during mitosis: evidence for its cortical localization in mitotic cell culture systems and its requirement for normal cell cycle progression*. Mol Biol Cell *14*, 3144-3155.

Yu,F., Cai,Y., **Kaushik,R**., Yang,X., and Chia,W. (2003). *Distinct roles of Galphai and Gbeta13F subunits of the heterotrimeric G protein complex in the mediation of Drosophila neuroblast asymmetric divisions*. J Cell Biol *162*, 623-633.

Yu,F., Morin,X., **Kaushik,R**., Bahri,S., Yang,X., and Chia,W. (2003). *A mouse homolog of Drosophila pins can asymmetrically localize and substitute for pins function in Drosophila neuroblasts*. J Cell Sci *116*, 887-896.

**Kaushik R**., Sleptsova-Friedrich I., Yang X. and Bahri, S. *Characterization of the LGN/AGS3 homologs from zebrafish: LGN is required for proper formation of primary motorneurons in the zebrafish embryo*. (Currently under review with Developmental Biology)

**Kaushik R**., Yu, F., Chia W., Yang X., and Bahri, S. *Characterization of DRapGAP2: its subcellular localization and role in dbd neuron formation.* (Manuscrpit in preparation)